



Università degli Studi di Ferrara

DOTTORATO DI RICERCA IN

"Farmacologia e oncologia molecolare"

CICLO XXVIII

coordinatore Prof. Antonio Cuneo

**New putative therapeutic targets
and biomarkers of epileptogenesis:
epigenetic, computational and neurochemical analyses**

Settore Scientifico Disciplinare BIO/14

Dottorando

Dott. Paolo Roncon

(firma)

Tutore

Prof. Michele Simonato

(firma)

Anni 2013/2015

Index

Abstract	1
Chapter 1. From patients to pre-clinical research: a translational overview in epilepsy	3
1.1 Epilepsy: definition	4
1.2 The classification of seizures	4
1.3 Diagnosis	5
1.4 Treatment	6
1.5 Temporal lobe epilepsy	13
1.6 Epileptogenesis	15
1.7 The role of the dentate gyrus	20
1.8 Experimental models of temporal lobe epilepsy	22
1.9 References	25
Chapter 2. Aims	32
Chapter 3. MicroRNAs as potential therapeutic targets and biomarkers of disease	34
3.1 MicroRNAs: biogenesis and functions	35
3.2 Circulating microRNAs as biomarkers of disease	36
3.3 MicroRNAs (dys)regulation in epilepsy	39
3.4 References	40

Identification of miRNAs differentially expressed in human epilepsy with or without granule cell pathology	46
MicroRNAs profile in hippocampal granule cells and plasma of rats with pilocarpine-induced epilepsy-comparison with human epileptic samples	54
Is autopsy tissue a valid control for epilepsy surgery tissue in microRNAs studies?	83
Meta-analysis of microRNAs dysregulated in different models of epilepsy	100
Chapter 4. Sestrin 3: a trans-regulator of a pro-convulsive gene network	132
4.1 Epilepsy and heritability	133
4.2 Sestrin 3	134
4.3 References	135
Systems genetics identifies Sestrin 3 as a regulator of a proconvulsant gene network in human epileptic hippocampus	138
Sestrin 3 as a regulator of a proconvulsant gene network: characterization of a rat knock out model	198
Silencing status epilepticus-induced BDNF expression with herpes simplex virus type-1 based amplicon vectors	201

Chapter 5. Excitatory/inhibitory unbalance in epilepsy	234
5.1 Neurotransmitter system involved in epileptic hyperactivity	235
5.2 Role of glutamatergic system in seizure activity	235
5.3 Human and animal studies evidencing the role of glutamate in epilepsy	236
5.4 Role of the GABAergic system in seizure activity	236
5.5 References	237
Impairment of GABA release in the hippocampus at the time of the first spontaneous seizure in the pilocarpine model of temporal lobe epilepsy	241
Increased extracellular levels of glutamate in the hippocampus of chronically epileptic rats	252
Chapter 6. Conclusions and futures perspectives	260
6.1 Summary	261
6.2 MiRNAs	261
6.3 Sestrin 3	264
6.4 Excitatory and inhibitory unbalance in the epileptic brain	265
6.5 References	266

New putative therapeutic targets and biomarkers of epileptogenesis: epigenetic, computational and neurochemical analyses

Temporal lobe epilepsy (TLE) arises in the limbic system of the brain, often after a latency period that follows a lesional event. During the latency phase (epileptogenesis) patients are apparently well, and the diagnosis of epilepsy is possible only when seizures begin to occur. Currently available antiepileptic drugs (AEDs) are effective for the treatment of the symptoms (seizures) but not for curing the disease. Furthermore, more than 30% of TLE patients are resistant to pharmacological treatments and, just for a small percentage of them, the only option is the surgical resection of the epileptogenic area.

Epileptogenesis is characterized by cellular and molecular modifications that transform a healthy brain in epileptic. The modifications occurring during epileptogenesis include “long-lasting” changes to gene expression and alterations in the release of neurotransmitters, like glutamate and GABA, which lead to an unbalance between excitation and inhibition.

In this thesis, I first investigated the role of microRNAs (miRNAs) in regulating pathogenetic mechanisms in the laser-microdissected dentate gyrus (DG) of epileptic rats, at different time points of the disease, and in drug-resistant patients that underwent surgery. Microarray analysis identified 64 miRNAs that are differentially expressed in the different phases of the disease (early and late latency, first spontaneous seizure and chronic stage) in the rat pilocarpine model of epilepsy. The comparison between epileptic rats and human DG revealed an overlap of 4 miRNAs (miR-21-5p, miR-23a-5p, miR-146a-5p and miR-181c-5p).

Changes observed in rats, however, may be model specific. A meta-analysis of different available datasets, obtained from the DG of animals made epileptic with different models of TLE, detected the dys-regulation of 44 and 8 miRNAs, respectively in the latency and in the chronic stages. Thus, these altered levels of miRNAs may be considered as disease-specific rather than model-specific. Moreover, a combinatorial histopathological and miRNAs signature identified miR-487a as highly expressed in human samples without granule cell pathology-type 2, a histological pattern that associates with a better prognosis after surgery. These findings suggest miR-487a as a putative biomarker for establishing the prognosis after surgery. In addition, levels of circulating miRNAs have been studied with a

microarray strategy, highlighting a significant up-regulation of the brain-enriched miR-9a-3p in plasma samples of rats killed in the early latency phase, suggesting its role as a putative biomarker of epileptogenesis.

Integrated analysis of transcriptional networks with genetic susceptibility data and phenotypic information allows to connect specific transcriptional programs to disease states. A computational analysis on TLE patients, pilocarpine-treated mice and pentilentetrazole-induced seizures in zebrafish identified the gene Sestrin 3 (SESN3) as a trans-regulator of a pro-convulsant gene network. SESN3-KO rats shown a significant delay in status epilepticus onset after pilocarpine injection. Moreover, a behavioral analysis of these rats revealed a phenotype less anxious and less prone to depression. These findings suggest a role of SESN3 as a common regulator of seizure onset and of comorbid disorders associated to epilepsy.

Seizure onset in the chronic stage of the disease may be due to an unbalance between excitatory and inhibitory neurotransmission. In this thesis, GABA and glutamate levels have been investigated through intra-cranial microdialysis at different phases of the disease in the rat pilocarpine model. The study revealed a significant impairment of GABA release starting with the first spontaneous seizure, when GABA-A receptor desensitization is also observed. In contrast, significantly higher levels of glutamate have been found in the hippocampus of epileptic rats, and may play a role in the maintenance of a chronic epileptic condition.

Taken together, the results presented in this thesis suggest a role of specific brain-enriched miRNAs and SESN3 as putative epigenetic regulators of mechanisms that can lead to epilepsy. MicroRNAs that are particularly relevant in the phase of epileptogenesis and may be further investigated as novel therapeutic targets for the treatment of epilepsy. Moreover, altered circulating levels of miRNAs in the early stages of latency have great potential for becoming biomarkers to help identifying those patients that will develop epilepsy after a brain lesion. In addition, miRNAs whose expression levels are modified and the gene SESN3 may be helpful for understanding the mechanisms of seizure onset and drugs-resistance. Indeed, analysis of the predicted targets of these miRNAs highlighted their involvement in the regulation of GABA and glutamate receptors that are already established actors in the pathogenesis of epilepsy.

Chapter 1

From patients to pre-clinical research: a translational overview in epilepsy

1.1 Epilepsy: definition

Epilepsy is a disease of the nervous system that affects people worldwide. The International League Against Epilepsy (ILAE) defined, in 2014, Epilepsy as “a disease characterized by an enduring predisposition to generate epileptic seizures and by the neurobiological, cognitive, psychological, and social consequences of this condition” (Fisher et al, 2014). Indeed, it is characterized by recurrent, unprovoked seizures resulting from episodes of unusually excessive electrical activity in the brain. One seizure does not mean epilepsy. A patient is considered to be affected by epilepsy, if at least one of these conditions is verified: (i) at least two unprovoked (or reflex) seizures occurring more than 24 hours apart; (ii) one unprovoked (or reflex) seizure and a probability of further seizures similar to the general recurrence risk (at least 60%) after two unprovoked seizures.

Epilepsy affects about 1% of the worldwide population, thus it is considered the most common chronic neurological disease. There are an estimated 70 million people with epilepsy in the world, of whom up to 75% live in resource-poor countries with little to or no access to medical services or treatment (Meinardi et al, 2001; Ngugi et al, 2010). Frequently, in these countries, people with epilepsy may not come to medical observation, either because of ignorance or of lack of awareness of the symptoms.

Epilepsy is one of the world’s oldest recognized disease conditions, with written records dating back to 4000 BC. Fear, misunderstanding, discrimination and social stigma have surrounded epilepsy for centuries. This stigma continues in many countries today and can impact on the quality of life for people with the disease and their families.

1.2 The classification of seizures

The starting point in diagnosis of epilepsy is to determine the type of seizures. The ILAE established a new electroclinical classification of seizure types in 2010 (Berg et al, 2010). Seizures have been divided in two categories: *focal* and *generalized*. Focal epileptic seizures are conceptualized as originating within networks limited to one hemisphere. They may be discretely localized or more widely distributed. Focal seizures may originate in subcortical structures. Generalized epileptic seizures are conceptualized as originating at some point

within, and rapidly engaging, bilaterally distributed networks. Such bilateral networks can include cortical and subcortical structures, but do not necessarily include the entire cortex. Although individual seizure onsets can appear localized, the location and lateralization are not consistent from one seizure to another. Generalized seizures can be classified as:

- ✓ Tonic-clonic, characterized by tonic and clonic muscular spasms;
- ✓ Absence, characterized by a sudden motor stop that lasts no more than 10 seconds;
- ✓ Myoclonic, associated with spasms in flexion;
- ✓ Clonic, characterized by clonic spasms;
- ✓ Tonic, characterized by tonic spasms;
- ✓ Atonic, characterized by a sudden loss of muscle tone that can cause the fall to the ground.

1.3 Diagnosis

The diagnosis of epilepsy needs an accurate evaluation of the symptoms and of the medical history. The neurologist has to test for brain abnormalities with an electroencephalogram (EEG) in order to detect changes in the normal pattern of brain waves, even when the patient is not having a seizure. A video-EEG monitoring may help in the identification of the kind of seizures that the patient experiences, leading to a more accurate diagnosis. In addition, anatomical alterations in the brain tissue have to be investigated through different imaging techniques. The computerized tomography (CT) scan and the magnetic resonance imaging (MRI) permit the identification of brain abnormalities that might be causing seizures. The positron emission tomography (PET) is used to identify active areas in the brain. If the EEG and MRI scans do not allow to pinpoint the site where seizures are originating, the single-photon emission computerized tomography (SPECT) provides a 3D map of the blood flow activity during seizures in the brain. After these imaging investigations, neurophysiological test, to assess thinking, memory and speech skills, are also needed to determine brain-areas is affected.

In our days, the diagnosis of epilepsy is possible when the patient shows the symptom of the disease, in the chronic period. Indeed, no biomarkers of epileptogenesis have been identified so far. Preclinical studies in animal models of epilepsy aim at the investigation of novel imaging approaches, at the discovery of genetic variations and regulatory molecules, such as the microRNAs, as putative biomarkers of epileptogenesis. These studies are expected to lead to the identification of those patients that are likely to develop epilepsy and to lead to new anti-epileptogenic strategies that will allow to prevent the development of the disease.

1.4 Treatment

Unfortunately, the currently available treatments are symptomatic, at best controlling seizure onset, frequency and severity.

Drugs. The elective therapy for the treatment of epileptic patients is based on the antiepileptic drugs (AEDs). Since the introduction of **bromide** as an anti-seizure drug in 1857, there has been an impressive expansion of therapies that are clinically effective. In 1910, **phenobarbital** (PHB), which then was then used to induce sleep, was found to have anti-seizure activity and became the drug of choice for many years. A number of medications similar to PHB were developed, including **primidone**. In 1940, **phenytoin** (PHT) was found to be an effective drug for the treatment of epilepsy, and since then it has become a major first-line AED in the treatment of partial and secondarily generalized seizures. In 1968, **carbamazepine** (CBZ) was approved, initially for the treatment of trigeminal neuralgia; later, in 1974, it was approved for the treatment of partial seizures. **Ethosuximide** has been used since 1958 as a first-choice drug for the treatment of absence seizures without generalized tonic-clonic seizures. **Valproate** (VPA) was licensed in Europe in 1960 and in the United States in 1978, and now is widely available throughout the world. It became the drug of choice in primary generalized epilepsies and in the mid-1990s was approved for treatment of partial seizures. These anticonvulsants were the drugs of choice for seizure treatment until the 1990s, when newer AEDs with good efficacy, fewer toxic effects, better tolerability, and no need for blood level monitoring were developed. A study of live-born infants in Denmark

found that exposure to the newer-generation AEDs **lamotrigine** (LTG), **oxcarbazepine** (OXC), **topiramate**, **gabapentin**, and **levetiracetam** (LEV) in the first trimester was not associated with an increased risk of major birth defects (Molgaard-Nielsen et al, 2011). However, the new AEDs have been approved in the United States as add-on therapy only, with the exception of topiramate and oxcarbazepine; lamotrigine is approved for conversion to monotherapy. In fact, a meta-analysis of 70 randomized clinical trials confirmed the clinical impression that efficacy does not significantly differ among AEDs used for refractory partial epilepsy (Costa et al, 2011).

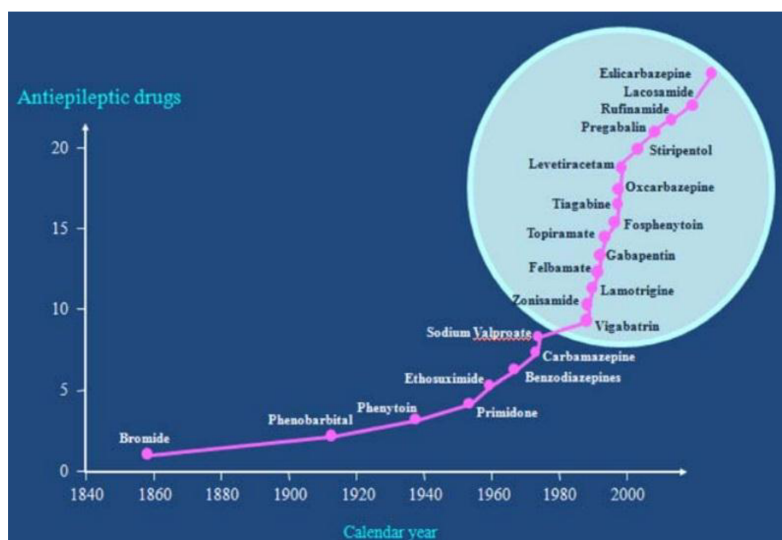


Figure 1. Chronology of AEDs available since the introduction of bromide in 1857. Brodie et al, 2000

Many structures and processes are involved in the development of a seizure, including neurons, ion channels, receptors, glia and inhibitory and excitatory synapses. The AEDs are designed to modify these processes so as to favor inhibition over excitation and thereby stop or prevent seizure activity. The AEDs can be grouped according to their main mechanism of action. The main groups include sodium channel blockers, calcium current inhibitors, gamma-aminobutyric acid (GABA) enhancers, glutamate blockers, carbonic anhydrase inhibitors, hormones, and drugs with unknown mechanisms of action.

Sodium channel blockade is the most common and best-characterized mechanism of currently available AEDs. Molecules that target sodium channels prevent the return of the channels to the active state by stabilizing the inactive form. Thus, repetitive firing of the axons is prevented. Presynaptic and postsynaptic blockade of sodium channels of the axons

causes stabilization of the neuronal membranes, blocks and prevents post-tetanic potentiation, limits the development of maximal seizure activity, and reduces the spread of seizures. AEDs that belong to this category are: CBZ, PHT, OXC and LTG.

Benzodiazepines and barbiturates are the most common drugs acting as GABA-receptor agonist. Since a seizure reflects an imbalance between excitatory and inhibitory activity in the brain, with an increment of excitation over inhibition, some benzodiazepine such as lorazepam, diazepam, clonazepam, and clobazam are used for the treatment of epilepsy. The first 2 drugs are used mainly for emergency treatment of seizures because of their quick onset of action, availability in intravenous (IV) forms, and strong anticonvulsant effects. Their use for long-term treatment is limited because of the development of tolerance. Moreover, 2 barbiturates mostly commonly used in the treatment of epilepsy are phenobarbital (PHB) and primidone. They are very potent anticonvulsants, but they have significant adverse effects that limit their use. Indeed, with the development of new drugs, the barbiturates now are used as second-line drugs.

Others molecules, such as the tiagabine, acts as GABA reuptake inhibitors. Reuptake of GABA is facilitated by specific GABA-transporting compounds; these carry GABA from the synaptic space into neurons and glial cells, where it is metabolized. This inhibition makes increased amounts of GABA available in the synaptic cleft prolonging inhibitory postsynaptic potentials (IPSPs). Similarly, vigabatrin inhibits the GABA transaminase in the extracellular compartment, leading to an increase in the extracellular concentration of the inhibitor neurotransmitter.

The enzyme glutamic acid decarboxylase (GAD) converts glutamate into GABA. Valproate (VPA) and gabapentin (GBP) are known to have some effect on this enzyme and thereby enhance the synthesis of GABA, in addition to other potential mechanisms of action. VPA also blocks the neuronal sodium channel during rapid sustained repetitive firing. GBP exerts a weak competitive inhibition of GABA transaminase.

Topiramate and perampanel act through a glutamate receptor blockade mechanism. Notably, topiramate has multiple mechanisms of action. It exerts an inhibitory effect on sodium conductance, decreasing the duration of spontaneous bursts and the frequency of generated action potentials, enhances GABA by unknown mechanisms, inhibits the amino-3-hydroxy-5-methyl-4-isoxazolepropionic acid (AMPA) subtype glutamate receptor, and is a

weak inhibitor of carbonic anhydrase. Perampanel is a noncompetitive antagonist of AMPA receptors.

The mechanism of action of LEV is possibly related to a brain-specific stereoselective binding site, synaptic vesicle protein 2A (SV2A). SV2A appears to be important for the availability of calcium-dependent neurotransmitter vesicles ready to release their content (Xu et al, 2001).

In spite of the numerous AEDs available, several patients are refractory to pharmacological treatments and continue to experience seizures (Simonato et al, 2014). Indeed, of those who develop epileptic seizures 47% will be controlled with the first prescribed AED, 32% with the second AED, and 9% with the third. Fourth and subsequent AEDs have at most a 5% chance of bringing remission. Accordingly, 30% of the individuals have no chances to obtain seizure control with a pharmacological treatment. Thus, there is an urgent need to develop new drugs for drug-resistant epilepsy or to prevent epileptogenesis. When drug treatments result ineffective and patients experience refractory seizures, other medical approaches may be attempted. These alternative treatments include ketogenic diet, vagus nerve or deep brain stimulation, and the surgical resection of the focus epilepticus.

Ketogenic diet. The ketogenic diet is one treatment option for children with epilepsy whose seizures are not controlled with AEDs. For some children who continue to have seizures, the ketogenic diet may help. However, the diet is very specialized, is a medical treatment and is usually only considered when at least two suitable medications have been tried and did not work. It should be carried out with the care, supervision and guidance of trained medical specialists.

The ketogenic diet is a high fat, low carbohydrate, controlled protein diet that has been used since the 1920s for the treatment of epilepsy. The word 'ketogenic' means that chemicals, called ketones, are made in the body (keto = ketone, genic = producing). Usually the body uses glucose from carbohydrates for its energy source. Ketones are made when the body uses fat for energy ("ketosis"). In the ketogenic diet the body uses ketones instead of glucose for its energy source.

A clinical trial in 2008 showed that the diet significantly reduced the number of seizures in some children whose seizures did not respond well to AEDs. After three months,

40% of children who started the diet had the number of their seizures reduced by over half and were able to reduce their medication. Although not all children had better seizure control, some had other benefits such as increased alertness, awareness and responsiveness.

So much work has centered on determining how these molecules may have anticonvulsant effects. Several mechanisms have been proposed, including changes in ATP production making neurons more resilient in the face of metabolic demands during seizures; altered brain pH affecting neuronal excitability; direct inhibitory effects of ketone bodies or fatty acids on ion channels; and shifts in amino acid metabolism to favor the synthesis of the inhibitory neurotransmitter GABA (Barañano and Hartman, 2008; Ma et al, 2007; Freeman et al, 2006).

In 1927, Wexler published the longer-term results of the use of the diet, of 91 patients suffering from idiopathic epilepsy, 32% became seizure-free, 22% improved, and the remaining 46% did not benefit from the diet (Wexler et al, 1997).

Vagus nerve stimulation. Vagus Nerve Stimulation (VNS) therapy is, similarly to the ketogenic diet, a treatment for people with epilepsy whose seizures are not controlled by drugs.

The VNS therapy requires a stimulator (or pulse generator) connected to the left vagus nerve in the neck (Figure 2).

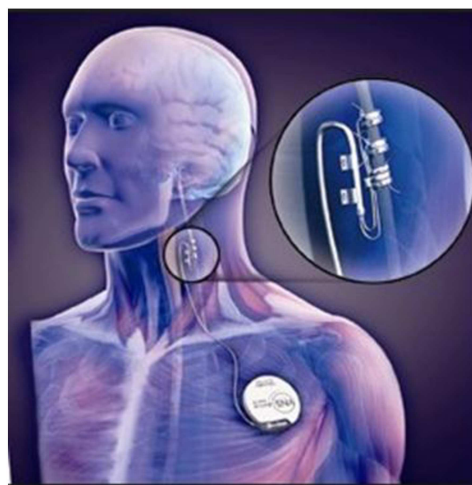


Figure 2. Vagus Nerve Stimulation

The stimulator delivers regular, mild electrical stimulations to the nerve that in turn projects these stimulations into the brain. The aim is to help slow down the irregular electrical brain activity that leads to seizures. The first surgically implanted automatic device for electrical stimulation of the left cervical vagus nerve was placed subcutaneously in a human patient with epilepsy in 1988 (Penry et al, 1990). In 1999, a report by the Therapeutics and Technology Assessment Subcommittee of the American Academy of Neurology stated that ‘VNS is indicated for adults and adolescents over 12 years of age with medically intractable partial seizures who are not candidates for potentially curative surgical resections, such as lesionectomies or mesial temporal lobectomies’ (Fischer et al, 1999; Labar, 2004). VNS is currently employed worldwide, and to date more than 22,000 people have been treated with this therapy. Indeed, Wasade and colleagues (2015) demonstrated, in a total of 207 epileptic patients, 50% seizure reduction in 68% of patients and seizure freedom in 20% of patients after the VNS treatment.

Surgery. There are different kinds of epilepsy surgery. One kind of surgery consists in removing a specific area of the brain, which is thought to be causing seizures. Another kind consists in separating the part of the brain that is causing seizures from the rest of the brain. For some patients surgery can stop or reduce the number of seizures they have. Surgery may be possible for both adults and children, and might be considered if:

- the patient tried several AEDs and none of them stopped or significantly reduced seizures;
- a cause for epilepsy could be found in a specific area of the brain, and this is an area where surgery is possible.

The effectiveness varies between subjects, depending on the type of surgery, with success rates varying between 50% and 80%. After surgical resection of the focus epilepticus, some patients are completely free of seizures. For others, the frequency of seizures is significantly reduced. In some cases, surgery may not be successful and a second surgery may be recommended. Most patients will need to continue taking anti-seizure medication for a year or more after surgery. Once seizure control is established, medications may be reduced or suspended. However, surgery can worsen existing problems or create new problems:

neurological deficits may appear, including loss of functions such as vision, speech, memory or movement.

Deep brain stimulation. The deep brain stimulation (DBS) therapy is a surgical treatment which aims to reduce seizures not controlled with medication, and where surgery to treat the cause of seizures is not possible. DBS consists of the application of low-intensity electric impulses, typically at or near a frequency of 130 Hz, to strategic sites in the brain through permanently implanted electrodes (Figure 3).

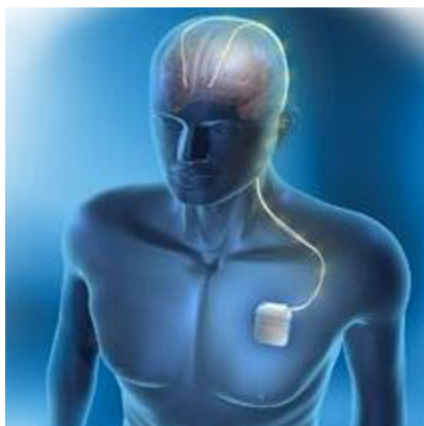


Figure 3. Deep brain stimulation.

These impulses are thought to transiently activate nearby axons (Coenen et al, 2015). During the first part of the surgery, two leads are placed deep inside the brain through small holes made in the skull. The neurosurgeon uses imaging techniques such as MRI to map the brain and place the leads in the correct position. The leads are connected to wires that run under the skin behind the ear, and down inside the skin of the neck where they are attached to a neuro-stimulator. During the second part of the surgery the neuro-stimulator is implanted under the skin in the upper chest (under the collar bone). The neuro-stimulator is a bit like a heart pacemaker: it contains a small battery and a computer chip programmed to send electrical impulses to the brain.

DBS is an established treatment for various neurological and psychiatric diseases. It is now considered a standard treatment for advanced Parkinson's disease. The safety and efficacy of DBS can be expected to improve with the application of new technical

developments in electrode geometry and new imaging techniques. Controlled trials would be helpful so that DBS could be extended to further indications, particularly psychiatric ones (Coenen et al, 2015).

1.5 Temporal lobe epilepsy

Temporal lobe epilepsy (TLE) is the most common form of focal epilepsy in adults. It frequently develops secondary to trauma, tumor or stroke, after a latency period in which patients are apparently well. During this period of time (epileptogenesis), that can last from months to year, modifications occur in the brain leading to the disease onset (Figure 4).

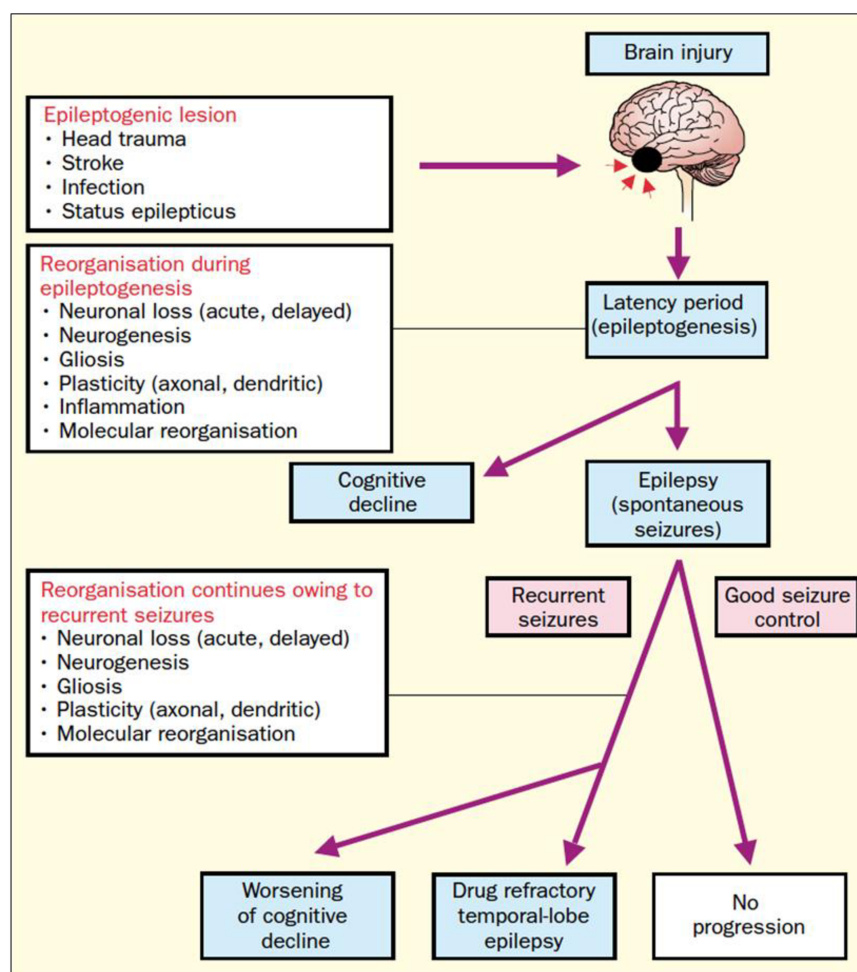


Figure 4. Transformation of a healthy brain into epileptic (Pitkanen and Sutula, 2002)

The ILAE recognizes two main types of temporal lobe epilepsy: lateral temporal lobe epilepsy (LTLE), the rarer type, arising in the neocortex at the outer (lateral) surface of the temporal lobe and mesial temporal lobe epilepsy (mTLE), arising in the hippocampus, the parahippocampal gyrus or the amygdala, which are located in the inner (medial) aspect of the temporal lobe. It is frequently associated with hippocampal sclerosis, reactive gliosis and synaptic rearrangement (Thom et al, 2009).

TLE is defined by seizure origination in only one or both lobes. About 40 to 80% of TLE-patients perform repetitive, automatic movements (called automatisms), such as lip smacking and rubbing the hands together. Seizures usually involve areas of the limbic system that control emotions and memory, and some individuals may have problems with memory, especially if seizures have occurred for more than 5 years. However, these memory problems are almost never severe.

The burden of comorbidity in people with epilepsy is high. Roughly 50% of adults with active epilepsy have at least one comorbid medical disorder (Feinstein, 1970; Forsgren, 1992; Keezer et al, 2015). Several diseases, including depression, anxiety, dementia, migraine, heart disease, peptic ulcers, and arthritis are up to eight times more common in people with epilepsy than in the general population (Gaitatzits et al, 2012; LaFrance et al, 2008; Keezer et al, 2015). Appreciation of the relevance of these comorbidities is increasing because they affect epilepsy prognosis and quality of life (Velioğlu et al, 2005; Taylor et al, 2011; Keezer et al, 2015). For instance, migraine has been associated with a reduced probability of early antiepileptic drug response and seizure freedom (Porta, 2014). Psychiatric disease was associated with a higher risk of pharmaco-resistance (Hitiris et al, 2007) and worsened outcome after anterior temporal lobectomy (Kanner et al, 2009).

Indeed, the presence of comorbidities may affect therapeutic decisions in people with epilepsy. Comorbid hepatic disease or renal insufficiency, migraine, or depression, for example, could be relevant in decisions about AEDs, while the risk of cognitive deficits might preclude some options, such as risk of severe memory impairment from temporal lobectomy (Keezer et al, 2015).

There is a pressing need for new and validated screening instruments and guidelines to help with the early detection and treatment of comorbid conditions. Preclinical and clinical research should continue to study the impact of comorbidities in epilepsy, not only focusing

on the description of the statistical relation between the different conditions, but also to uncover their common causal mechanisms.

1.6 Epileptogenesis

Epileptogenesis is most often defined as the seizure-free period between a precipitating injury event and the first observed clinical seizure. In this period, structural and functional changes arise in the brain that ultimately lead to epilepsy (Bertram, 2007). In other words, epileptogenesis refers to the phenomenon in which various kinds of brain insults –such as, traumatic brain injury, stroke, infection, prolonged febrile seizure trigger a cascade of events that eventually culminate in the occurrence of the first spontaneous seizure. Most of the data on the epileptogenic process originate from animal models in which epileptogenesis is initiated by status epilepticus, a relatively rare cause of epilepsy in humans. Further, typically the damage produced in animals exceeds that observed in humans. Thus, these models might distort our view of the severity of the pathology. However, these experiments provided a consistent set of information about the molecular and cellular changes in epilepsy: neurodegeneration, neurogenesis, gliosis, axonal damage or sprouting, dendritic plasticity, blood-brain barrier damage, reorganization of the extracellular matrix and reorganization of the molecular architecture of individual neuronal cells (Pitkänen and Lukasiuk, 2009).

Neurodegeneration. Neurodegeneration is the best described process associated with epileptogenesis and the chronic stage of the disease. Evidence obtained from surgical specimens or autopsy of TLE-patients demonstrates that neurodegeneration most often occurs in the hilus of the DG, in CA1 and CA3 pyramidal cell layer and interneurons, with milder damage in the CA2 pyramidal cell layer and in the granule cells of the DG (Pitkänen and Sutula, 2002). In addition, damaged areas have been observed in amygdala, entorhinal, perihinal and parahippocampal cortices and in extra-temporal areas, such as the thalamus and cerebellum (Jutila et al, 2002). Neuronal death in the hippocampal formation may compromise the hippocampal circuit and endanger the correct functioning of the synapses, contributing to the pathological processes that lead to epilepsy. However, it has been shown

that even a substantial protection of hippocampal neurons after SE does not prevent epileptogenesis (Brandt et al, 2003).

Neurogenesis. In rodents, it has been shown that even brief induced or spontaneous seizures, in addition to SE, can trigger neurogenesis (Pitkänen and Lukasiuk, 2009). After SE, increased neurogenesis can be detected within a few days and is maintained for several weeks (Parent et al, 1997). Moreover, seizures activity can disturb the migration of newly born neurons, resulting in their ectopic location in the hilus, aberrant connectivity and enhanced excitability (Scharfman et al, 2000). However, and in contrast with these observations, experimental evidence in the adult epileptic brain proved that newly born cells can develop specific synaptic properties to reduce excitability, becoming less sensitive to glutamate and more sensitive to GABA (Jakubs et al, 2006).

In human patients, it has been shown that epileptogenic brain insults such as stroke and TBI can also induce neurogenesis (Kluska et al, 2005; Pitkänen et al, 2006). Furthermore, altered neurogenesis has been found in learning and memory impairment and depression, which are common comorbid conditions of epilepsy (Scharfman and Her, 2007).

Gliosis. The main glial cells types include astrocytes, microglia, oligodendrocytes and polydendrocytes (NG2 cells). One major consequence of brain injury is a change in structure and function of the supporting glial cells, events that can contribute to the epileptogenic process in several ways: they can be involved in water and ion homeostasis, in the regulation of neurotransmission, in inflammatory responses and in the neurogenic potential. Specifically, astrocytes exhibit a hypertrophy of their processes and an altered expression of some proteins. When they display these alterations, the process is referred to as reactive astrocytosis. These changes represent a response of glia cells to primary modifications occurring in neurons.

Indeed, astrocytes are involved in a signaling dialog with neurons. Many synapses are associated with processes of astrocytes (the tripartite synapse). Here, astrocytes play a role in the uptake of the glutamate released by neurons, through the transporter GLT-1. Mice lacking this transporter develop spontaneous seizures and hippocampal pathology resembling that of patients with temporal lobe epilepsy (Haydon et al, 2009). In addition, astrocytes are important in the clearance of K^+ , preventing excess buildup of extracellular K^+ following repetitive neuronal activity. They can also respond to neurotransmitters with elevation in their

internal Ca^{2+} concentrations and release of transmitters. Astrocytes can release glutamate, which acts on neuronal NMDA receptors, D-serine, which is an endogenous agonist for the glycine binding site of NMDA receptors and ATP, which is hydrolyzed by extracellular ectonucleotidases to adenosine. Astrocyte-derived adenosine is not merely released at a background rate to maintain in its extracellular concentration. Indeed, neural activity can induce elevated release of ATP from astrocytes that, after hydrolysis to adenosine, causes the A1 receptor-dependent heterosynaptic repression of neighboring unstimulated synapses, exerting a powerful non-GABAergic mechanism of inhibition in the CNS. Adenosine is, indeed, considered an endogenous anticonvulsant. Unfortunately, is not feasible to use it as an AED, because of the variety of systemic actions. Other mechanisms of action including different pathways may be considered in the perspective to prevent epileptogenesis and seizures.

Astrocytes are involved in the neuroinflammatory response of the brain to the insult. They synthesize and release inflammatory mediators during the early post-injury phase, as well as in animals and patients with chronic epilepsy (Pitkänen and Lukasiuk, 2009; Vezzani and Baram, 2007). Astrocytes can produce a range of immunologically relevant molecules, including class II major histocompatibility complex antigens, many cytokines and chemokines, interleukins (IL-1, IL-6 and IL-10), interferons (INF- α and β), tumor necrosis factor (TNF) α and transforming growth factor (TGF).

Moreover, evidence is pointing to enhanced chemical signaling and disrupted linkage between water and potassium balance in epileptic tissue by reactive astrocytes, which together conspire to enhance local synchrony in hippocampal microcircuits (Wetherington et al, 2008). Brain tissue excitability is extremely sensitive to osmolality and to the size of the extracellular space. Indeed, hyperosmolar states and decreased extracellular space reduce seizure threshold (Binder and Steinhäuser, 2009).

Between the predominant glia-cells types, together with astrocytes, there is microglia. Microglia cells are extremely sensitive to disturbances in brain homeostasis and can secrete various compounds in the extracellular space. Moreover, microglia cells can respond quickly to pathological insults, such as damage to neighboring neurons (Heiler, 2008). Increases in the number of microglia cells and migration toward the place of injury can be observed. Microgliosis peaks at about 3-5 days and can remain elevated for several weeks (Jørgensen et

al, 1993; Heiler et al, 1999). Activated microglia can release a number of compounds potentially harmful to neurons, such as pro-inflammatory cytokines (IL-1, IL-6 and TNF α), proteases and nitric oxide. On the other hand, activated microglia can secrete TGF β and BDNF, which may exert neuroprotective effects (Elkabes et al, 1996; Miwa et al, 1997). The net effect (harmful versus protective) of microglia remains controversial and requires further study.

Oligodendrocytes and NG2 cells are the third and the fourth major glia-cells populations. There are relatively few studies on oligodendrocytes and NG2 cells in epilepsy or seizures. Oligodendrocytes are responsible for myelination. The contribution of myelin pathology to the epileptogenic process is poorly understood, even though white matter damage is often described in human acquired epilepsy (Lee et al, 1998). NG2 cells are progenitors cells expressing proteoglycan NG2 and are found in both gray and white matter. These cells receive synaptic contacts from excitatory and inhibitory neurons, suggesting that they transfer electrical and environmental cues to the myelination process (Kukley et al, 2008).

Axonal damage and mossy fibers sprouting. Axonal injury is common after epileptogenic brain insults like TBI and stroke. Indeed, histological studies have shown that, after TBI, axonal injury occurs within few minutes to hours, and continue for up to 1 year (Pitkänen and McIntosh, 2006). Whether axonal injury affects epileptogenesis and seizure spread is unknown.

Sprouting of glutamatergic granule cells axons (the mossy fibers) is the most widely studied form of axonal plasticity in epilepsy. Mossy fiber sprouting with recurrent excitation was proposed as a pro-epileptic mechanism in which denervated granule cells would be reinnervated by newly sprouted granule cell axons following seizure-induced neurogenesis, forming an excitatory network that predisposes to spontaneous spikes and epileptic discharges (Nadler, 2003). Experimental evidence from *in vivo* studies shown that many epileptogenic insults, including SE, TBI and stroke, trigger mossy fibers sprouting (Pitkanen et al, 2007). This has been described also in the hippocampus of surgical patients with epilepsy (Mathern et al, 1996). New mossy fiber synapses are predominantly excitatory (Sutula and Dudek,

2007), however sprouting may also generate new synapses with inhibitory interneurons (Sloviter et al, 2006).

The functional role of axonal sprouting in epileptogenesis and ictogenesis is controversial. However, many experimental treatments used to facilitate post-TBI/stroke recovery were found to enhance axonal sprouting of surviving neurons or provide transplanted cell that form new axonal connections and repair the damaged pathways (Marklund et al, 2006; Rao et al, 2006; Nudo, 2007; Pitkanen and Lukasiuk, 2009).

Dendritic plasticity. Changes in spine morphology, reduced dendritic branching and loss of dendritic spines have been described both in experimental model and in TLE-patients (Von Campe et al, 1997; Isokawa, 2000). These alterations can affect the availability of various receptors and, thus, compromise the information flow within the hippocampal circuit, promoting the epileptogenic process.

Blood-brain barrier damage. Damage to the blood-brain barrier (BBB) and consequent expression of angiogenic factors, proliferation of endothelial cells and angiogenesis are events that occur after various epileptogenic insults (Chopp et al, 2008; Rigau et al, 2007; Morgan et al, 2007; Pitkänen and Lukasiuk, 2009). Studies in animal models and humans suggest that prolonged seizure activity is associated with the opening of BBB and angiogenesis (Hellsten et al, 2005; Rigau et al, 2007; Van Villet et al, 2007).

Reorganization of the extracellular matrix. Molecular profiling studies have pinpointed the regulation of expression of a large number of enzymes contributing to extracellular matrix degradation and remodeling. Notably, the plasminogen system seems to be involved in brain-tissue remodeling following insult (Lukasiuk et al, 2003).

Epigenetic mechanisms. Epigenetics is the study of cellular and physiological phenotypic trait variations that are caused by external or environmental factors and affect how cells read genes instead of being caused by changes in the DNA sequence. These changes include chemical modification of DNA or chromatin, such as DNA methylation and alteration in the methylation or acetylation status of histones, post-transcriptional modification of the core structural subunits of chromatin, the histone proteins and certain classes of non-coding RNA (ncRNA), that are nuclear-localized, closely associated with chromatin and regulate

transcription. However, ncRNA classes that more typically regulate translation outside of the nucleus are also considered to have a role in the epigenetic mechanisms.

These modifications are of importance for cell function. Experimental evidences proved that such phenomena occur in mature, post-mitotic neurons and play a role in psychiatric disorders, such as addiction, depression and schizophrenia (Tzankova et al, 2007; Renthal et al, 2008). Moreover, recent studies revealed that epigenetic mechanisms may also be relevant to epileptogenesis and seizure control (Pitkanen and Lukasiuk, 2009). Notably, histone modifications for promoters of a few genes involved in neuronal plasticity (i.e. c-fos, c-jun, CREB, BDNF and GluR2) have been observed after SE (Tzankova et al, 2004) or seizures onset (Huang et al, 2002). For example, an acute increase in BDNF expression following SE is associated with histone H4 acetylation, whereas the BDNF chronic up-regulation may be controlled by the acetylation of the histone H3 (Tzankova et al, 2004).

Currently, the terms “epileptogenesis” and “latency period” are used synonymously as operational terms, to refer to a period that begins after the brain insult and ends at the time of the first spontaneous seizure. All the alterations that occur during this phase depict epileptogenesis as a dynamic process that progressively alters neuronal excitability, establishes critical interconnections and requires intricate structural changes before the first seizure. However, recent studies in animal models and TLE-patients suggest that the molecular and cellular changes triggered by an epileptogenic insult can continue to progress after the epilepsy diagnosis (Pitkänen and Lukasiuk, 2011, 2009). In line with these emerging data, we can use the term “epileptogenesis” to cover both the latency and the chronic phases of disease.

1.7 The role of the Dentate Gyrus

The dentate gyrus (DG) is a region explored in many TLE studies because of its suggested role as a “gate”, acting to inhibit over-excitation in the hippocampal circuitry through its unique synaptic, cellular and network properties that result in relatively low excitability.

Krook-Magnuson and colleagues (2015) demonstrated with an optogenetic strategy that first, the restoration of the DG gate through the selective inhibition of granule cells is sufficient to inhibit spontaneous seizures and second, the activation of DG granule cells worsens spontaneous seizures in a mouse model of TLE and can induce acute seizures in non-epileptic animals. These findings provide direct evidence to the basis of the “DG gate theory” of TLE, which posits that seizures occur when the gate function of the DG is disrupted such that excess excitation emerges from or passes through the DG to downstream regions.

In addition, the DG undergoes important functional changes during the phase of epileptogenesis, including mossy fiber sprouting (Zhang et al, 2012), altered intrinsic properties and receptor expression (Stegen et al, 2012) and reduced GABAergic inhibition (Coulter and Carlson, 2007). Moreover, the DG is very often involved in generation of seizures in TLE-patients and is very often surgically removed in drug-resistant patients.

Ninety-six surgically resected specimens, obtained from patients with TLE, have been histopathologically analyzed by Blümke et al (2009). A new neuropathological classification of epileptogenesis lesions has been proposed including focal cortical dysplasias (FCD; Blümke et al, 2011), hippocampal sclerosis (HS; Blümke et al, 2013) and granule cell pathology (GCP; Blümke et al, 2009) in order to define histopathological features and subtypes, allowing attempts to correlate clinical and pathological findings. Notably, the GCP can be classified as GCP-type 1 and 2. GCP-type 1 is characterized by loss of granule cells, and 2 different histopathologic patterns of the DG granule cell layer (GCL) can be described: thinned or containing cell-free gaps. In contrast, GCP-type 2 is characterized by a dispersion of the GCL that can appear also bilayered or containing ectopic neurons or clusters of neurons (Blümke et al, 2009; Figure 5). GCP-2 has been associated to a better prognosis after the surgical resection of the focus epilepticus in drug-resistant patients, but correlations with molecular markers have not been investigated before 2014, when Zucchini and colleagues identified a miRNA signature in patients with GCP-2 (full article reported in Chapter 2).

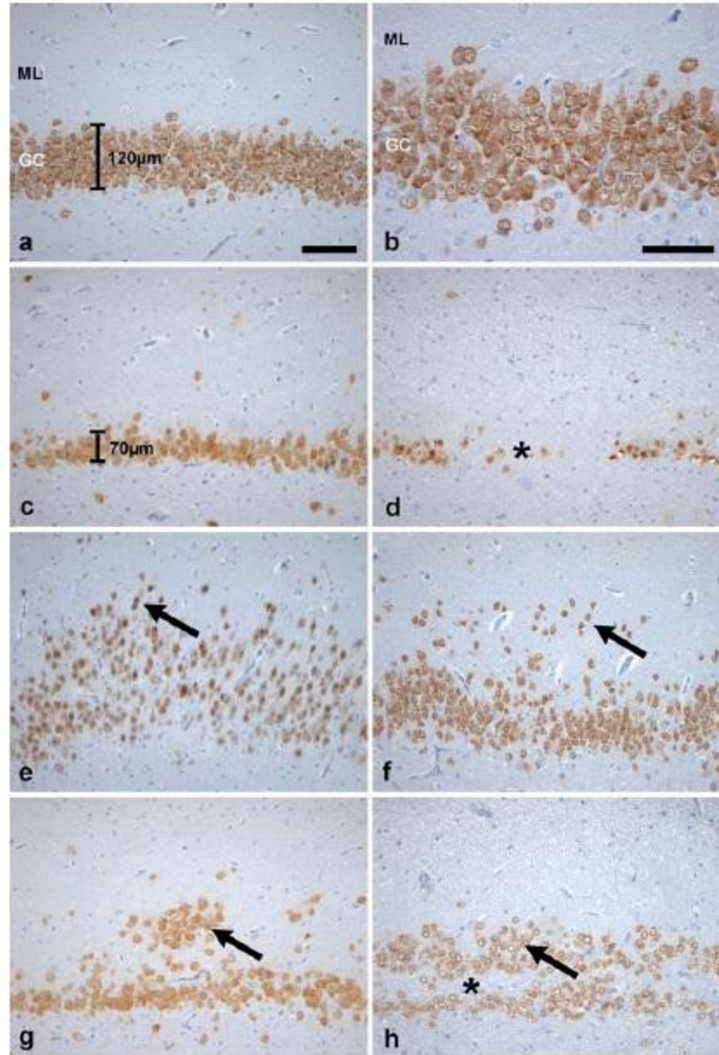


Figure 5. Histopathological spectrum of dentate gyrus pathology in TLE patients. **a** Normal appearance of the human dentate gyrus (no-GCP) with densely packed granule cells and sharp borders to subgranular and molecular layer (10 X magnification, bar 100 μ m, refers also to c–h). **b** Higher magnification of a (scale bar 50 μ m). Granule cell pathology Type 1 with significant granule cell loss indicated by thinning of dentate gyrus (c) or cell free gaps (d, asterisk). **e–h** Granule cell pathology Type 2 presenting with ectopic granule cells in the molecular layer, e.g., granule cell dispersion with spreading of granule cells into the molecular layer (e, arrow), single ectopic granule cells within the molecular layer (f, arrow), clusters of ectopic granule cells within the molecular layer (g, arrow) or with a bilaminar architecture (h, the arrow indicates the aberrant upper layer in the molecular layer, asterisk indicates a cell free gap between both layers). NeuN immunohistochemistry with hematoxylin counterstaining. GC granule cell layer, ML molecular layer TLE temporal lobe epilepsy (Blümcke et al, 2009).

1.8 Experimental models of temporal lobe epilepsy

The experimental models of epilepsy are important tools useful to develop new therapies. They have to show features that are characteristics of the disease, the same morphological and biochemical alterations, and they must be predictive for the development of new AEDs.

Experimental models of epilepsy, indeed, are employed to study the pathogenesis of epilepsy (epileptogenesis), to investigate putative biomarkers of disease and to identify new therapeutic targets.

The study of the basic mechanisms of epilepsy has obtained great advantages from the use of various *in vitro* experimental preparations, including the intact whole-brain preparation, brain slices, dissociated neurons, neuron fragments and single channel patches. As described above, epilepsy is characterized by active modifications in brain structure and function. Most of *in vitro* and *ex vivo* preparations cannot track neuronal alterations and epilepsy development. Thus, animal models are the best chance to study the development of the disease after an epileptogenic insult. Although researchers made a large use of non-human primates, dogs and especially cats (Gutnik and Prince 1975; Dichter and Spencer, 1969), starting from the 1980s small rodents, such as mice and rats, became the most common type of animal models.

The animal models of epilepsy may be classified in 3 main categories. (i) Acute models that are characterized by induced convulsive seizures without alterations in the neuro-electrical threshold and the onset of spontaneous seizures. (ii) Chronic models, such as kindling, characterized by a persistent decrease of seizure threshold but without spontaneous and recurrent seizures. (iii) Chronic models in which spontaneous and recurrent seizures occur, such as the pilocarpine model. These latter models are the only ones useful in the study of epileptogenesis.

The severity of seizures can be measured as reported in Table 1.

Table 1. Classification of seizures. Class 1-3 are focal seizures, class 4-6 are generalized seizures.

Classes	Description
1	Staring and mouth clonus
2	Automatisms
3	Monolateral forelimb clonus
4	Bilateral forelimb clonus
5	Bilateral forelimb clonus with rearing and falling
6	Tonic-clonic seizures

Rodents model of acquired epilepsy have contributed greatly to our understanding of the mechanisms that underlie epileptogenesis. Moreover, the administration of pro-convulsant agents, such as pilocarpine or kainate, evoking SE and, with time, recurrent spontaneous seizure led to better knowledge of the mechanisms that regulate seizures.

Although mice and rats are, in the present days, considered as the “normal” laboratory animals, new evidences in epilepsy research have been obtained with the employment of simpler vertebrate organisms, such as zebrafish. The zebrafish has great potential for modeling acute seizures. Indeed, acute seizures induced with 4-aminopyrimidine and pentylentetrazole (PTZ, Baraban et al, 2005; Johnson et al, 2015) or heat (Hunt et al, 2012) closely resemble those induced in rodents. Johnson and colleagues (2015, full article reported in Chapter 3), for example, performed a computational analysis on TLE-patients, pilocarpine-treated mice and PTZ-induced seizures in zebrafish, identifying the gene Sestrin 3 as regulator of a pro-convulsant gene-network.

In the last 10 years, computational biology has increased its power. Complex single-cell model approaches, derived from existing experimental data, have been combined into large-scale networks, to provide new understandings of the relationship between structure and function of particularly relevant brain areas, such as the DG (Johnsen et al, 2009).

1.9 References

Baraban SC, Taylor MR, Castro PA, Baier H (2005), Pentylentetrazole induced changes in zebrafish behavior, neural activity and c-fos expression. *Neuroscience*, 131:759-68.

Barañano KW, Hartman AL (2008), The ketogenic diet: uses in epilepsy and other neurologic illnesses. *Curr Treat Options Neurol*, 10(6): 410–419.

Bertram E, The relevance of kindling for human epilepsy (2007). *Epilepsia*, 48(2):65-74

Binder DK, Steinhäuser C (2009), Role of astrocyte dysfunction in epilepsy. *Encyclopedia of basic epilepsy research*, 1:412-7.

Blümcke I, Thom M, Aronica E, Armstrong DD, Bartolomei F, Bernasconi A, Bernasconi N, Bien CG, Cendes F, Coras R, Cross JH, Jacques TS, Kahane P, Mathern GW, Miyata H, Moshé SL, Oz B, Özkara Ç, Perucca E, Sisodiya S, Wiebe S, Spreafico R (2013), International consensus classification of hippocampal sclerosis in temporal lobe epilepsy: a Task Force report from the ILAE Commission on Diagnostic Methods. *Epilepsia*, 54(7):1315-29.

Blümcke I, Thom M, Aronica E, Armstrong DD, Vinters HV, Palmini A, Jacques TS, Avanzini G, Barkovich AJ, Battaglia G, Becker A, Cepeda C, Cendes F, Colombo N, Crino P, Cross JH, Delalande O, Dubeau F, Duncan J, Guerrini R, Kahane P, Mathern G, Najm I, Ozkara C, Raybaud C, Represa A, Roper SN, Salamon N, Schulze-Bonhage A, Tassi L, Vezzani A, Spreafico R (2011), The clinicopathologic spectrum of focal cortical dysplasias: a consensus classification proposed by an ad hoc Task Force of the ILAE Diagnostic Methods Commission. *Epilepsia*, 52(1):158-74.

Blümcke I, Kistner I, Clusmann H, Schramm J, Becker AJ, Elger CE, Bien CG, Merschhemke M, Meencke HJ, Lehmann T, Buchfelder M, Weigel D, Buslei R, Stefan H, Pauli E, Hildebrandt M (2009), Towards a clinic-pathological classification of granule cell dispersion in human mesial temporal lobe epilepsies. *Acta Neuropathol*, 117:535-44.

Brandt C, Potschka H, Löscher W, Ebert U (2003), N-Nethyl-D-aspartate receptor blockade after status epilepticus protects against limbic brain damage but not against epilepsy in the kainate model of temporal lobe epilepsy. *Neuroscience*, 118:727-40.

Chopp M, Li Y, Zhang J (2008), Plasticity and remodeling of brain. *J Neurol Sci*, 265:97-101.

Coenen VA, Amtage F, Volkmann J, Schlöpfer TE (2015), Deep Brain Stimulation in Neurological and Psychiatric Disorders. *Dtsch Arztebl Int*, 112(31-32):519-26.

Costa J, Fareleira F, Ascensão R, Borges M, Sampaio C, Vaz-Carneiro A (2011), Clinical comparability of the new antiepileptic drugs in refractory partial epilepsy: A systematic review and meta-analysis. *Epilepsia*, 52(7):1280-91.

Coulter DA, Carlson GC (2007), Functional regulation of the dentate gyrus by GABA-mediated inhibition. *Prog Brain Res*, 163:235-812.

Dichter M and Spencer WA (1969), Penicillin-induced interictal discharges from the cat hippocampus. I. Characteristics and topographical features. *J Neurophysiol*, 32:649-62.

Elkabes S, DiCicco-Bloom EM, Black IB (1996), Brain microglia/macrophages express neurotrophins that selectively regulate microglial proliferation and function. *J Neurosci*, 16:2508-21.

Engel J (2001). A proposed diagnostic scheme for people with epileptic seizures and with epilepsy: report of the ILAE Task Force on Classification and Terminology. *Epilepsia*, 42(6): 796–803.

Feinstein A (1970), Pre-therapeutic classification of co-morbidity in chronic disease. *J Chronic Dis* 23:455-68.

Fischer R, Handforth A (1999), Reassessment: VNS for epilepsy. *Neurology*, 53:666–9.

Fisher RS, Acevedo C, Arzimanoglou A, Bogacz A, Cross JH, Elger CE, Engel J Jr, Forsgren L, French JA, Glynn M, Hesdorffer DC, Lee BI, Mathern GW, Moshé SL, Perucca E, Scheffer IE, Tomson T, Watanabe M, Wiebe S (2014), ILAE official report: a practical clinical definition of epilepsy. *Epilepsia*, 55(4):475-82.

Forsgren L (1992), Prevalence of epilepsy in adults in northern Sweden. *Epilepsia*, 33:450-58.

Freeman J, Veggiotti P, Lanzi G, Tagliabue A, Perucca E (2006), The ketogenic diet: from molecular mechanisms to clinical effects. *Epilepsy Res*, 68:145–180.

Gaitatzis A, Sisodiya SM, Sander JW (2012), The somatic comorbidity of epilepsy: a weight but often unrecognized burden. *Epilepsia*, 53:1282-93.

Grone BP and Baraban S (2015), Animal models in epilepsy research: legacies and new directions. *Nat Neurosci*, 18(3):339-43.

Gutnick MJ and Prince DA (1975), Effect of projected cortical epileptiform discharges on neuronal activities in ventrobasal thalamus of the cat: ictal discharge. *Exp Neurol*, 46:418-31.

Hailer NP, Grampp A, Nitsch R (1999), Proliferation of microglia and astrocytes in the dentate gyrus following entorhinal cortex lesion: a quantitative bromodeoxyuridine-labelling study. *Eur J Neurosci*, 11:3359-64.

Haydon PG, Coulter DA, Yudkoff M, Moss SJ (2009), Astrocytic regulation of neuronal excitability. *Encyclopedia of basic epilepsy research*, 1:387-91.

Heiler NP (2008), Immunosuppression after traumatic or ischemic CNS damage: it is neuroprotective and illuminates the role of microglia cells. *Prog Neurobiol*, 84:211-33.

Hellsten J, West MJ, Arvidsson A, Ekstrand J, Jansson L, Wennström M, Tingström A (2005), Electroconvulsive seizures induce angiogenesis in adult rat hippocampus. *Bio Psychiatry*, 58: 871-8.

Hitiris N, Mohanraj R, Norrie J, Sills GJ, Brodie MJ (2007), Predictors of pharmacoresistant epilepsy. *Epilepsy Res*, 75:192-96

Huang Y, Doherty J, Dingledine R (2002), Altered histone acetylation at glutamate receptor 2 and brain-derived neurotrophic factor genes in an early event triggered by status epilepticus. *J Neurosci*, 22:8422-8.

Hunt RF, Hortopan GA, Gillepsie A, Baraban SC (2012), A novel zebrafish model of hyperthermia-induced seizures reveals a role for TRPV4 channels and NMDA-type glutamate receptors. *Exp Neurol*, 237:199-206.

Isokawa M (2000), Remodeling dendritic spines of dentate granule cells in temporal lobe epilepsy patients and the rat pilocarpine model. *Epilepsia*, 41(Suppl.6):S14-17.

Jakubs K, Nanobashvili A, Bonde S, Ekdahl CT, Kokaia Z, Kokaia M, Lindvall O (2006), Environment matters: synaptic properties of neurons born in the epileptic adult brain develop to reduce excitability. *Neuron*, 52:1047-59.

Johnsen JD, Morgan RJ, Soltesz I (2009), Computer models of seizures and epilepsy: understanding epileptogenesis using complex large-scale models. *Encyclopedia of basic epilepsy research*, 2:746-57.

Jørgensen MB, Finsen BR, Jensen MB, Castellano B, Diemer NH, Zimmer J (1993), Microglial and astroglial reactions to ischemic and kainic acid-induced lesions of the adult rat hippocampus. *Exp Neurol*, 120:70-88.

Jutila L, Immonen A, Partanen K, Partanen J, Mervaala E, Ylinen A, Alafuzoff I, Paljärvi L, Karkola K, Vapalahti M, Pitkänen A (2002), Neurobiology of epileptogenesis in the temporal lobe. *Adv Tech Stand Neurosurg*, 27:3-22.

Kanner AM, Byrne R, Chicharro A, Wu J, Frey M (2009), A lifetime psychiatric history predicts a worse seizure outcome following temporal lobectomy. *Neurology*, 72:793-99.

Keezer MR, Sisodiya SM, Sander JW (2015), Comorbidities of epilepsy: current concepts and future perspectives. *Lancet Neurol* S1474-4422(15)00225-2.

Kesner RP, Lee I, Gilbert P (2004), A behavioral assessment of hippocampal function based on a subregional analysis. *Rev Neurosci*, 15:333-51.

Kluska MM, Witte OW, Bolz J, Redcker C (2005), Neurogenesis in the adult dentate gyrus after cortical infarcts: effects of infarct location, N-methyl-D-aspartate receptor blockade and anti-inflammatory treatment. *Neuroscience*, 135:723-35.

Krook-Magnuson E, Armstrong C, Bui A, Lew S, Oijala M, Soltesz I (2015), In vivo evaluation of the dentate gate theory in epilepsy. *J Physiol*, 593(10):2379-88.

Kukley M, Kiladze M, Tognatta R, Hans M, Swandulla D, Schramm J, Dietrich D (2008), Glial cells are born with synapses. *FASEB J*, 22:2957-69.

Labar D, Vagus nerve stimulation for epilepsy (2004). *CNR* 4:81–87.

LaFrance WC Jr, Kanner AM, Hermann B (2008), Psychiatric comorbidities in epilepsy. *Int Rev Neurobiol*, 83:347-83.

Lee JW, Andermann F, Dubeau F, Bernasconi A, MacDonald D, Evans A, Reutens DC (1998), Morphometric analysis of the temporal lobe in temporal lobe epilepsy. *Epilepsia*, 39:727-36.

Lukasiuk K, Kontula L, Pitkänen A (2003), A CDNA profiling of epileptogenesis in the rat brain. *Eur J Neurosci*, 17:271-9.

Ma W, Berg J, Yellen G (2007), Ketogenic diet metabolites reduce firing in central neurons by opening K (ATP) channels. *J Neurosci*, 27:3618–3625.

Marklund N, Bakshi A, Castelbuono DJ, Conte V, McIntosh TK (2006), Evaluation of pharmacological treatment strategies in traumatic brain injury. *Curr Pharm Des*, 12:1645-80.

Miwa T, Furukawa S, Nakajima K, Furukama Y, Hohsaka S (1997), Lipopolysaccharide enhances synthesis of brain-derived neurotrophic factor in cultured rat microglia. *J neurosci Res*, 50(6):1023-9.

Molgaard-Nielsen D, Hviid A (2011), Newer-generation antiepileptic drugs and the risk of major birth defects. *JAMA*, 305(19):1996-2002.

Morgan R, Kreipke CW, Roberts G, Bagchi M, Rafols JA (2007), Neovascularization following traumatic brain injury: possible evidence for both angiogenesis and vasculogenesis. *Neurol Res*, 29:375-81.

Nudo RJ (2007), Postinfarct cortical plasticity and behavioral recovery. *Stroke*, 38(2, Suppl.):840-5.

Parent JM, Yu TW, Leibowitz RT, Geschwind DH, Sloviter RS, Lowenstein DH (1997), Dentate granule cell neurogenesis is increased by seizures and contributes to aberrant network reorganization in the rat hippocampus. *J Neurosci*, 17:3727-38.

Penry J, Dean J (1990), Prevention of intractable partial seizures by intermittent VNS in humans: preliminary results. *Epilepsia*, 31(Suppl 2):S40-3.

Pitkänen A, Lukasiuk K (2009), Molecular and cellular basis of epileptogenesis in symptomatic epilepsy. *Epilepsy Behav*, 14(1 Suppl. 1):16-25.

Pitkänen A, Lukasiuk K (2011), Mechanisms of epileptogenesis and potential treatment targets. *Lancet Neurol*, 10:173-86.

Pitkänen A, McIntosh TK (2006), Animal models of post-traumatic epilepsy. *J Neurotrauma*, 23:241-61.

Pitkänen A, Sutula T (2002), Is epilepsy a progressive disease? Prospect for new therapeutic approaches in temporal lobe epilepsy. *Lancet Neurol*, 1:173-81.

Porta M, ed. (2014), *A dictionary of epidemiology*. Oxford: Oxford University Press.

Rao MS, Hattiangady B, Shetty AK (2006), Fetal hippocampal CA3 cell grafts enriched with FGF-2 and BDNF exhibit robust long term survival and integration and suppress aberrant mossy fiber sprouting in the injured middle-aged hippocampus. *Neurobiol Dis*, 21:276-90.

Renthal W, Nestler EJ (2008), Epigenetic mechanisms in drug addiction. *Trends Mol Med*, 14:341-50.

Rigau V, Morin M, Rousset MC, de Bock F, Lebrun A, Coubes P, Picot MC, Baldy-Moulinier M, Bockaert J, Crespel A, Lerner-Natoli M (2007), Angiogenesis is associated with blood-brain barrier permeability in temporal lobe epilepsy. *Brain*, 130(Pt.7):1942-56.

Scharfman HE, Goodman JH, Sollas AL (2000), Granule-like neurons at the hilar/CA3 border after status epilepticus and their synchrony with area CA3 pyramidal cells: functional implications of seizure-induced neurogenesis. *J Neurosci*, 20:6144-58.

Scharfman HE, Hen R (2007), Neuroscience. Is more neurogenesis always better? *Science*, 315:336-8.

Scoville WB, Milner B (1975), Loss of recent memory after bilateral hippocampal lesions. *J Neurol Neurosurg Psychiatry*, 20:11-21.

Simonato M, Brooks-Kayal AR, Engel J Jr, Galanopoulou AS, Jensen FE, Moshé SL, O'Brien TJ, Pitkänen A, Wilcox KS, French JA (2014), The challenge and promise of anti-epileptic therapy development in animal models. *Lancet Neurol*, 13:949–60.

Stegen M, Kirchheim F, Hanuschkin A, Staszewski O, Veh RW, Wolfart J (2012), Adaptive intrinsic plasticity in human dentate gyrus granule cells during temporal lobe epilepsy. *Cereb Cortex*, 22: 2087-101.

Taylor RS, Sander JW, Taylor RJ, Baker GA (2011), Predictors of health-related quality of life and costs in adults with epilepsy: a systematic review. *Epilepsia*, 52:2160-80.

Thom M, Eriksson S, Martinian L, Caboclo LO, McEvoy AW, Duncan JS and Sisodya SM (2009), Temporal lobe sclerosis associated with hippocampal sclerosis in temporal lobe epilepsy: neuropathological features. *J Neuropathol Exp Neurol*, 68:928-938.

Tsankova N, Renthal W, Kumar A, Nestler EJ (2007), Epigenetic regulation in psychiatric disorders. *Nat Rev Neurosci*, 8:355-67.

Tsankova NM, Kumar A, Nestler EJ (2004), Histone modifications at gene promoter regions in rat hippocampus after acute and chronic electroconvulsive seizures. *J Neurosci*, 24:5603-10.

Van Vliet EA, da Costa Araújo S, Redeker S, van Schaik R, Aronica E, Gorter JA (2007), Blood-brain barrier leakage may lead to progression of temporal lobe epilepsy. *Brain*, 130(Pt.2):521-34.

Veliöğlu SK, Boz C, Ozmenoğlu M (2005), The impact of migraine on epilepsy: a prospective prognosis study. *Cephalgia*, 25:528-35.

Vezzani A, Baram TZ (2007), New roles for interleukin-1 beta in the mechanisms of epilepsy. *Epilepsy Curr*, 7:45-50.

Von Campe G, Spencer DD, de Lanerolle NC (1997), Morphology of dentate granule cells in the human epileptogenic hippocampus. *Hippocampus*, 7:472-88.

Wasade VS, Schultz L, Mohanarangan K, Gaddam A, Schwalb JM, Spanaki-Varelas M (2015), Long-term seizure and psychosocial outcomes of vagus nerve stimulation for intractable epilepsy. *Epilepsy & Behavior*, 53:31-36.

Wetherington J, Serrano G, Dingledine R (2008), Astrocytes in the epileptic brain. *Neuron*, 58:168-78

Wexler ID, Hemalatha SG, McConnell J, Buist NR, Dahl HH, Berry SA, Cederbaum SD, Patel MS, Kerr DS (1997), Outcome of pyruvate dehydrogenase deficiency treated with ketogenic diets. Studies in patients with identical mutations. *Neurology*, 49:1655–1661.

Xu T, Bajjalieh SM (2001), SV2 modulates the size of the readily releasable pool of secretory vesicles. *Nat Cell Biol*, 3(8):691-8.

Zhang W, Huguenard JR, Buckmaster PS (2012), Increased excitatory synaptic input to granule cells from hilar and CA3 regions in a rat model of temporal lobe epilepsy. *J Neurosci*, 32:1183-96.

Chapter 2

Aims

Currently available drugs can be effective for the symptomatic suppression of seizures in patients with epilepsy. However, seizures are not adequately controlled in a third of cases, no disease-modifying therapy exists, and comorbidities as well as unpredictable seizures impose a major burden on the quality of life of patients and caregivers. Therefore, we urgently need (i) treatments for drug-resistant seizures, (ii) disease-modifying treatments that prevent or attenuate epileptogenesis and (iii) treatments to prevent or attenuate the common comorbidities that contribute to disability in people with epilepsy.

This PhD project focused on the study of the molecular, cellular and neurochemical mechanisms that lead to the development of epilepsy (epileptogenesis) and to the occurrence of seizures in the chronic phase of the disease (ictogenesis). Specifically:

- 1) We investigated the alterations in miRNA expression in the epileptic brain tissue and the changes in miRNA levels in the peripheral blood. The former study was designed to identify new therapeutic approaches against epileptogenesis and drug-resistant epilepsy, via identification and validation of the predicted targets of de-regulated miRNAs. The latter study aimed at investigating circulating miRNAs as potential biomarkers of disease, useful to identify those individuals that will actually develop epilepsy (and should therefore be treated) among those at risk following an epileptogenic insult like a brain trauma or a stroke.
- 2) We used a systems genetics approach to identify from the human epileptic tissue a master regulator of a pro-convulsant gene network, Sestrin 3. After initial mechanistic studies in fish and mouse models, we generated Sestrin 3 knockout rats that were extensively characterized to substantiate the implication of the gene not only in seizure generation, but also in epilepsy co-morbidities.
- 3) We performed an extensive analysis of the adaptive and maladaptive changes occurring in the GABAergic and glutamatergic neurotransmission during the natural history of experimental temporal lobe epilepsy. This study allowed to evaluate the excitation to inhibition balance in a more compelling manner than in previously available studies, and can be useful to define a more rational and disease phase-oriented pharmacological treatment.

Chapter 3

MicroRNAs as potential therapeutic targets and biomarkers of disease

3.1 MicroRNAs: biogenesis and functions

MicroRNAs, or miRNAs, are small endogenous single strand RNAs that belong to the non-coding RNAs (ncRNAs) family. MiRNAs share with other identified ncRNAs the common function of regulators of gene expression, function that arises from their complementation with nucleic acids. MiRNAs are about 18-22 nucleotides (nt) in length and contain a 7-8 nt region that recognizes and binds mRNA targets, typically in the 3' untranslated region (3'UTR), to induce post-transcriptional silencing (Siegel et al, 2011; Qureshi and Mehler, 2012; Hwang et al, 2013).

MiRNAs are independently transcribed from intergenic or antisense regions or from intronic regions of coding DNA. They are transcribed as primary miRNAs (pri-miRNAs) constituted by 1-6 hairpin loop structures (>200 nt) that are cleaved in the nucleus by an endonuclease complex, called Drosha-DGCR8, into 60-70 nt hairpin intermediates known as miRNA precursors (pre-miRNAs). The pre-miRNAs are actively exported to the cytoplasm by exportin-5 and, here, processed by the endonuclease Dicer to yield mature miRNAs duplexes (Gregory et al, 2006). Thereafter, miRNAs interact with specific proteins called Argonaute (Ago) that are part of the catalytic core of the RNA-induced silencing complex (RISC). Ago are needed for miRNA-induced silencing and contain two conserved RNA binding domains: a PAZ domain that can bind the single stranded 3' end of the mature miRNA and a PIWI domain that structurally resembles ribonuclease-H and functions to interact with the 5' end of the guide strand. They bind the mature miRNA and orient it for interaction with a target mRNA. Generally, only one strand is incorporated into the RISC, selected on the basis of its thermodynamic instability and weaker base-pairing relative to the other strand. The other strand, called the passenger strand, due to its lower levels in the steady state, is normally inactive and gets degraded (Krol et al, 2004; Bartel, 2004; Khvorova et al, 2003; Schawarz et al, 2003). In some cases, both strands of the duplex are viable and become functional miRNAs that can silence an mRNA through different processes:

- ✓ cleavage of the mRNA strand into two pieces,
- ✓ destabilization of the mRNA through shortening of its poly(A) tail,
- ✓ less efficient translation of the mRNA into proteins by ribosomes.

MiRNAs play crucial regulatory roles in a wide range of biological processes, including cellular proliferation and differentiation, migration, apoptosis, development and metabolism (Pasquinelli et al, 2012; Pelaez et al, 2012; Kim et al, 2009) and their altered expression contributes to the pathogenesis of many human diseases. MiRNAs are found intracellularly in all cell types and have been shown to be present in plasma and serum samples in a stable form (Liang et al, 2013). Importantly, extracellular miRNAs levels are altered in different body fluids during the pathogenesis of many diseases (Mitchell et al, 2008; Chen et al, 2008).

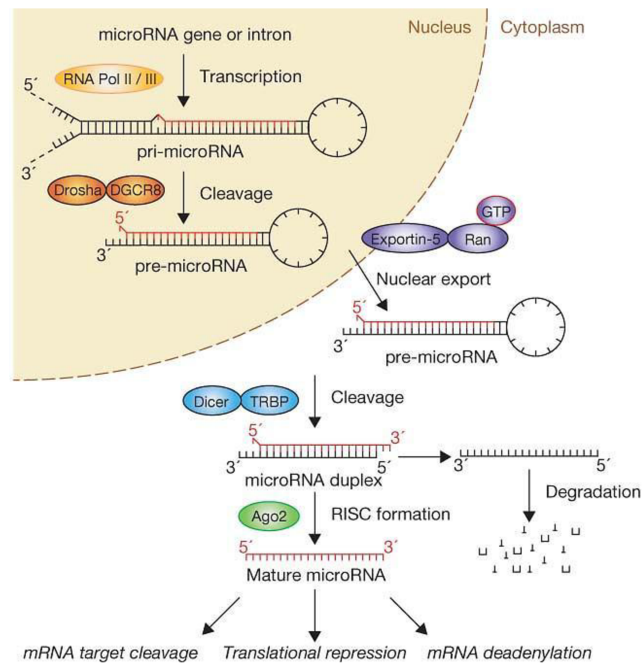


Figure 8. MicroRNAs biogenesis and functions (Winter et al, 2009)

3.2 Circulating microRNAs as biomarkers of disease

The origin and biological function of extracellular miRNAs remains not completely understood. The 2 most credible hypotheses suggest that (i) circulating miRNAs are derived from broken cells, particularly blood cells, or (ii) they are actively secreted from cells (Liang et al, 2013). Actually, only a few studies reported that the serum/plasma miRNAs may mainly derive from blood cells. However, tissue-enriched miRNAs from other organs have been detected in plasma (Laterza et al, 1983; Corsten et al, 2010; Lewis et al, 2010; Zhang et al, 2010; Wang et al, 2015a,b). These data strongly suggest that mechanisms may be in place to select specific miRNAs for release. Elucidating the origin of the extracellular miRNAs

would increase our understanding of their potential pathophysiological relevance (Liang et al, 2013). Several studies, indeed, focused on the stability and the biogenesis of the circulating miRNAs, proposing 3 different models.

- ✓ *Membranous vesicles.* MiRNAs can be secreted from donor cells via small membranous vesicles, which protect them from RNase activity (Skog et al, 2008; Valadi et al, 2007). Vesicles proposed as miRNA carriers include exosomes (30-100 nm) and shedding vesicles (100-1000 nm). Exosomes arise from multivesicular bodies (MVBs) and are released by exocytosis (Thery et al, 2002; Ratajczak et al, 2006; Simons et al, 2009; Mathivanan et al, 2010), whereas shedding vesicles are released by outward budding and fission of the plasma membrane.
- ✓ *High-density lipoproteins.* MiRNAs may be secreted from donor cells in association with high-density lipoprotein (HDL) that protect them to the extracellular RNase-dependent degradation (Cocucci et al, 2009).
- ✓ *RNA-binding proteins.* Recent studies showed that a significant portion of extracellular miRNAs in the plasma/serum is associated with AGO2 in a highly stable complex (Vickers et al, 2011). This may happen because they are passively leaked from broken cells owing to tissue injury and cell death.

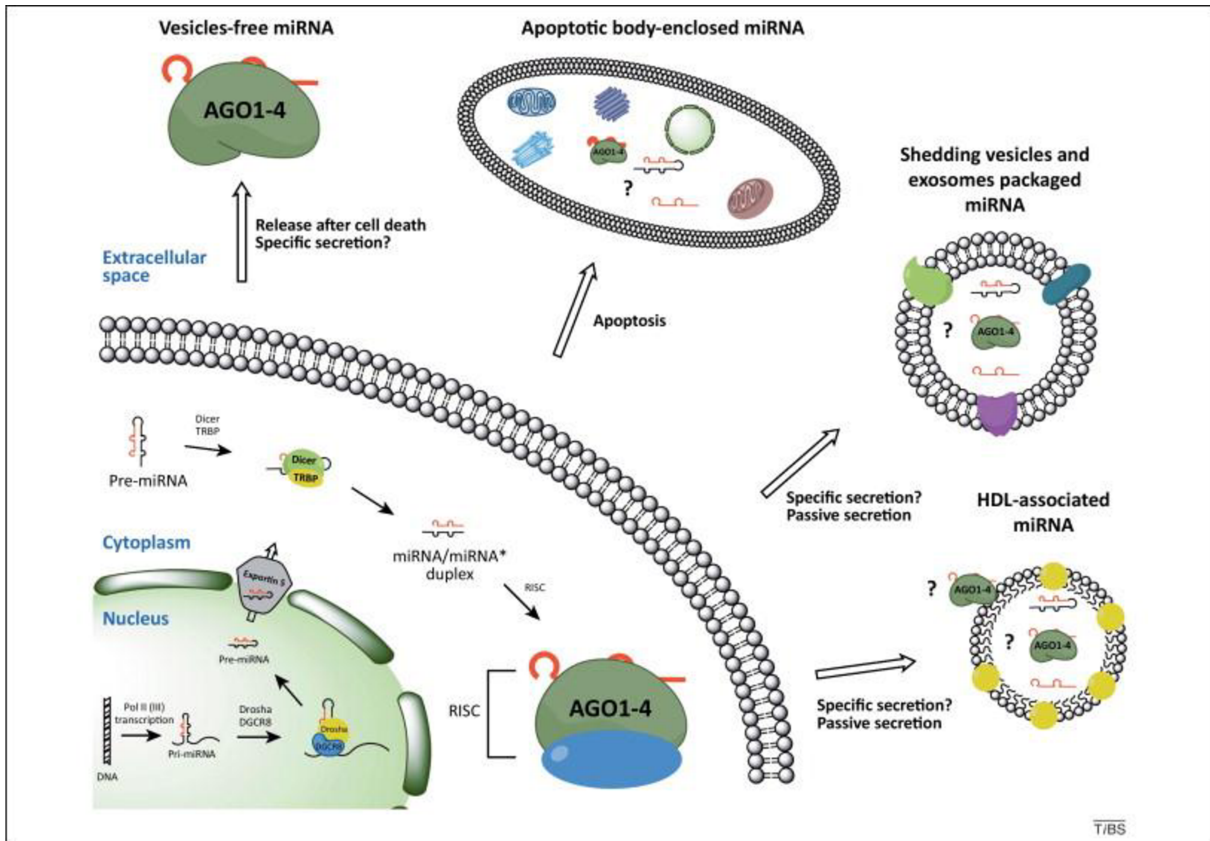


Figure 8. Biogenesis of extracellular microRNAs (Turchinovich et al, 2012).

An ideal biomarker should fulfill many criteria such as accessibility through noninvasive methods, high degree of specificity and sensitivity, ability to detect early stage of disease, long half-life within the sample, and capability for rapid and accurate detection. All these characteristics make the circulating miRNAs promising noninvasive or minimally invasive biomarkers to assess the pathological status of the body, the disease risk and treatments responses. Furthermore, from the point of view of the treatments, extracellular miRNAs may play a role. Many studies, indeed, are focused on the functional role and secretion of miRNA-containing vesicles. Notably, specific miRNA populations can be selectively packed into vesicles under certain pathological conditions. It has been demonstrated that miRNA-containing vesicles are actively secreted in the circulatory system or culture medium after different stimuli (Zhang et al, 2010). However, the mechanisms that control these vesicles are still partially uncovered. One possible mechanism is that the release of exosomal miRNAs may be regulated by a ceramide-dependent secretory mechanism (Kosaka et al, 2010).

Another important issue is the potential of the miRNAs-containing vesicles to be targeted and, thereby, recognized by recipient cells. These vesicles can be internalized by endocytosis, phagocytosis or direct fusion with the cell membrane (Liang et al, 2013). Indeed, it seems that extracellular miRNA-containing vesicles can play a role in the cellular communication system, representing a potential and novel approach to be investigated in the field of drug-delivery and gene therapy. However, prior to clinical translation, the application of exosomes in small RNAs delivery requires further studies aimed to define the strategies of isolation, purification, loading, delivery and the targeting protocols (Liang et al, 2013).

3.3 MicroRNA (dys)regulation in epilepsy

To date, more than 1000 miRNAs have been discovered in human tissues, about 50% of which have been found in the brain. Moreover, miRNAs have been involved in the regulation of various brain functions, many of which are implicated in epilepsy and epileptogenesis, such as neuronal and glial proliferation and differentiation (Dogini et al, 2013; Iyer et al, 2012; Delaloy et al, 2010; Zhao et al, 2009), neuronal migration (Diogini et al, 2013; Gaughwin et al, 2011) and neuronal organization (Diogini et al, 2013; Smrt et al, 2010; Edbauer et al, 2010).

Recently, several studies have investigated miRNAs expression levels in the hippocampus and/or in specific subareas of the hippocampus both in human (Kan et al, 2012; McKiernan et al, 2012; Kaalund et al, 2014) and in experimental models of epilepsy (Hu et al, 2011, 2012; Jimenez-Mateos et al, 2011; Song et al, 2011; McKiernan et al, 2012; Risbud and porter, 2013; Bot et al, 2013; Gorter et al, 2014; Kretschmann et al, 2015). Moreover, extracellular miRNA signatures have been studied in TLE-patients (Wang et al, 2015a,b) and in a rat model of epilepsy (Gorter et al, 2014). Therefore, a deeper comprehension of the role of miRNAs in epileptogenesis and seizures will provide potential diagnostic biomarkers and promising therapeutic targets for epilepsy (Alsharafi et al, 2015). Interestingly, miR-301a-3p was reported as one potential biomarker for drug-resistant epilepsy with high sensitivity and specificity (Wang et al, 2015b). On the other hand, two direct strategies of miRNA-based treatment have been tested: mimics or agomirs have been used to increase levels of specific

miRNAs after a loss of function, whereas inhibitors or antagomirs have been employed to block endogenous miRNAs, increasing the expression of their mRNA targets (Jimenez-Mateos et al, 2011).

3.4 References

Alsharafi WA, Xiao B, Abuhamed MM, Luo Z (2015), miRNAs: biological and clinical determinants in epilepsy. *Front Mol Neurosci*, 8:59.

Bartel DP (2004), MicroRNAs: target recognition and regulatory functions. *Cell*, 136(2):215-33.

Bot AM, Debski KJ, Lukasiuk K (2013), Alterations in miRNA levels in the dentate gyrus in epileptic rats. *PLoS ONE* 8:e76051. doi: 10.1371/journal.pone.0076051.

Chen X, Ba Y, Ma L, Cai X, Yin Y, Wang K, Guo J, Zhang Y, Chen J, Guo X, Li Q, Li X, Wang W, Zhang Y, Wang J, Jiang X, Xiang Y, Xu C, Zheng P, Zhang J, Li R, Zhang H, Shang X, Gong T, Ning G, Wang J, Zen K, Zhang J, Zhang CY (2008), Characterization of microRNAs in serum: a novel class of biomarkers for diagnosis of cancer and other diseases. *Cell Res*, 18:997-1006.

Cocucci E, Racchetti G, Meldolesi J (2009), Shedding microvesicles: srtefacts no more. *Trends Cell Biol*, 19:43-51.

Corsten MF, Dennert R, Jochems S, Kuznetsova T, Devaux Y, Hofstra L, Wagner DR, Staessen JA, Heymans S, Schroen B (2010), Circulating microRNA-208b and microRNA-499 reflect myocardial damage in cardiovascular disease. *Circ Cardiovasc Genet*, 3:499-506.

Delaloy C, Liu L, Lee JA, Su H, Shen F, Yang GY, Young WL, Ivey KN, Gao FB (2010), MicroRNA-9 coordinates proliferation and migration of human embryonic stem cell-derived neural progenitors. *Cell Stem Cell*, 6(4): 323-35. doi: 10.1016/j.stem.2010.02.015.

Dogini DB, Avansini SH, Vieira AS, Lopes-Cendes I (2013), MicroRNA regulation and dysregulation in epilepsy. *Front Cell Neurosci*, 7:1-7.

Dogini DB, Avansini SH, Vieira AS, Lopes-Cendes I (2013), MicroRNA regulation and dysregulation in epilepsy. *Front Cell Neurosci*, 7:172. doi: 10.3389/fncel.2013.00172.

Edbauer D, Neilson JR, Foster KA, Wang CF, Seeburg DP, Batterton MN, Tada T, Dolan BM, Sharp PA, Sheng M (2010), Regulation of synaptic structure and function by FMRP-associated microRNAs miR-125b and miR-132. *Neuron*. 2010 Feb 11;65(3):373-84. doi: 10.1016/j.neuron.2010.01.005.

Gaughwin P, Ciesla M, Yang H, Lim B, Brundin P (2011), Stage-specific modulation of cortical neuronal development by Mmu-miR-134. *Cereb Cortex*, 21(8):1857-69. doi: 10.1093/cercor/bhq262.

Gorter JA, Iyer A, White I, Colzi A, van Vliet EA, Sisodiya S, Aronica E (2014), Hippocampal subregion-specific microRNA expression during epileptogenesis in experimental temporal lobe epilepsy. *Neurobiol Dis*, 62:508-20.

Gregory RI, Chendrimada TP, Shiekhattar R (2006), MicroRNA biogenesis: isolation and characterization of the microprocessor complex. *Methods Mol Biol*, 342: 33-47.

Hu K, Xie YY, Zhang C, Ouyang DS, Long HY, Sun DN, Long LL, Feng L, Li Y, Xiao B (2012), MicroRNA expression profile of the hippocampus in a rat model of temporal lobe epilepsy and miR-34a-targeted neuroprotection against hippocampal neurone cell apoptosis post-status epilepticus. *BMC Neurosci*, 13:115. doi: 10.1186/1471-2202-13-115.

Hwang JY, Aromolaran KA, Zukin RS (2013). Epigenetic mechanisms in stroke and epilepsy. *Neuropsychopharmacol*, 38:167-82.

Iyer A, Zurolo E, Prabowo A, Fluiter K, Spliet WG, van Rijen PC, Gorter JA, Aronica E (2012), MicroRNA-146a: a key regulator of astrocyte-mediated inflammatory response. *PLoS One*, 7(9):e44789. doi: 10.1371/journal.pone.0044789.

Jimenez-Mateos EM, Bray I, Sanz-Rodriguez A, Engel T, McKiernan RC, Mouri G, Tanaka K, Sano T, Saugstad JA, Simon RP, Stallings RL, Henshall DC (2011), MiRNA Expression profile after status epilepticus and hippocampal neuroprotection by targeting miR-132. *Am J Pathol*, 179(5):2519-32.

Kaalund SS, Venø MT, Bak M, Møller RS, Laursen H, Madsen F, Broholm H, Quistorff B, Uldall P, Tommerup N, Kauppinen S, Sabers A, Fluiter K, Møller LB, Nossent AY, Silahatoglu A, Kjems J, Aronica E, Tümer Z (2014), Aberrant expression of miR-218 and miR-204 in human mesial temporal lobe epilepsy and hippocampal sclerosis-convergence on axonal guidance. *Epilepsia*, 55(12):2017-27. doi: 10.1111/epi.12839.

Kan AA, van Erp S, Derijck AA, de Wit M, Hessel EV, O'Duibhir E, de Jager W, Van Rijen PC, Gosselaar PH, de Graan PN, Pasterkamp RJ (2012), Genome-wide microRNA profiling of human temporal lobe epilepsy identifies modulators of the immune response. *Cell Mol Life Sci*, 69(18):3127-45. doi: 10.1007/s00018-012-0992-7.

Khvorova A, Reynolds A, Jayasena SD (2003), Functional siRNAs and miRNAs exhibit strand bias. *Cell*, 115(2):209-16.

Kim VN, Han J, Siomi MC (2009), Biogenesis of small RNAs in animals. *Nat Rev Mol Cell Biol*, 10:126-39.

Kosaka N, Iguchi H, Yoshioka Y, Takeshita F, Matsuky Y, Ochiya T (2010), Secretory mechanisms and intercellular transfer of microRNA in living cells. *J Biol Chem*, 285:17442-52.

Kretschmann A, Danis B, Andonovic L, Abnaof K, van Rikxoort M, Siegel F, Mazzuferi M, Godard P, Hanon E, Fröhlich H, Kaminski RM, Foerch P, Pfeifer A (2015), Different microRNA profiles in chronic epilepsy versus acute seizure mouse models. *J Mol Neurosci*, 55(2):466-79.

Krol J, Sobczak K, Wilczynska U, Drath M, Jasinska A, Kaczynska D, Krzyzosiak WJ (2004), Structural features of microRNA (miRNA) precursors and their relevance to miRNA biogenesis and small interfering RNA/short hairpin RNA design. *J Biol Chem*, 279(40):42230-9.

Laterza OF, Lim L, Garrett-Engele PW, Vlasakova K, Muniappa N, Tanaka WK, Johnson JM, Sima JF, Fare TL, Sistare FD, Glaab WE (2009), Plasma MicrorNAs as sensitive and specific biomarkers of tissue injury. *Clin Chem*, 55:1977-83.

Lewis AP, Jopling CL (2010), Regulation and biological function of the liver-specific miR-122. *Biochem Soc Trans*, 38:1553-7.

Liang H, Gong F, Zhang S, Zhang CY, Zen K, Chen Xi (2013), The origin, function, and diagnostic potential of extracellular microRNAs in human body fluids. *WIREs RNA*, doi: 10.1002/wrna.1208.

Mathivanan S, Ji H, Simpson RJ (2010), Exosomes: extracellular organelles important in intracellular communication. *J Proteomics*, 73:1907-20.

McKiernan RC, Jimenez-Mateos EM, Bray I, Engel T, Brennan GP, Sano T, Michalak Z, Moran C, Delanty N, Farrell M, O'Brien D, Meller R, Simon RP, Stallings RL, Henshall

DC (2012), Reduced mature microRNA levels in association with dicer loss in human temporal lobe epilepsy with hippocampal sclerosis. *PLoS One*, 7(5):e35921. doi: 10.1371/journal.pone.0035921.

McKiernan RC, Jimenez-Mateos EM, Sano T, Bray I, Stallings RL, Simon RP, Henshall DC (2012), Expression profiling the microRNA response to epileptic preconditioning identifies miR-184 as a modulator of seizure-induced neuronal death. *Exp Neurol*, 237(2):346-54.

Mitchell PS, Parkin RK, Kroh EM, Fritz BR, Wyman SK, Pogosova-Agadjanyan EL, Peterson A, Noteboom J, O'Briant KC, Allen A, Lin DW, Urban N, Drescher CW, Knudsen BS, Stirewalt DL, Gentleman R, Vessella RL, Nelson PS, Martin DB, Tewari M (2008), Circulating microRNAs as stable blood-based markers for cancer detection. *Proc Natl Acad Sci USA*, 105:10513-18.

Palaez N, Carthew RW (2012), Biological robustness and the role of MicroRNAs: a network perspective. *Curr Top Dev Biol*, 99:237-55.

Pasquinelli AE (2012), MicroRNAs and their targets: recognition, regulation and an emerging reciprocal relationship. *Nat Rev Gen*, 13:271-82.

Qureshi IA, Mehler MF (2012), Emerging roles of non-coding RNAs in brain evolution, development, plasticity and disease. *Nat Rev Neurosci*, 13:528-41.

Ratajczak J, Wysoczynsky M, Hayek F, Janowska-Wieczorek A, Ratajczak MZ (2006), Membrane-derived microvesicles: important and underappreciated mediators of cell-to-cell communication. *Leukemia*, 20:1487-95.

Risbud RM, Porter BE (2013), Changes in microRNA expression in the whole hippocampus and hippocampal synaptoneurosome fraction following pilocarpine induced status epilepticus. *PLoS One*, 8(1):e53464. doi: 10.1371/journal.pone.0053464.

Schwarz DS, Hutvagner G, Du T, Xu Z, Aronin N, Zamore PD (2003), Asymmetry in the assembly of the RNAi enzyme complex. *Cell*, 115(2): 199-208.

Siegel G, Saba R, Schratt G (2011), microRNAs in neurons: manifold regulatory roles at the synapse. *Curr Opin Genet Dev*, 21:491-7.

Simons M, Raposo G (2009), Exosomes-vesicular carriers for intercellular communication. *Curr Opin Cell Biol*, 21:575-81.

Skog J, Wurdiger T, van Rijn S, Meijer DH, Gainche L, Sena-Esteves M, Curry WT, Carter BS, Brichevsky AM, Breakefield XO (2008), Glioblastoma microvesicles transport RNA and proteins that promote tumor growth and provide diagnostic biomarkers. *Nat Cell Biol*, 10:1470-6.

Smrt RD, Szulwach KE, Pfeiffer RL, Li X, Guo W, Pathania M, Teng ZQ, Luo Y, Peng J, Bordey A, Jin P, Zhao X (2010), MicroRNA miR-137 regulates neuronal maturation by targeting ubiquitin ligase mind bomb-1. *Stem Cells*, 28(6):1060-70. doi: 10.1002/stem.431.

Song YJ, Tian XB, Zhang S, Zhang YX, Li X, Li D, Cheng Y, Zhang JN, Kang CS, Zhao W (2011), Temporal lobe epilepsy induces differential expression of hippocampal miRNAs including let-7e and miR-23a/b. *Brain Res*, 1387:134-40.

Thery C, Zitvogel L, Amigorena S (2002), Exosomes: composition, biogenesis and function. *Nat Rev Immunol*, 2:569-79.

Turchinovich A, Weiz L, Burwinkel B (2012), Extracellular miRNAs: the mystery of their origin and function. *Trends Biochem Sci*. 37(11):460-5.

Valadi H, Ekstrom K, Bossios A, Sjostrand M, Lee JJ, Lotvall JO (2007), Exosome-mediated transfer of mRNAs and microRNAs as a novel mechanism of genetic exchange between cells. *Nat Cell Biol*, 9:654-9.

Vickers KC, Palmisano BT, Shoucri BM, Shamburek RD, Remaley AT (2011), MicroRNAs are transported in plasma and delivered to recipient cells by high-density lipoproteins. *Nat Cell Biol*, 13:423-33.

Wang J, Tan L, Tan L, Tian Y, Ma J, Tan CC, Wang HF, Liu Y, Tan MS, Jiang T, Yu JT (2015b), Circulating microRNAs are promising novel biomarkers for drug-resistant epilepsy. *Sci Rep*. 5:10201. doi: 10.1038/srep10201.

Wang J, Yu JT, Tan L, Tian Y, Ma J, Tan CC, Wang HF, Liu Y, Tan MS, Jiang T, Tan L (2015a), Genome-wide circulating microRNA expression profiling indicates biomarkers for epilepsy. *Sci Rep*, 5:9522. doi: 10.1038/srep09522.

Winter J, Jung S, Keller S, Gregory RI, Diederichs S (2009), Many roads to maturity: microRNA biogenesis pathways and their regulation. *Nat Cell Biol*. 11(3):228-34.

Zhang Y, Jia Y, Zheng R, Guo Y, Wang Y, Guo H, Fei M, Sun S (2010), Plasma microRNA-122 as a biomarker for viral, alcohol-, and chemical-related hepatic diseases. *Clin Chem*, 56:1830-8.

Zhang Y, Liu D, Chen X, Li J, Li L, Bian Z, Sun F, Lu J, Yin Y, Cai X, Sun Q, Wang K, Ba Y, Wang Q, Wang D, Yang J, Liu P, Xu T, Yan Q, Zhang J, Zen K, Zhang CY (2010), Secreted monocytic miR-150 enhances targeted endothelial cell migration. *Mol Cell*, 39:133-44.

Zhao C, Sun G, Li S, Shi Y (2009), A feedback regulatory loop involving microRNA-9 and nuclear receptor TLX in neural stem cell fate determination. *Nat Struct Mol Biol*, 16: 365-71.



Identification of miRNAs Differentially Expressed in Human Epilepsy with or without Granule Cell Pathology

Silvia Zucchini^{1,2,3,9}, Gianluca Marucci^{4,9}, Beatrice Paradiso^{1,2,5}, Giovanni Lanza⁵, Paolo Roncon^{1,2}, Pierangelo Cifelli^{1,6}, Manuela Ferracin^{3,7}, Marco Giulioni⁸, Roberto Michelucci⁹, Guido Rubboli^{9,10,¶}, Michele Simonato^{1,2,3,¶*}

1 Department of Medical Sciences, Section of Pharmacology and Neuroscience Center, University of Ferrara, Ferrara, Italy, **2** National Institute of Neuroscience, Torino, Italy, **3** Laboratory for Technologies of Advanced Therapies (LTAA), University of Ferrara, Ferrara, Italy, **4** Department of Biomedical and NeuroMotor Sciences (DiBiNeM), Section of Pathology, Bellaria Hospital, Bologna, Italy, **5** Department of Morphology, Surgery and Experimental Medicine, Section of Pathology, University of Ferrara, Ferrara, Italy, **6** Ri.MED Foundation, Palermo, Italy, **7** Department of Morphology, Surgery and Experimental Medicine, Section of Pathology, Oncology and Experimental Biology, University of Ferrara, Ferrara, Italy, **8** IRCCS Institute of Neurological Sciences, Section of Neurosurgery, Bellaria Hospital, Bologna, Italy, **9** IRCCS Institute of Neurological Sciences, Section of Neurology, Bellaria Hospital, Bologna, Italy, **10** Danish Epilepsy Center, Epilepsihospital, Dianalund, Denmark

Abstract

The microRNAs (miRNAs) are small size non-coding RNAs that regulate expression of target mRNAs at post-transcriptional level. miRNAs differentially expressed under pathological conditions may help identifying mechanisms underlying the disease and may represent biomarkers with prognostic value. However, this kind of studies are difficult in the brain because of the cellular heterogeneity of the tissue and of the limited access to fresh tissue. Here, we focused on a pathology affecting specific cells in a subpopulation of epileptic brains (hippocampal granule cells), an approach that bypasses the above problems. All patients underwent surgery for intractable temporal lobe epilepsy and had hippocampal sclerosis associated with no granule cell pathology in half of the cases and with type-2 granule cell pathology (granule cell layer dispersion or bilamination) in the other half. The expression of more than 1000 miRNAs was examined in the laser-microdissected dentate granule cell layer. Twelve miRNAs were differentially expressed in the two groups. One of these, miR487a, was confirmed to be expressed at highly differential levels in an extended cohort of patients, using RT-qPCR. Bioinformatics searches and RT-qPCR verification identified ANTXR1 as a possible target of miR487a. ANTXR1 may be directly implicated in granule cell dispersion because it is an adhesion molecule that favors cell spreading. Thus, miR487a could be the first identified element of a miRNA signature that may be useful for prognostic evaluation of post-surgical epilepsy and may drive mechanistic studies leading to the identification of therapeutic targets.

Citation: Zucchini S, Marucci G, Paradiso B, Lanza G, Roncon P, et al. (2014) Identification of miRNAs Differentially Expressed in Human Epilepsy with or without Granule Cell Pathology. PLoS ONE 9(8): e105521. doi:10.1371/journal.pone.0105521

Editor: Giuseppe Biagini, University of Modena and Reggio Emilia, Italy

Received: May 8, 2014; **Accepted:** July 22, 2014; **Published:** August 22, 2014

Copyright: © 2014 Zucchini et al. This is an open-access article distributed under the terms of the Creative Commons Attribution License, which permits unrestricted use, distribution, and reproduction in any medium, provided the original author and source are credited.

Data Availability: The authors confirm that all data underlying the findings are fully available without restriction. All relevant data are within the paper.

Funding: This work has been supported by grants from the European Community [FP7-PEOPLE-2011-IAPP project 285827 (EPIXCHANGE) and FP7-HEALTH project 602102 (EPITARGET), to MS], and from the Ri.MED foundation (to PC). The funders had no role in study design, data collection and analysis, decision to publish, or preparation of the manuscript.

Competing Interests: The authors have declared that no competing interests exist.

* Email: michele.simonato@unife.it

¶ These authors contributed equally to this work.

¶ These authors are joint senior authors on this work.

¶ Current address: Institute of Clinical Medicine, University of Copenhagen, Copenhagen, Denmark

Introduction

The microRNAs (miRNAs) are small size endogenous non-coding RNAs that regulate the expression of target mRNAs at post-transcriptional level [1]. To date, more than 1000 human miRNAs have been identified, about 50% of which are expressed in the brain. miRNAs have been demonstrated to be involved in several brain functions, many of which may be implicated in epilepsy and epileptogenesis, like cell death, neurogenesis, synaptic plasticity [2],[3]. Indeed, silencing miR-134 using a specific antagomir exerted prolonged seizure-suppressant and neuroprotective actions in a murine model [4]. Thus, understanding which specific miRNAs are differentially expressed in epilepsy may help to identify the mechanisms underlying the disease. Moreover,

differentially expressed miRNAs may represent biomarkers that identify specific subpopulations of epileptic patients, holding a prognostic value [5].

Microarray platforms allow screening and identifying miRNAs differentially expressed under pathological conditions. Experimental studies have profiled miRNA expression in animal models of epilepsy [6],[7],[8],[9] and profiling studies have been also recently published using hippocampi resected from temporal lobe epilepsy (TLE) patients [10],[11]. However, some outstanding obstacles make difficult the interpretation of data from microarray analysis of human brain samples. First, in most studies tissue is derived from autopsies or, potentially even worse, pathological tissue is from surgery samples and control tissue from autopsies.

Post-mortem modifications are very likely to dramatically alter the molecular composition of the tissue, making the results questionable. Second, each brain area has a specific and complex cellular composition that changes (often markedly) in the course of diseases. Again, this makes interpretation of molecular data very difficult, because analysis of heterogeneous tissue homogenates does not allow identification of the cells where changes occur and because up-regulation of a molecule in one cell population may be obscured by down-regulation in another cell population.

One approach to overcome these problems is focusing on a well-defined cell population. For example, we focused here on a TLE-associated pathology of the granule cells of the hippocampus. Drug-resistant TLE is the most common type of epilepsy requiring surgical treatment, with a favorable postsurgical outcome in 60–70% of the patients. Based on the underlying etiology, TLE subtypes with different surgical prognosis have been described. Neuropathological classifications of epileptogenic lesions, including focal cortical dysplasias (FCD) [12], hippocampal sclerosis (HS) [13] and granule cell pathology (GCP) [14], define histopathological features and subtypes, allowing attempts to correlate clinical and pathological findings. Correlations with molecular markers, however, are still unavailable.

All patients included in this study underwent surgery for pharmacoresistant TLE and had HS type 1 [13]. All were similar for age, gender, clinical features of the disease. The most relevant difference was that half of the patients had no granule cell pathology (no GCP), whereas the other half had granule cell dispersion or bilamination (GCP type 2) [14], i.e. the single differential pathological feature was in a specific, isolable cell population. Therefore, the granule cell layer was laser-microdissected from all samples, total RNA was extracted from dissected tissues and the miRNAome profile was obtained using a miRNA microarray.

Materials and Methods

Patients

This study was approved by the Ethics Committee of Bologna (full name: *Comitato Etico Indipendente dell'Azienda USL della Città di Bologna*). A comprehensive written informed consent (also approved by the Ethics Committee of Bologna) was signed for the surgical treatment that produced the tissue samples, the related diagnostic procedures and the research use. All information regarding the human material used in this study was managed using anonymous numerical codes and samples were handled in compliance with the Helsinki declaration (<http://www.wma.net/en/30publications/10policies/b3/>).

Fourteen drug-resistant TLE patients candidate to epilepsy surgery were collected at the Epilepsy Surgery Center of the IRCCS Institute of Neurological Sciences of Bologna. All patients underwent detailed epileptological evaluation and wakefulness/sleep EEG. All patients also underwent continuous (24 hours) long-term video-EEG monitoring for seizure recording. Analysis of ictal clinical and EEG semiology and electroclinical correlations aimed to identify the epileptogenic area were performed.

Three Tesla MRI, and brain CT scan when necessary, were carried out. Electroclinical, neuroimaging, and neuropsychological data were discussed by the Epilepsy Surgery Team (epileptologists, neuroradiologists, neuropsychologists, neurosurgeons) to establish the site of the epileptogenic area and the surgical strategy.

Surgery

All patients underwent tailored temporal lobe resection to remove the epileptogenic area, according to the data obtained

during pre-surgical investigation. Essentially, surgery consisted of removing the temporal pole, the anterior neocortical lateral cortex, the uncus-entorhinal area and the hippocampus and parahippocampal gyrus. The main surgical specimens (hippocampus and/or temporal pole) were removed “en bloc” and spatially oriented to allow a proper histopathological examination.

Histology and microdissection

Specimens were formalin fixed and paraffin embedded. They were de-waxed using Bio-Clear (Bio-Optica, Milan, Italy), washed in ethanol and stained with hematoxylin and eosin for histological diagnosis. Neuropathological evaluation was performed using the most recent classifications of HS, GCP and FCD [12],[13],[14], applying the recommended histochemical and immunohistochemical stains. Specimens either displayed no GCP or GCP type 2. Four different types of neuropathological features can define GCP type 2: 1) dispersion: rows of granule cells spread into the molecular layer and the distance between granule cells is increased; 2) ectopic granule cells: single ectopic granule cells are dispersed into the molecular layer; 3) clusters: ectopic granule cells form clusters within the molecular layer; 4) bilaminar: two granule cell layers, separated by a cell-free gap [14]. While patterns of granule cell loss (thinning and/or cell free gaps, GCP 1) occur isolated, patterns of architectural abnormalities (GCP 2) can come along with cell loss. Therefore, only sections in which no cell loss was detected (based on NeuN staining) were included in analysis.

Ten-micron-thick sections were cut using a microtome and the dentate granule layer of the dentate gyrus was laser-dissected (**Fig. 1**) using the SL microcut microtest dissector (Nikon, Tokyo, Japan). Microdissected cells were captured in microcut transfer film (Nikon). Granule cells were collected in this manner from at least 3–4 slices per patient, in order to obtain an adequate quantity of RNA. Material from all sections of the same patient was pooled together, and total RNA extracted using an RNA purification kit (RecoverAll Total Nucleic Acid Isolation Kit, Ambion Life Technologies, CA, USA). Approximately 1.5 µg total RNA were obtained from each patient. Since miRNAs are more stable than mRNAs, they can be used for microarray analysis from formalin-fixed paraffin-embedded tissues [15]. We performed quality control checks on microarray hybridizations using the Agilent quality control (QC) tool in the Feature Extraction software. All samples passed the QC check.

Microarray

Total RNA was used for microarray analysis (Human micro-RNA Microarray V3, #G4470C, Agilent Technologies, Santa Clara, CA, USA). This chip consists of 60-mer DNA probes and allows simultaneous analysis of almost 1200 human miRNA obtained from the Sanger miR-BASE database (Release 10.1). We employed approximately 100 ng total RNA per sample in each experiment. RNA labeling and hybridization were performed in accordance to manufacturer's indications. Agilent scanner and the Feature Extraction 10.5 software (Agilent Technologies) were used to obtain the microarray raw-data.

Microarray results were analyzed using the GeneSpring GX 12 software (Agilent Technologies). Data transformation was applied to set all the negative raw values at 1.0, followed by Quantile normalization and log₂ transformation. Filters on gene expression were used to keep only the miRNAs detected in at least one sample (n = 536). The number of expressed miRNAs was 493 in the no GCP group, 464 in the GCP 2 group. Differentially expressed miRNAs were identified by comparing GCP type 2 vs. no GCP samples. A 2 fold-change filter (n = 141) and the unpaired t-test were applied (p < 0.05; False Discovery Rate-FDR = 7%). Differ-

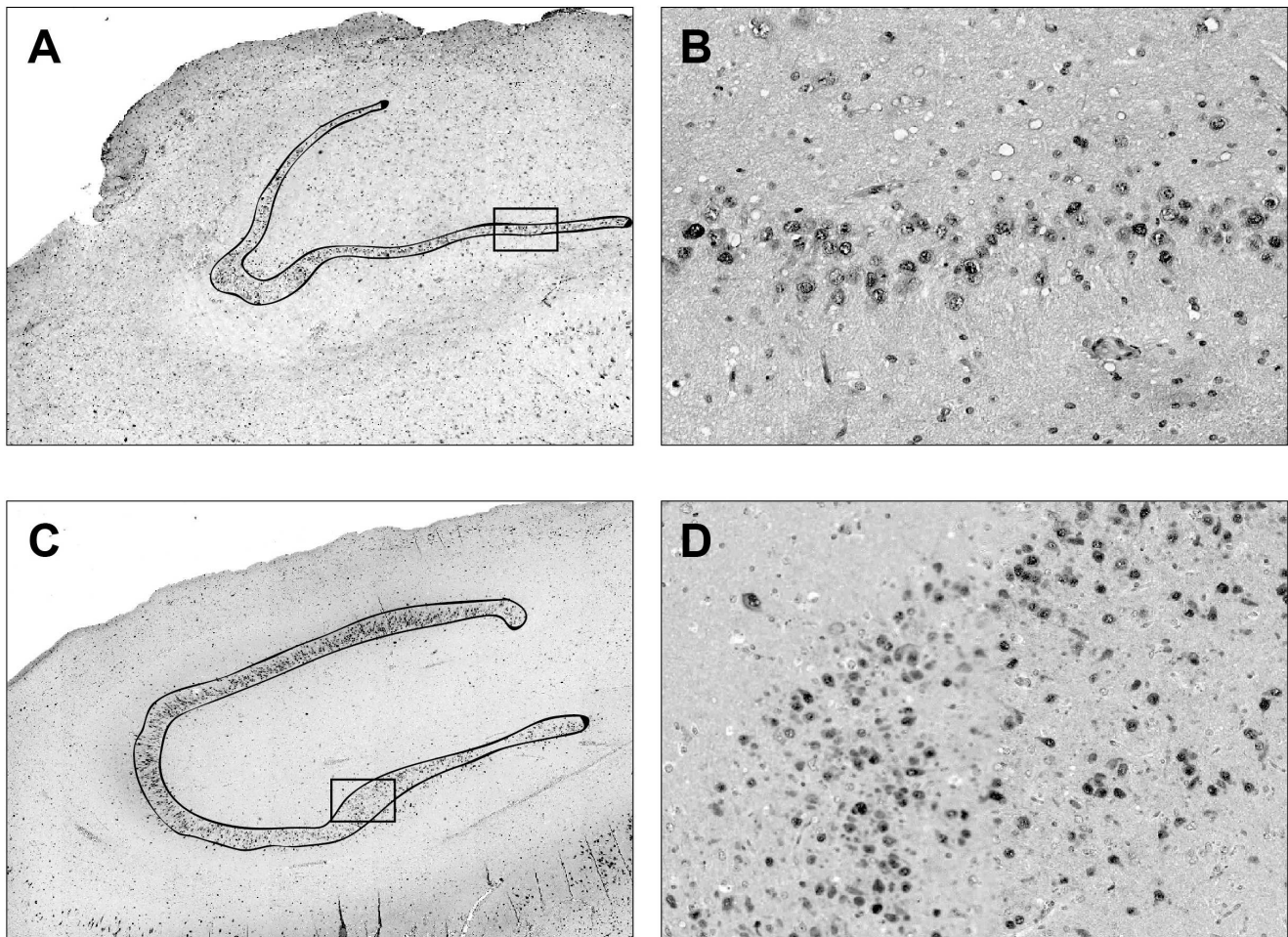


Figure 1. Laser microdissection of the human granule cell layer. Neu-N stained hippocampal sections prepared from a patient without granule cell pathology (A) and a patient with granule cell dispersion, i.e. type 2 granule cell pathology (C). The dissection line is in black. (B) and (D) are higher magnifications of the boxes in (A) and (C), respectively.
doi:10.1371/journal.pone.0105521.g001

entially expressed genes were employed in Cluster Analysis, using the Pearson correlation as a measure of similarity. For Cluster image generation, an additional step of normalization on gene median across all samples was added.

miRNA qRT-PCR

Quantitative real-time PCR (qRT-PCR) analysis of hsa-miR-338-3p, 219-5p and 487a was performed using a TaqMan miRNA assay kit (Applied Biosystems) according to the manufacturer's instructions. Samples were run in triplicate at 95°C for 15 s and 60°C for 1 min using a CFX96 Touch Real-Time PCR Detection System (Applied Biosystems). Analysis was performed by the comparative threshold cycle (CT) method. rRNA U48 was used as reference gene. The relative amount of each miRNA in epileptic samples was calculated using the equation $RQ = 2^{-CT}$, where $CT = (CT_{miRNA} - CT_{U6 RNA})$. Similar results were obtained using rRNA U6 as reference gene.

Bioinformatics

Target prediction was performed by comparative analysis of several databases, using an open-source database [16].

ANTXR1 qRT-PCR

mRNA levels of *antrax receptor 1* (ANTXR1) (assay ID: Hs01120394) and *neuronal enolase 2* (ENO 2) (assay ID: Hs01102367), were determined using TaqMan Real-Time PCR, according to manufacturer's instructions (Applied Biosystems). Ten ng of total RNA were retro-transcribed using iScript Reverse Transcription Supermix (BIO-RAD). cDNA templates were amplified with TaqMan PreAmp Master Mix (Applied Biosystems), using pooled assay mix for ANTXR1 and ENO 2 and then assayed for gene expression as described previously. Each sample was analyzed in triplicate, in two independent experiments. The level of each mRNA was measured using Ct (threshold cycle) and the amount of target was calculated as described above for miRNAs. Gene expression levels were normalized using ENO 2 expression, as reported previously for this particular tissue [17].

ANTXR1 immunohistochemistry

ANTXR1 immunostaining was performed by an automatic and clinically validated instrument based on Ventana Benchmark Ultra systems from Roche Tissue Diagnostics. This immunohistochemistry technique takes advantage of a new enhanced sensitivity biotin-free multimer technology system, based on direct linkers between peroxidase and secondary antibodies (ultraView

Universal DAB Detection Kit, Ventana Medical System). The protocol provided for the automatic CC1 Ventana pre-treatment (Cell Conditioning Solution, Ventana) for 52 min, then the incubation for 2 hours with the anti-ANTXR1 antibody by titration (rabbit polyclonal, by ThermoFisher Scientific; 1: 100). Staining was visualized with the UltraView DAB procedure by Benchmark Ultra System. Sections were then counterstained with haematoxylin. Negative controls were treated identically except that the primary antibody was omitted. Sections of metastatic breast cancer were used as positive controls [18],[19]. Evaluation of data was performed by two expert neuropathologists (GM and BP) under double-blind conditions.

Statistical analysis

For qRT-PCR data, comparisons between experimental groups were performed by using the Mann–Whitney U test. Differences between groups were considered significant when $P < 0.05$.

Results

Patients

Tissues from patients indicated in numbers in **Table 1** were employed for microarray analysis. Neuropathological examination evidenced that these patients had HS type 1 [13], which was associated with no granule cell pathology (no GCP) in 5 patients and with granule cell pathology (GCP type 2) in the other 5 [14]: GCP consisted of granule cell dispersion in 4 cases and bilaminar granule cell layer in one. The no GCP group was composed of 3 males and 2 females, with mean age at surgery of 44 (33–60), mean years after epilepsy diagnosis of 24 (7–38) and approximately 10 seizures per month before surgery (2 to >30); the GCP group was composed of 5 females, with mean age at surgery of 33 (31–37), mean years after epilepsy diagnosis of 23 (10–35) and approximately 10 seizures per month before surgery (3 to 15). An epileptogenic insult could be identified in only one of the no GCP cases (febrile convulsions), whereas all GCP cases had a history of febrile convulsions, one also a possible brain trauma (**Table 1**).

miRNA microarray

Twelve miRNAs were differentially expressed in patients without GCP compared with patients with type 2 GCP (**Fig. 2**). Of these, 6 had relatively higher expression in tissue from patients without GCP and 6 were higher in those with GCP 2 (**Fig. 2**). Differential expression of a subset of 3 miRNAs (namely miR-338-3p, miR-219-5p and miR-487a) was validated in an extended cohort of patients (the ten original patients plus another 2 per group, indicated in roman numbers in **Table 1**) using qRT-PCR. Expression levels of all these miRNAs were apparently different in the two groups, confirming microarray findings, but data were dispersed for miR-338-3p and miR-219-5p, not reaching significance level (**Fig. 3A and 3B**). In contrast, miR-487a expression was confirmed to be highly significantly reduced in GCP 2 (**Fig. 3C**).

Target identification and validation for miR-487a

Comparative analysis of several databases [16] indicated at least 10 highly likely targets for miR-487a, namely FAM126A, ANTXR1, NUDCD1, AP1S3, AP3D1, AFTPH, KIAA1217, ZNF57, PAG1 and PTGER3. All these mRNAs are expressed in the brain (www.genecards.org). A subset of these are associated with vesicle trafficking (AP1S3, AP3D1, AFTPH), others code for receptors (PTGER3), intracellular signaling (FAM126A) or transcription factors (ZNF57; www.genecards.org). More interestingly, two of these mRNAs (PAG1 and ANTXR1) may be

associated with cell adhesion (www.genecards.org). In particular, ANTXR1 (also known as *tumor endothelial marker 8*, TEM8) is expressed in the mouse dentate gyrus granule cell layer (Allen atlas; <http://mouse.brain-map.org/gene/show/45380>) and has been reported to promote cell spreading in human tumor tissues [20],[21]: therefore, it was hypothesized that reduced expression of miR487a will increase ANTXR1 levels, leading to granule cell spreading (i.e. dispersion or bilamination, i.e. GCP 2).

Evidence in support of this hypothesis has been pursued by analyzing ANTXR1 mRNA and protein levels in the same samples employed for validation of miR-487a. As predicted, using qRT-PCR ANTXR1 mRNA levels were increased in the GCP 2 group (**Fig. 4A**). Moreover, a clear increase of ANTXR1 immunoreactivity was observed in the granule cell layer of patients with type-2 GCP, as compared with those with no GCP (**Fig. 4B–C**).

Discussion

The main findings of this study were: (1) the identification of 12 miRNAs differentially expressed in the hippocampal granule cell layer of patients with hippocampal sclerosis associated with GCP 2 as compared with patients with no GCP; (2) the RT-qPCR confirmation of one of these, miR-487a, in an extended cohort of patients; (3) the identification of ANTXR1 as a possible target of miR-487a.

An important issue in evaluation of this data is the possible influence of medical treatments on miRNA expression. Indeed, there is evidence that antiepileptic drugs can interfere with miRNA expression: it has been reported that valproate can modulate miR-24, miR-34a, and miR-128 [22] and that phenobarbital can down-regulate miR-122 [23]. Although two patients in the no-GCP group were treated with valproate and five patients (three in the no-GCP group and two in the GCP 2 group) were treated with phenobarbital, none of the above miRNAs was found to be differentially expressed. More in general, a systematic bias due to pharmacological treatments seems unlikely, because all patients in both groups were using many drugs in combination. Therefore, although we cannot rule out an influence of the antiepileptic treatment on miRNAs expression, it seems more likely that the changes we observed are due to the pathology.

The prognosis of patients undergoing epilepsy surgery has been hypothesized to depend on the absence or presence of GCP but, thus far, results have been inconsistent. While some studies reported that GCP does not affect post-surgical outcome [24],[25], others suggested association between GCP and a favorable prognosis [14],[26]. Identification of molecular biomarkers that parallel and/or integrate the pathology findings would provide a valuable prognostic element, and miR-487a may represent a first component of this molecular signature that will allow better patient stratification. In the cohort of patients we analyzed in this study, however, no clear distinction of the outcome was observed in the early timeframe of post-surgical follow-up. Therefore, extension of the follow-up will be needed to verify this possibility.

MiR-487a has been reported to be down-regulated in Alzheimer disease [27] and up-regulated in schizophrenia [28]. Could it play a role in GCP? All miRNAs can have hundreds of targets, but target prediction based bioinformatics approaches is difficult for many reasons, most of all because of imperfect complementarity. However, comparative analysis of several databases [16] indicates at least 10 highly likely targets for miR-487a. ANTXR1 emerged as the most interesting, because it has been reported to promote cell spreading: ANTXR1 is a transmembrane protein that functions as an adhesion molecule,

Table 1. Patients included in the study.

Patient number	Gender	Age at surgery	Epileptogenic insult	Years after diagnosis	Seizures per month	Drug therapy (current)	Pathology MTS [29]	Pathology MTS [30]	Pathology GCP [14]	Outcome [31]
01	M	60	none	38	>30	VPA, CBZ, TGB	Grade IV	MTS 1B	no GCP	Ia
02	M	44	none	12	5–9	TPM, LVT	Grade III	MTS 1A	no GCP	Ia
03	M	36	none	7	8–10	LVT, PB, CLB	Grade III	MTS 1A	no GCP	Ia
04	F	47	none	33	2–3	PB, CBZ	Grade III	MTS 1A	no GCP	Ic
05	F	33	febrile convulsions	30	5–10	TPM, CBZ, VPA, PB	Grade III	MTS 1A	no GCP	Ia
I	M	55	none	51	10–15	OXC, LTG, CLB	Grade III	MTS 1A	no GCP	Ia
II	F	31	none	16	3–4	CBZ, ZNS	Grade III	MTS 1A	no GCP	Ia
06	F	31	febrile convulsions	10	8–12	PB, TPM	Grade III	MTS 1A	GCP 2	Ila
07	F	33	febrile convulsions	24	3–4	LTG, LVT, PB	Grade III	MTS 1A	GCP 2	Ia
08	F	32	febrile convulsions	27	4–10	CBZ	Grade III	MTS 1A	GCP 2	Ia
09	F	32	febrile conv. (trauma?)	20	9–10	OXC, LVT	Grade IV	MTS 1B	GCP 2	Ia
10	F	37	febrile convulsions	35	12–15	CBZ, TPM	Grade IV	MTS 1B	GCP 2	Ia
III	F	41	febrile convulsions	38	3–4	CBZ, PGB	Grade III	MTS 1A	GCP 2	Ia
IV	M	36	febrile convulsions	22	5–6	TPM, LVT	Grade III	MTS 1A	GCP 2	Ia

CBZ, carbamazepine; CLB, clobazam; LTG, lamotrigine; LVT, levetiracetam; OXC, oxcarbazepine; PB, pentobarbital; TGB, tiagabine; TPM, topiramate; VPA, valproic acid.
doi:10.1371/journal.pone.0105521.t001

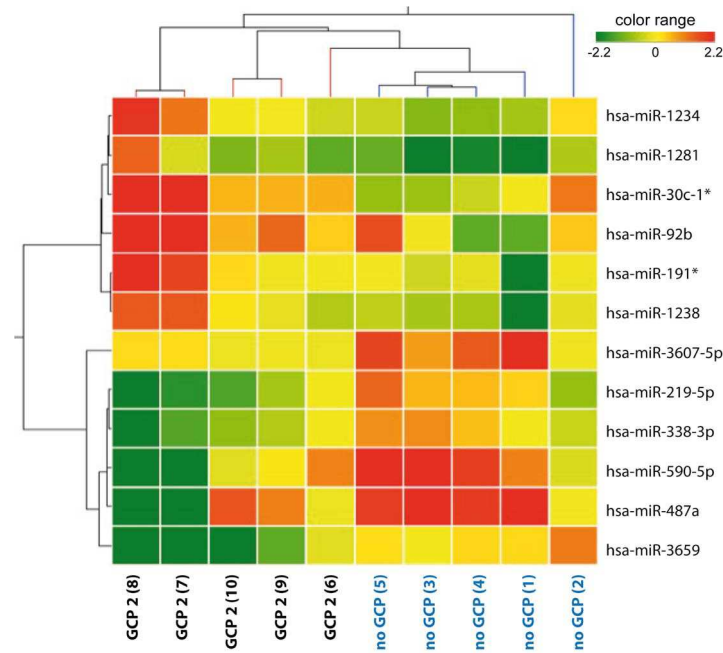


Figure 2. miRNAs differentially expressed in patients without granule cell pathology (no GCP) or with type 2 GCP (GCP 2). Heat-map representation of the average expression of the 12 differentially expressed miRNAs in no GCP and GCP 2 from ten different tissues. The colors of the genes represented on the heat map correspond to the expression values normalized on miRNA mean expression across all samples: green indicates down-regulated; red indicates up-regulated in the tissue. Patients are identified by numbers (in parenthesis) that correspond to those reported in the Table 1.

doi:10.1371/journal.pone.0105521.g002

coupling binding of an immobilized extracellular ligand and cell spreading through association to the actin cytoskeleton [20]. Thus, reduced expression of miR-487a could increase ANTXR1 mRNA and protein levels and thereby favor granule cell dispersion. Here, we have provided circumstantial evidence that this could indeed

be the case. Further studies in vitro and in animal models are currently ongoing to directly demonstrate this hypothesis.

In conclusion, miR-487a may be the first identified element of a miRNA signature that may be useful for a prognostic evaluation of post-surgical epilepsy and form the basis for mechanistic studies

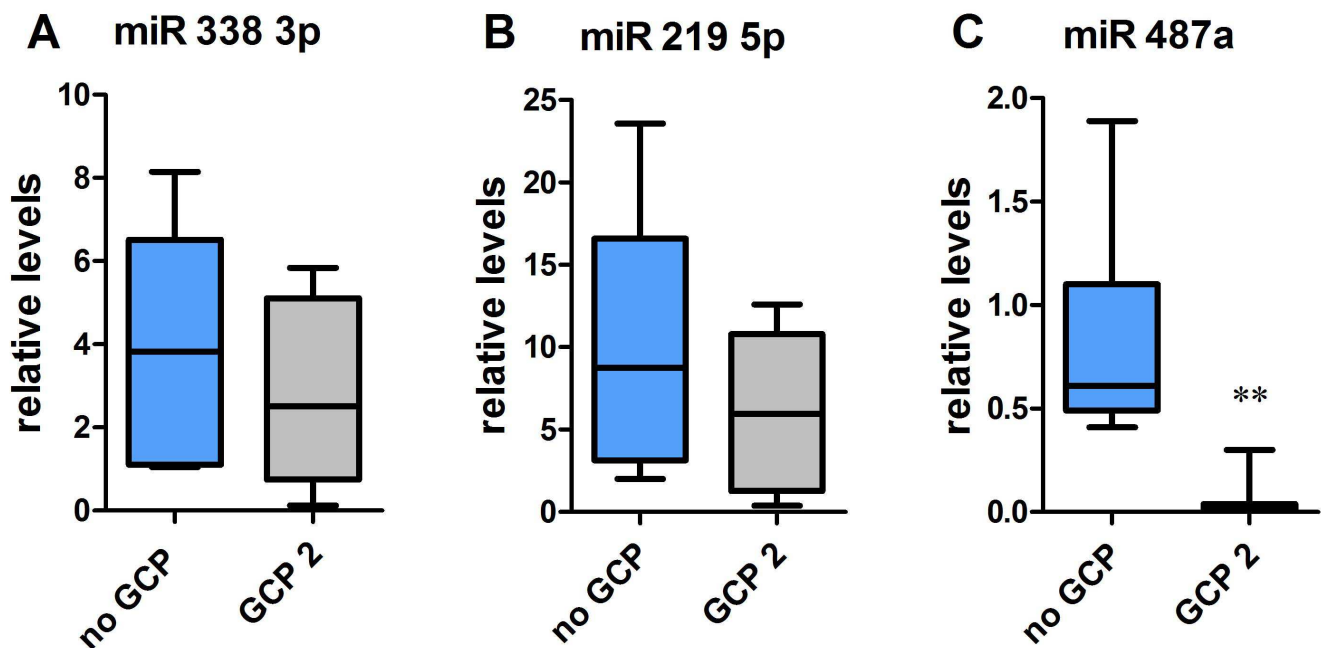


Figure 3. Relative expression of miR-338-3p (A), miR-219-5p (B) and miR-487a (C), evaluated by qRT-PCR in patients without granule cell pathology (no GCP, blue bars) or with type-2 GCP (black bars). Seven patients per group. **P<0.01 Mann-Whitney U test.

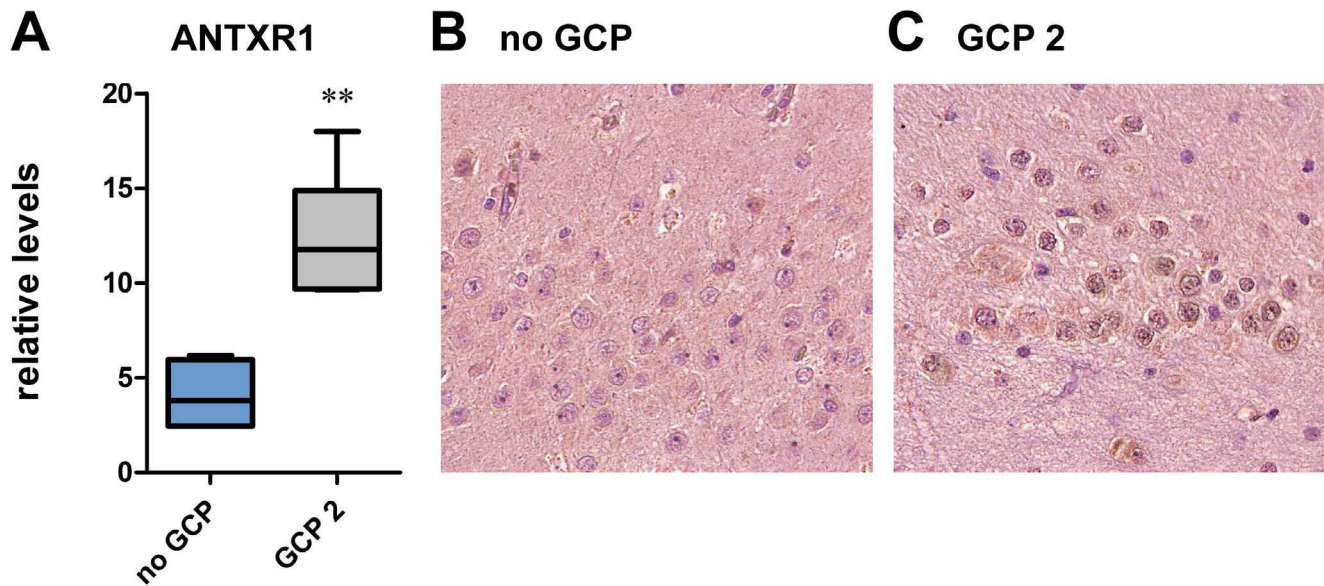


Figure 4. Relative expression of ANTXR1 (A), evaluated by qRT-PCR, in patients without granule cell pathology (no GCP, blue bars) or with type-2 GCP (black bars). Seven patients per group. $**P < 0.01$ Mann-Whitney U test. Representative granule cell layer hippocampal sections from patients without granule cell pathology (B) or with type-2 GCP (C) exhibiting DAB-labeled ANTXR1-like immunoreactivity (LI). Omitting the primary antibody to estimate nonspecific signal yielded completely negative labeling (data not shown). Note a widespread increase in ANTXR1-LI in granule cells from patients with type-2 GCP (C).
doi:10.1371/journal.pone.0105521.g004

that may lead to the identification of new therapeutic targets, like ANTXR1.

Acknowledgments

The authors are grateful to Dr. Pitt Niehusmann (University of Bonn) for helpful discussions; to Dr. Fulvio Chiesa (Roche, Italy) for technical advice; to Cristina Zampini, Patrizia Raisi, Maura Masiero, Maria Novi, Rosaria Morelli, Anna Cherubino and Elisa Zaffoni for technical support.

References

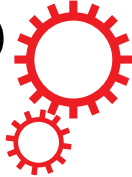
- Bartel DP (2004) MicroRNAs: genomics, biogenesis, mechanism, and function. *Cell* 116: 281–297.
- Im HI, Kenny PJ (2012) MicroRNAs in neuronal function and dysfunction. *Trends Neurosci* 35: 325–334.
- McNeill E, Van Vactor D (2012) MicroRNAs shape the neuronal landscape. *Neuron* 75: 363–379.
- Jimenez-Mateos EM1, Engel T, Merino-Serrais P, McKiernan RC, Tanaka K, et al. (2012) Silencing microRNA-134 produces neuroprotective and prolonged seizure-suppressive effects. *Nat Med* 18: 1087–1094.
- Henshall DC (2014) MicroRNA and epilepsy: profiling, functions and potential clinical applications. *Curr Opin Neurol* 27: 199–205.
- Song YJ, Tian XB, Zhang S, Zhang YX, Li X, et al. (2011) Temporal lobe epilepsy induces differential expression of hippocampal miRNAs including let-7c and miR-23a/b. *Brain Res* 1387: 134–140.
- Hu K, Xie YY, Zhang C, Ouyang DS, Long HY, et al. (2012) MicroRNA expression profile of the hippocampus in a rat model of temporal lobe epilepsy and miR-34a-targeted neuroprotection against hippocampal neuron cell apoptosis poststatus epilepticus. *BMC Neurosci* 13: 1–14.
- Bot AM, Debski KJ, Lukasiuk K (2013) Alterations in miRNA levels in the dentate gyrus in epileptic rats. *PLoS ONE* 8: e76051.
- Gorter JA, Iyer A, White I, Colzi A, van Vliet EA, et al. (2013) Hippocampal subregion-specific microRNA expression during epileptogenesis in experimental temporal lobe epilepsy. *Neurobiol Dis* 62: 508–520.
- Kan AA, van Erp S, Derijck AA, de Wit M, Hessel EV, et al. (2012) Genome-wide microRNA profiling of human temporal lobe epilepsy identifies modulators of the immune response. *Cell Mol Life Sci* 69: 3127–3145.
- McKiernan RC, Jimenez-Mateos EM, Bray I, Engel T, Brennan GP, et al. (2012) Reduced mature microRNA levels in association with dicer loss in human temporal lobe epilepsy with hippocampal sclerosis. *PLoS ONE* 7: e35921.
- Blümcke I, Thom M, Aronica E, Armstrong DD, Vinters HV, et al. (2011) The clinicopathologic spectrum of focal cortical dysplasias: a consensus classification proposed by an ad hoc Task Force of the ILAE Diagnostic Methods Commission. *Epilepsia* 52: 158–174.
- Blümcke I, Thom M, Aronica E, Armstrong DD, Bartolomei F, et al. (2013) International consensus classification of hippocampal sclerosis in temporal lobe epilepsy: a task force report from ILAE Commission on Diagnostic Methods. *Epilepsia* 54: 1315–1329.
- Blümcke I, Kistner I, Clusmann H, Schramm J, Becker AJ, et al. (2009) Towards a clinico-pathological classification of granule cell dispersion in human mesial temporal lobe epilepsies. *Acta Neuropathol* 117: 535–544.
- Peiró-Chova L1, Peña-Chilet M, López-Guerrero JA, García-Giménez JL, Alonso-Yuste E, et al. (2013) High stability of microRNAs in tissue samples of compromised quality. *Virchows Arch* 463: 765–774.
- Dweep H, Sticht C, Pandey P, Gretz N (2011) miRWalk - database: prediction of possible miRNA binding sites by "walking" the genes of 3 genomes. *J Biomed Inform* 44: 839–847.
- Maurer-Morelli CV, de Vasconcellos JF, Reis-Pinto FC, Rocha Cde S, Domingues RR, et al. (2012) A comparison between different reference genes for expression studies in human hippocampal tissue. *J Neurosci Methods* 208: 44–47.
- Chen D, Bhat-Nakshatri P, Goswami C, Badve S, Nakshatri H (2013) ANTXR1, a stem cell-enriched functional biomarker, connects collagen signaling to cancer stem-like cells and metastasis in breast cancer. *Cancer Res* 73: 5821–5833.
- Gutwein LG, Al-Quran SZ, Fernando S, Fletcher BS, Copeland EM, Grobmyer SR (2011) Tumor endothelial marker 8 expression in triple-negative breast cancer. *Anticancer Res* 31: 3417–3422.
- Werner E, Kowalczyk AP, Faundez V (2006) Anthrax toxin receptor 1/tumor endothelium marker 8 mediates cell spreading by coupling extracellular ligands to the actin cytoskeleton. *J Biol Chem* 281: 23227–23236.
- Gu J, Faundez V, Werner E (2010) Endosomal recycling regulates anthrax toxin receptor 1/tumor endothelial marker 8-dependent cell spreading. *Exp Cell Res* 316: 1946–1957.

Author Contributions

Conceived and designed the experiments: SZ GM BP MG RM GR MS. Performed the experiments: SZ GM BP PR PC MG. Analyzed the data: SZ GM BP MF GL MS. Contributed reagents/materials/analysis tools: SZ GM BP PR PC MG. Contributed to the writing of the manuscript: SZ GM GR MS.

22. Zhou R, Yuan P, Wang Y, Hunsberger JG, Elkahlon A, et al. (2009) Evidence for selective microRNAs and their effectors as common long-term targets for the actions of mood stabilizers. *Neuropsychopharmacology* 34: 1395–1405.
23. Shizu R1, Shindo S, Yoshida T, Numazawa S (2012) MicroRNA-122 down-regulation is involved in phenobarbital-mediated activation of the constitutive androstane receptor. *PLoS ONE* 7: e41291.
24. Thom M, Liagkouras I, Elliot KJ, Martinian L, Harkness W, et al. (2010) Reliability of patterns of hippocampal sclerosis as predictors of postsurgical outcome. *Epilepsia* 51: 1801-1808.
25. da Costa Neves RS, Jardim AP, Caboclo LO, Lancellotti C, Marinho TF, et al. (2013) Granule cell dispersion is not a predictor of surgical outcome in temporal lobe epilepsy with mesial temporal sclerosis. *Clin Neuropathol* 32: 24–30.
26. Marucci G, Rubboli G, Giulioni M (2010) Role of dentate gyrus alterations in mesial temporal sclerosis. *Clin Neuropathol* 29: 32–35.
27. Wang WX, Huang Q, Hu Y, Stromberg AJ, Nelson PT (2011) Patterns of microRNA expression in normal and early Alzheimer's disease human temporal cortex: white matter versus gray matter. *Acta Neuropathol* 121: 193–205.
28. Beveridge NJ, Cairns MJ (2012) MicroRNA dysregulation in schizophrenia. *Neurobiol Dis* 46: 263–271.
29. Wyler AR, Dohan FC Jr., Schweitzer JB, Berry AD III (1992) A grading system for mesial temporal pathology (hippocampal sclerosis) from anterior temporal lobectomy. *J Epil* 5: 220–225.
30. Blümcke I, Pauli E, Clusmann H, Schramm J, Becker A, et al. (2007) A new clinico-pathological classification system for mesial temporal sclerosis. *Acta Neuropathol* 113: 235–244.
31. Engel J Jr, Van Ness P, Rasmussen T, Ojemann L (1993) Outcome with respect to epileptic seizures. In Engel J Jr editor. *Surgical treatment of the epilepsies*, 2nd ed New York: Raven Press 609–621.

SCIENTIFIC REPORTS



OPEN

MicroRNA profiles in hippocampal granule cells and plasma of rats with pilocarpine-induced epilepsy – comparison with human epileptic samples

Received: 21 April 2015

Accepted: 12 August 2015

Published: 18 September 2015

Paolo Roncon¹, Marie Soukupová¹, Anna Binaschi², Chiara Falcicchia¹, Silvia Zucchini^{2,2,3}, Manuela Ferracin^{3,4}, Sarah R. Langley⁵, Enrico Petretto⁶, Michael R. Johnson⁵, Gianluca Marucci⁷, Roberto Michelucci⁸, Guido Rubboli^{8,9} & Michele Simonato^{2,2,3}

The identification of biomarkers of the transformation of normal to epileptic tissue would help to stratify patients at risk of epilepsy following brain injury, and inform new treatment strategies. MicroRNAs (miRNAs) are an attractive option in this direction. In this study, miRNA microarrays were performed on laser-microdissected hippocampal granule cell layer (GCL) and on plasma, at different time points in the development of pilocarpine-induced epilepsy in the rat: latency, first spontaneous seizure and chronic epileptic phase. Sixty-three miRNAs were differentially expressed in the GCL when considering all time points. Three main clusters were identified that separated the control and chronic phase groups from the latency group and from the first spontaneous seizure group. MiRNAs from rats in the chronic phase were compared to those obtained from the laser-microdissected GCL of epileptic patients, identifying several miRNAs (miR-21-5p, miR-23a-5p, miR-146a-5p and miR-181c-5p) that were up-regulated in both human and rat epileptic tissue. Analysis of plasma samples revealed different levels between control and pilocarpine-treated animals for 27 miRNAs. Two main clusters were identified that segregated controls from all other groups. Those miRNAs that are altered in plasma before the first spontaneous seizure, like miR-9a-3p, may be proposed as putative biomarkers of epileptogenesis.

Temporal lobe epilepsy (TLE) is the most common form of epilepsy in adults. It often develops secondary to an initial brain insult (e.g. trauma, tumor or stroke), after a latency period in which patients are apparently well. Thus, at-risk patients can often be identified, but it is currently impossible to predict who will actually develop epilepsy and who will not. Moreover, available antiepileptic drugs are symptomatic agents that are not useful in preventing the development of the disease and are ineffective in

¹Department of Medical Sciences, Section of Pharmacology and Neuroscience Center, University of Ferrara, Italy.

²National Institute of Neuroscience, Italy. ³Laboratory for Technologies of Advanced Therapies (LTTA), University of Ferrara, Italy. ⁴Department of Morphology, Surgery and Experimental Medicine, Section of Pathology, Oncology and Experimental Biology, University of Ferrara, Italy. ⁵Division of Brain Sciences, Imperial College London, Charing Cross Hospital, UK. ⁶Medical Research Council (MRC) Clinical Sciences Centre, Imperial College London, Hammersmith Hospital, UK. ⁷Department of Biomedical and NeuroMotor Sciences (DiBiNeM), Section of Pathology, Bellaria Hospital, Bologna, Italy. ⁸IRCCS Institute of Neurological Sciences, Section of Neurology, Bellaria Hospital, Bologna, Italy. ⁹Danish Epilepsy Center, Filadelfia/University of Copenhagen, Dianalund, Denmark. Correspondence and requests for materials should be addressed to P.R. (email: paolo.roncon@unife.it)

approximately one-third of patients with epilepsy¹. Thus, there is an urgent need not only to develop new therapies for drug-resistant epilepsy, but also to identify antiepileptogenic therapies that can prevent the disease in at-risk individuals^{1–3}. To do so, it is essential to better understand the mechanisms of epileptogenesis and drug-resistance. Moreover, the development of biomarkers for epileptogenesis following brain injury would facilitate clinical trials of novel antiepileptogenic therapies by allowing those patients at the greatest risk of epilepsy to be identified^{1,4,5}. MicroRNAs (miRNAs) provide an opportunity as both therapeutic targets and biomarkers of epileptogenesis.

MiRNAs are small (~22 nt) non-coding RNAs that regulate the expression of target mRNAs at the post-transcriptional level⁶. Experimental evidence has demonstrated that miRNAs are involved in heterogeneous brain functions^{7,8} including neuroinflammation⁹, synaptic remodeling¹⁰, and neuronal death¹¹. Thus, it can be hypothesized that specific miRNAs may regulate genetic programs leading to hyperexcitability in the brain and, as such, represent new therapeutic targets. Moreover, miRNAs are found in the blood, where their levels are affected by disease states^{12–15} and are therefore attractive candidates as biomarkers for stratifying patients at highest risk of epilepsy following brain injury^{16,17}.

Recently, alterations in miRNA expression levels have been described both in the brain of epilepsy patients and in animal models of epilepsy. In humans, Kan and colleagues performed a genome-wide profiling of TLE, identifying a miRNA signature of hippocampal sclerosis¹⁸. Likewise, a recent study demonstrated the implication of miR-487a in granule cell pathology¹⁹. In animal models, changes in miRNA expression levels in the hippocampus have been reported in multiple studies in the latency period after an epileptogenic insult and in the chronic epileptic state^{20–24}. Unfortunately, all these studies have multiple limitations. First, the brain tissue was the whole hippocampus or a mechanically-dissected hippocampal sub-region in most studies, which implicates not only great heterogeneity in terms of cell composition, but also a different representation of different cell types in controls and epileptic samples, as the epileptic hippocampus is characterized by cell loss and astrogliosis. Only Zucchini *et al.*¹⁹ micro-dissected a specific cell population (the granule cells), but the comparison was between epileptic samples with or without granule cell pathology, i.e. no healthy controls. Second, human studies lacked a proper control, in that the epileptic tissue was from surgeries and the control from autopsies. Third, no detailed evaluation of the changes in the course of disease was performed. Fourth, blood samples were not collected and analyzed, except for Gorter *et al.*²⁴

The aim of this study was to fill the gaps left by the previous ones of this kind. Specifically, we performed a systematic evaluation of the miRNAome in a specific cell population of the hippocampus (the laser microdissected granule cell) and in plasma samples, at multiple time-points in the course of pilocarpine-induced epilepsy in rats: early and late latency, at the time of the first spontaneous seizure and in the chronic period. Further, we compared results from rats in the chronic phase of epilepsy with post-mortem human epileptic and control granule cell samples.

Results

Granule cells. miRNA clustering. We first evaluated miRNA expression in the laser-microdissected granule cell layer (GCL) of rats sacrificed at multiple time-point following pilocarpine-induced SE: 4 and 7 days after SE, 12 h after the first spontaneous seizure and 50 days after the first spontaneous seizure. To detect changes in miRNA expression levels regardless of the time point, we first analyzed differential miRNA expression levels in the GCL between control and epileptic rats. We detected significant changes in the expression of 63 miRNAs (Supplementary Table S1). Hierarchical clustering of all samples performed with these 63 miRNAs revealed three main clusters that separated the control and chronic phase groups from rats sacrificed during latency (4 and 8 days after SE) and from those sacrificed after the first spontaneous seizure (Fig. 1). However, control and chronic formed distinguishable sub-clusters.

Changes in expression were also separately analyzed for each time point. As compared with controls, we detected significant changes in 33 miRNAs during latency (4 and 8 days after SE), 33 miRNAs at the time of the first spontaneous seizure, and 25 miRNAs in the chronic period (Supplementary Tables S2–S4).

miRNA expression pattern. Variations in miRNAs levels in the GCL at different time points were then analyzed in detail. Group to group comparison revealed 6 different miRNA expression patterns in the GCL. First, a subgroup of miRNAs (miR-15b-5p, miR-17-5p, miR-18a-5p, miR-19a-3p, miR-19b-3p, miR-20a-5p, miR-20b-5p, miR-21-5p, miR-23b-5p, miR-24-3p, miR-27a-3p, miR-92a-3p, miR-93-5p, miR-142-3p, miR-344b-2-3p, miR-431, miR-466b-5p and miR-674-3p) displayed increased expression levels during latency (4 and 8 days after SE), decreased their expression levels at the time of the first spontaneous seizure and returned to control levels in the chronic phase (Fig. 2, Supplementary Fig. S1). All these miRNAs displayed a peak in expression levels 8 days after SE, except for miR-21-5p, miR-27a-3p, miR-142-3p and miR-674-3p that peaked earlier (4 days after SE). Another subgroup of miRNAs displayed an opposite pattern, i.e. decreased expression during latency: miR-7a-1-3p, miR-107-3p, miR-138-5p, miR-139-3p, miR-186-5p, miR-204-5p, miR-222-3p, miR-324-3p and miR-505-3p were significantly decreased during latency (peak at 4 days after SE), then gradually returned to control levels (Fig. 2, Supplementary Fig. S2).

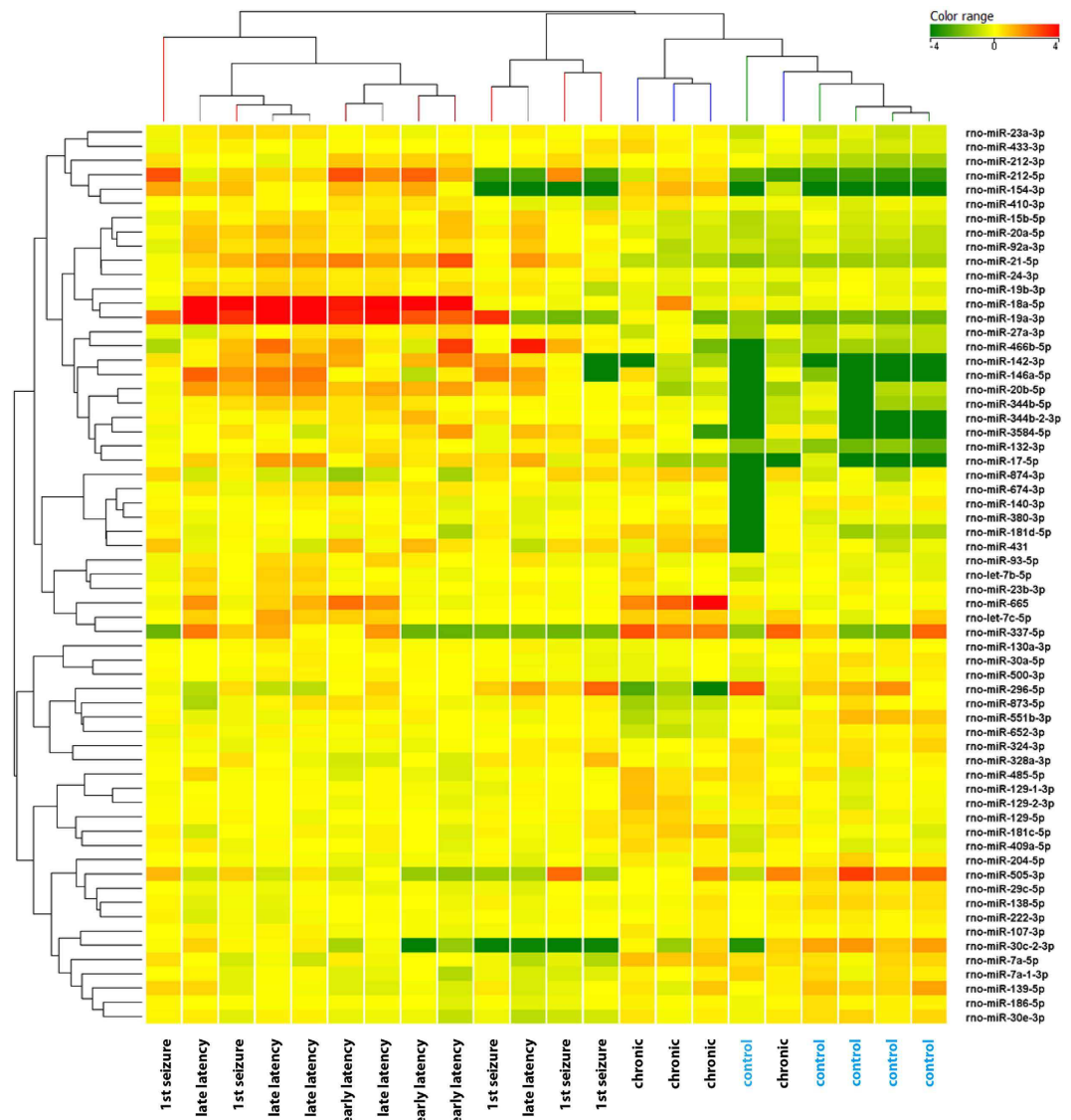


Figure 1. Cluster analysis of miRNAs differentially expressed in the granule cell layer (GCL) at different time points in the course of pilocarpine-induced epilepsy. Heat map representation of the average expression of the 63 differentially expressed miRNAs in the GCL of epileptic and control animals. Each column represents an individual animal and each row represents one miRNA, as indicated. Colors represent the expression level fold change: higher-red, lower-green. Analysis was performed on differentially expressed miRNAs (FDR > 10%), using the Person correlation; for cluster image preparation an additional step of normalization on gene median across all samples was added.

Some miRNAs (miR-129-1-3p; miR-129-2-3p, miR-129-5p, miR181c-5p, miR181d-5p, miR-409a-5p, miR-655 and miR-874-3p) were up-regulated (Fig. 2, Supplementary Fig. S3A), whereas others (miR-296-5p, miR-500-3p and miR-652-3p) were down-regulated only in the chronic phase, while not being significantly altered during latency (Fig. 2, Supplementary Fig. S3B). Finally, other subsets of miRNAs were either up-regulated (miR-23a-3p, miR132-3p, miR-146a-5p, miR-154-3p, miR-181d-5p, miR-212-3p, miR-212-5p, miR-344b-5p, miR-380-3p, miR-410-3p, miR-433-3p and miR-3584; Fig. 2, Supplementary Fig. S4), or down-regulated (miR-29c-5p, miR-30a-5p, miR-30c-2-3p, miR-30e-3p, miR-138-5p, miR-140-3p, miR-551b-3p and miR-652-3p; Fig. 2, Supplementary Fig. S5) during all phases of the disease.

Network analysis. We then performed a network analysis of miRNAs whose expression was significantly altered during latency, because pathways identified in this manner may play a role in epileptogenesis. Targets for each miRNA were obtained using the mirDB and TargetScan algorithms and filtered to include those which were expressed in the rat dentate gyrus. Seven significant clusters of miRNAs were identified at 10% false discovery rate (FDR) level (Fig. 3A). GO/KEGG enrichment highlighted five of them as having a potential role in epileptogenesis.

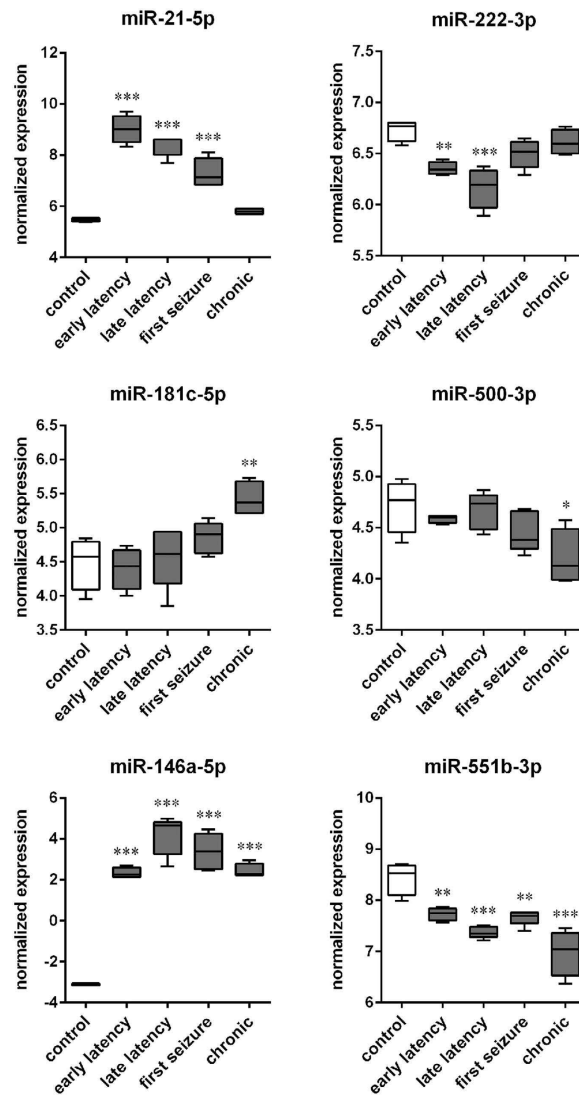


Figure 2. Time course patterns of miRNA expression in the rat granule cell layer (GCL). The boxplots depict the time course of expression for 6 of the miRNAs identified as significant with a false discovery rate (FDR) < 10% in the GCL by using one-way ANOVA. Each boxplot represents 4 animals. These miRNAs were chosen as representative of the different patterns that were observed: up-regulation (miR-21-5p) or down-regulation (miR-222-3p) during latency; up-regulation (miR-181c-5p) or down-regulation (miR-500-3p) in the chronic period; up-regulation (miR-146a-5p) or down-regulation (miR-551b-3p) in the entire course of the disease. The time courses of the other significantly modified miRNAs are shown in Supplementary Figs. S2, S3, S4, S5 and S6. * $p < 0.05$; ** $p < 0.01$; *** $p < 0.001$; Tukey's test.

Cluster 1, composed by miR-674-3p, miR-505-3p and miR-212-5p, was up-regulated during epileptogenesis (4 and 8 days after SE). Target analysis identified eight significant pathways: purine metabolism (adjusted $P = 0.016$); metabolic pathways (adjusted $P = 0.013$); axon guidance (adjusted $P = 0.013$); pyrimidine metabolism (adjusted $P = 0.0091$); peroxisome proliferator-activated receptors (PPAR) signaling pathway (adjusted $P = 0.0074$); adipocytokine signaling pathway (adjusted $P = 0.0074$); glycolysis and gluconeogenesis (adjusted $P = 0.0074$); SNAp REceptor (SNARE) interactions in vesicular transport (adjusted $P = 0.0064$; Fig. 3B). "Axon guidance" and "SNARE interactions in vesicular transport" were the categories most likely to play a role in latency. Two target genes per pathway were highlighted: the synaptosomal-associated protein 29kDa (Snap 29) and the vesicle-associated membrane protein 3 (Vamp 3) in the axon guidance pathway; the ephrin B1 (Efnb1) and the chemokine ligand 12 (Cxcl12) in the SNARE interactions in vesicular transport pathway (Supplementary Fig. S6A).

Cluster 3 was composed by two up-regulated microRNAs, miR-142-3p and miR-146a-5p. This cluster was associated with four different pathways including endocytosis (adjusted $P = 0.013$), cytokine-cytokine receptor interaction (adjusted $P = 0.013$), PPAR signaling pathway (adjusted $P = 0.003$) and general metabolic pathway (adjusted $P = 0.0008$; Fig. 3C). Two target genes in cytokine-cytokine receptor interaction

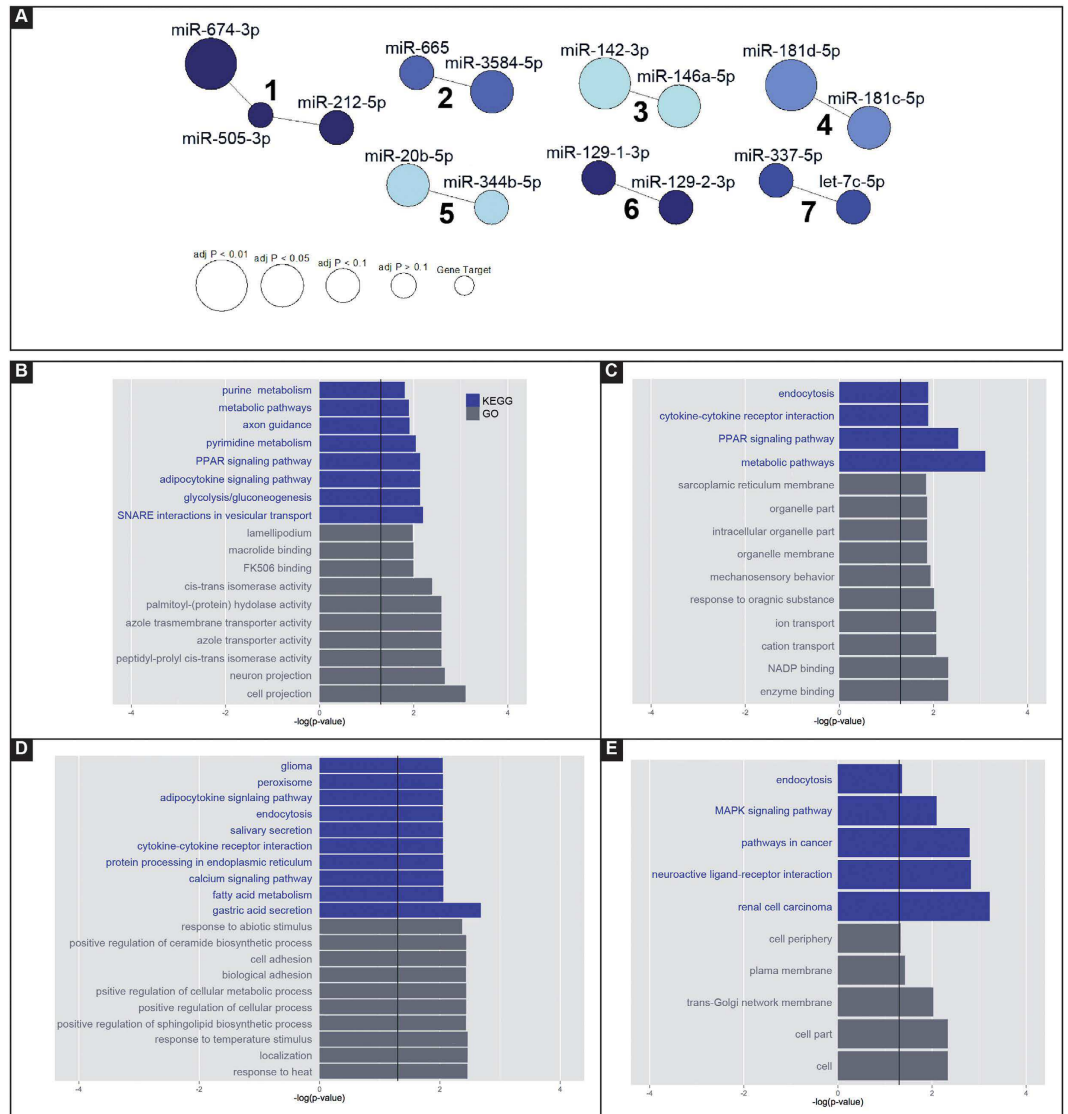


Figure 3. Network analysis. Predicted gene targets for each miRNA dys-regulated during latency (4 and 8 days after SE), obtained using the mirDB and TargetScan algorithms, were filtered with all miRNAs expressed in the dentate gyrus of rats (database GSE49850). **(A)** Clusters of miRNAs identified at 10% false discovery rate (FDR) level. **(B)** Cluster 1. **(C)** Cluster 3; **(D)** Cluster 4. **(E)** Cluster 5. Gene ontology (GO) and Kyoto Encyclopedia of Genes and Genomes (KEGG) analysis were performed using webgestalt, $p < 0.05$.

pathway were highlighted; the transforming growth factor β receptor 1 (Tgfb1) and the growth hormone receptor (Ghr; Supplementary Fig. S6B).

Cluster 4 included miR-181c-5p and miR-181d-5p. The KEGG analysis identified multiple pathways associated with the target genes of these two miRNAs. In particular, the neurotrophin signaling pathway (adjusted $P = 0.016$), with tumor necrosis factor receptor superfamily, member 11b (Tnfrsf11b), protein kinase C, delta (Prkcd) and calmodulin 1 (Calm1); and the cytokine-cytokine receptor interaction pathway (adjusted $P = 0.009$), with the platelet-derived growth factor receptor, alpha polypeptide (Pdgfra) and the chemokine ligand 10 (Cxcl10; Fig. 3D and Supplementary Fig. S6C).

MiR-344b-5p and miR-20b-5p were in cluster 5. They were associated with different cancer related pathways, endocytosis (adjusted $P = 0.044$), MAPK signaling (adjusted $P = 0.0081$) and neuroactive ligand-receptor interaction (adjusted $P = 0.0015$; Fig. 3E). Target genes involved in neuroactive ligand-receptor interaction category were the glycine receptor alpha 2 (Gla2), the gamma-aminobutyric acid B receptor 2 (Gabra2), the galanin receptor 1 (GalR1) and the glutamate receptor ionotropic AMPA 2 (Gria2; Supplementary Fig. S6D).

Interestingly, this combinatorial analysis revealed that some significant clusters of miRNAs might correlate with identical pathways.

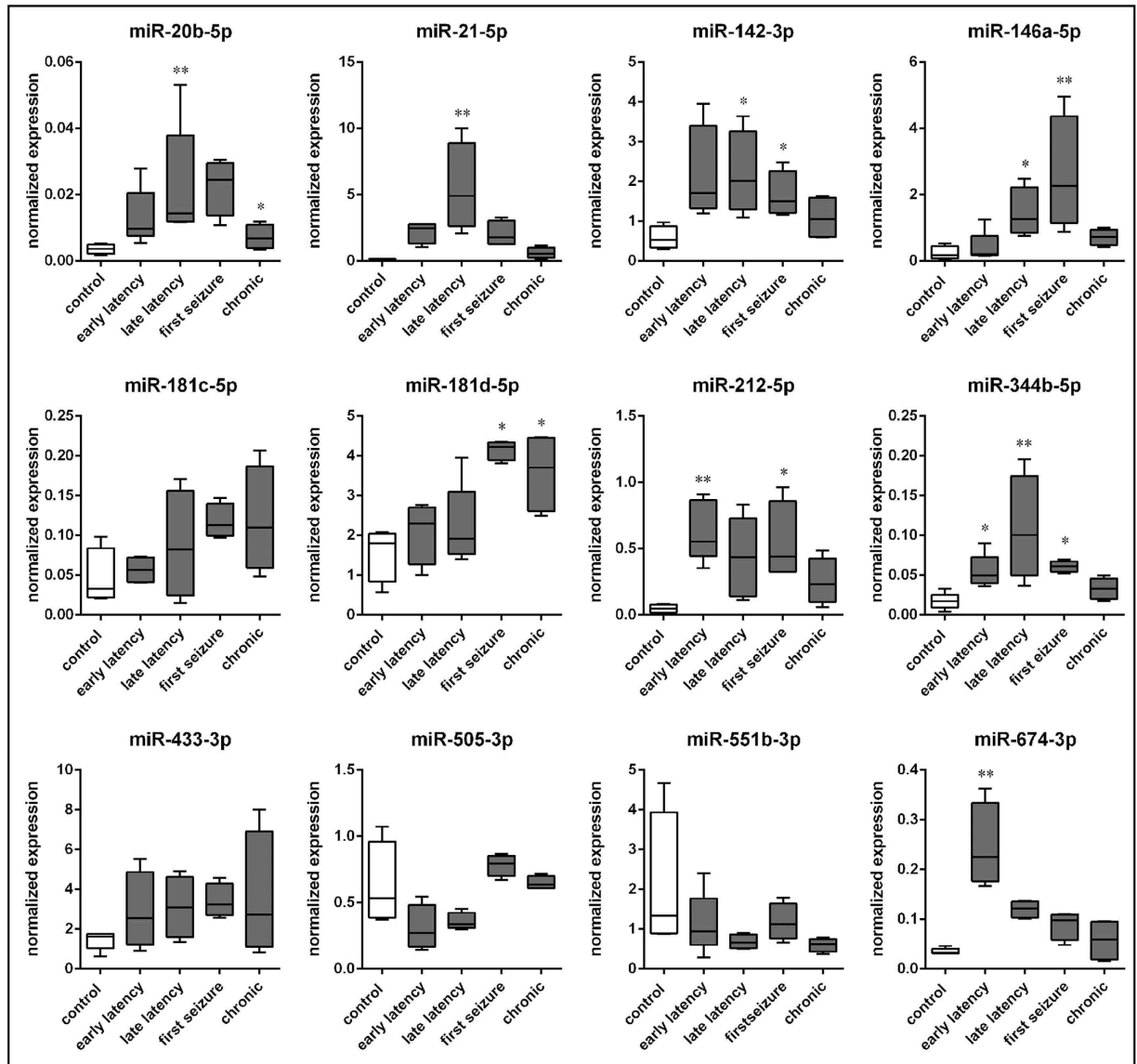


Figure 4. Relative expression of selected miRNAs in the granule cell layer, as detected using qPCR. Five rats per group. * $p < 0.05$; ** $p < 0.01$; Tukey's test.

RT-qPCR. A large subset of miRNAs whose expression was significantly modulated in the GCL in our model and that was identified in significant clusters through network analysis was validated using RT-qPCR in a different cohort of cases. Overall, the data were highly consistent with those obtained using microarray. In fact, the expression patterns of miR-20b-5p, miR-142-3p, miR-181d-5p, miR-212-5p, miR-344b-5p and miR-674-3p were identical to those observed using the microarray, and those of miR-21-5p and miR-146a-5p were very similar, although not identical (Fig. 4). Even if displaying the same patterns observed with the microarray, the expression levels of miR-181c-5p, miR-433-3p, miR-505-3p and miR-551b-3p were not significantly different from controls (Fig. 4).

Human tissue. Next, we asked what the relevance of these findings could be for human epilepsy. In humans, comparison can only be made between chronically epileptic and non-epileptic controls. However, a technical hurdle exists with human studies, because the only available human controls are from autopsies, whereas the epileptic tissue is generally from surgical resections. Thus, we first wanted to ensure that the comparison of autoptict and bioptict material was valid. We performed miRNA microarray on laser-microdissected GCLs from 10 epileptic patients who underwent surgery, two autopsies of epileptic patients and 10 aged-matched autopsy controls (epileptic: age 70 and 46, both females; non-epileptic: age 47 ± 7 , range 34–57, 3 males, 7 females; all 12 dead by acute pulmonary or cardiac disease). Unfortunately, the two autoptict epileptic did not segregate with the other epileptic as expected, but with the control autoptict. This indicates that the tissue origin (i.e. bioptict or autoptict) had greater

	Chronic rats		Patients	
	Fold change	Regulation	Fold change	Regulation
miR-21-5p	1.24	Up	1.93	Up
miR-23a-5p	1.83	Up	3.35	Up
miR-146a-5p	21.24	Up	3.63	Up
miR-181c-5p	1.91	Up	1.88	Up

Table 1. miRNAs expression patterns in chronically epileptic rats and patients.

importance than the disease background (data not shown, manuscript in preparation). Therefore, here we restricted the comparison between the 2 epileptic and the 10 non-epileptic autaptic samples.

We compared the miRNA species modulated in chronic epileptic rats and in human cases. We identified four miRNAs (miR-21-5p, miR-23a-5p, miR-146a-5p and miR-181c-5p) that were up-regulated in both epileptic humans and rats (Table 1). Moreover, the comparison displayed similar changes in expression levels between epileptic (human cases and rats) and controls, except for miR-146a-5p, that increased more in rats than in humans (fold change equals 21.24 in rats and 3.63 in humans).

Plasma. Finally, to investigate the possibility of using miRNAs in peripheral blood as potential biomarkers of epileptogenesis, we analyzed plasma samples collected from the experimental and control rats for the study of the hippocampal GCL.

This analysis revealed different levels between control and pilocarpine-treated animals in one miRNAs: only miR-91-3p showed significant differential expression at a 10% FDR level (adjusted $P = 0.08$). This may be due to the larger variability found in circulating miRNAs levels as compared to other tissues²⁵. Therefore, to gain an exploratory view of the miRNA expression patterns in plasma, we relaxed the significance threshold to an unadjusted $P < 0.05$, which resulted in 27 miRNAs of interest (Supplementary Table S5). Hierarchical clustering also generated two main clusters that separated controls from all other groups, with the exception of two animals in early latency group (4 days after SE) and one in the chronic phase group, which segregated with the controls (Fig. 5A). Within the cluster including all pilocarpine animals, rats belonging to the single experimental groups displayed a clear tendency to form distinct sub-clusters.

Within these 27 miRNAs, we detected 4 different expression patterns in the plasma of rats sacrificed at different time points of the disease history. MiR-9a-3p displayed highly increased levels at the earlier stage of latency (4 days after SE), then normalized to control levels at the following time points (Fig. 5B; Supplementary Fig. S7A). A second pattern was about the opposite: miR-466b-1-3p, miR-494-3p and miR-598-5p displayed significantly decreased plasma levels during latency, and a tendency to return to the control levels in the chronic stage (Supplementary Fig. S7B). Another couple of miRNAs (miR-32-3p and miR-300-3p) was down-regulated around the time of the first spontaneous seizure (Supplementary Fig. S7C). Finally, miR-30c-2-3p, miR-101b-3p, miR-142-3p, miR-142-5p, miR-181a-1-3p, miR-374-5p, miR-466c-3p, miR-1188-3p, miR-3065-3p and miR-3582 were significantly down-regulated in the chronic stage (Supplementary Fig. S7D).

The only miRNA dysregulated both in the GCL and in plasma was miR-142-3p. The patterns of dysregulation, however, were totally different: miR-142-3p was up-regulated in the GCL during latency and down-regulated in plasma in the chronic period. MiR-9a-3p and miR-142-3p were chosen for RT-qPCR validation in the same cohort of samples, displaying the same patterns observed in the microarray, even if they did not reach statistical significance.

Discussion

The main findings of the present study are the following. First, the overall analysis of the rat GCL revealed three main clusters of miRNAs that separated the control and chronic phase groups from rats sacrificed during latency (4 and 8 days after SE) and from those sacrificed after the first spontaneous seizure. This identifies a distinct miRNA expression pattern associated with the latency period between brain injury and first spontaneous seizure that may reveal epileptogenic pathways. Second, the chronic phase was accompanied by significant alterations in miRNA expression in the rat GCL, and comparison with data from epileptic patients identified several miRNAs (notably miR-21-5p, miR-23a-5p, miR-146a-5p and miR-181c-5p) that were up-regulated in both human and rat epileptic hippocampus. MiRNAs whose expression is altered in the GCL may be implicated in the mechanisms of epileptogenesis and/or in the generation of seizures, and may therefore represent new therapeutic targets. Third, analysis of plasma samples revealed that, while at relaxed threshold, 27 miRNAs were able to discriminate the controls from all other groups. Those miRNAs that are altered in plasma before the first spontaneous seizure, like miR-9a-3p, may be worth further investigation into their use as potential biomarkers of epileptogenesis.

The miRNA expression analysis revealed interesting overlaps between our work here and the two previously published studies focusing on the dentate gyrus (DG)^{23,24}, both in terms of miRNAs modulated

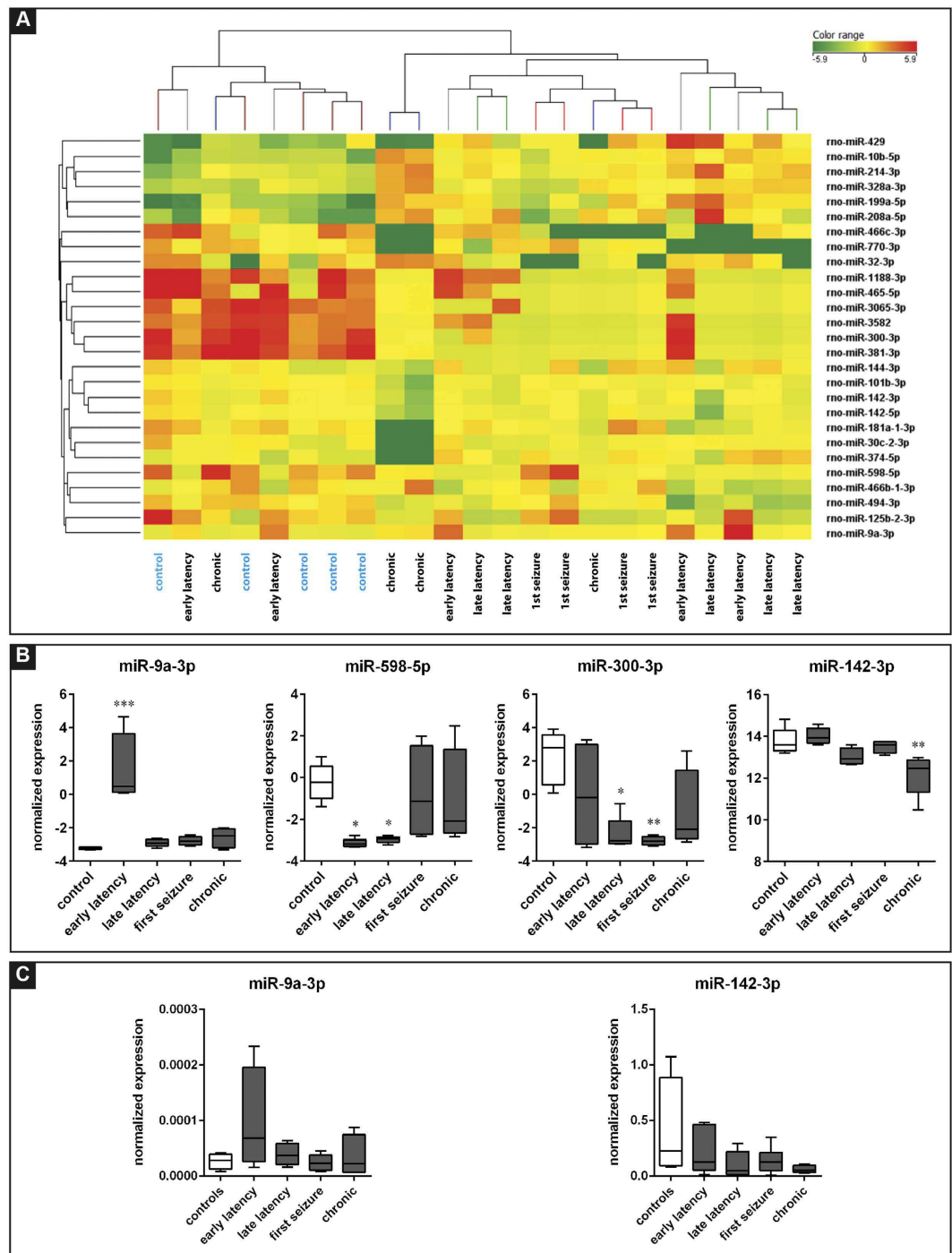


Figure 5. Plasma miRNA levels. (A) Heat map representation of the average levels of the 27 differentially expressed miRNAs in the plasma of epileptic and control animals. Each column represents an individual animal and each row represents one miRNA, as indicated. Colors represent the expression level fold change: higher-red, lower-green. Analysis was performed on differentially represented miRNAs using the Person correlation. (B) The boxplots depict the time course for 4 of the miRNAs identified as significant by using one-way ANOVA. Each boxplot represents 5 animals. These miRNAs were chosen as representative of the different patterns that were observed: up-regulation (miR-9a-5p) or down-regulation (miR-598-5p) during latency, down-regulation in the late latency - first spontaneous seizure period (miR-381-3p) and down regulation in the chronic stage (miR-142-5p). (C) Relative levels of miR-9a-5p and miR-142-3p, as detected using qPCR. Five rats per group. * $p < 0.05$; ** $p < 0.01$; *** $p < 0.001$; Tukey's test.

in the latency and in the chronic phase, even if: 1) different epilepsy models were employed in these other studies, namely amygdala and perforant path stimulation-induced SE; 2) the DG was mechanically dissected from other hippocampal regions in these other studies, and therefore the results are the combination of the varying alterations in miRNA levels occurring in multiple cell populations (in contrast with our laser-dissection approach, that ensures a nearly pure granule cell preparation). Other studies^{20–22} used the whole hippocampus, emphasizing the latter limitation, and therefore will not be used for comparison in the frame of the present discussion.

Commonalities with other studies are particularly interesting, because they may represent disease-specific, rather than model-specific alterations. Since the pathophysiological implications would be very different, we will here discuss separately findings related to latency (early and late latency in the present study) and findings related to the chronic state that follows diagnosis in humans (first seizure and chronic murine groups plus the human cases in this study). Finally, we will discuss the data obtained from peripheral blood.

Latency. Our study and other relevant data sets^{23,24} identified the up regulation of three miRNAs (miR-21-5p, miR-212-3p and miR-132-3p) during latency. Furthermore, we and Gorter *et al.*²⁴ observed the up-regulation of miR-17-5p, miR-20a-5p, miR-23a-3p and the down-regulation of miR-139-5p, whereas we and Bot *et al.*²³ observed the down-regulation of miR-551b-3p.

Alterations on these miRNA levels suggest a role in the mechanism of epileptogenesis, a concept that is supported by analysis of their potential targets. For example, the up-regulation of miR-21-5p may be involved in the initiation of the cell signaling pathway associated with epilepsy²⁶. Moreover, mutations in the myocyte enhancer factor 2C (MEF2C) gene, a neuronal transcription factor that may have a role in neuronal dysfunction and neurodegeneration²⁷, has been observed in patients with epilepsy²⁸ and has been identified as a target of miR-21-5p and miR-21-3p²⁷. Sestrin 1 (SESN1), a predicted target of miR-21-5p, is down-regulated during latency after amygdala stimulation²³. This finding, combined with the evidence that another member of the sestrins family, SESN3, controls a proconvulsant transcriptional program in human TLE²⁹, suggests a correlation between miR-21-5p and the mechanisms that lead to seizures onset.

Further evidence for a direct involvement of the identified miRNAs in the mechanisms of epileptogenesis derived from network analysis. Our network analysis, based on miRNAs dysregulated during latency in the GCL, highlighted the presence of 4 clusters of miRNAs. Cluster 3 (that includes miR-142-3p and miR-146a-5p) and cluster 4 (including miR-181c-5p and miR-181c-5p) are connected to the “cytokine-cytokine receptor interaction” signaling pathway, which suggests a neuroinflammatory role for those miRNAs. In keeping with this idea, evidence in the literature supports that miR-146a-5p regulates the astrocyte-mediated inflammatory response by influencing IL-1 β , IL-6 and COX-2 signaling^{24,30}. Cluster 4, together with cluster 1 (that includes miR-674-3p, miR-505-3p and miR-212-5p) and cluster 5 (including miR-144b-5p and miR-20b-5p), may also strongly influence neuronal activity. In fact, their predicted targets in the rat DG are involved in axon guidance and SNARE interaction (cluster 1), neurotrophin signaling (cluster 4) and neuroactive ligand receptor (cluster 5). Axon guidance has been linked to epilepsy, the sprouting of mossy fibers (the axons of granule cells) being the best characterized of axonal reorganization in TLE. Although epilepsy-associated mossy fiber sprouting has been extensively studied^{31–33}, its underlying molecular mechanisms are still poorly understood, and the present findings suggest a role for this cluster of miRNAs. Interestingly, the predicted targets of cluster 5 include the gamma-aminobutyric acid B receptor 2 (Gabra2), the galanin receptor 1 (GalR1) and the glutamate receptor ionotropic AMPA 2 (Gria2), all genes whose products are implicated in the regulation of excitability and in epilepsy. Specifically, 1) a polymorphism of Gabra2 is associated with mTLE³⁴; 2) GalR1 deletion exacerbates hippocampal neuronal loss after kainate administration in mice³⁵, and GalR1 knock-out mice exhibit spontaneous epilepsy, abnormal EEGs, and altered inhibition in the hippocampus³⁶; 3) Gria2 in the hippocampus is related to the mechanisms of seizure and neurodegeneration³⁷. Thus, this cluster of miRNAs may play a role as a master regulator of multiple mechanisms of epileptogenesis. Functional studies aimed at establishing the functional role of these miRNAs in TLE will represent the obvious continuation of this study.

Most of the miRNAs up-regulated during latency in the GCL displayed peak expression levels in the late phase of latency (7 days after SE), but a subset (miR-21-5p, miR-674-3p and miR-3564-5p) was increased the most 4 days after SE. It can be hypothesized that these changes correspond to different “waves” of the epileptogenesis process, which may represent different windows of opportunity for therapy³⁸.

Chronic period. Regarding the chronic group, both the present dataset and the other two that we considered relevant to this Discussion^{23,24} identified the up-regulation of miR-21-5p, miR-23a-5p and miR-146a-5p. Up-regulation of these miRNAs has been reported also in other studies^{21,39,40}. Moreover, we and Gorter *et al.*²⁴ observed the up-regulation of miR-212-5p, whereas we and Bot *et al.*²³ observed the up-regulation of miR-433-3p.

MiR-23a-5p has been proven to be a regulator of cell growth and apoptosis⁴¹. Furthermore, it has been identified as a negative regulator of lamin B1, thereby contributing to the process of oligodendroglia

development and myelin formation⁴². MiR-146a-5p is strictly associated with the astrocyte-associated immune response both in epileptic patients and *in vivo* models^{24,39}.

As described, we identified different expression patterns of miRNAs that were up or down-regulated at the time of the first seizure and during the chronic period, showing slight but significant differences between the two phases. Continuing modifications in the expression pattern of miRNAs in the course of chronic epilepsy support the hypothesis that epileptogenesis is a dynamic process that continues even after the initial diagnosis of the disease, i.e. after the initial spontaneous seizures¹.

The comparison between chronic epileptic rats and the human cases identified four miRNAs (miR-21-5p, miR-23a-5p, miR-146a-5p and miR-181c-5p) that are similarly up-regulated in expression levels in both species. Interestingly, miR-23a-5p and miR-146a-5p are in common with the other two rat data sets that were taken as primary comparator in this Discussion^{23,24}. As for miR-181c-5p, it was highlighted by network analysis in cluster 4, and implicated in cytokine-cytokine receptor interaction and in the inflammatory response. Thus, even if preliminary being based on a small number of patients, human data appear to confirm those obtained in animal models, suggesting that animal data may be representative of the human situation also under conditions (latency) that cannot be directly explored in humans.

Blood. There is great need of diagnosis tools to identify those individuals, among those at risk, that will actually develop epilepsy or to stratify epileptic patients with different prognosis. Changes in extracellular miRNA levels have been observed in association with neurological diseases in various body fluids including plasma, putting forward the concept that miRNAs may represent noninvasive or minimally invasive, clinically useful biomarkers^{16,17,24}, even if the biological function of plasmatic miRNAs is still obscure (it has been hypothesized that they represent a form of cellular communication whereby cells can interact at distance by transfer of exosomes or microvesicles containing miRNAs through the systemic circulation^{43,44}).

Two previous studies performed microarrays on blood samples. One described changes in circulating miRNA levels 24 h after ischemic stroke, intracerebral hemorrhage and kainate seizures⁴⁵. The other²⁴ performed the analysis in plasma samples obtained from the trunk blood, reporting an increase in miR-142-5p levels during the acute phase, miR-21-5p in the early stage and of miR-146a-5p in the chronic stage, that reflect parallel changes in miRNAs expression observed in the brain. Unfortunately, the complete dataset has not been made available by this study, and it is therefore unclear if all plasma miRNAs or only those 3 change in the same manner in plasma and in the brain.

Here, we studied the expression levels of circulating miRNAs in plasma separated by blood collected from animals through an intracardiac withdrawal, a technique that avoids contamination with others cell populations. Analysis of plasma samples revealed different levels between control and pilocarpine-treated animals for 27 miRNAs that segregated controls from all other groups. We identified a single miRNA, miR-142-3p that was altered both in plasma and in the brain, but the pattern of expression was different in that it was down-regulated in the former and up-regulated in the latter. Based on our data, therefore, it seems unlikely that changes in circulating miRNAs levels are correlated to the changes in miRNAs expression in the brain.

Although it is impossible, at the current stage of knowledge, to speculate on the biological significance of changes in plasma, it can nonetheless be proposed that those miRNAs that are altered in plasma before the first spontaneous seizure, like miR-9a-3p, are putative biomarkers of epileptogenesis. Further studies are needed to gain insight into the origin and the biological significance of circulating miRNAs, and to understand their functional role in TLE and other neurological disorders. The present data, however, are relevant to the identification of biomarkers that can predict the development of epilepsy in at-risk subjects.

In conclusion, the present results identify a distinct miRNA expression pattern associated with latency in the rat pilocarpine model and reveal putative epileptogenic pathways, suggesting that miRNAs represent attractive therapeutic targets for the prevention of epilepsy. Moreover, we found overlap human and rat databases in the chronic stage, supporting the notion that animal data are representative of the human situation. There are many commonalities between our data and other publicly available datasets obtained from *in vivo* models of TLE. Those miRNAs whose expression changes are in common through different datasets are particularly attractive candidates for further investigation, being disease-, rather than model-specific. Finally, results obtained from rat plasma samples suggest that circulating miRNAs may be used as biomarkers of epilepsy. The major hits identified in this study, like miR-9a-3p, should be now challenged in other epilepsy models in which only a subset of animals develop spontaneous seizures, in order to verify that they can actually stratify subjects that will or will not develop the disease.

Methods

Animals. Male Sprague-Dawley rats (250–350 g; Harlan, Italy) were used for pilocarpine experiments. They were housed under standard conditions: constant temperature (22–24 °C) and humidity (55–65%), 12 h light/dark cycle, free access to food and water. Procedures involving animals and their care were carried out in accordance with European Community, national and local approved guidelines, laws and policies. All experimental protocols were approved by the University of Ferrara Ethical Committee for Animal Experimentation and by the Italian Ministry of Health. All animals were (i) acclimatized to laboratory conditions for at least 1 h before the start of the experiment, (ii) used only once during the

pilocarpine protocol and (iii) euthanized at different times points by anesthetic overdose. The number of animals was kept as small as possible and the ARRIVE (Animal Research: Reporting *In Vivo* Experiments⁴⁶) have been followed.

Surgery. Surgery was carried out to implant the electrodes for EEG recordings. Rats were secured to a stereotaxic apparatus, with the nose bar positioned at +5 mm, under ketamine/xylazine (43 and 7 mg/Kg i.p.) anesthesia. Anesthesia was then maintained using isoflurane (1.4% in air; 1.2 ml/min). A recording electrode was implanted into the right ventral hippocampus (A: -3.4 mm; L: +4.5 mm; P: +6.5 mm to bregma⁴⁷). A reference electrode was placed on the skull. Rats were allowed 7 days to recover from surgery.

Pilocarpine. Rats were randomly assigned to groups that received a single injection of methyl-scopolamine (1 mg/kg, s.c.) 30 min prior to pilocarpine (370 mg/kg, i.p.) or a single injection of methyl-scopolamine 30 min prior to vehicle (0.9% NaCl solution; control animals), and their behavior was observed by experienced researchers for at least 6 h thereafter. Within the first 20–25 min after pilocarpine injection, 83% of the animals developed seizures evolving into recurrent generalized convulsions (status epilepticus, SE). SE was interrupted 3 h after onset by administration of diazepam (20 mg/kg, i.p.). For 1–2 days following SE interruption, animals occasionally exhibited short-lasting seizures and lost weight (15–20%). Thereafter, they recovered and entered a period of apparent wellbeing (latency). However, one fourth of the animals that entered SE (i.e. 21% of those administered pilocarpine) died during SE or within 1–2 days.

Test and interspersed control animals were then randomly assigned to four experimental groups representing different phases of the natural history of the disease: early latency (4 days after SE), late latency (8 days after SE), first spontaneous seizure (11 ± 1 days after SE), chronic (50 days after the first spontaneous seizure). Inclusion criteria were (i) development of convulsive SE within 1 h after pilocarpine administration and (ii) weight gain within the first week after SE.

Video and electroencephalography recordings. Video and video-EEG recordings were used to verify the hippocampal seizure onset and the disease progression in chronic animals. Convulsive seizures were assessed by 24/24-h video monitoring, performed using a digital video surveillance system DSS1000 (V4.7.0041FD, AverMedia Technologies, USA). Video monitoring was started approximately 6 h after pilocarpine administration (i.e. at the end of direct observation by the researchers – see above) and continued until day 5 when EEG recording was applied for proper identification of the first spontaneous seizure. Continuous video-EEG monitoring was started from day 5 after SE until the day of the first spontaneous seizure. Video-EEG monitoring (hardware system MP150 and software AcqKnowledge 4.3, all from Biopac, USA) was started at day 5 because, as previously reported^{48,49}, we do not observe spontaneous seizures earlier than 8–9 days after pilocarpine administration under the experimental conditions employed in this study. EEG seizures were categorized and measured as periods of paroxysmal activity of high frequency (>5 Hz) characterized by a >3-fold amplitude increment over baseline with progression of the spike frequency that lasted for a minimum of 3 s^{33,50}. Seizure severity was scored using the scale of Racine⁵¹: 1, chewing or mouth and facial movements; 2, head nodding; 3, forelimb clonus; 4, generalized seizure with rearing; 5, generalized seizure with rearing and falling. In the chronic phase, animals were continuously video-EEG recorded for a week after the first spontaneous seizure, for a week before the sacrifice and 48 h per week between the first spontaneous seizure and the killing.

Tissue preparation. Rats were killed by decapitation under an anesthetic overdose. Before being killed, rats were anesthetized with ketamine (870 mg/kg) and xylazine (13 mg/Kg), and a blood sample was collected through intracardiac withdrawal. Blood samples were added EDTA (ethylenediaminetetraacetic acid disodium salt dehydrate, Sigma, Germany) to prevent clotting and plasma was separated by centrifugation at 1000 rcf for 2 minutes and the supernatant was centrifuged at 2500 rcf for 2 minutes. This procedure ensured low platelet contamination⁵². Samples were separated in 200 µl aliquots and stored at -80 °C.

Brains were rapidly removed, frozen in isopentane and stored at -80 °C until use. Coronal sections (20 µm thick) were cut across the entire hippocampus, plates 40–52 of Pellegrino *et al.*⁴⁷ and mounted onto slides for laser microdissection (MembraneSlides PEN-Membrane 2,0 µm, Leica). Sections were fixed according to a slight modification of a published protocol⁵³: ethanol 70% in diethyl pyrocarbonate (DEPC) water for 5 min, rinse in distilled DEPC water, incubation in Mayer's hematoxylin solution 0.1% (Sigma) for 5 min, another wash in DEPC water; finally, section were dried at room temperature for 10 min before being stored at -80 °C. This procedure ensured the best yield and quality of extracted RNA, as compared to other published procedures, in side-by-side testing experiments conducted in the lab before initiating the processing of the tissue employed in the present study.

Human Samples. All human hippocampal tissue was from autopsies of 2 epileptic and 10 non-epileptic patients who died of acute lung or heart pathologies. All autoptic material was from the tissue archives of the Bellaria Hospital (Bologna, Italy). The study was approved by the Ethics Committee of Bologna (Comitato Etico Indipendente dell'Azienda USL della Città di Bologna). Since this was a pilot study in

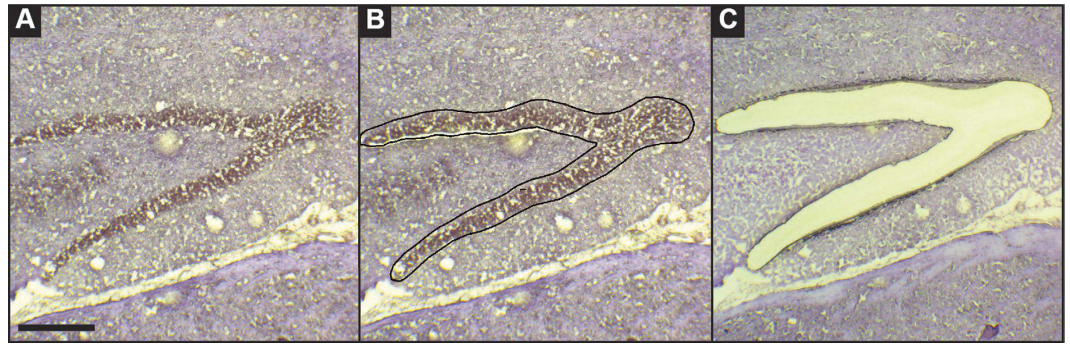


Figure 6. Laser microdissection of the rat granule cell layer. Representative hematoxylin stained hippocampal section prepared from a pilocarpine treated rat (level: dentate gyrus of the hippocampus). (A) Intact section before laser microdissection. (B) Identification of the region of interest, the granular layer (black line). (C) The section after the laser microdissection, without the granular layer. Horizontal bar = 320 μ m.

a small cohort of cases, all from archive samples of patients who died years ago, the Ethical Committee acknowledged the impossibility to collect informed consents and approved the study under the condition to strictly ensure anonymity. All the methods were carried out in accordance with the approved guidelines, and all information regarding the human material was managed using anonymous numerical codes and samples were handled in compliance with the Helsinki declaration (<http://www.wma.net/en/30publications/10policies/b3/>). Specimens were formalin-fixed and paraffin-embedded. They were de-waxed using Bio-Clear (Bio-Optica, Milan, Italy), washed in ethanol and stained with hematoxylin and eosin, as indicated in Zucchini *et al.*¹⁹.

Laser microdissection, RNA purification and profiling. Ten-micron-thick sections were cut using a microtome and collected in slides for laser microdissection (LMD). LMD was performed essentially as previously described^{19,54,55}. Briefly, PEN-membrane slides were mounted on a Leica LMD6000B system (Leica Microsystems, Wetzlar, Germany) with the sections facing downwards. The intensity, aperture and cutting velocity were calibrated to obtain the sharpest cut with the minimal intensity, then the pulsed UV laser beam was carefully directed along the borders of the dentate gyrus GCL (Fig. 6). The microdissected region was then transferred by gravity into a 0,2 ml Eppendorf tube cap placed directly underneath the tissue section. Tissue collection was verified by inspecting the tube cap. Granule cells were collected from at least 9 slices per animal and 3–4 slices per patient, in order to obtain an adequate amount of tissue for RNA extraction. Material from all sections from the same animal or patient was pooled together, and total RNA purified using an RNA purification kit (miRNeasy Micro kit from QIAGEN Germany, was used to purify the RNA in animal samples and RecoverAll™ Total Nucleic Acid Isolation kit from Life Technologies, Milan, Italy for human samples). Approximately 250 ng of total RNA were obtained from each sample. Every RNA sample was analyzed using an Agilent 2100 Bioanalyzer in order to evaluate the quality of total RNA. RNA samples with a RNA Integrity Number (RIN) <5 (in a 1 to 10 scale) were excluded from further analysis.

Total RNA, including microRNAs, was also purified from 200 μ l of plasma samples with a specific RNA purification kit (miRNeasy Serum/Plasma kit, Qiagen). To ensure effective denaturation of proteins, 10 volumes of Qiazol solution were added to one volume of plasma or serum. Samples were then thoroughly mixed by vortexing and incubated at room temperature for 5 min⁵⁶. As internal control, we employed *c. elegans* miR-39 miRNA mimic (miRNeasy Serum/Plasma Spike-In Control, Qiagen; 3.5 μ l, 1.6×10^8 copies/ μ l). Total RNA was eluted from column by two sequential elutions with 16 μ l of RNase-free water to yield 30 μ l RNA solution. Prior to RNA isolation, all samples were carefully ordered to alternate samples from different groups, in order to avoid biases related to batch effects and geographic location of samples in the thermocycler block⁵⁶.

Total RNA was used for microarray analysis (Rat miRNA MicroArray Kit, Human micro-RNA Microarray V3, #G4470C, Agilent Technologies, Santa Clara, CA, USA). The chip consisted of 60-mer DNA probes and allowed simultaneous analysis of 677 rat miRNAs and 1200 human miRNAs obtained from the Sanger miR-BASE database (Release 16.0 for rats and 10.1 for humans). We employed approximately 100 ng total RNA per sample in each experiment. RNA labeling and hybridization were performed according to the manufacturer's indications. Agilent scanner and the Feature Extraction 10.5 software (Agilent Technologies) were used to obtain the raw-data.

Data analysis. Microarray results were analyzed by using the GeneSpring GX 13 software (Agilent Technologies). Data transformation was applied to set all the negative raw values at 1.0, followed by quantile normalization. Filters on gene expression were used to keep only those miRNAs that were

detected in at least one sample. Comparisons among all experimental groups (controls, early latency, late latency, 12h within the first seizure and chronic) were performed with ANOVA analysis and differences were considered significant when adjusted P was <0.1. Comparisons between two groups were performed with moderated t-test and considering an adjusted $p < 0.1$ as significant. For plasma, we applied ANOVA analysis and a P cutoff of 0.05. Gaussian graphical models (GGM) based on partial correlation were constructed using a FDR threshold of 1%. Principle components analysis (PCA) and boxplots were generated in R. Hierarchical clustering was performed on differentially expressed miRNAs with GeneSpring GX 12 software (Agilent Technologies), using the Pearson correlation as a measure of similarity. For cluster image generation, expression data was centered on gene median across samples.

Predicted target genes for each miRNA that was deregulated during the two earlier time point (4 and 7 days after SE) were obtained from miRWalk using the miRDB and TargetScan algorithms⁵⁷. Only those genes that were predicted by both algorithms were taken in consideration. The list of targets was further filtered using publicly available rat gene expression from the dentate gyrus (GSE49850). The predicted targets were filtered out if they were not present in the top two-thirds of expressed genes assayed in the control rats. Gene ontology (GO) and Kyoto encyclopedia of genes and genomes (KEGG) enrichment was performed using webgestalt (<http://bioinfo.vanderbilt.edu/webgestalt/>) and the terms enriched with adjusted p-values < 0.05 were deemed significant.

RT-qPCR. Reverse transcription (RT) reactions were performed using the Taq-Man miRNA Reverse Transcription kit and miRNA-specific stem-loop primers (Applied Biosystems, Inc) in a scaled down (7.5 μ l) reaction. Samples were run at 16 °C for 30 min, 42 °C for 30 min, 85 °C for 5 min and hold at 4 °C. RT products were stored undiluted at –20 °C prior to running real-time PCR.

For GCL samples, real-time PCR reactions were performed using the TaqMan miRNA assay kit (Applied Biosystems, Santa Clara, CA, USA) according to the manufacturer's instructions; for plasma, they were performed as described by others⁵⁶. Samples were run in triplicate at 95 °C for 15 sec and 60 °C for 1 min using CFX96 Touch™ (Biorad, Milan, Italy). Analysis was performed by the comparative delta threshold cycle (Δ CT) method⁵⁸. For brain samples, U6 and snoRNA were used as reference genes⁵⁹. For plasma, data normalization was obtained using the synthetic spiked-in *c. elegans* miR-39.

References

1. Simonato, M. *et al.* The challenge and promise of anti-epileptic therapy development in animal models. *Lancet Neurol* **13**, 949–60 (2014).
2. Simonato, M. *et al.* Finding a better drug for epilepsy: preclinical screening strategies and experimental trial design. *Epilepsia* **53**, 1860–7 (2012).
3. Simonato, M., French, J. A., Galanopoulou, A. S. & O'Brien, T. J. Issues for new antiepilepsy drug development. *Curr Opin Neurol* **26**, 195–200 (2013).
4. Galanopoulou, A. S. *et al.* Identification of new epilepsy treatments: issues in preclinical methodology. *Epilepsia* **53**, 571–82 (2012).
5. Engel, J. Jr. *et al.* Epilepsy biomarkers. *Epilepsia* **4**, 61–9 (2013).
6. Bartel, D. P. MicroRNAs: genomics, biogenesis, mechanism, and function. *Cell* **116**, 281–97 (2004).
7. Im, H. I. & Kenny, P. J. MicroRNAs in neuronal function and dysfunction. *Trends Neurosci* **35**, 325–34 (2012).
8. McNeill, E. & Van Vactor, D. MicroRNAs shape the neuronal landscape. *Neuron* **75**, 363–79 (2012).
9. Vezzani, A., Aronica, E., Mazarati, A. & Pittman, Q. J. Epilepsy and brain inflammation. *Exp Neurol* **244**, 11–21 (2013).
10. Mikkonen, M. *et al.* Remodeling of neuronal circuitries in human temporal lobe epilepsy: increased expression of highly polysialylated neural cell adhesion molecule in the hippocampus and the entorhinal cortex. *Ann Neurol* **44**, 923–34 (1998).
11. Blümcke, I. *et al.* International consensus classification of hippocampal sclerosis in temporal lobe epilepsy: a Task Force report from the ILAE Commission on Diagnostic Methods. *Epilepsia* **54**, 1315–29 (2013).
12. Wu, J. *et al.* MicroRNA-421 is a new potential diagnosis biomarker with higher sensitivity and specificity than carcinoembryonic antigen and cancer antigen 125 in gastric cancer. *Biomarkers* **16**, 1–6 (2014).
13. Sepramanian, S. *et al.* Circulating microRNA as biomarkers of acute stroke. *Int J Mol Sci* **15**, 1418–32 (2014).
14. Tan, L. *et al.* Genome-wide serum microRNA expression profiling identifies serum biomarkers for Alzheimer's disease. *J Alzheimers Dis* **40**, 1017–27 (2014).
15. Cloutier, F., Marrero, A., O'Connell, C. & Morin, P. J. MicroRNAs as Potential Circulating Biomarkers for Amyotrophic Lateral Sclerosis. *J Mol Neurosci* **56**, 102–112 (2014).
16. Jin, X. F., Wu, N., Wang, L. & Li, J. Circulating microRNAs: a novel class of potential biomarkers for diagnosing and prognosing central nervous system diseases. *Cell Mol Neurobiol* **33**, 601–13 (2013).
17. Zhang, Y. *et al.* Altered expression levels of miRNAs in serum as sensitive biomarkers for early diagnosis of traumatic injury. *J Cell Biochem* **112**, 2435–42 (2011).
18. Kan, A. A. *et al.* Genome-wide microRNA profiling of human temporal lobe epilepsy identifies modulators of the immune response. *Cell Mol Life Sci* **69**, 3127–45 (2012).
19. Zucchini, S. *et al.* Identification of miRNAs differentially expressed in human epilepsy with or without granule cell pathology. *PLoS One* **9**, e105521. doi: 10.1371/journal.pone.0105521 (2014).
20. Risbud, R. M. & Porter, B. E. Changes in microRNA expression in the whole hippocampus and hippocampal synaptoneurosome fraction following pilocarpine induced status epilepticus. *PLoS One* **8**, e53464. doi: 10.1371/journal.pone.0053464 (2013).
21. Hu, K. *et al.* MicroRNA expression profile of the hippocampus in a rat model of temporal lobe epilepsy and miR-34a-targeted neuroprotection against hippocampal neurone cell apoptosis post-status epilepticus. *BMC Neurosci* **13**, 115 (2012).
22. Jimenez-Mateos, E. M. *et al.* miRNA Expression profile after status epilepticus and hippocampal neuroprotection by targeting miR-132. *Am J Pathol* **179**, 2519–32 (2011).
23. Bot, A. M., Dębski, K. J. & Lukasiuk, K. Alterations in miRNA levels in the dentate gyrus in epileptic rats. *PLoS One* **8**, e76051. doi: 10.1371/journal.pone.0076051 (2013).
24. Gorter, J. A. *et al.* Hippocampal subregion-specific microRNA expression during epileptogenesis in experimental temporal lobe epilepsy. *Neurobiol Dis* **62**, 508–20 (2013).

25. Lucherini, O. M. *et al.* First report of circulating microRNAs in tumour necrosis factor receptor-associated periodic syndrome (TRAPS). *PLoS One* **8**, e73443. doi: 10.1371/journal.pone.0073443 (2013).
26. Meng, F. *et al.* Neuronal calcium signaling pathways are associated with the development of epilepsy. *Mol Med Rep* **11**, 196–202 (2015).
27. Yelamanchili, S. V. & Fox, H. S. Defining larger roles for “tiny” RNA molecules: role of miRNAs in neurodegeneration research. *J Neuroimmune Pharmacol* **5**, 63–9 (2010).
28. Bienvenu, T., Diebold, B., Chelly, J. & Isidor, B. Refining the phenotype associated with MEF2C point mutations. *Neurogenetics* **14**, 71–5 (2013).
29. Johnson, M. R. *et al.* Systems genetics identifies Sestrin 3 as a regulator of a proconvulsant gene network in human epileptic hippocampus. *Nat Commun* **6**, 6031 (2015).
30. Iyer, A. *et al.* MicroRNA-146a: a key regulator of astrocyte-mediated inflammatory response. *PLoS One* **7**, e44789. doi: 10.1371/journal.pone.0044789 (2012).
31. Pitkänen, A. & Sutula, T. P. Is epilepsy a progressive disorder? Prospects for new therapeutic approaches in temporal-lobe epilepsy. *Lancet Neurol* **1**, 173–81 (2002).
32. Curia, G., Longo, D., Biagini, G., Jones, R. S. & Avoli, M. The pilocarpine model of temporal lobe epilepsy. *J Neurosci Methods* **172**, 143–57 (2008).
33. Paradiso, B. *et al.* Localized overexpression of FGF-2 and BDNF in hippocampus reduced mossy fibers sprouting and spontaneous seizures up to 4 weeks after pilocarpine-induced status epilepticus. *Epilepsia* **52**, 572–78 (2011).
34. Wang, X. *et al.* M129V polymorphism in the prion protein gene is not associated with mesial temporal lobe epilepsy in a Han Chinese population. *Eur J Neurol* **15**, 827–30 (2008).
35. Schauwecker, P. E. Galanin receptor 1 deletion exacerbates hippocampal neuronal loss after systemic kainate administration in mice. *PLoS One* **5**, e15657. doi: 10.1371/journal.pone.0015657 (2010).
36. McColl, C. D., Jacoby, A. S., Shine, J., Iismaa, T. P. & Bekkers, J. M. Galanin receptor-1 knockout mice exhibit spontaneous epilepsy, abnormal EEGs and altered inhibition in the hippocampus. *Neuropharmacology* **50**, 209–18 (2006).
37. Szczurowska, E. & Mareš, P. NMDA and AMPA receptors: development and status epilepticus. *Physiol Res* **62**, S21–38 (2013).
38. Pitkänen, A. *et al.* Issues related to development of antiepileptogenic therapies. *Epilepsia* **4**, 35–43 (2013).
39. Aronica, E. *et al.* Expression pattern of miR-146a, an inflammation-associated microRNA, in experimental and human temporal lobe epilepsy. *Eur J Neurosci* **31**, 1100–7 (2010).
40. Song, Y. J. *et al.* Temporal lobe epilepsy induces differential expression of hippocampal miRNAs including let-7e and miR-23a/b. *Brain Res* **1387**, 134–40 (2011).
41. Cheng, A. M., Byrom, M. V., Shelton, J. & Ford, L. P. Antisense inhibition of human miRNAs and indications for an involvement of miRNA in cell growth and apoptosis. *Nucleic Acids Res* **33**, 1290–7 (2005).
42. Song, Y. J. *et al.* miR-23 regulation of lamin B1 is crucial for oligodendrocyte development and myelination. *Dis Model Mech* **2**, 178–88 (2009).
43. Valadi, H. *et al.* Exosome-mediated transfer of mRNAs and microRNAs is a novel mechanism of genetic exchange between cells. *Nat Cell Biol* **9**, 654–9 (2007).
44. Hunter, M. P. *et al.* Detection of microRNA expression in human peripheral blood microvesicles. *PLoS One* **3**, e3694. doi: 10.1371/journal.pone.0003694 (2008).
45. Liu, D. Z. *et al.* Brain and blood microRNA expression profiling of ischemic stroke, intracerebral hemorrhage, and kainate seizures. *J Cereb Blood Flow Metab* **30**, 92–101 (2010).
46. Kilkeny, C. *et al.* Animal research: reporting *in vivo* experiments: the ARRIVE guidelines. *J Cereb Blood Flow Metab* **31**, 991–3 (2011).
47. Pellegrino, L. J., Pellegrino, A. S. & Cushman, A. J. *A stereotaxic atlas of the rat brain*. Plenum Press, New York and London (1979).
48. Paradiso, B. *et al.* Localized delivery of fibroblast growth factor-2 and brain-derived neurotrophic factor reduces spontaneous seizures in an epilepsy model. *Proc Natl Acad Sci USA* **106**, 7191–6 (2009).
49. Mazzuferi, M. *et al.* Enhancement of GABA(A)-current run-down in the hippocampus occurs at the first spontaneous seizure in a model of temporal lobe epilepsy. *Proc Natl Acad Sci USA* **107**, 3180–5 (2010).
50. Soukupova, M. *et al.* Impairment of GABA release in the hippocampus at the time of the first spontaneous seizure in the pilocarpine model of temporal lobe epilepsy. *Exp Neurol* **257**, 39–49 (2014).
51. Racine, R. J. Modification of seizure activity by electrical stimulation. II. Motor seizure. *Electroencephalogr Clin Neurophysiol* **32**, 281–94 (1972).
52. Cheng, H. H. *et al.* Plasma processing conditions substantially influence circulating microRNA biomarkers levels. *PLoS One* **8**, e64795. doi: 10.1371/journal.pone.0064795 (2013).
53. Goldsworthy, S. M., Stocktown, P. S., Trempus, C. S., Foley, J. F. & Maronpot, R. R. Effects of fixation on RNA extraction and amplification from laser capture microdissected tissue. *Mol Carcinog* **25**, 86–91 (1999).
54. Burbach, G. J., Dehn, D., Del Turco, D. & Deher, T. Quantification of layer-specific gene expression in the hippocampus: effective use of laser microdissection in combination with quantitative RT-PCR. *J Neurosci Methods* **131**, 83–91 (2003).
55. Baj, G. *et al.* Regulation of the spatial code for BDNF mRNA isoform in the rat hippocampus following pilocarpine-treatment: a systematic analysis using laser microdissection and quantitative real-time PCR. *Hippocampus* **23**, 413–23 (2013).
56. Kroh, E. M., Parkin, R. K., Mitchell, P. S. & Tewari, M. Analysis of circulating microRNA biomarkers in plasma and serum using quantitative reverse transcription-PCR (qRT-PCR). *Methods* **50**, 298–301 (2010).
57. Dweep, H., Sticht, C., Pandey, P. & Gretz, N. miRWalk-database: prediction of possible miRNA binding sites by “walking” the genes of 3 genomes. *J Neurosci Methods* **208**, 44–7 (2011).
58. Livak, K. J. & Schmittgen, T. D. Analysis of relative gene expression data using real-time quantitative PCR and the $2^{-\Delta\Delta CT}$ method. *Methods* **25**, 402–8 (2001).
59. de Araújo, M. A. *et al.* Identification of endogenous reference genes for the analysis of microRNA expression in the hippocampus of the pilocarpine-induced model of mesial temporal lobe epilepsy. *PLoS One* **9**, e100529. doi: 10.1371/journal.pone.0100529 (2014).

Acknowledgements

This work was supported by a grant from the European Union (EPITARGET) to MRJ, EP and MS.

Author Contributions

P.R. and M.Si. designed the study and wrote the manuscript. P.R., M.So., A.B., C.F. and S.Z. performed the experiments. M.F., S.R.L., E.P. and M.R.J. performed bioinformatics analyses. G.M., R.M. and G.R. prepared the human samples.

Additional Information

Supplementary information accompanies this paper at <http://www.nature.com/srep>

Competing financial interests: The authors declare no competing financial interests.

How to cite this article: Roncon, P. *et al.* MicroRNA profiles in hippocampal granule cells and plasma of rats with pilocarpine-induced epilepsy - comparison with human epileptic samples. *Sci. Rep.* **5**, 14143; doi: 10.1038/srep14143 (2015).



This work is licensed under a Creative Commons Attribution 4.0 International License. The images or other third party material in this article are included in the article's Creative Commons license, unless indicated otherwise in the credit line; if the material is not included under the Creative Commons license, users will need to obtain permission from the license holder to reproduce the material. To view a copy of this license, visit <http://creativecommons.org/licenses/by/4.0/>

Supplementary information

MicroRNA profiles in hippocampal granule cells and plasma of rats with pilocarpine-induced epilepsy – comparison with human epileptic samples.

Paolo Roncon, Marie Soukupová, Anna Binaschi, Chiara Falcicchia, Silvia Zucchini, Manuela Ferracin, Sarah R Langley, Enrico Petretto, Michael R Johnson, Gianluca Marucci, Roberto Michelucci, Guido Rubboli, Michele Simonato

Contents

- Supplementary Tables S1-S5
- Supplementary Figures S1-S7

Supplementary Table S1. Significantly dys-regulated miRNAs in the GCL of epileptic compared with control animals.

miRNA	P	P adjusted
miR-21-5p	6,57 ⁻⁰⁹	1,73 ⁻⁰⁶
miR-132-3p	1,36 ⁻⁰⁷	1,19 ⁻⁰⁵
miR-20a-5p	1,35 ⁻⁰⁷	1,19 ⁻⁰⁵
miR-212-3p	5,71 ⁻⁰⁷	3,75 ⁻⁰⁵
miR-29c-5p	8,57 ⁻⁰⁷	4,5 ⁻⁰⁵
miR-652-3p	4,55 ⁻⁰⁶	1,99 ⁻⁰⁴
miR-551b-3p	1,31 ⁻⁰⁵	4,91 ⁻⁰⁴
miR-92a-3p	1,64 ⁻⁰⁵	5,38 ⁻⁰⁴
miR-344b-2-3p	2,16 ⁻⁰⁵	6,32 ⁻⁰⁴
miR-15b-5p	5,61 ⁻⁰⁵	1,46 ⁻⁰³
miR-24-3p	6,12 ⁻⁰⁵	1,46 ⁻⁰³
miR-23a-3p	0,0001	2,44 ⁻⁰³
miR-222-3p	0,0002	3,23 ⁻⁰³
miR-181d-5p	0,0002	3,97 ⁻⁰³
miR-674-3p	0,0002	4,28 ⁻⁰³
miR-142-3p	0,0003	4,96 ⁻⁰³
miR-17-5p	0,0003	4,96 ⁻⁰³
miR-874-3p	0,0004	6,00 ⁻⁰³
miR-27a-3p	0,0004	6,00 ⁻⁰³
miR-19b-3p	0,001	1,37 ⁻⁰²
miR-93-5p	0,0011	1,39 ⁻⁰²
miR-433-3p	0,0012	1,45 ⁻⁰²
miR-30a-5p	0,0013	1,47 ⁻⁰²
miR-18a-5p	0,0016	1,53 ⁻⁰²
miR-146a-5p	0,0015	1,53 ⁻⁰²
miR-20b-5p	0,0014	1,53 ⁻⁰²
miR-138-5p	0,0015	1,53 ⁻⁰²
miR-431	0,0024	2,21 ⁻⁰²
miR-130a-3p	0,0024	2,21 ⁻⁰²
miR-7a-5p	0,0025	2,22 ⁻⁰²
miR-3584-5p	0,0028	2,41 ⁻⁰²
miR-23b-3p	0,0035	2,87 ⁻⁰²
miR-181c-5p	0,0051	4,14 ⁻⁰²
miR-30e-3p	0,0056	4,34 ⁻⁰²
miR-129-5p	0,0062	4,67 ⁻⁰²
miR-296-5p	0,0065	4,72 ⁻⁰²
miR-505-3p	0,0073	5,05 ⁻⁰²
miR-19a-3p	0,0073	5,05 ⁻⁰²

miR-154-3p	0,0077	5,19 ⁻⁰²
miR-139-5p	0,0084	5,51 ⁻⁰²
miR-204-5p	0,009	5,81 ⁻⁰²
miR-410-3p	0,0096	6,04 ⁻⁰²
miR-129-1-3p	0,0100	6,13 ⁻⁰²
miR-186-5p	0,0107	6,40 ⁻⁰²
miR-337-5p	0,0114	6,48 ⁻⁰²
miR-324-3p	0,0111	6,48 ⁻⁰²
miR-485-5p	0,0115	6,48 ⁻⁰²
miR-466b-5p	0,0124	6,81 ⁻⁰²
let-7c-5p	0,0127	6,85 ⁻⁰²
miR-873-5p	0,0142	7,50 ⁻⁰²
miR-344b-5p	0,0154	7,89 ⁻⁰²
miR-380-3p	0,0157	7,89 ⁻⁰²
let-7b-5p	0,0162	7,89 ⁻⁰²
miR-107-3p	0,0162	7,89 ⁻⁰²
miR-140-3p	0,0174	8,33 ⁻⁰²
miR-409a-5p	0,0182	8,56 ⁻⁰²
miR-7a-1-3p	0,0186	8,60 ⁻⁰²
miR-30c-2-3p	0,0195	8,70 ⁻⁰²
miR-129-2-3p	0,0192	8,70 ⁻⁰²
miR-500-3p	0,0202	8,87 ⁻⁰²
miR-212-5p	0,0217	9,37 ⁻⁰²
miR-328a-3p	0,0222	9,43 ⁻⁰²
miR-665	0,0231	9,64 ⁻⁰²

Supplementary Table S2. Significantly dys-regulated miRNAs in the GCL in latency (four and eight days after SE) compared with control animals.

	P	Fold change	Regulation
miR-142-3p	0,067	34,11	up
miR-344b-2-3p	0,030	23,32	up
miR-3584-5p	0,089	18,28	up
miR-17-5p	0,047	18,16	up
miR-30c-2-3p	0,077	11,94	down
miR-181a-1-3p	0,093	9,02	down
miR-132-3p	0,002	4,58	up
miR-21-5p	0,008	3,56	up
miR-212-3p	0,002	2,95	up
miR-181d-5p	0,022	2,57	up
miR-27a-3p	0,026	2,08	up
miR-30e-3p	0,030	2,06	down
miR-92a-3p	0,046	2,04	up
miR-20a-5p	0,030	2,00	up
miR-874-3p	0,093	2,00	up
miR-139-5p	0,094	1,97	down
miR-431	0,091	1,88	up
miR-30a-3p	0,094	1,82	down
miR-551b-3p	0,030	1,71	down
miR-23a-3p	0,070	1,65	up
miR-433-3p	0,033	1,59	up
miR-330-3p	0,091	1,58	down
miR-370-3p	0,071	1,53	up
miR-138-5p	0,022	1,50	down
miR-140-3p	0,030	1,48	down
miR-128-3p	0,053	1,43	down
miR-380-3p	0,041	1,43	up
miR-29c-5p	0,008	1,43	down
miR-30a-5p	0,030	1,39	down
miR-300-3p	0,077	1,30	up
miR-652-3p	0,070	1,29	down
miR-186-5p	0,100	1,24	down
miR-103-3p	0,070	1,11	down

Supplementary Table S3. Significantly dys-regulated miRNAs in the GCL of rats at the time of the first spontaneous seizure compared with controls.

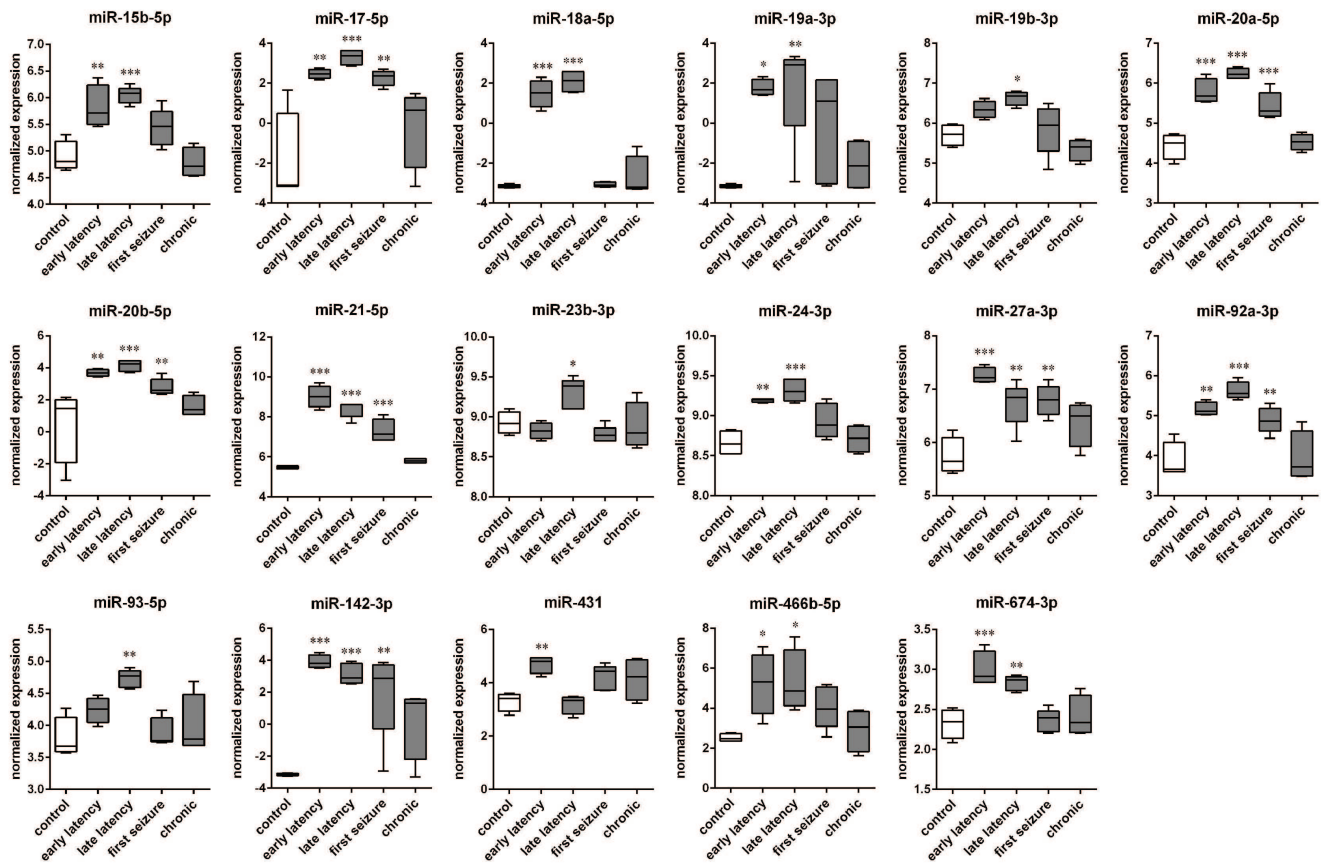
	P	Fold change	Regulation
miR-142-3p	0,067	34,11	up
miR-344b-2-3p	0,030	23,32	up
miR-3584-5p	0,089	18,28	up
miR-17-5p	0,047	18,16	up
miR-30c-2-3p	0,077	11,94	down
miR-181a-1-3p	0,093	9,02	down
miR-132-3p	0,002	4,58	up
miR-21-5p	0,008	3,56	up
miR-212-3p	0,002	2,95	up
miR-181d-5p	0,022	2,57	up
miR-27a-3p	0,026	2,08	up
miR-30e-3p	0,030	2,06	down
miR-92a-3p	0,046	2,04	up
miR-20a-5p	0,030	2,00	up
miR-874-3p	0,093	2,00	up
miR-139-5p	0,094	1,97	down
miR-431	0,091	1,88	up
miR-30a-3p	0,094	1,82	down
miR-551b-3p	0,030	1,71	down
miR-23a-3p	0,070	1,65	up
miR-433-3p	0,033	1,59	up
miR-330-3p	0,091	1,58	down
miR-370-3p	0,071	1,53	up
miR-138-5p	0,022	1,50	down
miR-140-3p	0,030	1,48	down
miR-128-3p	0,053	1,43	down
miR-380-3p	0,041	1,43	up
miR-29c-5p	0,008	1,43	down
miR-30a-5p	0,030	1,39	down
miR-300-3p	0,077	1,30	up
miR-652-3p	0,070	1,29	down
miR-186-5p	0,100	1,24	down
miR-103-3p	0,070	1,11	down

Supplementary Table S4. Significantly dys-regulated miRNAs in the GCL of chronically epileptic compared with control animals.

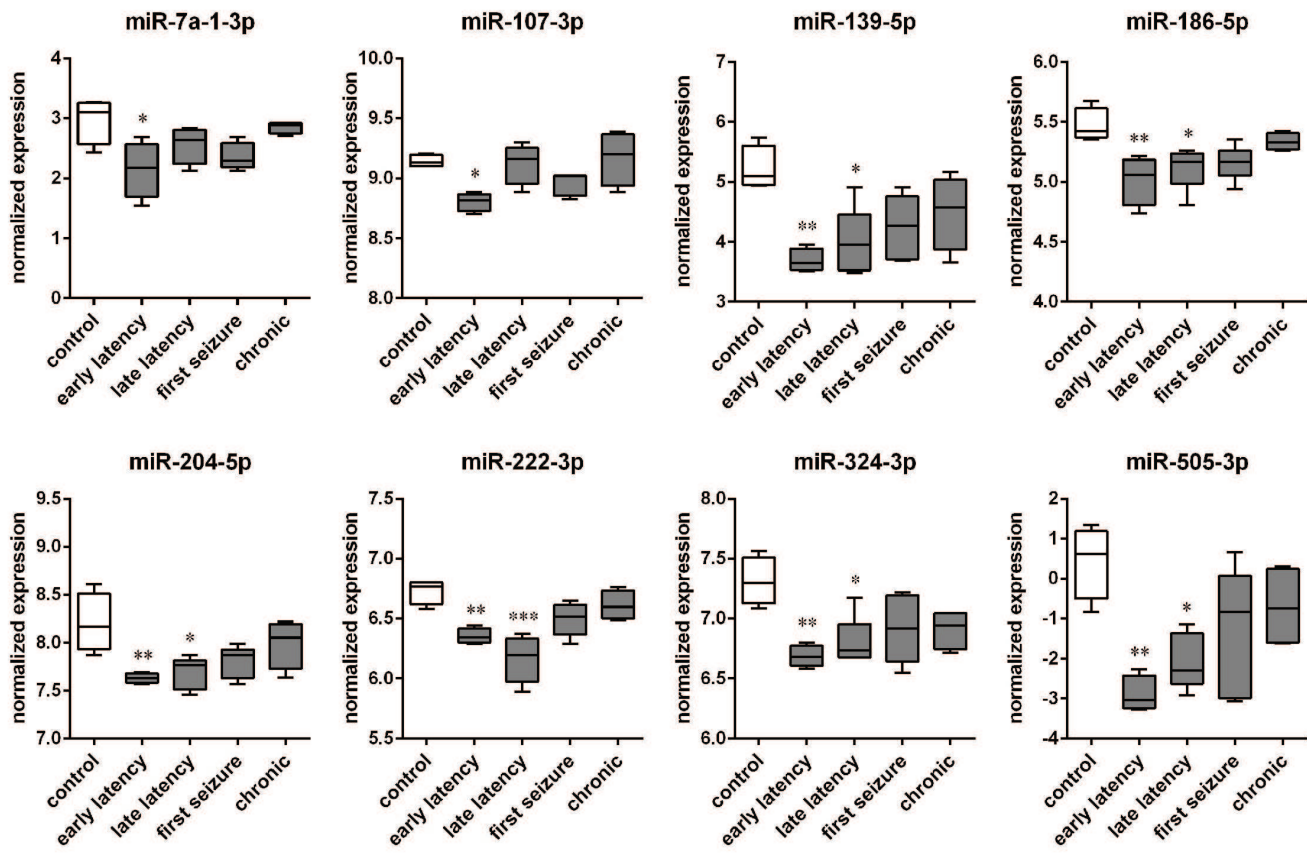
	P	Fold change	Regulation
miR-154-3p	8,608 ⁻⁰⁴	36,68	up
miR-146a-5p	4,274 ⁻⁰²	21,24	up
miR-344b-2-3p	8,079 ⁻⁰²	18,01	up
miR-31a-5p	4,962 ⁻⁰²	4,53	down
miR-181d-5p	2,018 ⁻⁰²	3,62	up
miR-132-3p	2,018 ⁻⁰²	3,51	up
miR-551b-3p	2,357 ⁻⁰²	2,75	down
miR-212-3p	2,018 ⁻⁰²	2,39	up
miR-873-5p	2,768 ⁻⁰²	2,28	down
miR-652-3p	2,018 ⁻⁰²	1,93	down
miR-181c-5p	5,467 ⁻⁰²	1,91	up
miR-23a-3p	2,018 ⁻⁰²	1,84	up
miR-433-5p	2,357 ⁻⁰²	1,71	up
miR-433-3p	5,082 ⁻⁰²	1,70	up
miR-409a-5p	8,079 ⁻⁰²	1,60	up
miR-410-3p	8,079 ⁻⁰²	1,53	up
miR-1949	4,274 ⁻⁰²	1,48	down
miR-380-3p	8,079 ⁻⁰²	1,45	up
miR-30a-5p	2,392 ⁻⁰²	1,45	down
miR-411-3p	8,079 ⁻⁰²	1,40	up
miR-140-3p	8,079 ⁻⁰²	1,32	down
miR-664-3p	8,079 ⁻⁰²	1,31	down
miR-29c-5p	2,018 ⁻⁰²	1,28	down
miR-21-5p	5,214 ⁻⁰²	1,25	up
miR-148b-3p	8,079 ⁻⁰²	1,23	down

Supplementary Table S5. Significantly dys-regulated miRNAs in the plasma of epileptic compared with control animals.

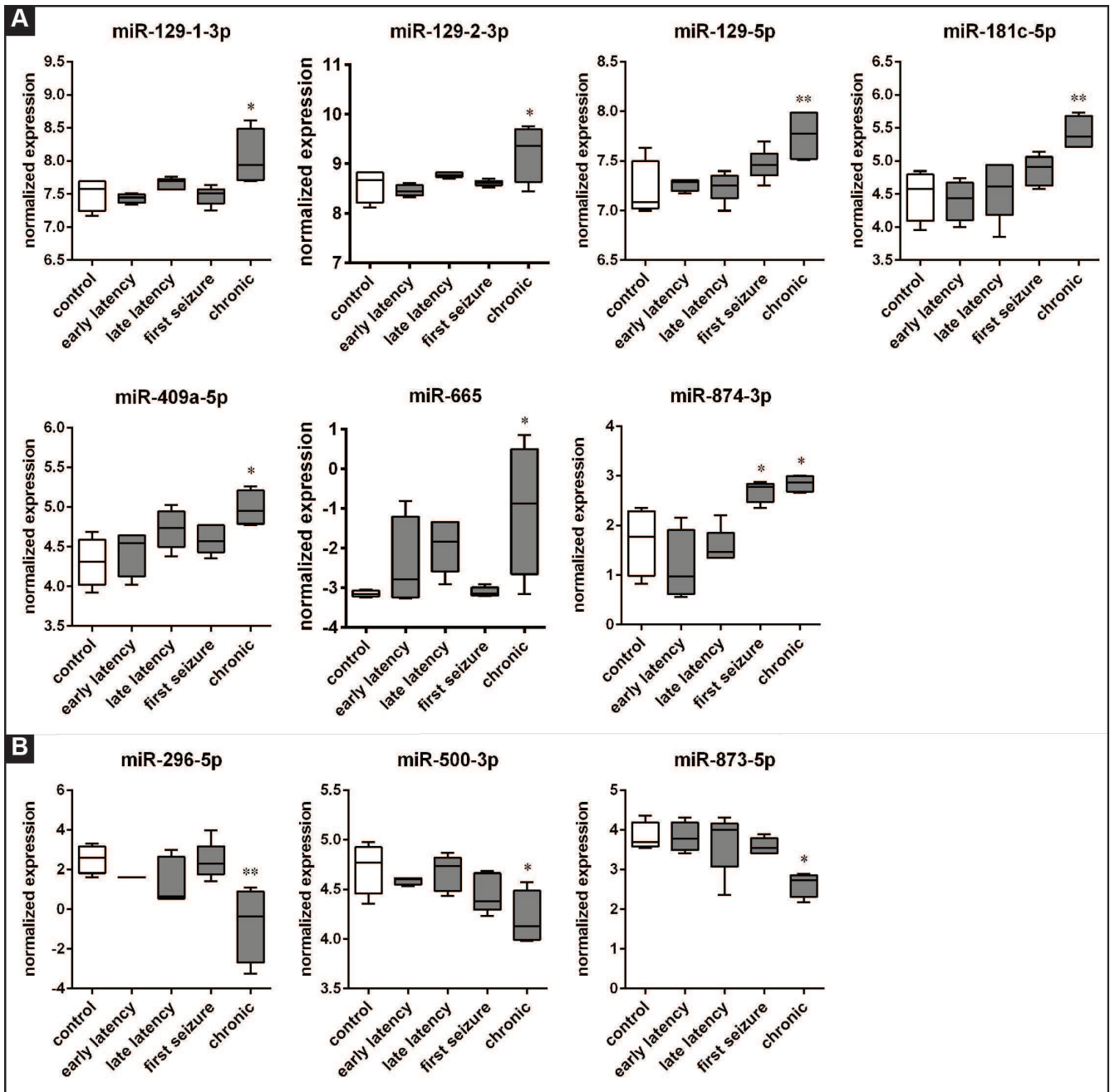
miRNA	P	P adjusted
miR.598.5p	0,0002	0,0833
miR.300.3p	0,0160	0,4286
miR.381.3p	0,0069	0,4286
miR.3582	0,0027	0,4286
miR.199a.5p	0,0076	0,4286
miR.181a.1.3p	0,0131	0,4286
miR.30c.2.3p	0,0103	0,4286
miR.10b.5p	0,0164	0,4286
miR.214.3p	0,0097	0,4286
miR.466b.1.3p	0,0099	0,4286
miR.144.3p	0,0141	0,4286
miR.142.3p	0,0154	0,4286
miR.3065.3p	0,0074	0,4286
miR.125b.2.3p	0,0263	0,4853
miR.466c.3p	0,0300	0,4853
miR.429	0,0326	0,4853
miR.32.3p	0,0329	0,4853
miR.374.5p	0,0234	0,4853
miR.208a.5p	0,0323	0,4853
miR.328a.3p	0,0278	0,4853
miR.210.3p	0,0328	0,4853
miR.494.3p	0,0231	0,4853
miR.465.5p	0,0324	0,4853
miR.142.5p	0,0375	0,5293
miR.1188.3p	0,0395	0,5353
miR.770.3p	0,0467	0,5676
miR.101b.3p	0,0486	0,5676
miR.598.5p	0,0477	0,5676
miR.300.3p	0,0160	0,4286



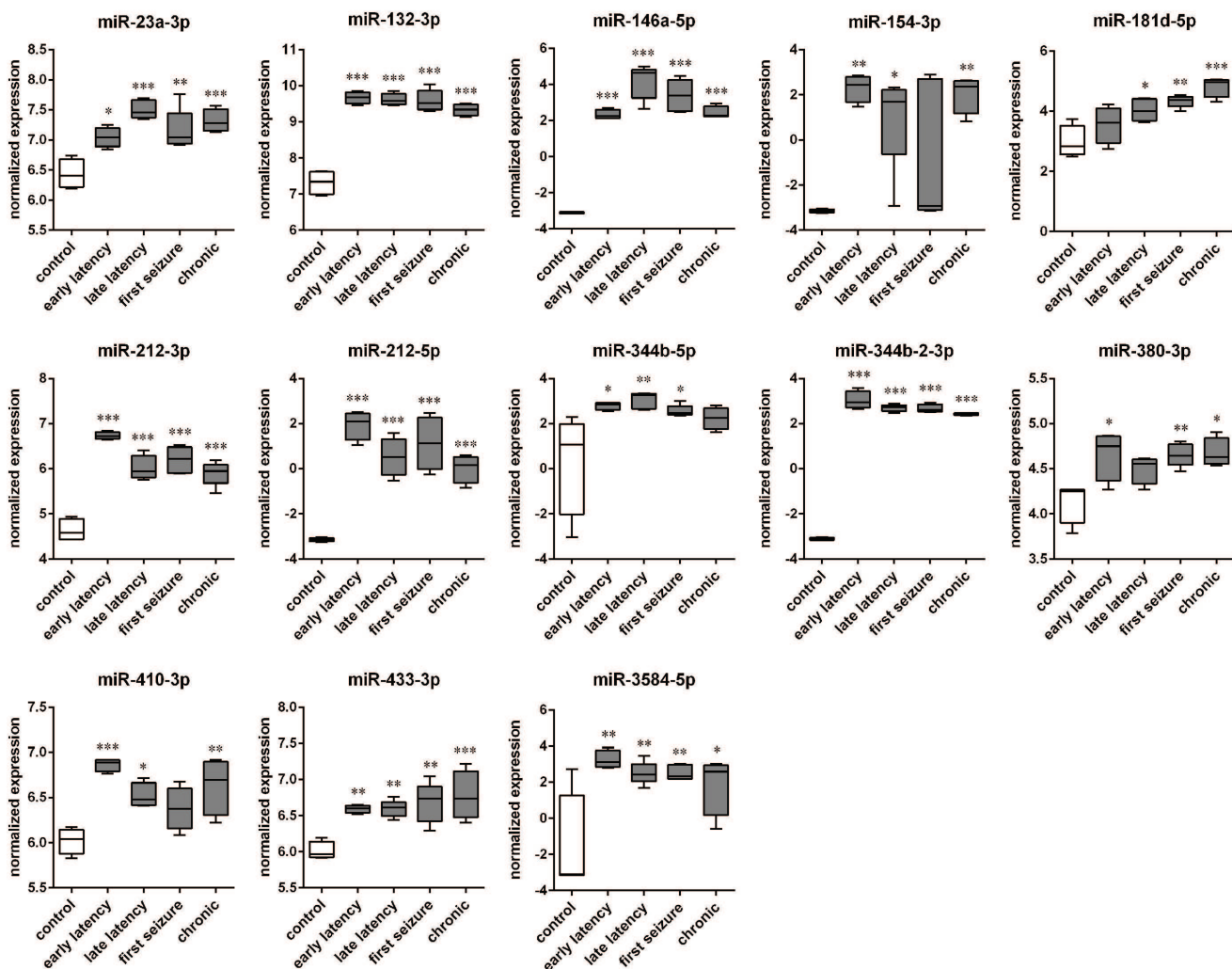
Supplementary Fig. S1. Up-regulated miRNAs in the rat granule cell layer (GCL) during latency. The boxplots depict the time course of expression for 17 of the miRNAs identified as significant with a false discovery rate (FDR)<10% in the GCL by using one-way ANOVA. Each boxplot represents 4 animals. * $p < 0.05$; ** $p < 0.01$; *** $p < 0.001$; Tukey's test.



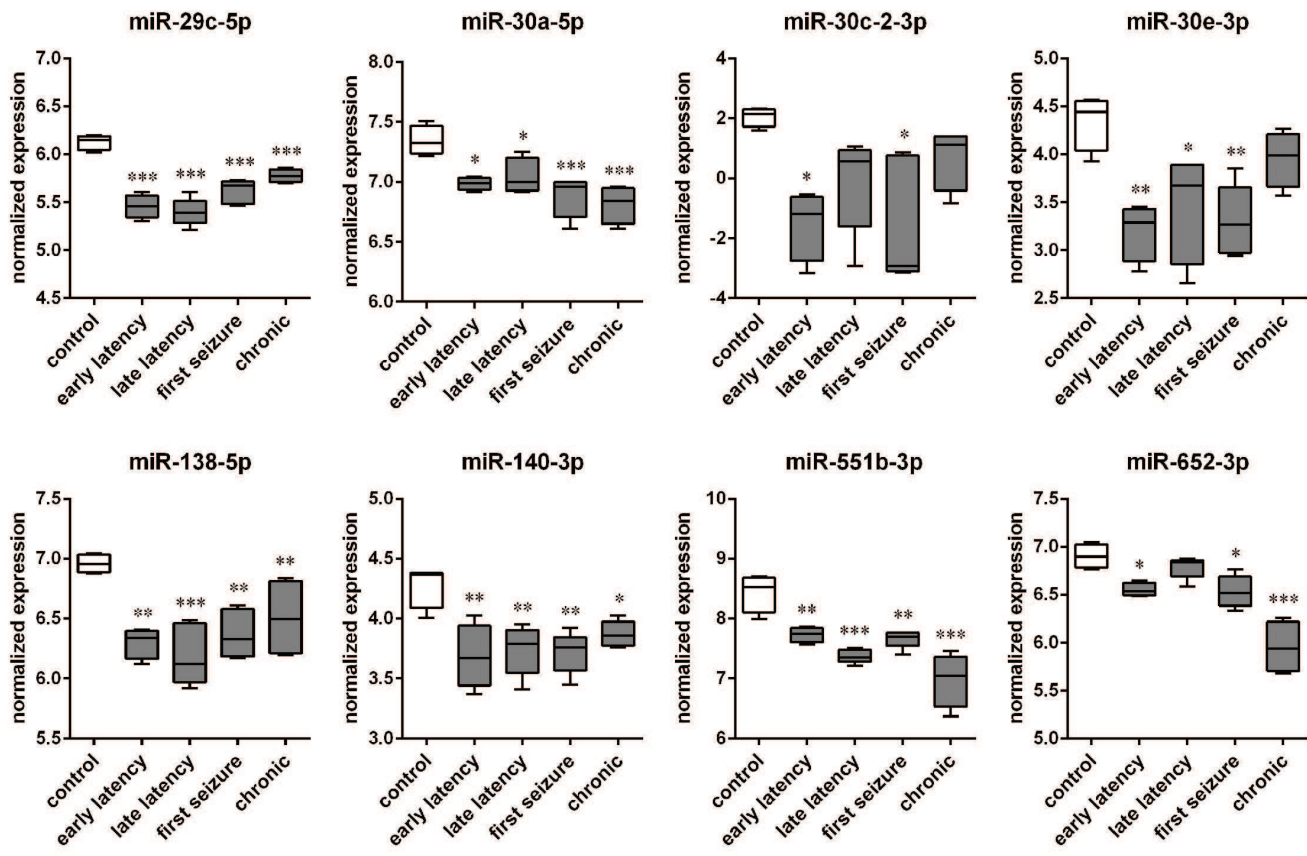
Supplementary Fig. S2. Down-regulated miRNAs in the rat granule cell layer (GCL) during latency. The boxplots depict the time course of expression for 8 of the miRNAs identified as significant with a false discovery rate (FDR)<10% in the GCL by using one-way ANOVA. Each boxplot represents 4 animals. * $p < 0.05$; ** $p < 0.01$; *** $p < 0.001$; Tukey's test.



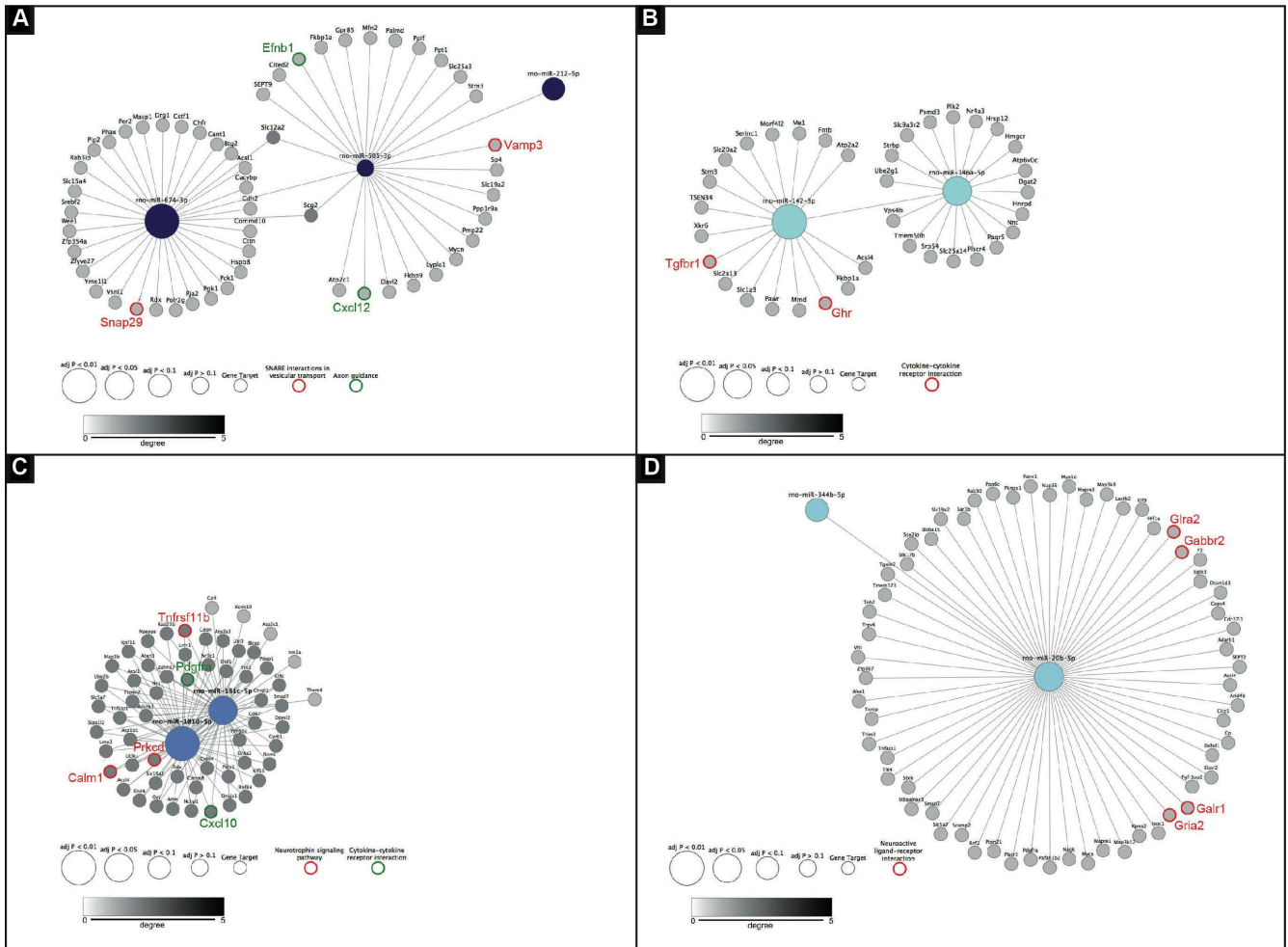
Supplementary Fig. S3. Deregulated miRNAs in the rat granule cell layer (GCL) during the chronic phase. The boxplots depict the time course of expression for 7 up-regulated (A) and 3 down-regulated (B) miRNAs identified as significant with a false discovery rate (FDR)<10% in the GCL by using one-way ANOVA. Each boxplot represents 4 animals. * $p < 0.05$; ** $p < 0.01$; *** $p < 0.001$; Tukey's test.



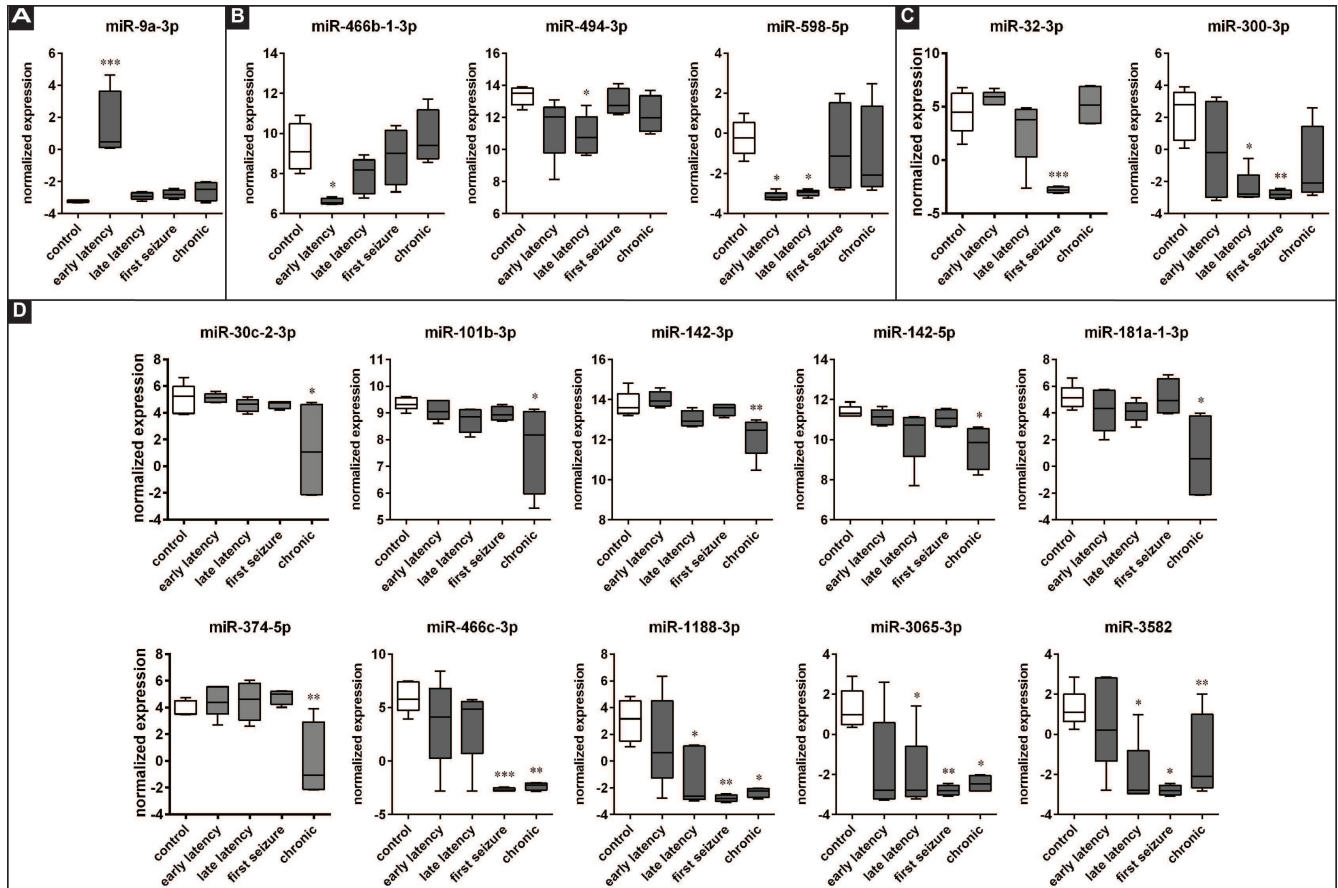
Supplementary Fig. S4. Up-regulated miRNAs in the rat granule cell layer (GCL) during latency. The boxplots depict the time course of expression for 13 of the miRNAs identified as significant with a false discovery rate (FDR)<10% in the GCL by using one-way ANOVA. Each boxplot represents 4 animals. * p<0.05; ** p < 0.01; *** p<0.001; Tukey's test.



Supplementary Fig. S5. Down-regulated miRNAs in the rat granule cell layer (GCL) during latency. The boxplots depict the time course of expression for 8 of the miRNAs identified as significant with a false discovery rate (FDR)<10% in the GCL by using one-way ANOVA. Each boxplot represents 4 animals. * $p < 0.05$; ** $p < 0.01$; *** $p < 0.001$; Tukey's test.



Supplementary Fig. S6. Network analysis. Predicted gene targets for each miRNA dys-regulated during latency (4 and 8 days after SE), obtained using the mirDB and TargetScan algorithms, were filtered with all miRNAs expressed in the dentate gyrus of rats (database GSE49850). (A) Cluster 1. (B) Cluster 3; (C) Cluster 4. (D) Cluster 5. Gene ontology (GO) and Kyoto Encyclopedia of Genes and Genomes (KEGG) analysis were performed using webgestalt, $p < 0.05$.



Supplementary Fig. S7. Deregulated miRNAs in the rat plasma during the all phases of the disease. The boxplots depict the time course for 16 of the miRNAs identified as significant by using one-way Anova. Each boxplot represents 5 animals. (A) miRNAs up-regulated during latency; (B) miRNAs down-regulated during latency; (C) miRNAs down-regulated in the first spontaneous seizure period; (D) miRNAs down regulated in the chronic period.

Is autopsy tissue a valid control for epilepsy surgery tissue in microRNA studies?

Running head: Microarray: autaptic vs bioptic tissues

Paolo Roncon MS¹, Silvia Zucchini PhD^{1,2,3}, Manuela Ferracin PhD^{3,4}, Gianluca Marucci MD⁵, Marco Giulioni MD⁶, Roberto Michelucci MD⁷, Guido Rubboli MD^{7,8}, Michele Simonato MD^{1,2,3}

¹ *Department of Medical Sciences, Section of Pharmacology and Neuroscience Center, University of Ferrara, 44121, Italy;*

² *National Institute of Neuroscience, Italy;*

³ *Laboratory for Technologies of Advanced Therapies (LTTA), University of Ferrara, 44121, Italy;*

⁴ *Department of Morphology, Surgery and Experimental Medicine, Section of Pathology, Oncology and Experimental Biology, University of Ferrara, 44121, Italy;*

⁵ *Section of Pathology "M. Malpighi", Bellaria Hospital, Azienda USL - IRCCS Institute of Neurological Sciences, Bologna, 40139, Italy;*

⁶ *IRCCS Institute of Neurological Sciences, Section of Neurosurgery, Bellaria Hospital, Bologna, 40139, Italy;*

⁷ *IRCCS Institute of Neurological Sciences, Section of Neurology, Bellaria Hospital, Bologna, 40139, Italy;*

⁸ *Danish Epilepsy Center, Filadelfia/University of Copenhagen, Dianalund, 4293, Denmark.*

Corresponding author:

Paolo Roncon
Department of Medical Sciences, Section of Pharmacology
University of Ferrara
Via Fossato di Mortara 17-19
44121 Ferrara, Italy

Tel: (+39) 0532 455345

Fax: (+39) 0532 455205

e-mail address: paolo.roncon@unife.it

Number of characters in the title: 82

Number of characters in the running head: 38

Number of words in the abstract: 186

Number of words in the manuscript: 1644

Number of figures: 1

Number of tables: 3

Abstract

Background

MicroRNAs (miRNA) are differentially expressed in the brain under pathological conditions and may therefore represent both therapeutic targets and diagnostic or prognostic biomarkers for neurological diseases, including epilepsy. In fact, miRNA expression profiles have been investigated in the hippocampi of epileptic patients in comparison with control, non-epileptic cases. Unfortunately, the interpretation of these data is difficult because surgically resected epileptic tissue was compared with control tissue obtained from autopsies.

Materials and methods

To challenge the validity of this approach, we performed a miRNA microarray on the laser micro-dissected granule cell layer of the human hippocampus obtained from surgical samples of epileptic patients, autoptic non-epileptic controls and autoptic epileptic patients, using the latter as internal control.

Results and conclusions

Hierarchical clustering of all samples showed that those obtained from autopsies of epilepsy patients segregated with the other autoptic samples (controls) and not with the bioptic tissues from the surgery patients, i.e. that the origin of the tissue (surgery or autopsy) was prevalent over the underlying pathology (epilepsy or not epilepsy). This observation arises serious concerns on the use of autopsy controls for this kind of studies.

Introduction

MicroRNAs, or miRNAs, are small, endogenous, non-coding RNAs of about 18-24 nucleotides that regulate gene expression at post-transcriptional level, inhibiting mRNA translation with or without transcript degradation¹. About 70% of the known miRNAs are expressed in the brain, and many are specific to neurons². Based on these observations, it has been hypothesized that miRNAs might actively participate to the pathogenesis of central nervous system (CNS) diseases, and their expression levels and functions have been investigated in many neurological disorders, including Alzheimer disease, Parkinson disease^{3,4} and the temporal lobe epilepsy (TLE)⁵⁻⁹.

MiRNAs may represent novel therapeutic targets for these diseases. For example, the silencing of miR-134 has been demonstrated to exert prolonged seizure-suppressant and neuroprotective actions in a murine model of epilepsy¹⁰. Moreover, miRNAs may serve as disease biomarkers^{11,12}. With reference to epilepsy, studies in rodents found a correlation between specific miRNA expression patterns (in the brain and in the peripheral blood) and the phase of the disease^{5,7,8}. If confirmed in humans, these may help to predict patients that will develop epilepsy after a potentially epileptogenic insult. Moreover, analysis of miRNA expression patterns in surgical samples may help in the prognostic evaluation of post-surgical epilepsy⁶.

MiRNAs expression profiles have been also investigated in the hippocampus of TLE patients in comparison with control, non-epileptic cases¹³⁻¹⁵. Unfortunately, the interpretation of these data remains difficult because the control tissue used to investigate miRNA expression levels was from autopsies whereas the epileptic tissue was from surgical specimens, and it is questionable if autopsy samples are valid controls for surgical epilepsy

samples. Therefore, the aim of this study was to challenge the validity of this approach. We performed a miRNA microarray on the laser micro-dissected granule cell layer of the hippocampus obtained from bioptic (surgical) samples of TLE patients, autoptic (non-epileptic) controls and autoptic epileptic patients, using these last as “internal control” for the hierarchical cluster analysis. The assumption was that, if autopsy controls were valid, the autopsy epilepsy group would segregate with the surgery epilepsy group. If instead the controls were not valid, i.e. if the post-mortem condition was prevalent over the disease condition, the autopsy epilepsy group would segregate with the autopsy control group.

Materials and methods

Patients and controls

The present study was approved by the Ethics Committee of Bologna (Comitato Etico Indipendente dell’Azienda USL della Città di Bologna). Surgical hippocampal samples from 12 drug resistant TLE patients (3 males and 9 females) were collected at the Epilepsy Surgery Center of the IRCCS Institute of Neurological Sciences of Bologna (Table 1). Patients signed a comprehensive written informed consent for the research use of the tissue obtained from surgery. Epileptological evaluation, wakefulness/sleep EEG and continuous long-term video EEG monitoring for seizure recording were performed on all epileptic patients before surgery. Ictal clinical and EEG semiology and electroclinical correlations were used to identify the epileptogenic area. Brain MRI and CT scan (when necessary) were also used for proper

identification of the epileptogenic focus. The main surgical specimens (hippocampus and/or temporal pole) were removed “en bloc” and spatially oriented to allow a proper histopathological examination. All the methods were carried out in accordance with the approved guidelines, all information regarding the human material was managed using anonymous numerical codes, and samples were handled in compliance with the Helsinki declaration (<http://www.wma.net/en/30publications/10policies/b3/>).

Autoptic hippocampal tissue was from 2 epileptic patients (both females) who died of lung pathologies (Table 2) and 10 patients (3 males and 7 females) without history of epilepsy or seizures (Table 3).

Histology and microdissection

Tissue obtained from surgeries and autopsies was formalin fixed and paraffin embedded. Ten-micron-thick sections were cut using a microtome and mounted on slides for laser microdissection (LMD). Samples were de-waxed using Bio-Clear (Bio-Optica, Milan, Italy), washed in ethanol and stained with hematoxylin. LMD was then performed essentially as previously described (Zucchini et al, 2014). Briefly, slides were positioned in a stencil laser (SL) microcut microtest dissector (Nikon, Tokio, Japan). The intensity, aperture and cutting velocity were calibrated to obtain the sharpest cut with the minimal intensity, and the pulsed UV laser beam was carefully directed along the borders of the dentate gyrus granule cell layer (GCL). GCLs were then collected in microcut transfer film (Nikon). In order to obtain an adequate amount of tissue for RNA purification, the microdissected GCL from at least 3-4 slices per patient was pooled together. Total RNA was extracted using an RNA purification kit (RecoverAll Total Nucleic Acid Isolation kit, Life Technologies, CA, USA). All samples were analyzed using an Agilent 2100 Bioanalyzer to evaluate the quality of total RNA; the

concentration and quality of the RNA were confirmed using a NanoDrop 1000 spectrophotometer (Thermo Scientific, Waltham, MA, U.S.A.).

Hierarchical clustering

One hundred ng of total RNA per sample were employed for microarray analysis (Human micro-RNA Microarray V3, #G4470C, Agilent Technologies, Santa Clara, CA, USA). The chip consisted of 60-mer DNA probes and allowed simultaneous analysis of 1200 human miRNAs obtained from the Sanger miR-BASE database (Release 10.1). RNA labeling and hybridization were performed according to the manufacturer's indications. Row data were obtained using a Agilent scanner and the Feature Extraction 10.5 software (Agilent Technologies).

The GeneSpring GX 12 software (Agilent Technologies) was employed to analyze microarray results. All negative values were transformed at 1.0, followed by Quantile normalization and log₂ transformation. Differentially expressed miRNAs were identified by comparing autoptic controls with autoptic and bioptic epileptic samples, applying a 2 fold-change filter, the Mann Whitney test and Benjamini-Hochberg correction (adjusted $p < 0.05$). Manhattan correlation was used for cluster analysis.

Results

Subjects

Surgical specimens from twelve TLE patients indicated in numbers in Table 1 were laser-microdissected and employed for microarray analysis. Neuropathological examination evidenced that all these patients had type 1 hippocampal sclerosis¹⁷. This group was composed of 3 males and 9 females, with mean age at surgery of 39 (31-60), mean years after epilepsy diagnosis of 24 (7-38) and approximately 10 seizures per month before surgery (2 to >30). The two autoptic TLE specimens (Table 2, cases 13 and 14) also had type 1 hippocampal sclerosis. They were from two females with mean age at death of 58 (46,70), who died for lung diseases (pulmonary edema, pneumonia). Information on time from diagnosis and number of seizures per day was available only for case 13 (death 48 years after diagnosis; 4-30 seizures/month).

Control specimens were from ten non epileptic individuals listed in Table 3 (cases 15-24). This group was composed of 3 males and 7 females with mean age at death of 46 (34-57), who died for lung or heart diseases (pulmonary edema, pneumonia, pulmonary thromboembolism, myocardial infarction) except for cases 15 and 20, who died for cerebral infarction.

Microarray

We investigated miRNAs expression in the laser-microdissected granule cell layer (GCL) from the three groups: surgical specimens of epileptic patients, autoptic samples of cases without history of epilepsy and autoptic samples from TLE patients. After comparing epileptic (both autoptic and bioptic) and control samples, we detected significant changes in the expression levels of 106 miRNAs. Hierarchical clustering of all samples showed that all surgical epilepsy samples except one (case 10) separated from the autopsy controls. However, the 2 samples obtained from autopsies of TLE patients segregated with the other autoptic

samples (controls) and not with the bioptic tissues from the surgery patients (Fig 1), suggesting a relevant difference between the two specimen types.

Discussion

Previous studies have explored differences between miRNA expression patterns in surgical epileptic tissue compared with autoptic control tissue¹³⁻¹⁵. However, the possible bias generated by the utilization of post-mortem tissue was not evaluated in depth. This study aimed at addressing this specific issue, by introducing in the comparison a third group, i.e. autopsy specimens from individuals with epilepsy. We acknowledge that a limitation of the present study is the very limited number of cases in this group (two only). Unfortunately, it is very difficult to obtain autopsy tissue from patients with a documented history of epilepsy, who died for non-epilepsy-related causes. Even if it would have been desirable to have a larger cohort of such cases, the segregation of these two cases with the other autopsy, non-epileptic ones (and not with the surgical epileptic, as expected) is very clear. This may depend on post-mortem modifications and/or on differences in tissue preparation (formalin fixation vs. fresh tissue). In any event, the observation poses very serious concerns on the use of autopsy controls for this kind of studies.

A possible approach that may be proposed to use control autopsy cases in these studies, thereby integrating the limited number of epilepsy autopsy cases with the much more readily available surgical ones, may be to first run cluster analysis of microarray data to compare autoptic epileptic with autoptic controls, and then perform a further hierarchical

clustering based on those miRNAs identified as differentially expressed in the first step while including the surgical samples. We explored this possibility with our samples, and observed significant changes in the expression levels of 36 miRNAs between autoptic epileptic and autoptic controls. When cluster analysis has been run including all groups, the two autoptic epileptic cases segregated with the other epileptic and not with the other autopsies (data not shown). Although these data must be viewed as preliminary, being based on the only two autoptic epilepsy cases, they appear to provide more accurate information than the surgery-epilepsy vs. autopsy-control approach. In fact, this analysis identified some up-regulated miRNAs that were found positive also in animal models^{5,7,8}. Nonetheless, further analysis with increased cohorts of autoptic TLE cases will be needed to unequivocally identify TLE-dependent miRNA expression changes.

In conclusion, microarrays platforms can provide important insights in the search for novel biomarkers or therapeutic targets, but limitations in the experimental approach must be carefully considered. The present results show that tissue origin and/or processing can have greater impact than the disease background on the data generated, with a serious hindrance in their interpretation.

Authors contribution

P.R. and M.S. designed the study and wrote the manuscript. P.R. and S.Z. performed the experiments. M.F. performed bioinformatics analyses. M.G., G.M., R.M. and G.R. prepared the human samples.

Acknowledgements

The research leading to these results has received funding from the European Union's Seventh Framework Programme (FP7/2007-2013) under grant agreement no. 602102 (EPITARGET).

Submitted

References

1. Bartel DP. MicroRNAs: genomics, biogenesis, mechanism, and function. *Cell* 2004; 116(2): 281-97.
2. Cao X, Yeo G, Muotri RA et al. Noncoding RNAs in the mammalian central nervous system. *Annu Rev Neurosci* 2006; 29:77-103.
3. Femminella GD, Ferrara N, Rengo G. The emerging role of microRNAs in Alzheimer's disease. *Front Physiol* 2015; 12: 6-40.
4. Margis R, Margis R, Rieder CRM. Identification of blood microRNAs associated with Parkinson's disease. *J of Biotech* 2011; 152:96-101.
5. Roncon P, Soukupová M, Binaschi A, et al. MicroRNA profiles in hippocampal granule cells and plasma of rats with pilocarpine-induced epilepsy – comparison with human epileptic samples. *Sci Rep* 2015; 5:14143. doi: 10.1038/srep14143.
6. Zucchini S, Marucci G, Paradiso B, et al. Identification of miRNAs differentially expressed in human epilepsy with or without granule cell pathology. *PLoS ONE* 2014; 9(8):e105521. doi:10.1371/journal.pone.0105521.
7. Gorter JA, Iyer A, White I, et al. Hippocampal subregion-specific microRNA expression during epileptogenesis in experimental temporal lobe epilepsy. *Neurobiol Dis* 2014; 62: 508-20.
8. Bot AM, Dębski KJ, Lukasiuk K. Alterations in miRNA levels in the dentate gyrus in epileptic rats. *PLoS One* 2013; 8(10): e76051. doi: 10.1371/journal.pone.0076051.
9. Jimenez-Mateos EM, Bray I, Sanz-Rodriguez A, et al. miRNA Expression profile after status epilepticus and hippocampal neuroprotection by targeting miR-132. *Am J Pathol* 2011; 179(5): 2519-32.

10. Jimenez-Mateos EM, Engel T, Merino-Serrais P, et al. Silencing microRNA-134 produces neuroprotective and prolonged seizure-suppressive effects. *Nat Med* 2012; 18(7):1087-94.
11. Wang J, Chen J, Sen S. microRNA as biomarkers and diagnostics. *J Cell Physiol* 2016; 231(1):25-30.
12. Rossignol E, Kobow K, Simonato M, et al. WONOEP appraisal: new genetic approaches to study epilepsy. *Epilepsia* 2014; 55(8):1170-86.
13. Kaalund SS, Venø MT, Bak M, et al. Aberrant expression of miR-218 and miR-204 in human mesial temporal lobe epilepsy and hippocampal sclerosis-convergence on axonal guidance. *Epilepsia* 2014; 55(12):2017-27.
14. Kan AA, van Erp S, Derijck AA, et al. Genome-wide microRNA profiling of human temporal lobe epilepsy identifies modulators of the immune response. *Cell Mol Life Sci* 2012; 69(18): 3127-45.
15. McKiernan RC, Jimenez-Mateos EM, Bray I, et al. Reduced mature microRNA levels in association with dicer loss in human temporal lobe epilepsy with hippocampal sclerosis. *PLoS ONE* 2012; 7: e35921. doi: 10.1371/journal.pone.0035921.
16. Blümcke I, Thom M, Aronica E, et al. International consensus classification of hippocampal sclerosis in temporal lobe epilepsy: a Task Force report from the ILAE Commission on Diagnostic Methods. *Epilepsia* 2013; 54(7):1315-29.

Figure Legends

Figure 1. Cluster analysis of miRNAs differentially expressed in the granule cell layer (GCL) in TLE patients (including 2 autoptic epileptic cases) and in the control group. Each column represents an individual case and each row represents one miRNA. Colors represent the miRNA expression level in each sample, referred to miRNA average expression: higher-red, lower-green. Differentially expressed miRNAs were identified applying a 2 fold-change filter, the Mann Whitney test and Benjamini-Hochberg correction (adjusted $p < 0.05$).

Submitted

Tables

Table 1. Epileptic patients who underwent surgery.

Patient number	Gender	Age at surgery	Epileptogenic insult	Years after diagnosis	Seizures per month	Drug therapy
01	M	60	None	38	>30	VPA, CBZ, TGB
02	F	50	None	38	5-12	CBZ, TPM, PB
03	M	44	None	12	3-8	TPM, LVT
04	M	36	None	7	8-10	LVT, PB, CLB
05	F	47	None	33	2-3	PB, CBZ
06	F	33	Febrile convulsions	30	4-5	TPM, CBZ, VPA, PB
07	F	31	Febrile convulsions	18	3-8	LVT, CBZ, CLB
08	F	31	Febrile convulsions	10	8-12	PB, TPM
09	F	33	Febrile convulsions	24	3-4	LTG, LVT, PB
10	F	32	Febrile convulsions	27	4-10	CBZ
11	F	32	Febrile convulsions	20	9-10	OXC, LVT
12	F	37	Febrile convulsions	35	7-10	CBZ, TPM

Abbreviations: CBZ, carbamazepine; CLB, clobazam; LTG, lamotrigine; LVT, levetiracetam; OXC, oxcarbazepine; PB, pentobarbital; TGB, tiagabine; TPM, topiramate; VPA, valproic acid.

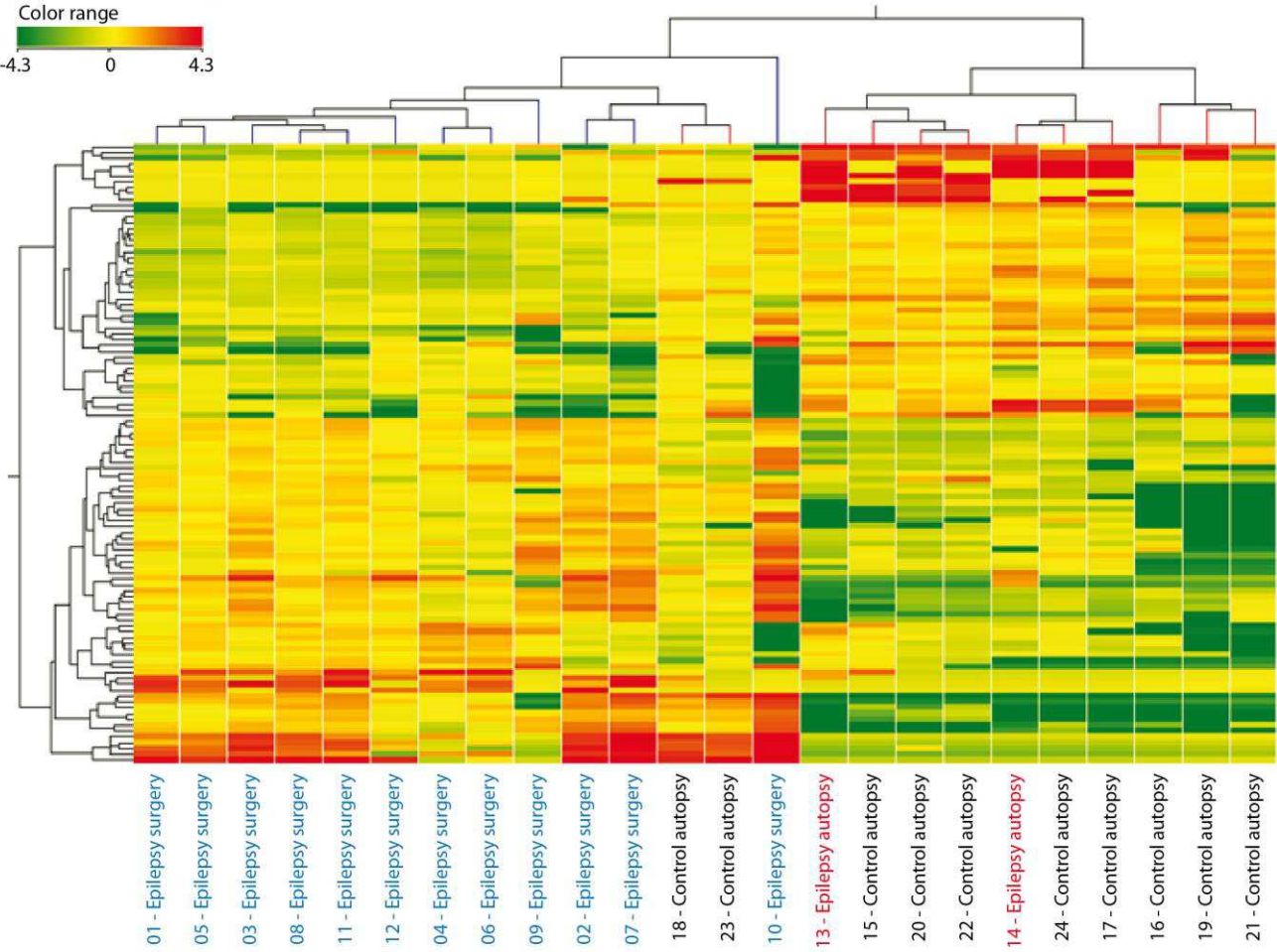
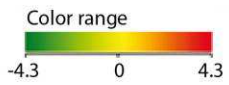
Table 2. Autoptic epileptic cases included in the study.

Patient number	Gender	Age at death	Epileptogenic insult	Years after diagnosis	Seizures per month	Post mortem delay (hrs)	Cause of death
13	F	70	Trauma	48	4-30	44	Pneumonia
14	F	46	Cryptogenic	4	25-30	26	Pulmonary edema

Submitted

Table 3. Autoptic non-epileptic cases included in the study.

Case number	Gender	Age at death	Post mortem delay (hrs)	Cause of death
15	M	40	38	Cerebral infarction
16	F	47	35	Myocardial infarction
17	F	51	26	Pulmonary edema
18	F	34	34	Pneumonia
19	M	38	24	Myocardial infarction
20	F	48	25	Cerebral infarction
21	F	44	28	Pulmonary thromboembolism
22	F	57	55	Pulmonary thromboembolism
23	F	50	42	Pulmonary edema
24	M	56	20	Pulmonary thromboembolism



Meta-analysis of microRNAs dysregulated in different models of epilepsy

Roncon P^{1*}, Srivastava P^{2*}, Lukasiuk K³, Gorter JA⁴, Aronica E⁴, Petretto E⁵, Pitkänen A⁶,
Johnson MR², Simonato M.^{1,7,8}

¹ *Department of Medical Sciences, Section of Pharmacology and Neuroscience Center, University of Ferrara, Italy;*

² *Division of Brain Sciences, Imperial College London, Charing Cross Hospital, UK;*

³ *Nencki Institute of Experimental Biology, Polish Academy of Sciences, Warsaw, Poland;*

⁴ *Department of (Neuro)Pathology, Academic Medical Center and Swammerdam Institute for Life Sciences, Center for Neuroscience University of Amsterdam, The Netherlands; SEIN – Stichting Epilepsie Instellingen Nederland, Heemstede, The Netherlands;*

⁵ *Duke-NUS Graduate Medical School, 8 College Road, Singapore 169857, Singapore;*

⁶ *Department of Neurobiology, Head A.I. Virtanen Institute for Molecular Sciences University of Eastern Finland (UEF), Kuopio, Finland;*

⁷ *National Institute of Neuroscience, Italy;*

⁸ *Laboratory for Technologies of Advanced Therapies (LTTA).*

** These authors contributed equally to this work.*

Corresponding author:

Paolo Roncon
Department of Medical Sciences, Section of Pharmacology
University of Ferrara
Via Fossato di Mortara 17-19
44121 Ferrara, Italy

Tel: (+39) 0532 455345
Fax: (+39) 0532 455205
e-mail address: paolo.roncon@unife.it

Abstract

Background

Temporal lobe epilepsy (TLE) often develops secondary to an initial brain insult after a latency period in which patients are apparently well. Patients at-risk of developing epilepsy following brain injury cannot be identified, and the available anti-epileptic drugs are ineffective in preventing the development of epilepsy. MicroRNAs (miRNAs) are promising candidates to become therapeutic targets for both prevention and treatment. Since it is impossible to study miRNA changes in the human brain during the latency phase, animal models have been used. However, individual studies have been relatively underpowered to detect the spectrum of miRNA changes associated with epileptogenesis and epilepsy.

Aims

We performed a meta-analysis of miRNA microarray studies in the latency and in the chronic phases of experimental animal models of TLE, in order to (a) provide increased power to identify miRNAs associated with epileptogenesis and epilepsy and (b) detect miRNA changes across heterogeneous models of epilepsy.

Methods

Following Z-score transformation of miRNA expression in each dataset, we performed the meta-analysis using a random effects model with the DerSimonian and Laird method.

Results and Conclusions

The analysis identified 44 miRNAs that are significantly dysregulated during latency and 8 miRNAs dysregulated in the chronic epileptic phase, as compared to the control group. The dysregulation of these miRNAs may be disease-mediated rather than model-dependent. Gene Ontology enrichment analysis on the validated targets of those miRNAs that are differentially

expressed in latency revealed terms connected to specific neuronal fields. However, further analyses are required to establish which miRNAs regulate epileptogenic pathways.

Introduction

Epilepsy is a neurological disorder affecting 1% of the world's population. Temporal lobe epilepsy (TLE) is the most common form in adults, often arising after a latent period that can range from months to years, secondary to an initial brain insult (i.e. trauma, tumor or stroke). Available antiepileptic drugs are symptomatic agents that cannot prevent the development of the disease and are ineffective in approximately one-third of patients with epilepsy (Simonato et al, 2014). Thus, the studies are focusing on uncover the mechanisms of epileptogenesis and drug-resistance in order to develop antiepileptogenic therapies that can potentially prevent the disease in at-risk individuals and to identify new putative therapeutic targets for the cure of drug-resistance patients (Simonato et al, 2012; 2013; 2014). Evidence is emerging that microRNAs (miRNAs) may be crucial to the pathogenesis and have potential as therapeutic tools in prevention and treatment of neurological conditions (Gupta et al, 2015).

MiRNAs represent a family of small, noncoding RNAs of ~22 nucleotides that post-transcriptionally regulate gene expression through degradation or translational repression of the messenger RNA (mRNA) transcripts (Bartel, 2004). It is estimated that miRNAs regulate about the 60% of the mRNAs, indeed one miRNA can target hundreds of mRNAs, while a single target transcript may be regulated by many different miRNAs (Ebert and Sharp, 2012). Approximately the 70 % of all miRNA species are present in the brain (Cao et al, 2006).

These evidence highlight the putative role of miRNAs as powerful players in the regulation of specific neuronal functions and alterations in miRNAs levels have been demonstrated to produced effects in the pathogenesis of various neurological diseases (Hill and Lukiw, 2015; Cogoni et al, 2015; Filatova et al, 2012).

Increasing evidences have been described, through microarray analysis that miRNAs levels are altered in the brains of both epileptic patients as well as in animal models of disease. A miRNAs signature of hippocampal sclerosis has been identified through a genome-wide profiling of TLE-patients (Kan et al, 2012) and similarly, a recent study demonstrated the implication of miR-487a in the granule cell pathology (Zucchini et al, 2014). In animal models, changes in miRNA expression levels in the hippocampus have been reported in multiple studies in the latency period after an epileptogenic insult and in the chronic epileptic state (Jimenez-Mateos et al, 2011; Hu et al, 2012; Risbud et al, 2013; Bot et al, 2013; Gorter et al, 2014; Kretschmann et al, 2015; Roncon et al, 2015). Unfortunately, all these studies presented many methodological differences making them not easily comparable. For instance, the human studies lacked a proper control groups (i.e. autopsy) and in Zucchini et al (2014) the comparison had been made between epileptic patients with or without the granule cell pathology. Studies in animal models solved the problem of the proper controls and permitted the evaluation of the alterations of miRNAs expression levels in the phase of epileptogenesis, however few studies (Jimenez-Mateos et al, 2011; Hu et al, 2012; Risbud et al, 2013; Kretschmann et al, 2015) had been performed in total hippocampus with the use of different chip technologies. Only 3 microarray studies investigated the changes in the miRNA expression levels during the phase of epileptogenesis and in the chronic stage in the dentate gyrus (DG) of the hippocampus of epileptic rats (Bot et al, 2013; Gorter et al, 2014; Roncon

et al, 2015), avoiding the bias of cellular and molecular heterogeneity that may differentially influence the miRNAs enrichment in the RNA samples. These studies agreed in the up-regulated miRNAs: miR-21-5p, miR-212-3p and the miR-132-3p during the phase of latency, suggesting a role in the pathogenesis of the temporal lobe epilepsy. This “inconsistency” may be due to different animal models, and small samples size for the varying results obtained by different groups, accomplished by different laboratory protocols, microarray platforms and analysis techniques (Siddiqui et al, 2006). Studies have shown that the systematic combination of gene expression data from multiple datasets, so-called meta-analyses, can increase statistical power for detecting differentially expressed genes while allowing for an assessment of heterogeneity. Thus leading to more robust, reproducible and accurate predictions (Ramasamy et al, 2005; Yang et al, 2014).

A combinatorial-analysis has been performed by Kretschmann and colleagues (2015) on the miRNomes obtained from epileptic mice from different models: pilocarpine, SSSE and the 6-Hz model; although total hippocampus was employed for RNA purification. In this study we have performed a meta-analysis of miRNAs expression in the DG obtained from three different animal models of epilepsy. The aim of our analysis is standardize and solve the inconsistencies within the datasets, to overcome the limitations of individual studies. Finally, get more insights for uncovering the epileptogenesis and those mechanisms that lead to the seizures onset, and further generating new miRNA-candidate to become putative therapeutic targets for the cure of epilepsy.

Methods

Inclusion criteria and studies design

Animal models of epilepsy are widely used as a proxy for human epilepsy. Although, each model differ with each other in some aspects and there is a need to characterize the changes that are common to all animal model of epilepsy which might be translated to human epilepsy. To this end we studied the role of microRNAs for different stages of TLE in the DG. The choice of DG as tissue was based on the observation that as it has most homogenous population of in the hippocampus.

Here, we have collected datasets for meta-analysis on the available genome-wide expression profiles for the miRNAs that were generated on the DG from epileptic and control hippocampi during the phase of latency (for animal models), in this period rodents did not show any behavioral seizures and chronic phase of epilepsy where animals developed spontaneous seizures. The data were collected from the following models that were generated within the framework. To assess the functional classification of those miRNAs resulted significant from the meta-analysis, we included in the further investigation, miRNA and the gene expression data obtained from DG or the whole hippocampus from epileptic rodents and patients.

First, data were collected within the EPITARGET consortium. Second, we have undertaken a comprehensive systematic search to identified all published studies that deal with the comparison of miRNAs expression levels and/or the gene expression between cases (epileptic) and controls, in the DG of *in vivo* models of epilepsy and human patients. We conducted Pubmed/Google search based on the keywords: “microarray, epilepsy, dentate

gyrus”. MiRNAs or genes expression profiles data obtained from the whole hippocampi or different brain regions from the DG were not involved in the meta-analysis. However we have used these datasets to verify the conservation through species of those miRNAs and the pathways, in which they are involved, identified with the meta-analysis. Third, since experimental evidences in RNA analyses shown biases related to the tissue origins i.e. bioptic and autoptic (van der Linden et al, 2014), we did not consider human studies that performed the comparison between epileptic bioptic and “healthy” autoptic cases for the meta-analysis.

Considering different time points for each stage for the latency and the chronic phases have not been standardized we have considered data from those animals killed 7-8 days after status epilepticus (SE) for the “latency phase” and those killed more than 2 months after SE for the “chronic phase”. Further, to ensure the validity of the chosen time points, we have checked each study if the behavioral analysis were reported and we considered only those animals that did not show seizures at 7-8 days after the SE for the latency period and those that shown spontaneous recurrent seizures were considered for the investigation of chronic stage.

Moreover, we have made sure if the latency period duration for each study was in agreement with already published data (Gorter et al, 2001; Guzik-Kornacka et al, 2011; Soukupova et al, 2014, 2015).

Following models were considered for the meta-analysis : A, Pilocarpine model: a microarray study based on the investigation of miRNAs differential expression levels in the laser-microdissected granule cell layer of the dentate gyrus (DG) of the hippocampi of pilocarpine-induced epileptic rats and matched-controls, killed during the late phase of late latency, 8 days the status epilepticus and in the chronic stage, 50 days after the first spontaneous seizure (Roncon et al, 2015). B, Amygdala stimulation: a microarray study focused on the differential

expression miRNA and genes expression levels in handled dissected DG in the amygdala stimulation rat model during the phase of latency, 7 days after the stimulation, and in the chronic stage, 60 days after the stimulation (Bot et al, 2013). C, Perforant path stimulation: a microarray miRNAs study based on the perforant path stimulation rat model of epilepsy, and we have considered in the present study, just the DG samples obtained from stimulated and controls rat hippocampi, 8 days and 3-4 months after the stimulation, respectively for the latency and chronic stages (Gorter et al, 2014). The datasets considered for the meta-analysis is summarized in Table 1. For the first step of identification of an overlap of miRNAs expressed in different animal models, we considered also a dataset (not publicly available) obtained from rats that received a trauma brain injury (Figure 1).

Data preprocessing

The following information was extracted, from each identified study: platform, number of cases and controls, and miRNAs expression data at different time points of the disease. When available, GEO accession number and gene expression data were extracted (Table 1).

We have performed Z-score transformation for each miRNAs in considered models to reduce the variability within/between the datasets caused by different platforms, animal models and tissue collection methods may make difficult to directly compared the data. It may run a high risk of skewing comparison results reducing the reliability of measurements of individual miRNA expression changes (Yang et al, 2014). The Z-score transformation approach has been applied on each single miRNA through the different datasets. Z-score was calculated according to the formula:

$$Z - \text{score} = \frac{X_i - X}{\delta}$$

Where X_i is the normalized intensity data for each miRNA, X is the average normalized miRNA intensity within a single study and δ is the standard deviation (SD) of cases and controls within respective studies.

Estimation of effect size

To estimate the efficacy of each individual study, the effect size of each of them has been estimated. The all effects size, defined as the standardized mean difference (SMD) between cases and the control

group, has been calculated using the Hedge's method with the following formula:

$$g = \frac{X_1 - X_2}{\delta}$$

Where X_1 is the mean of the cases, X_2 the mean of the control group and δ the SD.

Estimation of statistical heterogeneity: random effect model

Statistical heterogeneity was assessed using a meta-regression approach i.e. by considering Cochran's Q-test, I^2 - statistic and Tau²-statistic. These measures were applied at each data set to assess the overall heterogeneity (Higgins et al, 2003; Ioannidis et al, 2007). To test the total variance of each miRNAs within the studies, the Cochran's Q-test have been run, according to the formula:

$$Q = k(k - 1) \frac{\sum_{T=1}^k (xT - \frac{N}{k})^2}{\sum_{i=1}^b xT(k-xT)}$$

Where k is the number of the studies included in the meta-analysis, T is the number of variables observed, b is the number of miRNAs included in the test and N is the total number. A p value < 0.1 was considered statistically significant for the Cochran's Q -statistic test.

Furthermore, I^2 statistic has been employed to describe the percentage of the variability in the effect size estimates, following the formula:

$$I^2 = \left(\frac{Q-df}{Q} \right) * 100\%$$

Where Q is the value derived from the Cochran's Q -statistics test and df are the degrees of freedom.

Finally, to estimate the variance across studies the Tau^2 has been applied:

$$\text{Tau}^2 = \frac{Q-df}{C}$$

Where Q is the value derived from the Cochran's Q -statistic test, df are the degrees of freedom and C is a scaling factor which take in consideration that the Q -value is the weighted sum of squares.

The presence of statistical heterogeneity among the miRNAs in all data sets has led the analysis to a random-effect rather than a fix-effect model. The pooled effect size for each microRNAs has been obtained applying the random effect size model based on the DerSimonian and Laird method (DerSimonian and Laird, 1986; DerSimonian and Kacker, 2007). We generated one forest plot for each miRNA involved in the study, for the latency and the chronic phase to depict the SMD along with its 95% confidence interval (95% CI) for

individual studies as well as the pooled mean difference by combining all of them. The statistical significance of the pooled effect size was performed by z-test, Bonferroni correction was applied to the p values ($p < 0.05$).

miRNA targets functional classification

Gene Ontology (GO) enrichment and pathways enrichment analysis based on the Kyoto Encyclopedia of Genes and Genomes (KEGG) database have been run using Webgestalt webserver (Wang et al, 2013) to gain insight into the functional role of those miRNAs identified as significant during the phase of latency and the chronic stage of epileptic DG. As first analysis, only validated mRNA target were considered. The enrichment was performed with an hyper-geometric test separately for the list of targets based on those miRNAs dysregulated in latency and in the chronic stage. Significant canonical pathways maps were selected according to a False Discovery Rate (FDR) $< 5\%$. The analysis was run using the validated mRNA targets obtained by miRwalk database (Dweep et al, 2011). Secondly, we use miRwalk to predict putative mRNA targets of those miRNAs (n=44) that were differentially expressed in latency. The software allows a comparative analysis by 6 prediction programs (miRMap, RNA22, miRanda, RNAhybrid, PITCAR 2 and Targetscan) and we restricted the miRNAs-binding site prediction within the 3' untranslated region (UTR), with a minimum seed length of seven nucleotides.

Results

Animal models of epilepsy have played a fundamental role in advancing our understanding of basic mechanisms underlying ictogenesis and epileptogenesis (Loscher, 2011). Epilepsy could potentially be induced by either incorporating chemical or electrical insults. Each model has its own merits and drawbacks so this warrants a need to characterize the genome-wide microRNA (miRNA) changes that is common to all animal model of induced epilepsy, which in turn would have a better chance to be translated into human epilepsy. To this end we have studied the role of miRNA for different stages of TLE in the DG.

Effect size and meta-regression

A total of 176 miRNAs were expressed in all three models (Figure 1). Next we performed z-score transformation to scale miRNA expressions in the datasets to derive Q-statistics for the estimation of the heterogeneity between the studies. Meta-regression analysis have been run separately for the phase of latency and for the chronic stage. The Cochran's Q-test suggested there was a significant overall heterogeneity ($p < 0.1$, Figure 1A), then to assess the percentage of miRNAs that shown different expression profiles during latency, between studies, we calculate the I^2 - statistic. A total of 25.44% of 178 miRNAs revealed a high level of heterogeneity, whereas the 30.50% and the 42.94% shown respectively a moderate and a low rate of variability based on the heterogeneity classification described by Higgings et al (2003; Figure 1B). In the chronic stage the same statistical approach revealed a significant overall heterogeneity with the Cochran's Q-test ($p < 0.1$, Figure 1D). Furthermore, the 10.22% of the total 178 miRNAs shown high variance within studies, instead the 20.45% (moderate) and the

69.32% (low) of the total results more homogeneous (Figure 1E). The tau²-statistics, calculated for each miRNA, revealed that 7 miRNAs, out of 8 significantly deregulated between chronic and control groups, shown a tau-squared equal to zero (Table 2, Figure 1F).

Meta-analysis: the random effect model

To incorporate the statistical heterogeneity in the data we used random effect model for performing meta-analysis. The analysis identified 44 significant miRNAs (Bonferroni adjusted pvalue <0.05) that were differentially expressed between epileptic cases and controls in the phase of latency and 8 significant miRNAs (Bonferroni adjusted pvalue <0.05) with different expression levels between the two groups at the chronic stage. The miRNAs that were identified as significant compared to the control group, are listed in Table 2 for the phase of latency and in Table 3 for the chronic stage. In both tables, are reported the pooled effect size (PES) estimation, the I² and the tau² values and the adjusted p value for each miRNAs analyzed, after Bonferroni correction. As an example, we reported the forest plot of miR-21-5p, miR-132-3p, miR-212-3p and miR-551b-5p (Figure 3A-D).

The comparison between the list of miRNAs that resulted as significant after the meta-analysis in the latency phase highlighted 3 miRNAs (miR-212-3p, miR-21-5p and miR-132-3p) in common within the meta-analysis and the miRNAs significantly de-regulated in each individual study. Moreover, the meta-analysis revealed, as significant, 23 miRNAs in latency (Table 4), and 4 in the chronic stage (Table 5), that did not rise up in the published datasets (Roncon et al, 2015; Gorter et al, 2014; Bot et al, 2013).

miRNAs functional classification

GO analysis of the validated mRNA targets of those miRNAs that were significantly downregulated 8 days after SE revealed an high enrichment in neuronal GO terms (Figure 4). Specifically, we identified genes as significantly enriched in neuronal cellular component (Supplementary figure 4A) such as dendritic spine (adjusted $p=0.0364$), neuron spine (adjusted $p=0.0364$), axon (adjusted $p=0.01$), postsynaptic membrane (adjusted $p=0.0291$), terminal bottom (adjusted $p=0.0291$), synaptic vesicle membrane (adjusted $p=0.0288$), presynaptic membrane (adjusted $p=0.0047$) and active zone (adjusted $p=0.0069$), synapse (adjusted $p=0.0044$) and neuron projection (adjusted $p=0.0037$). Regarding the molecular functions (Supplementary figures 4B) we observed a significant involvement of these in genes in voltage-gated ion and cation channels (adjusted $p=0.03$, $p=0.02$), in the SNARE binding ($p=0.03$). Moreover, the enrichment analysis on the validated targets genes of the miRNAs revealed as significant several biological processes (Supplementary figure 4C) that are connected to an neuronal/hippocampal involvement: memory (adjusted $p=5.73^{-05}$), membrane depolarization (adjusted $p=4.59^{-05}$), regulation of postsynaptic membrane potential (adjusted $p=9.17^{-06}$), regulation of excitatory postsynaptic potential (adjusted $p=5.51^{-06}$), but also few epileptogenic processes such as regulation of cell death (adjusted $p=5.51^{-06}$), cell differentiation (adjusted $p=7.5^{-05}$) and regulation of cells proliferation (adjusted $p=5.26^{-06}$). The KEGG analysis, interestingly, revealed 4 “epileptogenic” pathways in which these validated targets genes are involved (Supplementary figure 5). The pathways are: cytokine-cytokine receptor interaction (adjusted $p=0.0128$), TGF-beta signaling pathway (adjusted $p=0.003$), neuroactive ligand receptor interaction (adjusted $p=0.003$) and the MAPK signaling pathway (adjusted $p=0.003$).

Discussion

Several genome-wide miRNAs screens provided relevant evidence that miRNAs are differentially expressed, both in humans and in different animal models of TLE. The animal models appear to be a good system to study the miRNAs involvement in the phase of epileptogenesis. However, the available epilepsy models differ in several parameters (SE induction, latency duration, seizures frequency and duration), that can influence miRNA expression (Jimenez-Mateos and Henshall, 2013; Kretschmann et al, 2015). The current meta-analysis identified differentially expressed miRNAs among 3 datasets obtained by different rat models, both in latency and in the chronic stage of the disease, supporting the idea that miRNAs expression may be disease-mediated rather than model-dependently dys-regulated.

An expression of 176 miRNAs were observed to be common between 3 available rat models (Bot et al, 2013; Gorter et al, 2014; Roncon et al, 2015). To avoid the bias of model specificity we consider also a dataset, not published but available between the EPITARGET consortium partner, obtained from rats that underwent the trauma brain injury (TBI) model, which one is considered closer to the human scenario. Actually, just the 30% of the rats become epileptic after the brain insult, showing few electroencephalographic seizures. Surprisingly, the overlap was exactly the same. Thus confidently, we performed the meta-analysis identifying 44 miRNAs that were differentially expressed between the latency and the control groups and just 8 that shown altered expression levels in the chronic compared to the control rats within the 3 models. The relevant different amount of miRNAs that shown significant changes between the 2 phases suggesting a major role of these molecules in regulating those molecular and cellular processes that lead to the transformation of an “healthy” brain to epileptic (epileptogenesis). Our study confirm the up-regulation of miR-21-

5p (adjusted $p=8.54^{-32}$), miR-132-3p (adjusted $p=4.19^{-18}$) and miR-212-3p (adjusted $p=1.74^{-47}$) that were commonly de-regulated in the phase of latency within the studies involved.

Moreover, the meta-analysis highlighted the down-regulation of miR-551b-3p (adjusted $p=1.58^{-12}$) in the chronic period that, instead, stood out just in Roncon et al (2015).

Interestingly, among the list of significant differentially expressed miRNAs there are 23 miRNAs in the phase of latency and 4 miRNAs in the chronic stage that were not identified previously as significantly dys-regulated in either of the studies involved, demonstrating more robust and accurate predictions made by the meta-analysis.

Within the list of miRNAs that were significant both in the latency and the chronic stage we found some brain-enriched families (Landgraf et al, 2007; Liang et al, 2007) that are highly conserved through species (Agarwal et al, 2015). For example, we identified in the phase of latency the miR-132/212-3p family that resulted highly significant up-regulated. Moreover, we observed the presence of let-7b-3p and let-7d-3p as component of the highly conserved brain let-7/miR-98 family, such as miR-17-5p and miR-20a-5p belong to the same miRNA family. In the chronic stage we observed the presence of just one brain-enriched miRNA, miR-130a-3p.

Latency

We observed the dys-regulation of miR-132-3p and miR-212-3p that are the components of the miR-132/212-3p brain enriched family (Landgraf et al, 2007; Liang et al, 2007). Indeed, these two miRNAs are transcribed by the same primary transcript and exhibit identical seed sequences (Wanet et al, 2012). The fact that they are part of the same miRNA-family and they are two of the most significantly differentially expressed between the latency and the control

groups, suggests that there is potentially a role in regulating the same cellular and molecular mechanisms that lead to the disease development.

Epileptogenesis refers to a dynamic process that progressively alters neuronal excitability, establishes abnormal interconnections, and perhaps requires complex structural changes before the first spontaneous seizure occurs (Engel et al, 2005; Pitkanen and Lukasiuk, 2011). These changes can include neurodegeneration, neurogenesis, gliosis, axonal damage or sprouting, dendritic plasticity, blood–brain barrier (BBB) damage, recruitment of inflammatory cells into brain tissue, re-organization of the extracellular matrix, and re-organization of the molecular architecture of individual neuronal cells (Pitkanen and Lukasiuk, 2009, 2011). Transcriptomic analyses have highlighted groups of genes contributing to the generation of specific network alterations linked to those mechanisms. Importantly, interpretation of transcriptomics seems to be focused on pinpointing regulating modules of genes (or miRNAs), able to affect gene expression levels and signaling pathways (Johnson et al, 2015). At the proteins level, neurotrophins show remarkable changes during epileptogenesis in different animal models, notably the brain-derived neurotrophic factor (BDNF). Paradiso et al demonstrated, in 2009, that enhancing repair by neurotrophins alleviates epileptogenesis.

One of the differentially expressed miRNA, Mir-132-3p is a CREB-regulated miRNA, induced by BDNF/TrkB signaling and neural activity, highly conserved and enriched in neurons (Remenyi et al., 2010; Vo et al., 2015). Moreover, it has been demonstrated that the *in vitro* overexpression of miR-132-3p in cultured hippocampal neurons influenced the BDNF mRNA (Xiang et al., 2015) and caused neurite (Vo et al., 2005) and dendritic outgrowth (Wayman et al., 2008) and increase excitatory currents (Edbauer et al., 2008). Indeed, recent

experimental evidence proved the involvement of miR-132-3p in the post-epileptic enhancement of high voltage-calcium channels influencing neuronal epileptiform discharges (Xiang et al, 2015). The reduction of miR-132-3p, through the antagomir approach, in a mice model of temporal lobe epilepsy significantly reduce damage in hippocampus after the status epilepticus (Jimenez-Mateos et al., 2011). MiR-132-3p and miR-212-3p share an identical seed region (Wanet et al, 2012), supposing to commonly target the same mRNAs. In our knowledge, just Xiang and collaborators (2015) studied *in vitro* the combinatorial expression control of these miRNAs on SOX 11, one transcription factor which expression was strictly confined to neuronal committed precursors and immature neurons, but absent in mature neurons (Mu et al, 2012). Their results suggested a strong control of SOX 11 mRNA via interaction with miR-132-3p and miR-212-3p. Taken together, these findings, already available in the scientific literature, and our meta-analysis highlighted their relevant involvement in the phase of epileptogenesis both *in vitro* and *in vivo* models of temporal lobe epilepsy.

Our meta-analysis confirmed the up-regulation of the miR-21-5p that was first identified as relevantly significant in all studies considered. Significant changes in this miRNA levels have been observed in the DG and the whole hippocampus of epileptic rats in different animal model (Bot et al, 2013; Gorter et al, 2014; Roncon et al, 2015; Risbud and Porter, 2013) strongly suggesting its involvement in regulating several mechanisms of epileptogenesis, hypothesizing a role in the initiation of the cell-signaling pathway associated with epilepsy (Meng et al, 2015). Roncon and colleagues (2015), indeed, discussed the hypothesis that miR-21-5p may be involved in the epileptogenesis regulating the expression of one predicted target, the myocyte enhancer factor 2C (MEF2C) gene. This is a neuronal

transcription factor that has been related to the regulation of neuronal dysfunction and neurodegeneration (Yelamanchilli et al, 2013), moreover a polymorphism in this gene has been identified in TLE-patients (Benvienu et al, 2013).

In addition, the present study highlighted a list of 23 miRNAs as significant in the phase of latency, that were not previously identified to be significantly de-regulated in the studies included (Table 5). Within this miRNAs, miR-34c-5p was of particular interest. Haenisch and colleagues (2015) observed an increasing of miR-34c-5p levels more than 5-fold in focal hippocampal tissue compared to temporal neocortical non-focal tissue obtained from surgical specimens of drug-resistant TLE-patients. Indeed, they discuss the potential of this miRNA as putative therapeutic targets of epileptogenesis, a concept that is supported by the analysis of its mRNAs targets. Notably, in the same study, has been demonstrated, *in vitro*, a strong negative interaction between miR-34c-5p, the glutamate receptor metabotropic 7 (GRM7) and the GABA B receptor 2 (GABBR 2) and the GABA B receptor alpha 3 (GABRA3), suggesting a role in the regulation of the glutamatergic and GABAergic transmission. It has been observed that glutamate regulates the survival and the integration of newborn granule cells in the DG, inhibiting proliferation of neuronal stem cells (Berg et al, 2013). Instead, GABA is the most important inhibitory neurotransmitter in the nervous system, leading to the hyperpolarization of neuronal membranes through GABA receptors, playing an important role in the excitatory-inhibitory unbalance in the epilepsy. Moreover, a polymorphism in GABRA3 was associated with altered response to the antiepileptic drug-therapy in TLE-patients (Hung et al, 2013).

Chronic stage

In the chronic stage we have identified 8 miRNAs to be significantly de-regulated compared to the control group. Four of these miRNAs (miR-551b-3p, miR-652-3p, miR-29c-5p and miR-148b-3p) were de-regulated in the chronic stage of the laser-microdissected DG of pilocarpine-epileptic rats (Roncon et al, 2015). Whereas 4 of them (miR-324-3p, miR-130a-3p, miR-345-5p and miR-328a-3p) stood out as significantly deregulated just after our meta-analysis. miR-130a-3p belongs to a brain-enriched family (Landgraf et al, 2007; Liang et al, 2007). This miRNA shown decreased expression levels in the DG of chronic epileptic rats (Table 3) and higher circulating levels of miR-130a-3p have been detected in serum of TLE-patients (Wang et al, 2015). This inverse correlation lead to the idea that miR-130a-3p may join peripheral tissues from the brain, becoming a putative biomarker of epilepsy maybe useful for the stratification of TLE-patients. Further analysis are needed to investigate its role in epilepsy.

Conclusions

In summary, the current meta-analysis confirm and revealed the dys-regulation of 44 miRNAs in the phase of latency and 8 in the chronic stage in the DG of epileptic rats through different models. The larger amount of miRNAs, dys-regulated 8 days after the SE, validate the hypothesis that miRNAs have a role in the regulation of the pathogenesis of disease and in those mechanisms that lead to the seizure onset. GO and KEGG enrichments, indeed, confirmed their involvement in post-transcriptional regulation of genes that are involved in neuronal-epileptogenic pathways. Their regulation activity seems to decrease in the chronic stage. Our analysis highlighted the dys-regulation of just 8 miRNAs (the majority were down-regulated) in the latest phase of the disease, phase in which, rats showed several recurrent spontaneous seizures. The right evaluation should be for example to investigate, at different

time point in the chronic stage, which miRNAs are involved in the regulation of those mechanisms that lead to the seizures onset and to the comorbidities development. In conclusion, our results leads further investigations aimed to uncover how the gene expression can be miRNAs-modulated, moreover highlights the role of few miRNAs (or families of miRNAs), such as the miR-132/212-3p family, as putative new therapeutic targets for the cure of epilepsy.

References

Simonato, M. *et al.* The challenge and promise of anti-epileptic therapy development in animal models. *Lancet Neurol* **13**, 949–60 (2014).

Simonato, M. *et al.* Finding a better drug for epilepsy: preclinical screening strategies and experimental trial design. *Epilepsia* **53**, 1860–7 (2012).

Simonato, M., French, J. A., Galanopoulou, A. S. & O'Brien, T. J. Issues for new antiepilepsy drug development. *Curr Opin Neurol* **26**, 195–200 (2013).

Gupta S, Verma S, Mantri S, Berman NE, Sandhir R, Targeting MicroRNAs in Prevention and Treatment of Neurodegenerative Disorders. *Drug Dev Res.* doi: 10.1002/ddr.21277 Epub ahead of print (2015).

Bartel, D. P. MicroRNAs: genomics, biogenesis, mechanism, and function. *Cell* **116**, 281–97 (2004).

Ebert MS, Sharp PA (2012), Roles of microRNAs in conferring robustness to biological processes. *Cell* 149:515-524.

Cao X, Yeo G, Muotri RA, Kuwabara T, Goge KH (2006) Noncoding RNAs in the mammalian central nervous system. *Annu Rev Neurosci* 29:77-103

Hill JM, Lukiw WJ, microRNA (miRNA)-Mediated Pathogenetic Signaling in Alzheimer's Disease (AD), *Neurochem Res* (2015). Head of print

Cogoni C, Ruberti F, Barbato C (2015), MicroRNA landscape in Alzheimer's disease. *CNS Neurol Disord Drug Targets*. 2015;14(2):168-75.

Filatova EV, Alieva AKh, Shadrina MI, Slominsky PA (2012), MicroRNAs: possible role in pathogenesis of Parkinson's disease. *Biochemistry (Mosc)* 77(8):813-9.

Kan, A.A. *et al.* Genome-wide microRNA profiling of human temporal lobe epilepsy identifies modulators of the immune response. *Cell Mol Life Sci* **69**, 3127-45 (2012).

Zucchini, S. *et al.* Identification of miRNAs differentially expressed in human epilepsy with or without granule cell pathology. *PLoS One* **9**, e105521. doi: 10.1371/journal.pone.0105521 (2014).

Jimenez-Mateos, E.M. *et al.* miRNA Expression profile after status epilepticus and hippocampal neuroprotection by targeting miR-132. *Am J Pathol* **179**, 2519-32 (2011).

Hu, K. *et al.* MicroRNA expression profile of the hippocampus in a rat model of temporal lobe epilepsy and miR-34a-targeted neuroprotection against hippocampal neurone cell apoptosis post-status epilepticus. *BMC Neurosci* **13**, 115 (2012).

● Risbud, R.M., Porter, B.E. Changes in microRNA expression in the whole hippocampus and hippocampal synaptoneurosomal fraction following pilocarpine induced status epilepticus. *PLoS One* **8**, e53464. doi: 10.1371/journal.pone.0053464. (2013).

Bot, A.M., Dębski, K.J., Lukasiuk, K. Alterations in miRNA levels in the dentate gyrus in epileptic rats. *PLoS One* **8**, e76051. doi: 10.1371/journal.pone.0076051. (2013).

Gorter, J.A. *et al.* Hippocampal subregion-specific microRNA expression during epileptogenesis in experimental temporal lobe epilepsy. *Neurobiol Dis* **62**, 508-20 (2013).

Kretschmann A, Danis B, Andonovic L, Abnaof K, van Rikxoort M, Siegel F, Mazzuferi M, Godard P, Hanon E, Fröhlich H, Kaminski RF, Foerch P, Pfeifer A, Different MicroRNA Profiles in Chronic Epilepsy Versus Acute Seizure Mouse Models. *J Mol Neurosci* 55:466-479 (2015).

Roncon P *et al.*, MicroRNA profiles in hippocampal granule cells and plasma of rats with pilocarpine-induced epilepsy – comparison with human epileptic samples. *Sci Rep* **5**: 141-43 (2015)

Siddiqui AS, Delaney AD, Schnerch A, Griffith OL, Jones SJ, Marra MA: Sequence biases in large scale gene expression profiling data. *Nucleic Acids Res* 2006, 34(12):e83-e83.

Ramasamy A, Mondry A, Holmes CC, Altman DG: Key issues in conducting a meta-analysis of gene expression microarray datasets. *PLoS Med* 5(9):e184 (2005).

Yang Z, Chen Y, Fu Y, Yang Y, Zhang Y, Chen Y, Li D, Meta-analysis of differentially expressed genes in osteosarcoma based on gene expression data. *BMC Medical Genetics* 15:80 (2014).

JP Higgins, SG Thompson, JJ Deeks and DG Altman. (2003). Measuring inconsistency in meta-analyses. *BMJ* 327:557–560.

Ioannidis JP, NA Patsopoulos and E Evangelou. (2007). Heterogeneity in meta-analyses of genome wide association investigations. *PLoS One* 2:e841.

Yang Z, Chen Y, Fu Y, Yang Y, Zhang Y, Chen Y and Li D. (2014). Meta-analysis of differentially expressed genes in osteosarcoma based on gene expression data. *BMC Medical Genetics* 15:80.

Soukupova M, Binaschi A, Falcicchia C, Zucchini S, Roncon P, Palma E, Magri E, Grandi E, Simonato M. (2014) Impairment of GABA release in the hippocampus at the time of the first spontaneous seizure in the pilocarpine model of temporal lobe epilepsy. *Exp Neurol.* 257:39-49.

Soukupova M, Binaschi A, Falcicchia C, Palma E, Roncon P, Zucchini S, Simonato M. (2015) Increased extracellular levels of glutamate in the hippocampus of chronically epileptic rats. *Neuroscience.* 301:246-53.

Gorter JA, van Vliet EA, Aronica E, Lopes da Silva FH (2001). Progression of spontaneous seizures after status epilepticus is associated with mossy fibre sprouting and extensive bilateral loss of hilar parvalbumin and somatostatin-immunoreactive neurons. *Eur J Neurosci.* 13(4):657-69.

van der Linden A, Blokker BM, Kap M, Weustink AC, Riegman PHJ, Oosterhuis JW (2014) Post-Mortem Tissue Biopsies Obtained at Minimally Invasive Autopsy: An RNA-Quality Analysis. *PLoS ONE* 9(12): e115675. doi:10.1371/journal.pone.0115675. pmid:25531551

DerSimonian R, Laird N (1986) Meta-analysis in clinical trials. *Control Clin Trials*;7:177–87. DerSimonian R, Kacker R (2007) Random-effects model for meta-analysis of clinical trials: An update. *Cont Clin Trials*; 28: 105–114.

Wang, J., Duncan, D., Shi, Z., Zhang, B. WEB-based GENE SeT ANALYSIS Toolkit (WebGestalt): update 2013. *Nucleic Acids Res*, 41 (Web Server issue), W77-83 (2013).

Dweep H, Sticht C, Pandey P, Gretz N. miRWalk-database: prediction of possible miRNA binding sites by “walking” the genes of three genomes. *J Biomed Informatics* 44:839-847 (2011).

Löscher W. Critical review of current animal models of seizures and epilepsy used in the discovery and development of new antiepileptic drugs. *Seizure* 20(5):359-68 (2011).

Higgins JP, Thompson SG, Deeks JJ, Altman DG. Measuring inconsistency in meta-analyses. *BMJ* 327(7414):557-60 (2003).

Agarwal V, Bell GW, Nam JW, Bartel DP. Predicting effective microRNA target sites in mammalian mRNAs. *Elife*. 4. doi: 10.7554/eLife.05005 (2015).

Landgraf P, Rusu M, Sheridan R, Sewer A, Iovino N, Aravin A, Pfeffer S, Rice A, Kamphorst AO, Landthaler M, Lin C, Socci ND, Hermida L, Fulci V, Chiaretti S, Foà R, Schliwka J, Fuchs U, Novosel A, Müller RU, Schermer B, Bissels U, Inman J, Phan Q, Chien M, Weir DB, Choksi R, De Vita G, Frezzetti D, Trompeter HI, Hornung V, Teng G, Hartmann G, Palkovits M, Di Lauro R, Wernet P, Macino G, Rogler CE, Nagle JW, Ju J, Papavasiliou FN, Benzing T, Lichter P, Tam W, Brownstein MJ, Bosio A, Borkhardt A, Russo JJ, Sander C, Zavolan M, Tuschl T, A mammalian microRNA expression atlas based on small RNA library sequencing. *Cell* 129(7):1401-14 (2007)

Liang Y, Ridzon D, Wong L, Chen C. Characterization of microRNA expression profiles in normal human tissues. *BMC Genomics* 8:166 (2007).

Wanet A, Tacheny A, Arnould T, Renard P. miR-212/132 expression and functions: within and beyond the neuronal compartment. *Nucleic Acids Res.* 40, 4742-4753 (2012).

Engel J Jr, Pedley TA. What is epilepsy? In: *Epilepsy: A comprehensive textbook*. Philadelphia: Lippincott-Raven. 1–11 (2005).

Pitkänen A, Lukasiuk K. Mechanisms of epileptogenesis and potential treatment targets. *Lancet Neurol.* 10(2):173-86 (2011).

Lukasiuk K, Pitkänen A. Seizure-induced gene expression. In: Encyclopedia of basic epilepsy research. Oxford: Academic Press. 1302–09 (2009).

Michael R. Johnson, Jacques Behmoaras, Leonardo Bottolo, Michelle L. Krishnan, Katharina Pernhorst, Paola L. Meza Santoscoy, Tiziana Rossetti, Doug Speed, Prashant K. Srivastava, Marc Chadeau-Hyam, Nabil Hajji, Aleksandra Dabrowska, Maxime Rotival, Banafsheh Razzaghi, Stjepana Kovac, Klaus Wanisch, Federico W. Grillo, Anna Slaviero, Sarah R. Langley, Kirill Shkura, Paolo Roncon, Tisham De, Manuel Mattheisen, Pitt Niehusmann, Terence J. O'Brien, Slave Petrovski, Marec von Lehe, Per Hoffmann, Johan Eriksson, Alison J. Coffey, Sven Cichon, Matthew Walker, Michele Simonato, Be'ne'dicte Danis, Manuela Mazzuferi, Patrik Foerch, Susanne Schoch, Vincenzo De Paola, Rafal M. Kaminski, Vincent T. Cunliffe, Albert J. Becker & Enrico Petretto. Systems genetics identifies Sestrin 3 as a regulator of a proconvulsant gene network in human epileptic hippocampus. *Nat Comm* 6:6031 (2015).

Paradiso B, Marconi P, Zucchini S, Berto E, Binaschi A, Bozac A, Buzzi A, Mazzuferi M, Magri E, Navarro Mora G, Rodi D, Su T, Volpi I, Zanetti L, Marzola A, Manservigi R, Fabene PF, Simonato M. Localized delivery of fibroblast growth factor-2 and brain-derived neurotrophic factor reduces spontaneous seizures in an epilepsy model. *PNAS*.106(17):7191-6 (2009).

● Remenyi, J., Hunter, C.J., Cole, C., Ando, H., Impey, S., Monk, C.E., Martin, K.J., Barton, G.J., Hutvagner, G., Arthur, J.S. Regulation of the miR-212/132 locus by MSK1 and CREB in response to neurotrophins. *Biochem. J.* 428, 281–291 (2010).

Vo, N., Klein, M.E., Varlamova, O., Keller, D.M., Yamamoto, T., Goodman, R.H., Impey, S. A cAMP-response element binding protein-induced microRNA regulates neuronal morphogenesis. *Proc. Natl. Acad. Sci. USA* 102, 16426–16431 (2005).

Xiang L, Ren Y, Cai H, Zhao W, Song Y. MicroRNA-132 aggravates epileptiform discharges via suppression of BDNF/TrkB signaling in cultured hippocampal neurons. *Brain Res.* 1622:484-95. doi: 10.1016/j.brainres.2015.06.046 (2015).

Wayman, G.A., Davare, M., Ando, H., Fortin, D., Varlamova, O., Cheng, H.Y., Marks, D., Obrietan, K., Soderling, T.R., Goodman, R.H., Impey, S. An activity-regulated microRNA controls dendritic plasticity by down-regulating p250GAP. *Proc. Natl. Acad. Sci. USA* 105, 9093–9098 (2008).

Edbauer, D., Neilson, J.R., Foster, K.A., Wang, C.F., Seeburg, D.P., Battersby, M.N., Tada, T., Dolan, B.M., Sharp, P.A., Sheng, M. Regulation of synaptic structure and function by FMRP-associated microRNAs miR-125b and miR-132. *Neuron* 65, 373–384 (2008).

Mu, L., Berti, L., Masserdotti, G., Covic, M., Michaelidis, T.M., Doberauer, K., Merz, K., Rehfeld, F., Haslinger, A., Wegner, M., Sock, E., Lefebvre, V., Couillard-Despres, S., Aigner, L., Berninger, B., Lie, D.C. SoxC transcription factors are required for neuronal differentiation in adult hippocampal neurogenesis. *J. Neurosci.* 32, 3067–3080 (2012).

Risbud RM, Porter BE. Changes in microRNA expression in the whole hippocampus and hippocampal synaptoneurosome fraction following pilocarpine induced status epilepticus. *PLoS One.* 11(1):196-202. doi: 10.3892/mmr.2014.2756.

Meng F, You Y, Liu Z, Liu J, Ding H, Xu R. Neuronal calcium signaling pathways are associated with the development of epilepsy. *Mol Med Rep* 11, 196–202 (2015).

Berg DA, Belnoue L, Song H, Simon A. Neurotransmitter-mediated control of neurogenesis in the adult vertebrate brain. *Development* 140, 2548-2561 (2013).

Yelamanchili, S. V. & Fox, H. S. Defining larger roles for “tiny” RNA molecules: role of miRNAs in neurodegeneration research. *J Neuroimmune Pharmacol* 5, 63–9 (2010).

Bienvenu, T., Diebold, B., Chelly, J. & Isidor, B. Refining the phenotype associated with MEF2C point mutations. *Neurogenetics* **14**, 71–5 (2013).

Hung CC, Chen PL, Huang WM, Tai JJ, Hsieh TJ, Ding ST, Hsieh YW, Liou HH. Gene-wide tagging study of the effects of common genetic polymorphisms in the α subunits of the GABA(A) receptor on epilepsy treatment response. *Pharmacogenomics*. 14(15):1849-56 (2013).

Wang J, Yu JT, Tan L, Tian Y, Ma J, Tan CC, Wang HF, Liu Y, Tan MS, Jiang T, Tan L. Genome-wide circulating microRNA expression profiling indicates biomarkers for epilepsy. *Sci Rep* 5:9522. doi: 10.1038/srep09522 (2015).

Tables

Table 1. Studies characteristics.

	Study A	Study B	Study C
GEO ID	-	GSE49849	-
Rat model	Pilocarpine	Amygdala stimulation	Electrical tetanic stimulation of the angular bundle
Sample count for latency cases:controls	5:5	5:5	8:10
Sample count for chronic stage cases:controls	4:5	5:5	6:10
Latency duration (days after SE)	11±1*	~8**	7.2±1.5***
Platform	Rat miRNA MicroArray Kit, Agilent Technologies	miRCURY LNA™ microRNA Array 7 th , Exiqon services	miRCURY LNA™ microRNA Array 6 th , Exiqon Services
Tissue collection	Laser-microdissected DG	Handily dissected DG	Handily dissected DG

* Soukupova et al, 2014; ** Bot et al, 2013;*** Gorter et al, 2001

Table 2. Differentially expressed microRNAs in the latency period compared with controls.

miRNA	Adjusted p	Q statistics	I² statistics	Tau² statistics	Regulation
miR-212-3p	1.74 ⁻⁴⁷	1.586803	0	0	Up
miR-21-5p	8.54 ⁻³²	3.427403	0.416468	0.171964	Up
miR-7a-5p	3.44 ⁻²⁴	0.824368	0	0	Down
miR-33-5p	4.92 ⁻¹⁹	0.216389	0	0	Down
miR-132-3p	4.19 ⁻¹⁸	5.279402	0.621169	0.240867	Up
miR-139-5p	4.40 ⁻¹⁷	0.294917	0	0	Down
miR-3573-3p	4.68 ⁻¹⁷	1.384298	0	0	Down
miR-344b-2-3p	5.43 ⁻¹⁴	1.568536	0	0	Up
miR-551b-3p	9.09 ⁻¹⁴	0.5054	0	0	Down

miR-146a-5p	4.05 ⁻¹⁰	2.659351	0.247937	0.246412	Up
miR-138-5p	3.98 ⁻⁰⁸	0.5946	0	0	Down
miR-29c-5p	1.48 ⁻⁰⁷	2.912197	0.313233	0.269093	Down
miR-667-3p	1.62 ⁻⁰⁷	1.874378	0	0	Down
let-7d-3p	2.03 ⁻⁰⁷	6.746476	0.703549	0.378224	Down
miR-345-5p	1.46 ⁻⁰⁶	1.751763	0	0	Down
miR-330-3p	1.94 ⁻⁰⁶	0.165092	0	0	Down
miR-101a-3p	5.15 ⁻⁰⁶	0.635355	0	0	Down
let-7b-3p	8.36 ⁻⁰⁶	7.400298	0.729741	0.423699	Down
miR-324-5p	8.55 ⁻⁰⁶	2.048405	0.023631	0.07768	Down
miR-212-5p	1.15 ⁻⁰⁵	0.362442	0	0	Down
miR-92b-3p	1.70 ⁻⁰⁵	1.08194	0	0	Down
miR-335	2.47 ⁻⁰⁵	1.405846	0	0	Down
miR-383-5p	6.11 ⁻⁰⁵	4.003288	0.500411	0.337541	Down
miR-150-5p	6.17 ⁻⁰⁵	1.937471	0	0	Down
miR-30e-5p	6.98 ⁻⁰⁵	1.28534	0	0	Down
miR-7a-2-3p	0.000602	4.340783	0.539254	0.35599	Down
miR-153-3p	0.000795	0.206011	0	0	Down
miR-136-3p	0.001277	0.661483	0	0	Down
miR-27a-3p	0.003317	3.340617	0.401308	0.347921	Up
miR-331-3p	0.00448	0.988975	0	0	Down
miR-218a-5p	0.010095	1.670054	0	0	Down
miR-1188-3p	0.010911	0.738942	0	0	Down
miR-17-5p	0.012311	3.014118	0.336456	0.378571	Up
miR-30e-3p	0.01427	0.676731	0	0	Down
miR-34c-5p	0.014285	1.855119	0	0	Down
miR-31a-5p	0.021707	2.332326	0.142487	0.205825	Down
miR-148b-3p	0.022782	2.345195	0.147192	0.210386	Down
miR-340-3p	0.022859	2.470099	0.190316	0.218127	Down
miR-20a-5p	0.023111	4.312947	0.53628	0.490022	Up
miR-140-5p	0.031974	0.889134	0	0	Down
miR-30d-5p	0.033385	3.668404	0.454804	0.428528	Down
miR-376a-3p	0.039635	0.874285	0	0	Down
miR-136-5p	0.043962	1.544642	0	0	Down
miR-125b-5p	0.044755	1.531211	0	0	Down

Table 3. Differentially expressed microRNAs in the chronic stage compared with controls.

miRNA	Adjusted p	Q statistics	I ² statistics	Tau ² statistics	Regulation
miR-551b-3p	1.58 ⁻¹²	1.633425	0	0	Down
miR-324-3p	1.18 ⁻⁰⁷	1.030138	0	0	Down
miR-652-3p	1.71 ⁻⁰⁷	2.546169	0.214506	0.258625	Down
miR-130a-3p	2.65 ⁻⁰⁵	1.012496	0	0	Down
miR-345-5p	0.000316	1.299491	0	0	Down
miR-328a-3p	0.001197	1.269087	0	0	Down
miR-148b-3p	0.002188	0.161368	0	0	Down
miR-29c-5p	0.020336	0.421915	0	0	Down

Table 4. Differentially expressed microRNAs in common between latency and the chronic phases.

miRNA	Latency		Chronic phase	
	Adjusted p	Regulation	Adjusted p	Regulation
miR-551b-3p	9.09 ⁻¹⁴	Down	1.58 ⁻¹²	Down
miR-29c-5p	1.48 ⁻⁰⁷	Down	0.02033552	Down
miR-345-5p	1.46 ⁻⁰⁶	Down	0.00031551	Down
miR-148b-3p	0.02278224	Down	0.00218784	Down

Table 5. Differentially expressed microRNAs uncovered with the meta-analysis in the latency period.

miRNA	Adjusted p	Regulation
miR-3573-3p	4.68 ⁻¹⁷	Down
miR-667-3p	1.62 ⁻⁰⁷	Down
let-7d-3p	2.03 ⁻⁰⁷	Down
miR-345-5p	1.46 ⁻⁰⁶	Down
miR-101a-3p	5.15 ⁻⁰⁶	Down
let-7b-3p	8.36 ⁻⁰⁶	Down
miR-335	2.47 ⁻⁰⁵	Down
miR-383-5p	6.11 ⁻⁰⁵	Down
miR-150-5p	6.17 ⁻⁰⁵	Down
miR-30e-5p	6.98 ⁻⁰⁵	Down

miR-153-3p	7.95^{-04}	Down
miR-136-3p	1.28^{-03}	Down
miR-331-3p	4.48^{-03}	Down
miR-218a-5p	1.01^{-02}	Down
miR-1188-3p	1.09^{-02}	Down
miR-34c-5p	1.43^{-02}	Down
miR-31a-5p	2.17^{-02}	Down
miR-148b-3p	2.28^{-02}	Down
miR-340-3p	2.29^{-02}	Down
miR-140-5p	3.20^{-02}	Down
miR-376a-3p	3.96^{-02}	Down
miR-136-5p	4.40^{-02}	Down
miR-125b-5p	4.48^{-02}	Down

Table 6. Differentially expressed microRNAs uncovered with the meta-analysis in the chronic phase.

miRNA	Adjusted p	Regulation
miR-324-3p	1.18031^{-07}	Down
miR-130a-3p	2.6508^{-05}	Down
miR-345-5p	0.000315506	Down
miR-328a-3p	0.001196532	Down

Supplementary table 1. Commonly expressed microRNAs in the datasets.

let-7b-3p	miR-146b-5p	miR-29b-3p	miR-341	miR-466b-5p
let-7b-5p	miR-148b-3p	miR-29c-3p	miR-342-3p	miR-466c-3p
let-7c-5p	miR-150-5p	miR-29c-5p	miR-344a-3p	miR-485-5p
let-7d-3p	miR-151-5p	miR-300-3p	miR-344b-2-3p	miR-487b-3p
let-7d-5p	miR-153-3p	miR-300-5p	miR-345-5p	miR-488-3p
let-7e-5p	miR-154-5p	miR-301a-3p	miR-34a-5p	miR-495
miR-100-3p	miR-15b-5p	miR-30a-3p	miR-34b-5p	miR-497-5p
miR-101a-3p	miR-16-5p	miR-30a-5p	miR-34c-5p	miR-500-3p
miR-103-3p	miR-17-5p	miR-30b-3p	miR-352	miR-505-3p
miR-106b-5p	miR-181a-5p	miR-30b-5p	miR-3573-3p	miR-505-5p
miR-107-3p	miR-181b-5p	miR-30c-5p	miR-361-3p	miR-539-5p
miR-1188-3p	miR-181d-5p	miR-30d-5p	miR-365-3p	miR-541-5p

miR-124-3p	miR-185-5p	miR-30e-3p	miR-369-5p	miR-551b-3p
miR-124-5p	miR-186-5p	miR-30e-5p	miR-374-5p	miR-582-5p
miR-1249	miR-1949	miR-31a-5p	miR-376a-3p	miR-598-3p
miR-125a-5p	miR-195-5p	miR-32-3p	miR-376b-3p	miR-652-3p
miR-125b-5p	miR-204-5p	miR-320-3p	miR-376b-5p	miR-664-3p
miR-126a-3p	miR-20a-5p	miR-323-3p	miR-379-5p	miR-665
miR-127-3p	miR-21-5p	miR-324-3p	miR-380-3p	miR-667-3p
miR-127-5p	miR-212-3p	miR-324-5p	miR-382-5p	miR-672-5p
miR-128-3p	miR-212-5p	miR-325-3p	miR-383-5p	miR-674-3p
miR-129-2-3p	miR-218a-5p	miR-325-5p	miR-384-5p	miR-702-3p
miR-129-5p	miR-22-3p	miR-326-3p	miR-410-3p	miR-7a-1-3p
miR-130a-3p	miR-22-5p	miR-328a-3p	miR-411-3p	miR-7a-2-3p
miR-132-3p	miR-221-3p	miR-328b-5p	miR-411-5p	miR-7a-5p
miR-135a-5p	miR-222-3p	miR-329-3p	miR-423-5p	miR-7b
miR-136-3p	miR-23a-3p	miR-33-5p	miR-425-5p	miR-872-5p
miR-136-5p	miR-23b-3p	miR-330-3p	miR-431	miR-92b-3p
miR-137-3p	miR-24-3p	miR-331-3p	miR-433-3p	miR-93-5p
miR-138-2-3p	miR-25-3p	miR-335	miR-433-5p	miR-98-5p
miR-138-5p	miR-26a-5p	miR-337-3p	miR-434-3p	miR-99a-5p
miR-139-5p	miR-26b-5p	miR-337-5p	miR-434-5p	miR-99b-3p
miR-140-3p	miR-27a-3p	miR-338-3p	miR-451-5p	miR-99b-5p
miR-140-5p	miR-27b-3p	miR-340-3p	miR-466b-1-3p	miR-9a-3p
miR-143-3p	miR-299a-5p	miR-340-5p	miR-466b-2-3p	miR-9a-5p
miR-146a-5p	miR-29a-3p			

Figures

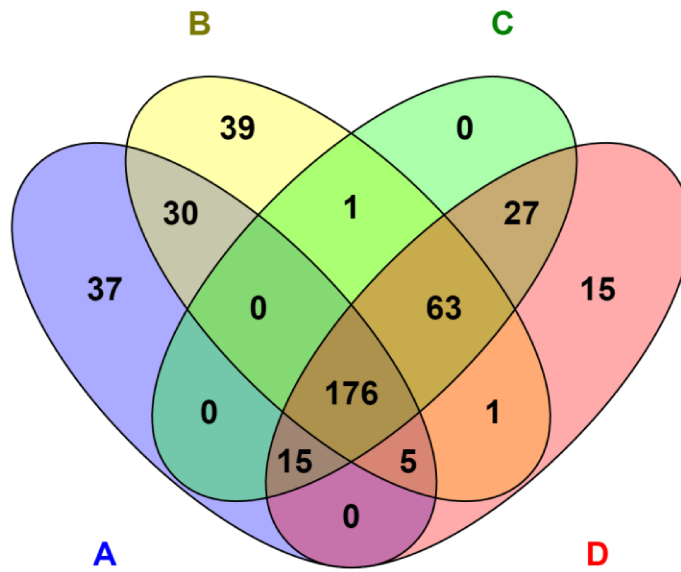


Figure 1. Commonly expressed miRNAs in the four datasets. Venn diagram showing the 176 miRNAs commonly expressed through the available datasets. The 176 miRNAs are those on which the meta-analysis has been run.

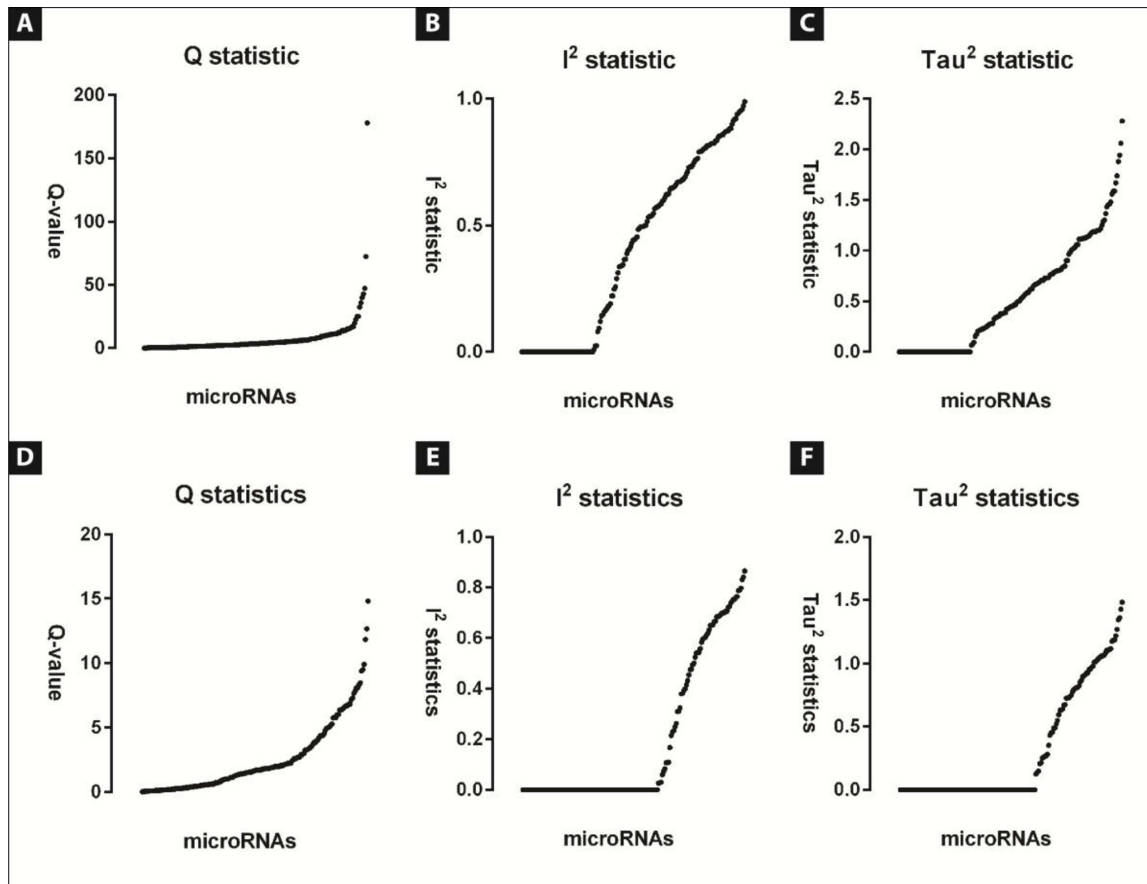


Figure 2. Statistical heterogeneity. Heterogeneity estimation of 176 miRNAs commonly expressed within the datasets both in latency (A,B,C) and in the chronic stage (D, E, F). A and D, Q-statistics, $p < 0.1$. B and E, I^2 statistic (%). C and F, Tau^2 statistic, $p < 0.05$.

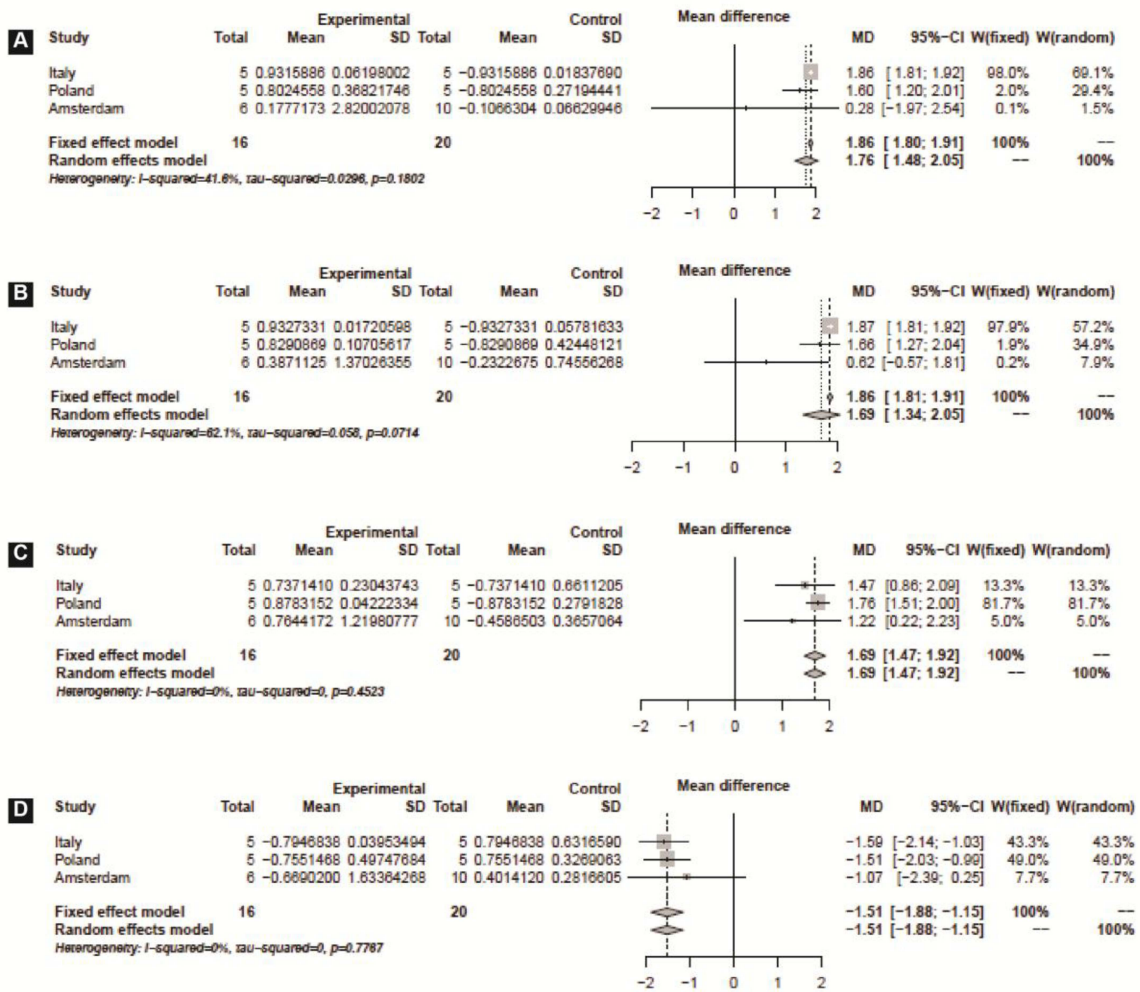
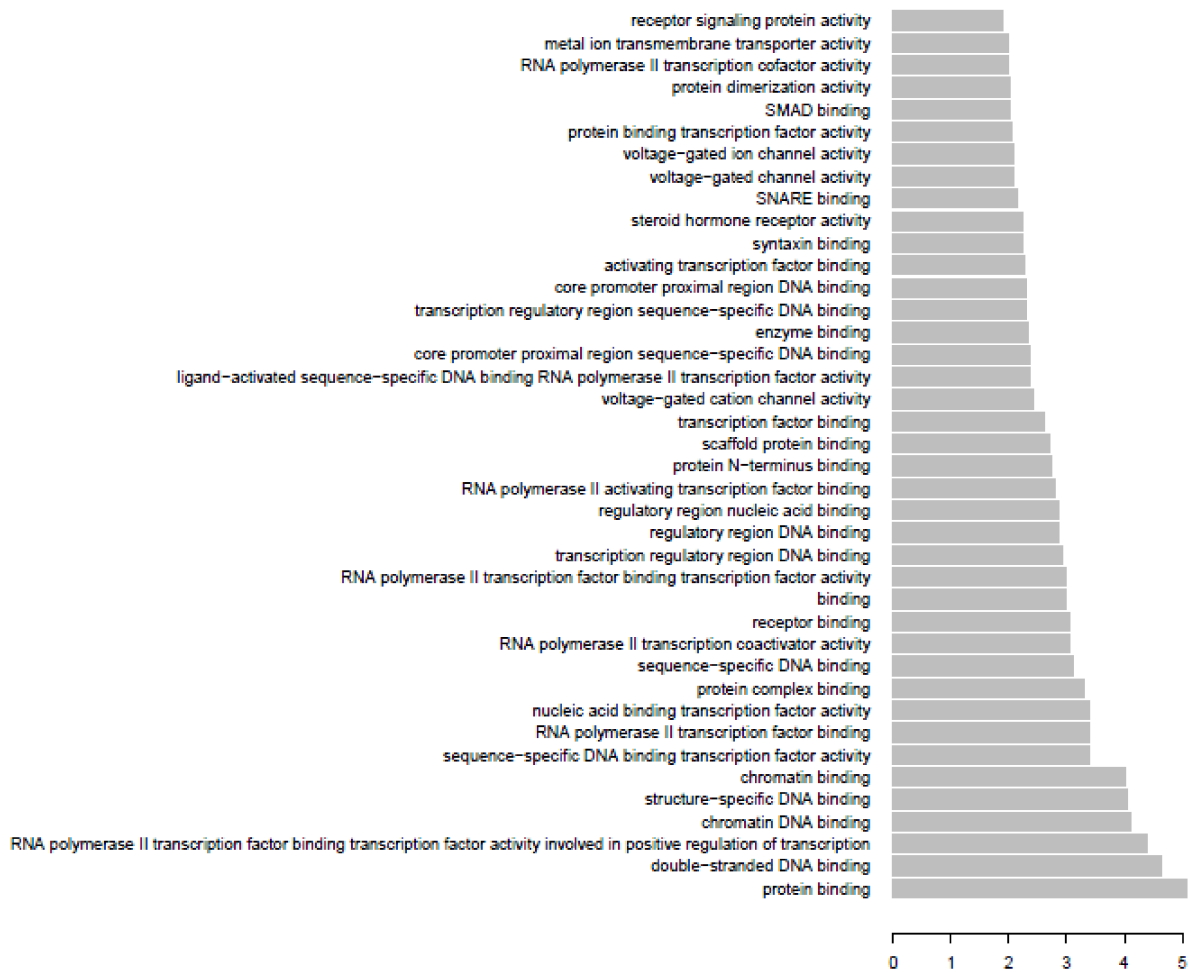
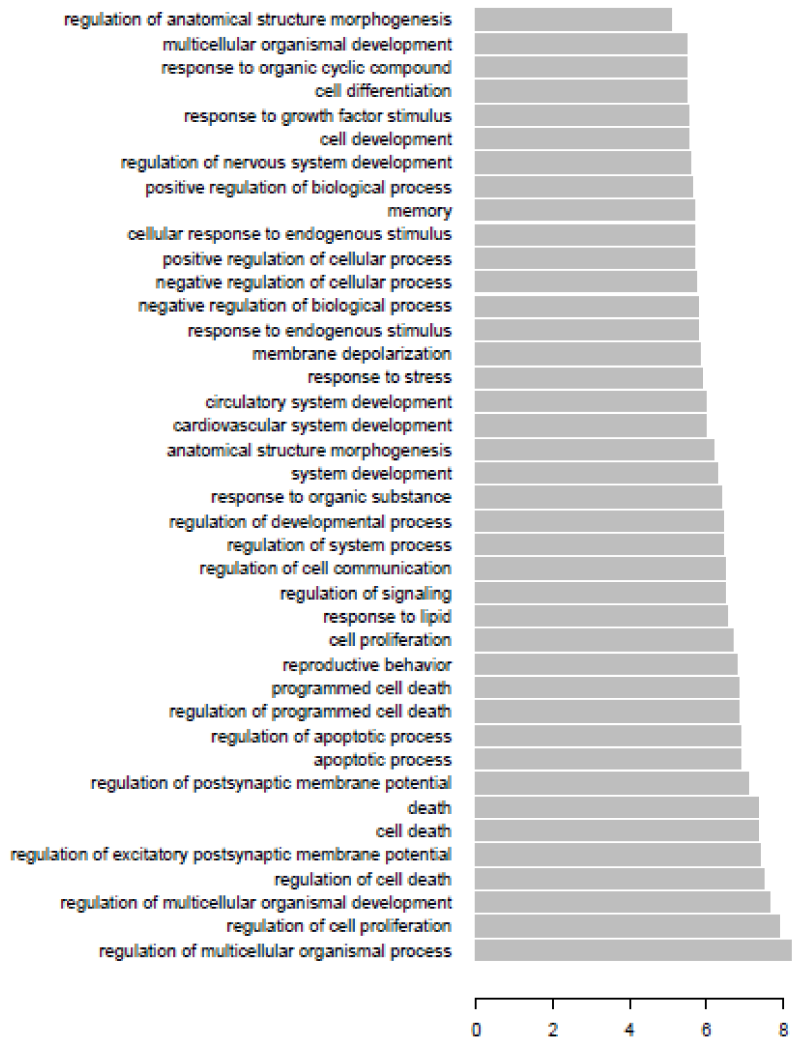


Figure 3. Graphical representation of the mean difference. Forest plots of miR-21-5p (A), miR-132-3p (B), miR-212-3p (C) and miR-551b-3p (D).



in SUL



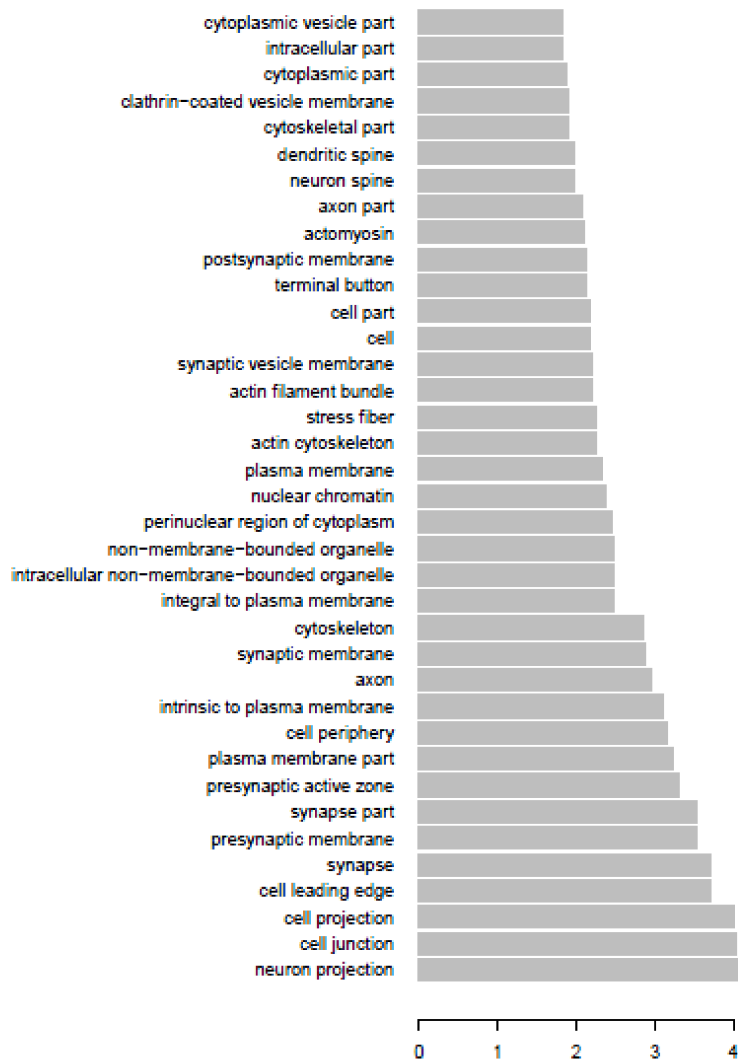


Figure 4. Gene ontology enrichment. (A) Molecular function, (B) Biological processes, (C) cellular components. The analysis was run on the validated mRNAs targets calculated on 44 miRNAs differentially expressed in the phase of latency after the meta-analysis; adjusted $p < 0.05$.

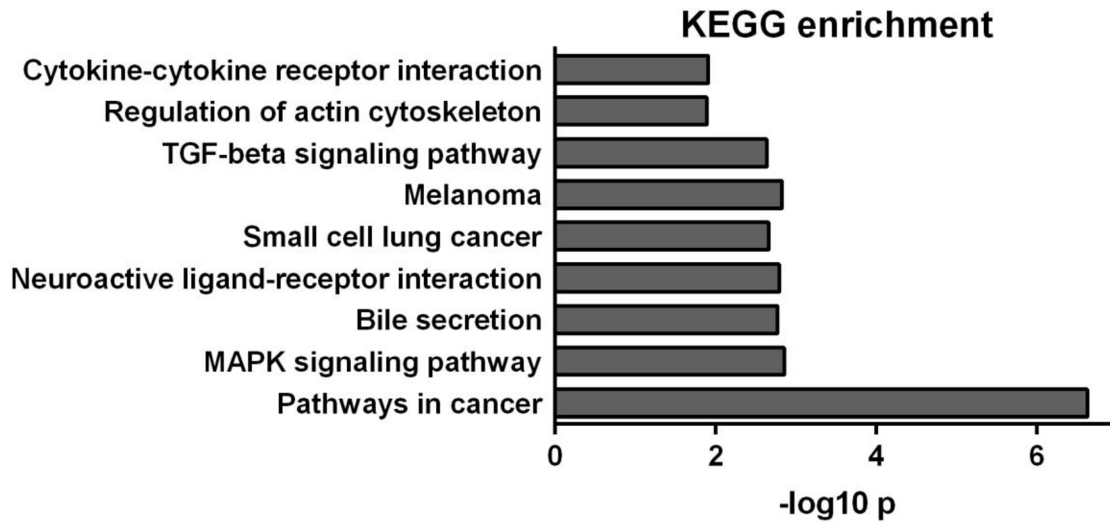


Figure 5. Kyoto encyclopedia of genes and genomes enrichment. The analysis was run on the validated mRNAs targets calculated on 44 miRNAs differentially expressed in the phase of latency after the meta-analysis; adjusted $p < 0.05$.

Chapter 4

Sestrin 3: a trans-regulator of a pro-convulsive gene network

4.1 Epilepsy and heritability

Although the causes of epilepsy are diverse and heterogeneous, epilepsies are a group of diseases with high genetic component and heritability. An inherited predisposition to seizures (epileptic diathesis) combined with some trigger and/or additional factors have been hypothesized as a cause of many types of epilepsy (Lennox and Lennox, 1960). However, genetic association studies and exome sequencing approaches have provided limited insight in underlying disease susceptibility. Traditional estimates of heritability for epilepsy vary greatly, depending on the method used, the population sampled and the different clinical subtypes considered in the analysis (Speed et al, 2014). Consequently, genetic factors affecting common forms of epilepsy remain poorly understood.

Epilepsies are clinically divided into generalized and focal forms. Epidemiological studies in familial aggregation and in twins revealed some genetic factors that may contribute to both (Miller et al, 1998; Berkovic et al, 1998; Steinlein, 2004; Kjeldsen et al, 2002). Notably, causative mutations in many genes, such as those coding for ion channel subunits or others involved in synaptic function and brain development have been reported (Helbig et al, 2008; Poduri and Lowenstein, 2011). Despite the high heritability of epilepsy investigated in twins' studies, gene-wide association studies (GWAS) independently provided findings explaining a small fraction of the overall population susceptibility to epilepsy (Kasperavičirūte et al, 2010; Guo et al, 2011; EPICURE Consortium et al, 2012). In 2014, the ILAE published a meta-analysis of GWASs through which the authors identified 3 loci associated with epilepsy. They identified one locus in the region 2q24.3, that implicate the gene encoding sodium channel type-1A (SCN1A), as described in previous studies (Kasperavičirūte et al, 2010; Baum et al, 2014); one locus in the regions 4p15.1 involving the gene encoding the protocadherin 7 (PCDH7), newly associated with epilepsy; and the locus 2p16, previously reported in the EPICURE cohort, where the genes VRK2 and FANCL are in close proximity.

Integrated analysis of transcriptional networks with genetic susceptibility data and phenotypic information allows specific transcriptional programs to be connected to disease states, and thereby can identify disease pathways and their genetic regulators as new therapeutic approaches. In the following paper, we identify a gene-regulatory network

associated with epilepsy, we probe the genome for key regulators of the network in the human brain and, finally, we pinpoint the Sestrin 3 gene as a trans-active genetic regulator of a proconvulsant gene network in the human epileptic hippocampus.

4.2 Sestrin 3

Sestrins (Sesn) are a family of genes involved in reactive oxygen species (ROS) regulation. The Sesn family is composed of three members: Sesn1, Sesn2 and Sesn3. They are a p53 target and have dual biochemical functions: as antioxidants, controlling the activity of peroxiredoxins that scavenge ROS (Budanov et al, 2004), and as inhibitors of the rapamycin complex 1 (TORC1) signaling (Budanov et al, 2008; Lee et al, 2010). Additionally, it has been demonstrated that all three members of the Sesn family are activated by the forkhead transcription factor (FoxO3A) and Fox1. Notably, Sesn3 has the highest degree of activation by the FoxO proteins (Nogueira et al, 2008), which are enriched in brain. The position of Sesn3 in the neuronal network between TORC1 and the FoxOs suggest its role in the development of epilepsy and its comorbidities.

Indeed, recently, the TORC1 pathway has been implicated in mechanisms of epileptogenesis and the TORC1 inhibitor, rapamycin, has been proposed to have antiepileptogenic effects in preventing some types of epilepsy (Guo et al, 2013). Moreover, alterations in the upstream molecules of FoxOs, such as brain derived neurotrophic factor (BDNF) or protein kinase B, are also involved in the development of major depressive disorders. FoxOs could be regulated by serotonin and norepinephrine receptor signaling as well as by the hypothalamic-pituitary-adrenal axis, all of which are involved in the pathogenesis of depression. FoxOs also regulate neuronal morphology, synaptogenesis and adult hippocampal neurogenesis, which are viewed as candidate mechanisms for the etiology of depression (Wang et al, 2015), a comorbid disorder of epilepsy.

In this Chapter we studied the behavior of Sesn3-knock out (KO) rats in order to understand the involvement of this gene in epilepsy and its comorbidities. However, a more refined silencing approach should be used. For example, amplicon-vectors may be used to silence the gene only in the hippocampus. This new strategy has been well characterized to

silence BDNF in the hippocampus of epileptic rats. All the data are reported in the following article.

4.3 References

Baum L, Haerian BS, Ng HK (2005), Case-control association study of polymorphisms in the voltage-gated sodium channel genes SCN1A, SCN2A, SCN3A, SCN1B and SCN2B and epilepsy. *Hum Genet*, 133:651-9.

Berkovic SF, Howell RA, Hay DA, Hopper JL (1998), Epilepsies in twins: genetics of the major epilepsy syndromes. *Ann Neurol*, 43:435-445.

Budanov AV, Karin M (2008), p53 target genes sestrin1 and sestrin2 connect genotoxic stress and mTOR signaling. *Cell*, 134:451-60.

Budanov AV, Sablina AA, Feinstein E, Koonin EV, Chumakov PM (2004), Regeneration of peroxiredoxins by p53-regulated sestrins, homologs of bacterial AhpD. *Science*, 304:596-600.

Epi4K Consortium; Epilepsy Phenome/Genome Project, Allen AS, Berkovic SF, Cossette P, Delanty N, Dlugos D, Eichler EE, Epstein MP, Glauser T, Goldstein DB, Han Y, Heinzen EL, Hitomi Y, Howell KB, Johnson MR, Kuzniecky R, Lowenstein DH, Lu YF, Madou MR, Marson AG, Mefford HC, Esmaceli Nieh S, O'Brien TJ, Ottman R, Petrovski S, Poduri A, Ruzzo EK, Scheffer IE, Sherr EH, Yuskaitis CJ, Abou-Khalil B, Alldredge BK, Bautista JF, Berkovic SF, Boro A, Cascino GD, Consalvo D, Crumrine P, Devinsky O, Dlugos D, Epstein MP, Fiol M, Fountain NB, French J, Friedman D, Geller EB, Glauser T, Glynn S, Haut SR, Hayward J, Helmers SL, Joshi S, Kanner A, Kirsch HE, Knowlton RC, Kossoff EH, Kuperman R, Kuzniecky R, Lowenstein DH, McGuire SM, Motika PV, Novotny EJ, Ottman R, Paolicchi JM, Parent JM, Park K, Poduri A, Scheffer IE, Shellhaas RA, Sherr EH, Shih JJ, Singh R, Sirven J, Smith MC, Sullivan J, Lin Thio L, Venkat A, Vining EP, Von Allmen GK, Weisenberg JL, Widdess-Walsh P, Winawer MR (2013), De novo mutations in epileptic encephalopathies. *Nature*, 501(7466):217-21.

EPICURE Consortium, EMINet Consortium, Steffens M, Leu C, Ruppert AK, Zara F, Striano P, Robbiano A, Capovilla G, Tinuper P, Gambardella A, Bianchi A, La Neve A,

Crichiutti G, de Kovel CG, Kasteleijn-Nolst Trenité D, de Haan GJ, Lindhout D, Gaus V, Schmitz B, Janz D, Weber YG, Becker F, Lerche H, Steinhoff BJ, Kleefuß-Lie AA, Kunz WS, Surges R, Elger CE, Muhle H, von Spiczak S, Ostertag P, Helbig I, Stephani U, Møller RS, Hjalgrim H, Dibbens LM, Bellows S, Oliver K, Mullen S, Scheffer IE, Berkovic SF, Everett KV, Gardiner MR, Marini C, Guerrini R, Lehesjoki AE, Siren A, Guipponi M, Malafosse A, Thomas P, Nabbout R, Baulac S, Leguern E, Guerrero R, Serratosa JM, Reif PS, Rosenow F, Mörzinger M, Feucht M, Zimprich F, Kasper C, Schankin CJ, Suls A, Smets K, De Jonghe P, Jordanova A, Caglayan H, Yapici Z, Yalcin DA, Baykan B, Bebek N, Ozbek U, Gieger C, Wichmann HE, Balschun T, Ellinghaus D, Franke A, Meesters C, Becker T, Wienker TF, Hempelmann A, Schulz H, Rüschenhoff F, Leber M, Pauck SM, Trucks H, Toliat MR, Nürnberg P, Avanzini G, Koeleman BP, Sander T (2012), Genome-wide association analysis of genetic generalized epilepsies implicates susceptibility loci at 1q43, 2p16.1, 2q22.3 and 17q21.32. *Hum Mol Genet*, 21(24):5359-72.

Guo D, Zeng L, Brody DL, Wong M (2013), Rapamycin attenuates the development of posttraumatic epilepsy in a mouse model of traumatic brain injury. *PLoS One*, 8(5):e64078. doi: 10.1371/journal.pone.0064078.

Guo D, Zeng L, Brody DL, Wong M (2013), Rapamycin attenuates the development of posttraumatic epilepsy in a mouse model of traumatic brain injury. *PLoS One*;8(5):e64078. doi: 10.1371/journal.pone.0064078.

Guo Y, Baum LW, Sham PC, Wong V, Ng PW, Lui CH, Sin NC, Tsoi TH, Tang CS, Kwan JS, Yip BH, Xiao SM, Thomas GN, Lau YL, Yang W, Cherny SS, Kwan P (2012), Two-stage genome-wide association study identifies variants in *CAMSAP1L1* as susceptibility loci for epilepsy in Chinese. *Hum Mol Genet*, 21(5):1184-9.

Guo Y, Baum LW, Sham PC, Wong V, Ng PW, Lui CH, Sin NC, Tsoi TH, Tang CS, Kwan JS, Yip BH, Xiao SM, Thomas GN, Lau YL, Yang W, Cherny SS, Kwan P (2012), Two-stage genome-wide association study identifies variants in *CAMSAP1L1* as susceptibility loci for epilepsy in Chinese. *Hum Mol Genet*, 21(5):1184-9.

Helbig I, Scheffer IE, Mulley JC, Berkovic SF (2008), Navigating the channels and beyond: unraveling the genetics of the epilepsies. *Lancet Neurol*, 7:231-45.

International League Against Epilepsy Consortium on Complex Epilepsies. Electronic address: epilepsy-austin@unimelb.edu.au (2014), Genetic determinants of common

epilepsies: a meta-analysis of genome-wide association studies. *Lancet Neurol*, 13(9):893-903.

Kasperaviciūte D, Catarino CB, Heinzen EL, Depondt C, Cavalleri GL, Caboclo LO, Tate SK, Jamnadas-Khoda J, Chinthapalli K, Clayton LM, Shianna KV, Radtke RA, Mikati MA, Gallentine WB, Husain AM, Alhusaini S, Leppert D, Middleton LT, Gibson RA, Johnson MR, Matthews PM, Hosford D, Heuser K, Amos L, Ortega M, Zumsteg D, Wieser HG, Steinhoff BJ, Krämer G, Hansen J, Dorn T, Kantanen AM, Gjerstad L, Peuralinna T, Hernandez DG, Eriksson KJ, Kälviäinen RK, Doherty CP, Wood NW, Pandolfo M, Duncan JS, Sander JW, Delanty N, Goldstein DB, Sisodiya SM (2010), Common genetic variation and susceptibility to partial epilepsies: a genome-wide association study. *Brain*, 133(Pt 7):2136-47.

Kasperaviciute D, Catarino CB, Matarin M (2013), Epilepsy, hippocampal sclerosis and febrile seizures linked by common genetic variation around SCN1A. *Brain*, 136:3140-50.

Kjeldsen MJ, Kyvik KO, Friis ML, Christensen K (2002), Genetic and environmental factors in febrile seizures: a Danish population-based twin study. *Epilepsy Res*, 51:167-177.

Lee JH, Budanov AV, Park EJ, Birse R, Kim TE, Perkins GA, Ocorr K, Ellisman MH, Bodmer R, Bier E, Karin M (2010), Sestrin as a feedback inhibitor of TOR that prevents age-related pathologies. *Science*, 327:1223-8.

Lennox WG, Lennox MA (1960), *Epilepsy and related disorders*. Little, Brown; Boston. The genetic of epilepsy.

Miller LL, Pellock JM, DeLorenzo RJ, Meyer JM, Corey LA (1998), A univariate genetic analyses of epilepsy and seizures in a population-based twin study: the Virginia twin registry. *Genet Epidemiol*, 15:33-49.

Nogueira V, Park Y, Chen CC, Xu PZ, Chen ML, Tonic I, Unterman T, Hay N (2008), Akt determines replicative senescence and oxidative or oncogenic premature senescence and sensitized cells to oxidative apoptosis. *Cancer Cell*, 14:458-70.

Poduri A, Lowenstein D (2013), Epilepsy genetics-past, present, and future. *Curr Opin Genet Dev*, 21:325-32.

Speed D, O'Brien TJ, Palotie A, Shkura K, Marson AG, Balding DJ, Johnson MR (2014), Describing the genetic architecture of epilepsy through heritability analysis. *Brain*, 137(Pt 10):2680-9.

Steinlein OK (2004), Genes and mutations in human idiopathic epilepsy. *Brain Dev*, 26:213-218.

Wang H, Quirion R, Little PJ, Cheng Y, Feng ZP, Sun HS, Xu J, Zheng W (2015), Forkhead box O transcription factors as possible mediators in the development of major depression. *Neuropharmacology*, 99:527-37.

ARTICLE

Received 1 Sep 2014 | Accepted 4 Dec 2014 | Published 23 Jan 2015

DOI: 10.1038/ncomms7031

Systems genetics identifies Sestrin 3 as a regulator of a proconvulsant gene network in human epileptic hippocampus

Michael R. Johnson^{1,§}, Jacques Behmoaras^{2,*}, Leonardo Bottolo^{3,*}, Michelle L. Krishnan^{4,*}, Katharina Pernhorst^{5,*}, Paola L. Meza Santoscoy^{6,*}, Tiziana Rossetti⁷, Doug Speed⁸, Prashant K. Srivastava^{1,7}, Marc Chadeau-Hyam⁹, Nabil Hajji¹⁰, Aleksandra Dabrowska¹⁰, Maxime Rotival⁷, Banafsheh Razzaghi⁷, Stjepana Kovac¹¹, Klaus Wanisch¹¹, Federico W. Grillo⁷, Anna Slaviero⁷, Sarah R. Langley^{1,7}, Kirill Shkura^{1,7}, Paolo Roncon^{12,13}, Tisham De⁷, Manuel Mattheisen^{14,15,16}, Pitt Niehusmann⁵, Terence J. O'Brien¹⁷, Slave Petrovski¹⁸, Marec von Lehe¹⁹, Per Hoffmann^{20,21}, Johan Eriksson^{22,23,24}, Alison J. Coffey²⁵, Sven Cichon^{20,21}, Matthew Walker¹¹, Michele Simonato^{12,13,26}, Bénédicte Danis²⁷, Manuela Mazzuferi²⁷, Patrik Foerch²⁷, Susanne Schoch^{5,28}, Vincenzo De Paola⁷, Rafal M. Kaminski²⁷, Vincent T. Cunliffe⁶, Albert J. Becker^{5,§} & Enrico Petretto^{7,29,§}

Gene-regulatory network analysis is a powerful approach to elucidate the molecular processes and pathways underlying complex disease. Here we employ systems genetics approaches to characterize the genetic regulation of pathophysiological pathways in human temporal lobe epilepsy (TLE). Using surgically acquired hippocampi from 129 TLE patients, we identify a gene-regulatory network genetically associated with epilepsy that contains a specialized, highly expressed transcriptional module encoding proconvulsive cytokines and Toll-like receptor signalling genes. RNA sequencing analysis in a mouse model of TLE using 100 epileptic and 100 control hippocampi shows the proconvulsive module is preserved across-species, specific to the epileptic hippocampus and upregulated in chronic epilepsy. In the TLE patients, we map the *trans*-acting genetic control of this proconvulsive module to Sestrin 3 (*SESN3*), and demonstrate that *SESN3* positively regulates the module in macrophages, microglia and neurons. Morpholino-mediated *Sesn3* knockdown in zebrafish confirms the regulation of the transcriptional module, and attenuates chemically induced behavioural seizures *in vivo*.

¹ Division of Brain Sciences, Imperial College London, Hammersmith Hospital Campus, Burlington Danes Building, London W12 0NN, UK. ² Centre for Complement and Inflammation Research, Imperial College London, Hammersmith Hospital, Du Cane Road, London W12 0NN, UK. ³ Department of Mathematics, Imperial College London, 180 Queen's Gate, London SW7 2AZ, UK. ⁴ Centre for the Developing Brain, Department of Perinatal Imaging and Health, St Thomas' Hospital, King's College London, London SE1 7EH, UK. ⁵ Section of Translational Epileptology, Department of Neuropathology, University of Bonn, Sigmund Freud Street 25, Bonn D-53127, Germany. ⁶ Department of Biomedical Science, Bateson Centre, University of Sheffield, Firth Court, Western Bank, Sheffield S10 2TN, UK. ⁷ Medical Research Council (MRC) Clinical Sciences Centre, Imperial College London, Hammersmith Hospital, Du Cane Road, London W12 0NN, UK. ⁸ UCL Genetics Institute, University College London, Gower Street, London WC1E 6BT, UK. ⁹ Department of Epidemiology and Biostatistics, School of Public Health, MRC/PHE Centre for Environment and Health, Imperial College London, St Mary's Hospital, Norfolk Place, W21PG London, UK. ¹⁰ Department of Medicine, Centre for Pharmacology and Therapeutics, Imperial College London, Du Cane Road, London W12 0NN, UK. ¹¹ Institute of Neurology, University College London, London WC1N 3BG, UK. ¹² Department of Medical Sciences, Section of Pharmacology and Neuroscience Center, University of Ferrara, 44121 Ferrara, Italy. ¹³ National Institute of Neuroscience, 44121 Ferrara, Italy. ¹⁴ Department of Genomics, Life and Brain Center, University of Bonn, D-53127 Bonn, Germany. ¹⁵ Institute of Human Genetics, University of Bonn, D-53127 Bonn, Germany. ¹⁶ Institute for Genomic Mathematics, University of Bonn, D-53127 Bonn, Germany. ¹⁷ Department of Medicine, RMH, University of Melbourne, Royal Melbourne Hospital, Royal Parade, Parkville, Victoria 3050, Australia. ¹⁸ Department of Neurology, Royal Melbourne Hospital, Melbourne, Parkville, Victoria 3050, Australia. ¹⁹ Department of Neurosurgery, University of Bonn Medical Center, Sigmund-Freud-Strasse 25, 53105 Bonn, Germany. ²⁰ Institute of Human Genetics, University of Bonn, Sigmund-Freud-Strasse 25, 53127 Bonn, Germany. ²¹ Department of Biomedicine, University of Basel, Hebelstrasse 20, 4056 Basel, Switzerland. ²² Folkhälsan Research Centre, Topeliussgatan 20, 00250 Helsinki, Finland. ²³ Helsinki University Central Hospital, Unit of General Practice, Haartmaninkatu 4, Helsinki 00290, Finland. ²⁴ Department of General Practice and Primary Health Care, University of Helsinki, 407, PO Box 20, Tukholmankatu 8 B, Helsinki 00014, Finland. ²⁵ Wellcome Trust Sanger Institute, Wellcome Trust Genome Campus, Hinxton CB10 1SA, UK. ²⁶ Laboratory for Technologies of Advanced Therapies (LTAT), University of Ferrara, 44121 Ferrara, Italy. ²⁷ Neuroscience TA, UCB Biopharma SPRL, Avenue de l'industrie, R9, B-1420 Braine l'Alleud, Belgium. ²⁸ Department of Epileptology, University of Bonn Medical Center, Sigmund-Freud-Strasse 25, Bonn D-53127, Germany. ²⁹ Duke-NUS Graduate Medical School, 8 College Road, Singapore 169857, Singapore. * These authors contributed equally to this work. § These authors jointly supervised this work. Correspondence and requests for materials should be addressed to M.R.J. (email: m.johnson@imperial.ac.uk) or to A.J.B. (email: albert_becker@uni-bonn.de) or to E.P. (email: enrico.petretto@duke-nus.edu.sg).

Epilepsy is a serious neurological disorder affecting about 1% of the world's population. Recently, a growing body of experimental and clinical data has implicated Toll-like receptor (TLR) signalling¹ and release of proconvulsant inflammatory molecules (that is, interleukin (IL)-1 β) in both seizure generation and epileptogenesis^{2,3}. However, the pathogenetic mechanisms linking these inflammatory processes with the development (and recurrence) of epileptic seizures in humans are unclear. Despite high heritability of epilepsy^{4–6}, both genome-wide association studies (GWAS) and exome sequencing approaches have so far provided limited insights into the genetic regulatory mechanisms underlying inflammatory pathways in epilepsy aetiology^{7–11}, and traditional single-variant association approaches are likely to be underpowered to detect complex gene network interactions that underlie disease susceptibility¹². As the molecular processes driving complex disease usually affect sets of genes acting in concert, one alternative strategy is to use systems-level approaches to investigate transcriptional networks and pathways within pathologically relevant cells and tissues^{13,14}. Integrated analysis of transcriptional networks with genetic susceptibility data and phenotypic information allows specific transcriptional programmes to be connected to disease states, and thereby can identify disease pathways and their genetic regulators as new targets for therapeutic intervention¹⁵.

Almost uniquely among disorders of the human brain, epilepsy surgery offers opportunities for gene expression profiling in ante-mortem brain tissue from pathophysiologically relevant brain structures such as the hippocampus¹⁶. This allows direct investigation of transcriptional programmes in brain tissue from living epilepsy patients. In this study, we integrate unsupervised network analysis of global gene expression in the hippocampi of patients with temporal lobe epilepsy (TLE) with GWAS data in a systems genetics approach¹⁷. We uncover pathways and transcriptional programmes associated with epilepsy that are conserved in mouse epileptic hippocampus, including a proconvulsant gene network encoding IL-1 β ³ and TLR-signalling genes¹ previously implicated in epilepsy. Using genome-wide Bayesian expression QTL mapping¹⁸, we probe the genome for key genetic regulators of the network in human brain. We pinpoint an unexpected gene, *Sestrin 3* (*SESN3*) whose protein product controls the intracellular response to reactive oxygen species^{19–22}, as a *trans*-acting genetic regulator of the proconvulsant gene network in the human epileptic hippocampus. We carry out validation experiments in independent *in vitro* and *in vivo* systems, which confirm the genetic regulation of the proconvulsant transcriptional programme in epilepsy by *Sestrin 3*, therefore providing a first evidence of a function for *SESN3* in disorders of the human brain.

Results

Identification of a gene network associated with epilepsy. We first assessed the degree of variation in gene expression between hippocampal subfields in TLE patients with hippocampal sclerosis, and compared this with the total variation in gene expression measured both across subjects and between subfields (Supplementary Fig. 1). We found higher variability in gene expression across TLE subjects than between the hippocampal subfields alone, suggesting that variation in whole hippocampus expression can be used to infer co-expression networks in the hippocampus of TLE patients (Supplementary Fig. 1). After excluding subjects with incomplete clinical data or non-hippocampal sclerosis pathology, whole-genome expression profiles in surgically resected hippocampi from 129 TLE patients (median age at surgery 35 years, range 1–64 years, male/female ratio of 1.2:1; Supplementary Table 1) were available for gene co-expression network analysis.

We then investigated whether the transcriptome in the hippocampus of these 129 TLE patients is organized into discrete gene co-expression networks, and if these have functional implications for susceptibility to epilepsy. Gene co-expression networks were reconstructed genome wide using Graphical Gaussian Models (GGMs)²³, which identified a large co-expression network comprising 442 annotated genes (false discovery rate (FDR) < 5%, Fig. 1a and Supplementary Data 1). To investigate whether the protein products of the TLE-hippocampus derived transcriptional network (TLE-network) genes have a shared function at the protein level, we used the DAPPLE algorithm²⁴. This method interrogates high-confidence protein–protein interactions to assess the physical connections among proteins encoded by the genes in the network. Genes comprising the TLE-network were found to have increased protein–protein interconnectivity as compared with random protein–protein interaction networks ($P = 9.9 \times 10^{-5}$, Supplementary Fig. 2). This provides evidence that proteins encoded by the co-expressed genes in the TLE-network interact physically, supporting the validity of the gene network topography.

As gene expression may vary both as a cause and a consequence of disease, we investigated the causal relationship between the TLE-network and epilepsy by integration with genetic susceptibility data. Here, DNA variation was used to infer causal relationships between the network and epilepsy by assessing whether the network as a whole was genetically associated with epilepsy. To this aim, we used focal epilepsy GWAS data^{6,25} from a separate cohort of 1,429 cases (consisting mainly of patients with TLE) and 7,358 healthy controls. Although no single-nucleotide polymorphism (SNP) achieved genome-wide significance in the epilepsy GWAS (Supplementary Fig. 3), we found that the TLE-network as a whole was highly enriched for genetic associations to focal epilepsy compared with genes not in the network ($P = 2 \times 10^{-7}$; Fig. 1a and Supplementary Table 2). These integrated analyses of co-expression network and genetic susceptibility data from a focal epilepsy GWAS provide independent evidence to support the causal involvement of the TLE-network in epilepsy aetiology.

Conservation and functional specialization of the network. The TLE-network was significantly enriched for genes belonging to several biological pathways involving cell-to-extracellular matrix adhesion including ‘extracellular matrix–receptor interaction’ ($P = 3.9 \times 10^{-5}$), ‘focal adhesion’ ($P = 1.4 \times 10^{-4}$) and inflammation, such as the ‘cytokine–cytokine receptor interaction’ ($P = 2.4 \times 10^{-5}$) and ‘TLR signalling’ ($P = 3.9 \times 10^{-5}$; Fig. 1b). The observation that the TLE-network was enriched for multiple pathways led us to investigate whether the network contained functionally homogenous transcriptional modules (that is, sub-networks of highly correlated genes) with implications for epilepsy aetiology. Using unsupervised agglomerate clustering approaches (see Supplementary Methods), we identified two transcriptional modules comprising 69 (Module-1) and 54 (Module-2) unique genes, respectively (Fig. 1c and Supplementary Data 1). Module-1 was specifically enriched for gene ontology categories related to inflammatory mechanisms, whereas Module-2 was enriched for cell-to-extracellular matrix adhesion processes (Fig. 1d and Supplementary Table 3), indicating functional sub-specialization within the larger TLE-network. We observed that Module-1 genes were significantly upregulated as compared with genes in the larger TLE-network, Module-2, or with respect to all other genes profiled in the hippocampus of TLE patients (Fig. 1e). This increased hippocampal expression of Module-1 genes in TLE patients was not observed

in separate gene expression data sets from the hippocampus of healthy subjects (that is, individuals clinically classified as neurologically normal; Supplementary Fig. 4). Notably, Module-1 was markedly enriched for highly expressed inflammatory cytokines (16-fold enrichment, $P = 6.6 \times 10^{-13}$) many of which belong to the IL-1 signalling cascade (*IL-1 β* , *IL-1RN*, *IL-1 α* , *TNF α*) and the TLR-signalling pathway (11-fold enrichment, $P = 1.4 \times 10^{-6}$), previously implicated in epileptogenesis¹ and brain inflammation^{2,3} (Supplementary Fig. 5). Taken together, these data indicate the presence of a coordinated transcriptional programme (Module-1), encompassing TLR activation and release of proinflammatory cytokines (including IL-1 β), in chronic human epileptic hippocampus as previously hypothesized^{3,26}.

We then investigated whether the TLE-network and Module-1 genes, in particular, were conserved across-species and to this aim we carried out high-throughput sequencing of mRNA (RNA-Seq) in whole hippocampus from 100 epileptic (pilocarpine model)²⁷ and 100 control naïve mice (full details of this model are reported in the Supplementary Methods). We employed GGMs to assess the co-expression relationships between the 371 mouse orthologues of the human TLE-network genes, and found that 312 genes (84%) had significant co-expression (FDR < 5%) with at least another network gene in mouse epileptic hippocampus

(Fig. 2a). The conserved TLE-network genes formed 1,119 significant partial correlations in mouse epileptic hippocampus, which is significantly higher than expected by chance ($P = 0.001$ by 10,000 bootstrap permutations; Fig. 2b). In contrast, only 615 significant partial correlations between the same 312 genes were detected in healthy hippocampus ($P = 0.659$ by 10,000 bootstrap permutations), suggesting that the TLE-network is specifically conserved in the epileptic mouse hippocampus (Fig. 2b). In keeping with the high expression of proinflammatory genes observed in the hippocampus of TLE patients (Supplementary Fig. 5), the mouse orthologues of Module-1 genes that were significantly upregulated in epileptic hippocampus were enriched for TLR-signalling and cytokines (gene set enrichment analysis²⁸, $P = 9.03 \times 10^{-4}$, Fig. 2c). These comparative genomics analyses revealed that, to a large extent, the hippocampal TLE-network is conserved across-species, and confirm that genes for TLR signalling and proinflammatory cytokines within the TLE-network are upregulated in chronic epileptic hippocampus.

SESN3 is a genetic regulator of the proinflammatory network.

We set out to identify genetic variants that regulate the gene co-expression modules (that is, regulatory ‘hotspots’) by employing genome-wide Bayesian expression QTL mapping approaches^{18,29}.

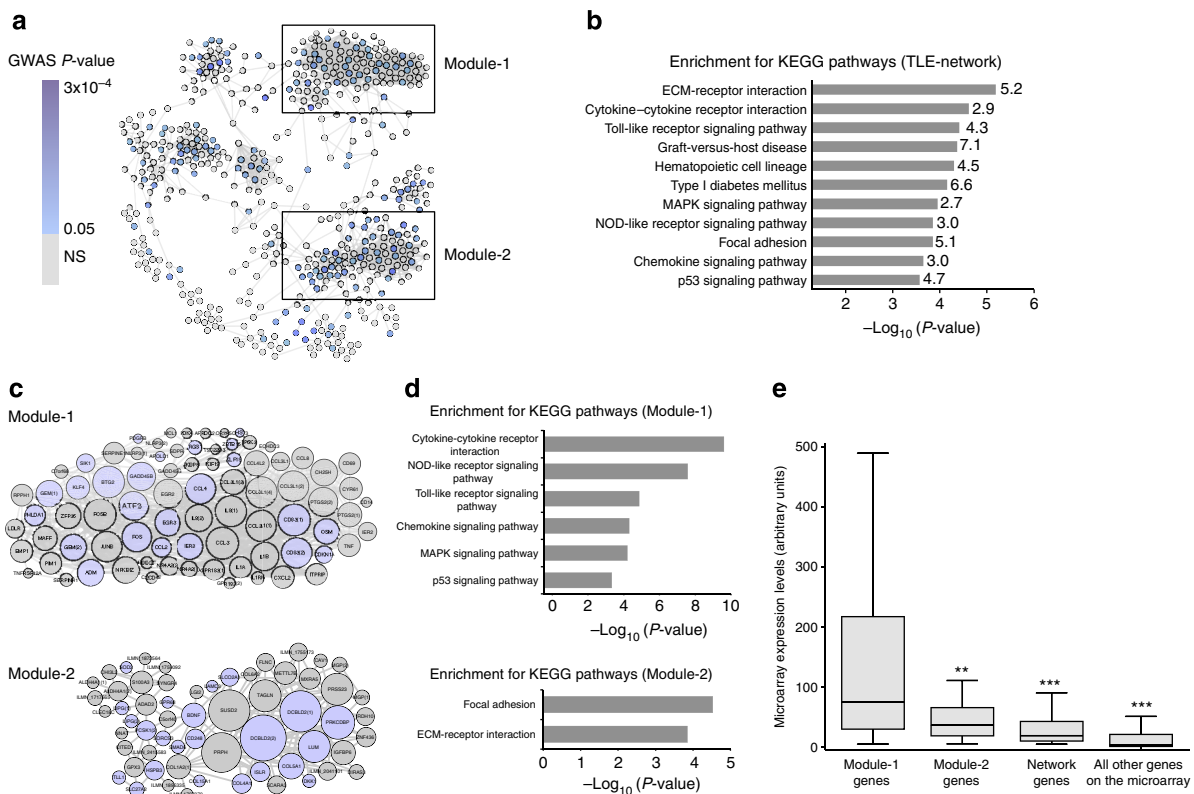


Figure 1 | Identification of the TLE-network and functionally specialized transcriptional modules in human epileptic hippocampus. (a) Gene co-expression network identified in the hippocampus of TLE patients (TLE-network). Nodes represent genes and edges represent significant partial correlations between their expression profiles (FDR < 5%). Node colour indicates the best GWAS P-value of association with focal epilepsy for SNPs within 100 kb of each gene (Supplementary Data 1). Boxes mark two transcriptional modules within the network. (b) Kyoto Encyclopedia of Genes and Genome (KEGG) pathways significantly enriched in the TLE-network (FDR < 5%). The fold enrichment for each KEGG pathway is reported on the side of each bar. (c) Module-1 and Module-2 details. The size of each node is proportional to its degree of interconnectivity within each module. Light blue indicates genes showing nominal association with susceptibility to focal epilepsy by GWAS. Numbers in parenthesis indicate multiple microarray probes representing the same gene. (d) KEGG pathways significantly enriched in Module-1 (top) and Module-2 (bottom; FDR < 5%). (e) Module-1 is significantly highly expressed in the hippocampus of TLE patients. mRNA expression of Module-1 ($n = 80$ probes, representing 69 unique annotated genes) as compared with Module-2 ($n = 60$ probes, representing 54 unique annotated genes), other network genes ($n = 371$ probes, representing 319 unique annotated genes) and all other probes represented on the microarray ($n = 48,256$). ** $P = 3.8 \times 10^{-4}$; *** $P < 10^{-10}$, Mann-Whitney test, two-tailed.

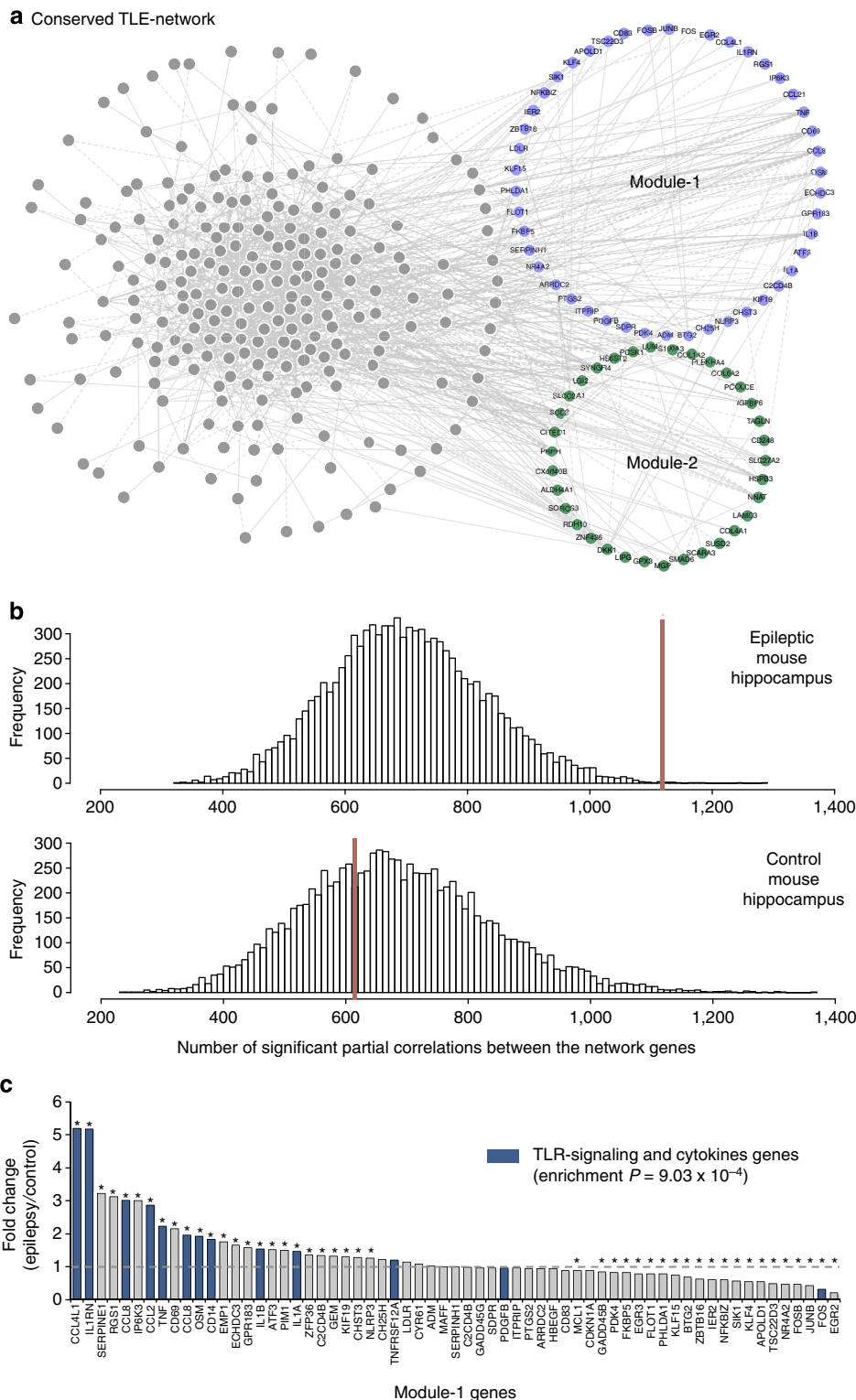


Figure 2 | TLE-network conservation in mouse epileptic hippocampus. (a) Human TLE-network genes that are conserved and co-expressed (84%) in the mouse hippocampus. Each node in the network represents a transcript that had significant partial correlation with at least another transcript in the network (FDR < 5%). Conserved Module-1 and Module-2 genes are indicated in blue and green, respectively. (b) Distribution of significant partial correlations (FDR < 5%) between pairs of transcripts from 10,000 bootstrap permutation samples in epileptic (top) and control (bottom) mouse hippocampus. In each case, the red line indicates the actual number of significant partial correlations (FDR < 5%) between all genes in the network. The number of significant partial correlations observed in control hippocampus was not different from chance expectation ($P = 0.659$). In contrast, the number of significant partial correlations detected in epileptic hippocampus was significantly higher than expected by chance ($P = 0.001$). (c) Differential expression of Module-1 genes between control and epileptic mouse hippocampus shows specific enrichment for TLR-signalling and cytokine genes among the upregulated genes (gene set enrichment analysis²⁸). Stars denote significant fold changes between epileptic and control mouse hippocampus (FDR < 5%); blue bars indicate TLR-signalling and cytokine genes.

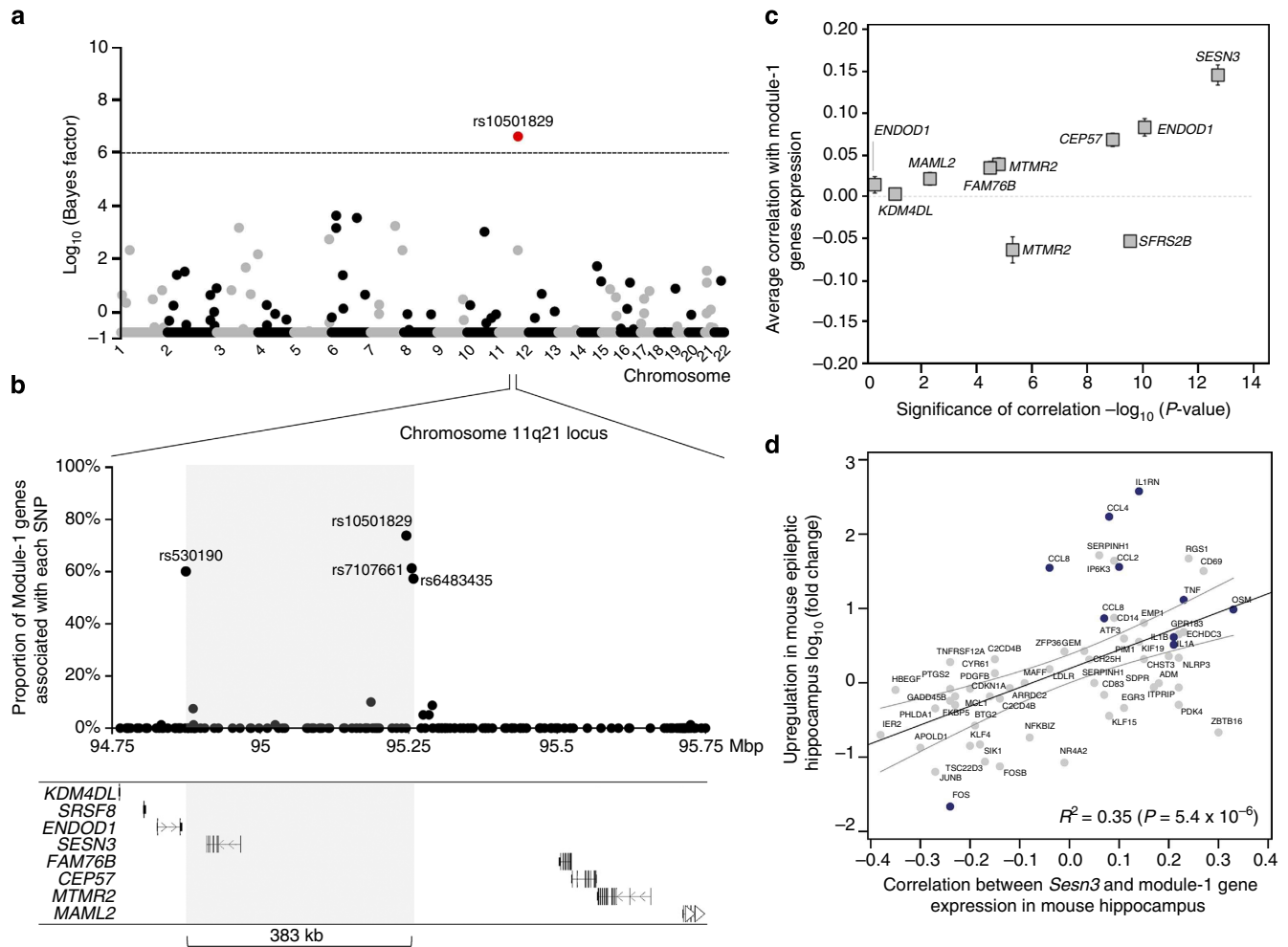


Figure 3 | *SESN3* is a trans-acting genetic regulator of Module-1 in epileptic hippocampus. (a) Genome-wide mapping of the genetic regulation of Module-1. For each autosome (horizontal axis), the strength of evidence for each SNP (filled dot) being a regulatory locus for the first PC of Module-1 expression is measured by the log₁₀(Bayes factor) (vertical axis). The Bayes factor quantifies evidence in favour of genetic regulation versus no genetic control of module expression, and is reported as a ratio between the strengths of these models. At 5% FDR (that is, log₁₀(Bayes factor) > 6, dashed line), SNP rs10501829 (11q21, highlighted in red) was significantly correlated with Module-1 expression. (b) Joint mRNA levels and SNPs analysis within the 1-Mbp region centred on SNP rs10501829, comprising 178 SNPs genotyped in the TLE patient cohort. We carried out multivariate Bayesian regression modelling¹⁸ of all Module-1 probes ($n = 80$) and all SNPs ($n = 178$) to identify the most informative SNPs in the region predicting Module-1 expression. For each SNP, we report the proportion of associated genes in Module-1 (vertical axes): four SNPs (rs10501829, rs530190, rs7107661 and rs6483435) that are individually associated with 58–74% of Module-1 genes are highlighted. The grey box indicates the boundaries of the associated regulatory region (delimited by SNPs rs530190 and rs6483435), spanning 383 kb. (c) For each candidate gene at the 1-Mbp regulatory locus, we report the average Pearson correlation (r , \pm s.e.m.) between the candidate gene’s expression and the expression of Module-1 genes (y axes) and its statistical significance for deviation from $r = 0$ (x axes). Two-tailed P -values are reported on a negative log scale and were calculated using one sample Wilcoxon Signed Rank test. Two genes (*ENDOD1* and *MTMR2*) were represented by two microarray probes and were analysed separately. (d) Association between increased *Sesn3* mRNA expression and upregulation of Module-1 genes in epileptic mouse hippocampus. For each gene, we report its log₁₀(fold change) in epilepsy versus control (y axes) and its correlation with *Sesn3* mRNA expression (x axes). The 95% confidence interval of the slope of the regression line is indicated. TLR-signalling and cytokines genes are highlighted in blue.

To this aim, we have developed a multi-step strategy to identify SNPs that regulate the expression of a transcriptional module (or network) as a whole. As first step, we summarize the expression of the genes in each module using principal component (PC) analysis and detect regulatory ‘hotspots’ using a Bayesian regression model at the genome-wide level²⁹. This analysis prioritizes genomic regions associated with variation in mRNA expression of the genes in each module. As a second step, to refine the genetic mapping results, we regress jointly the mRNA levels of module genes to all SNPs within the regulatory locus identified in the first step¹⁸. Given the functional specialization within the large TLE-network (Fig. 1d), we investigated the genetic regulation of both Module-1 and Module-2, by analysing

527,684 genome-wide SNPs in the TLE patient cohort. In the first step, we identified a single locus on chromosome 11q21 centred on SNP rs10501829, which was significantly associated with the first PC of Module-1 expression (FDR < 5%; Fig. 3a). Module-2 showed no significant genome-wide associations (Supplementary Fig. 6). In the second step, we investigated in detail the locus on chromosome 11q21 regulating Module-1 and carried out joint mRNA levels-SNPs analysis of all genes in Module-1 and all SNPs genotyped within a 1-Mbp region centred on SNP rs10501829. This analysis identified three additional SNPs (rs530190, rs7107661 and rs6483435) in the Best Model Visited (that is, the best combination of SNPs predicting mRNA level of module genes, see Supplementary Methods) that were associated with the

majority of genes of Module-1 (58–74% of Module-1 genes are predicted by individual SNPs, Fig. 3b). The set of SNPs regulating *in trans* the expression of Module-1 genes defined the boundaries of a minimal regulatory region spanning ~383 kb (Fig. 3b).

The larger 1-Mbp region centred on SNP rs10501829 contained eight annotated protein-coding genes (Fig. 3b). To further prioritize candidate genes, we carried out co-expression analysis between each of these genes and all genes in Module-1, and found that Sestrin 3 (*SESN3*) was, on average, most strongly and positively correlated with Module-1 gene expression ($P = 1.7 \times 10^{-13}$, Fig. 3c). The positive association between *SESN3* and Module-1 gene expression remained significant following genome-wide correlation analysis in human hippocampus ($P < 0.00001$, Supplementary Fig. 7). In summary, *SESN3* is the only gene within the minimal regulatory region and, when compared with all genes within a 1-Mbp window around SNP rs10501829, showed the strongest correlation with Module-1 gene expression. Similarly, in the epileptic mouse hippocampus, we found that increased *Sesn3* mRNA expression was also significantly associated with upregulation of Module-1 genes ($P = 5.4 \times 10^{-6}$, Fig. 3d), therefore providing independent, cross-species evidence supporting *SESN3* as a positive regulator of Module-1 genes in epileptic hippocampus.

Taken together, these data prioritize *SESN3* as a candidate gene for the *trans*-acting genetic regulation of Module-1. To test this hypothesis, we first carried out gene knockdown experiments followed by transcriptional analysis of Module-1 genes by means of RNA interference using short interfering RNA (siRNA). Initially, we used murine bone marrow-derived macrophages (BMDMs) and BV2 microglia cell line as an *in vitro* system as Module-1 recapitulates the ATF3/API transcriptional complex and IL-1 signalling (Supplementary Fig. 8), known to be highly expressed in lipopolysaccharide (LPS)-stimulated macrophages³⁰. Consistent with the positive correlation of Module-1 genes with *SESN3* mRNA expression (Fig. 3c,d and Supplementary Fig. 7), we observed decreased expression of Module-1 genes after siRNA-mediated knockdown of *SESN3* in both LPS-stimulated BMDMs and BV2 microglia cells (Fig. 4a,b). Similar results were found in unstimulated BV2 microglial cells, suggesting that *SESN3* can modulate expression of proinflammatory genes (for example, *IL-1 β* , *IL-1RN*, *IL-1 α* , *TNF α*) even in the absence of a strong inflammatory stimulus (Fig. 4c). Within the human brain we localized *SESN3* expression to neurons by immunohistochemistry (Fig. 4d), and found that it is highly expressed in the hippocampus of TLE patients as compared with hippocampus from control autopsy samples (Fig. 4e and Supplementary Fig. 9). In keeping with this, we found increased

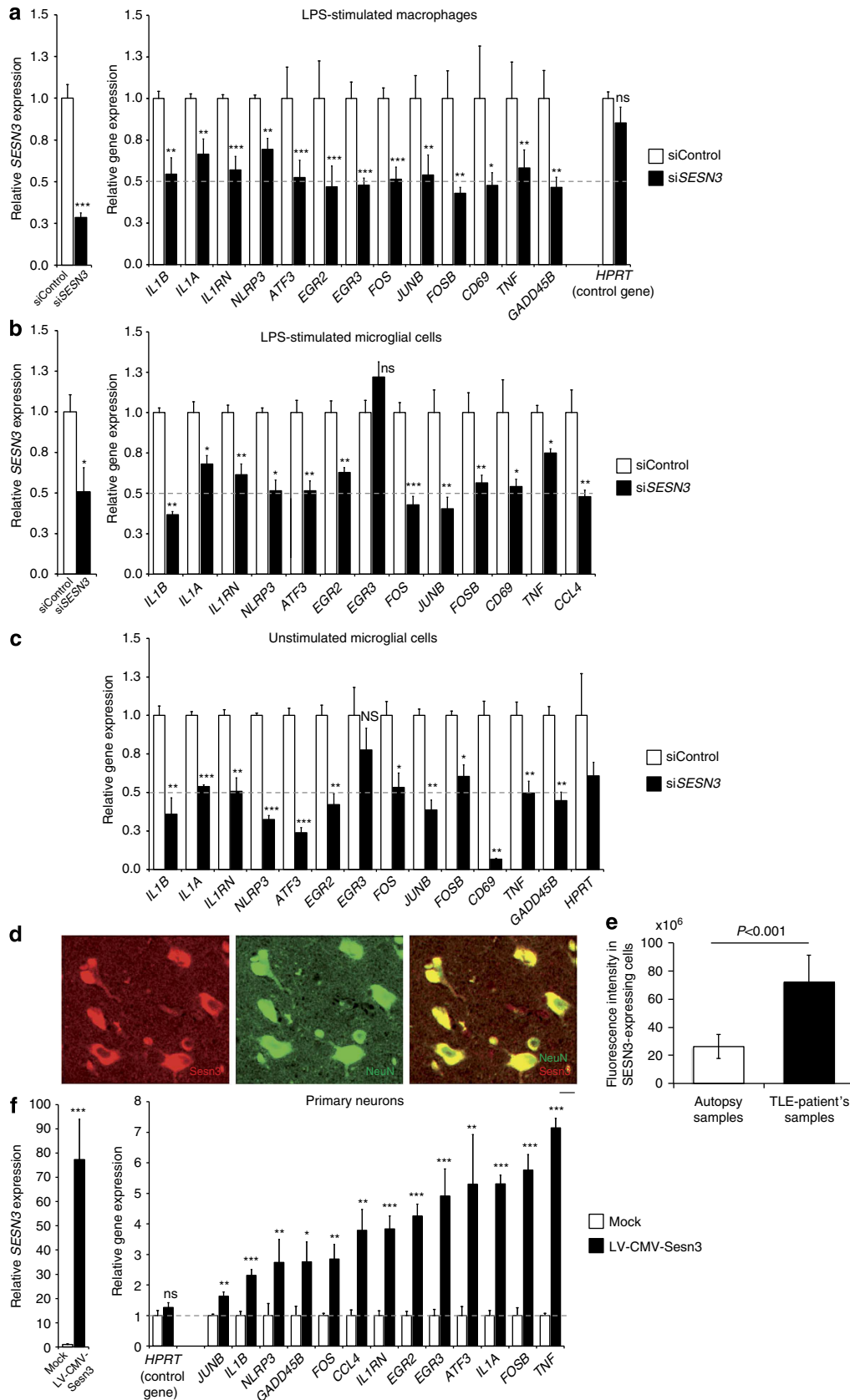
Sesn3 mRNA expression in the mouse hippocampus after pilocarpine-induced status epilepticus (Supplementary Fig. 10), suggesting an association between *SESN3* gene expression and epilepsy that is conserved across-species. We then tested whether Module-1 genes are upregulated when *SESN3* is overexpressed in neurons. To address this aim, we used an integrating lentiviral vector (LV) for gene overexpression in primary murine neurons (see Supplementary Methods) and quantitative PCR analysis showed that the relative levels of *Sesn3* mRNA were markedly increased in transduced neurons compared with the levels observed in mock transduction (Fig. 4f). Consistent with the observed positive correlation between increased *Sesn3* expression and Module-1 genes in the hippocampus (Fig. 3c,d), lentiviral-mediated overexpression of *Sesn3* resulted in significant upregulation of Module-1 genes in hippocampal neurons (Fig. 4f). These *in vitro* experiments show that *Sesn3* is capable of regulating Module-1 gene expression in different cell types and in particular of inducing upregulation of proinflammatory genes in hippocampal neuronal cells. Our findings in primary neurons are in keeping with previous data reporting the activity of several inflammatory molecules in neuronal cells under pathological conditions³¹, including IL-1 β and its receptor³². Furthermore, the upregulation of proinflammatory genes in neurons supports the ‘neurogenic inflammation’ hypothesis, wherein neurons are proposed as triggers of innate and adaptive immune-cell activation in the central nervous system (CNS; reviewed in Xanthos and Sandkuhler³³).

SESN3 regulates chemically induced behavioural seizures. The *in vitro* data, combined with the positive association between *SESN3* and Module-1 gene expression in human and mouse epileptic hippocampus, indicate that *SESN3* is a positive regulator of Module-1. We hypothesized that inhibiting *SESN3* would reduce the activity of genes in functional pathways enriched in Module-1, including proconvulsant signalling molecules, and thus by extension could have seizure-suppressing effects. To test this hypothesis *in vivo*, we investigated the role of *SESN3* in a zebrafish model of convulsant-induced seizures^{34,35}. In this model, exposure of 2- or 3-day-old zebrafish larvae to the convulsant agent pentylenetetrazole (PTZ) rapidly induces the expression of synaptic activity-regulated genes in the CNS and causes vigorous episodes of calcium flux in muscle cells as well as intense locomotor activity characteristic of epileptic seizures^{34,35}. This acute seizure model has been primarily used to investigate the anti-/proconvulsant activity of compounds³⁶ and for *in vivo* drug discovery³⁴. In particular, molecular and behavioural

Figure 4 | *SESN3* regulates expression of Module-1 genes in macrophages, microglial cells and neurons. Effect of siRNA-mediated knockdown of *Sesn3* as compared with control siRNA (siControl), showing significant inhibition of *Sesn3* mRNA expression and downregulation of Module-1 genes in murine LPS-stimulated (1 h) BMDM (a) and BV2 microglial cells (b), as well as in unstimulated BV2 microglial cells (c). Five independent biological replicates were used for BMDM experiments and at least three replicates in the BV2 microglia cells experiments. Data normalized to β -actin levels are shown as means relative to control \pm s.e.m. (d) *SESN3* immunofluorescence of human hippocampal slices from TLE patients: co-immunostainings with NeuN (green) antibody showed that *SESN3* (red) is localized in neurons. Scale bar, 100 μ m. (e) Quantification of *SESN3* expression in human hippocampal tissue by immunofluorescence analysis. Maximum intensity projections of confocal z-stack images of immunohistochemical stainings with antibody against *SESN3* were used. For determination of *SESN3* cell fluorescence as a measure of *SESN3* expression level, *SESN3*-expressing cells in the CA2 region of the hippocampus in both TLE patients samples ($n = 7$) and autopsy samples ($n = 8$) were measured using ImageJ software. Cell fluorescence was assessed as follows: integrated density—(area of selected cell \times mean fluorescence of background readings). *SESN3* total cell fluorescence in TLE patients is significantly increased as compared with the *SESN3* total cell fluorescence in autopsy samples (two-tailed Mann-Whitney test, $P < 0.001$). Fluorescence intensity data are reported as means \pm s.e.m. (f) Effect of lentiviral-mediated *Sesn3* overexpression on Module-1 genes in primary hippocampal neurons. Left, relative levels of *Sesn3* mRNA in transduced neurons (LV-CMV-*Sesn3*) compared with the levels in mock transduction (Mock). Right, relative mRNA levels of Module-1 genes and a control gene not in the network (*Hprt*) in transduced neurons compared with levels in mock transduction. Data normalized to *Gapdh* levels are shown as means relative to control \pm s.e.m. Four (Mock group) and twelve (LV-CMV-*Sesn3* group) replicates were used in neuronal cell experiments. Statistical significance of the differences (P -value) between si*SESN3* (or LV-CMV-*Sesn3*) and siControl (or Mock) was assessed by t -test (two-tailed) and adjusting for unequal variances across different groups. * $P < 0.05$; ** $P < 0.01$; *** $P < 0.001$; **** $P < 0.0001$; NS, not significant ($P > 0.05$).

phenotypes in the zebrafish PTZ-induced seizure model have been employed to identify compounds that attenuate seizure activity³⁷. We employed this model to correlate the locomotor responses with gene network dynamics, that is, transcriptional

activation of the neuronal activity-regulated gene *c-fos*³⁸ and an additional subset of Module-1 genes in response to PTZ treatment in *Sesn3* morphant and control morphant larvae. *Sesn3* showed widespread expression in the brain of 3 and 4 days



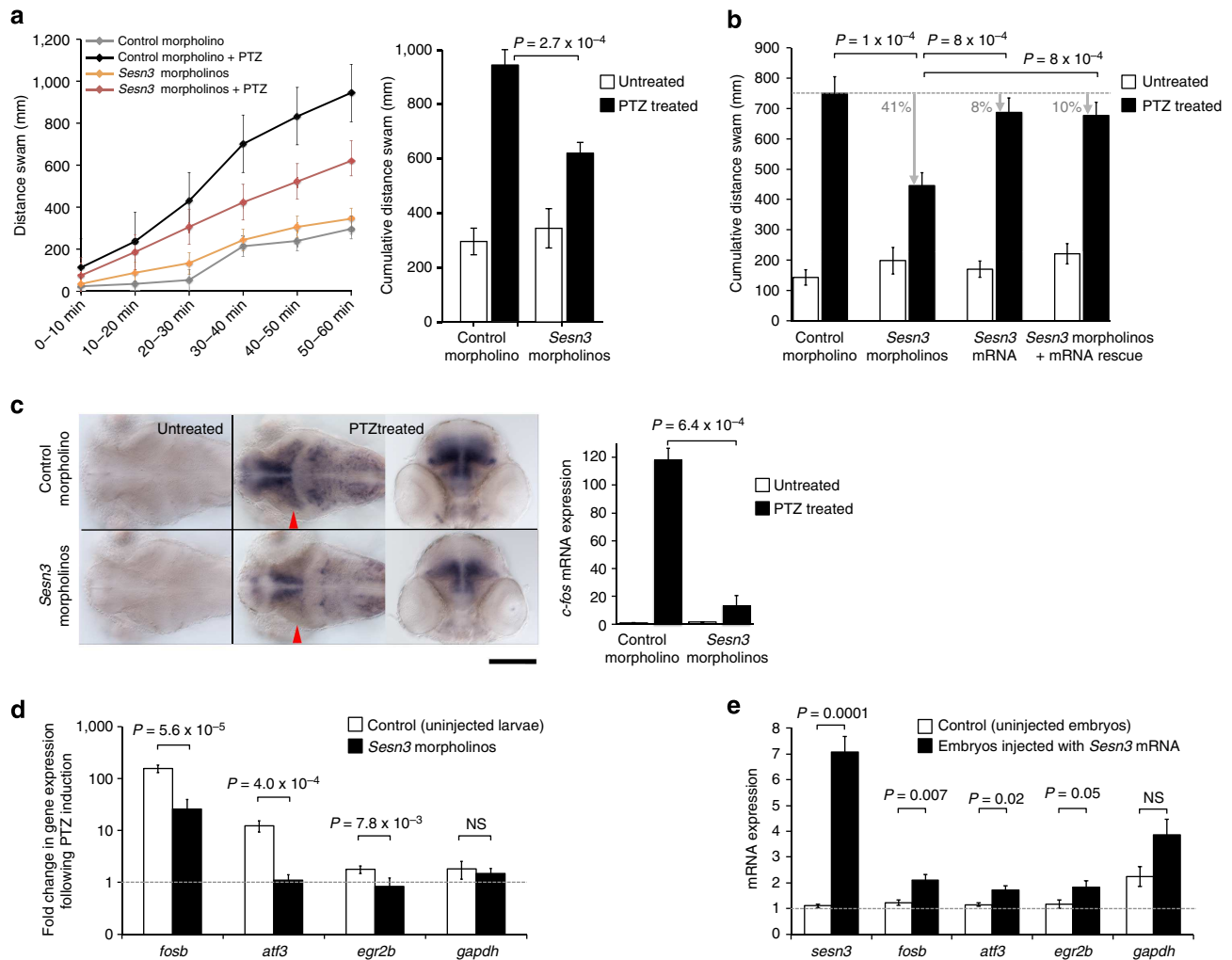


Figure 5 | *Sesn3* modulates PTZ-induced *c-fos* expression, locomotor convulsions and Module-1 genes in zebrafish. (a) Left, *Sesn3* promotes convulsive locomotor response of zebrafish larvae exposed to PTZ. Three days post fertilization (d.p.f.) zebrafish larvae were incubated with and without 20 mM PTZ for 1 h and locomotor activity was monitored continuously. Larvae microinjected with *Sesn3* morpholinos exhibited a sustained reduction in locomotor activity throughout the period of PTZ incubation, in comparison with control morphant larvae. Both *Sesn3* morphant and control morphant larvae ($n = 12$) exhibited similarly low levels of locomotor activity in the absence of PTZ. Right, *Sesn3* morpholinos reduced the cumulative locomotor activity of zebrafish exposed to 20 mM PTZ (black columns) without appreciably affecting basal locomotor activity of larvae incubated in the absence of PTZ (white columns). (b) Co-injecting *Sesn3* morpholinos with synthetic *Sesn3* mRNA showed that *Sesn3* mRNA rescued the locomotor activity phenotype (total distance swam, y axis). For each group, 16–18 larvae were analysed. Black bars, 1 h PTZ treatment (20 mM). (c) *Sesn3* morpholinos attenuate seizure-induced expression of the synaptic activity-regulated gene *c-fos*. Left and central images, dorsal views of the brains of 3 d.p.f. control morphant (top) and *Sesn3* morphant larvae (bottom) maintained for 1 h in the absence and presence of 20 mM PTZ, after which larvae were fixed and analysed for *c-fos* expression by whole-mount *in situ* hybridization. Red arrowheads: position of the transverse sections of the brains; scale bar, 200 μ m. Following PTZ treatment (20 mM, 1 h), quantitative PCR (qPCR) analysis revealed that *Sesn3* morphant larvae exhibited significantly lower mRNA expression of *c-fos* in the brain than control morphant larvae (c, right panel). (d) PTZ-induced transcriptional response of Module-1 genes was significantly lower in *Sesn3* morphants as compared with uninjected larvae; six samples were used in the qPCR experiments (one sample = 15–20 pooled larvae). (e) Upregulation of Module-1 genes upon injection of synthetic mRNA (1 ng) in zebrafish embryos ($n = 30$) as compared with uninjected control embryos ($n = 30$). Total RNA was extracted 28 h post fertilization and qPCR experiments were performed for the two pools of embryos using six technical replicates. Data reported as means \pm s.e.m. were determined by the $2^{-\Delta\Delta C_t}$ method and normalized to the housekeeping gene β -actin. *P*-values calculated by *t*-test (two-tailed) adjusting for unequal variances across different groups. NS, not significant ($P > 0.05$).

post fertilization (d.p.f.) zebrafish larvae (Supplementary Fig. 11) and, following PTZ treatment, we found that *Sesn3* morphant zebrafish larvae exhibited significantly reduced locomotor activity as compared with control morphant larvae (Fig. 5a). To test the specificity of the morpholino effect, we co-injected the *Sesn3* morpholinos (Supplementary Fig. 12) along with synthetic *Sesn3* mRNA, which cannot be targeted by either of the splice-blocking morpholinos (see Supplementary Methods), and assessed whether the *Sesn3* mRNA could rescue the morphant phenotype. We observed an almost complete rescue of the locomotor activity

phenotype (only 10% difference between uninjected larvae and larvae co-injected with *Sesn3* morpholinos and *Sesn3* mRNA), with no significant differences in the locomotor activities between the uninjected larvae and the larvae injected with synthetic *Sesn3* mRNA alone (Fig. 5b).

To further confirm *Sesn3*-dependent modification of neuronal response to PTZ, we measured transcriptional activation of the neuronal activity-regulated gene *c-fos*, an important regulator for cellular mechanisms mediating neuronal excitability and survival³⁸. Consistent with the behavioural assay (Fig. 5a), there

was decreased expression of *c-fos* in the brain (mostly in forebrain and midbrain) following PTZ exposure in *Sesn3* morphant larvae as compared with control morphant larvae (Fig. 5c and Supplementary Fig. 12). As silencing of *Sesn3* resulted in downregulation of Module-1 genes *in vitro* (Fig. 4a–c), we tested whether inhibiting *Sesn3* could similarly reduce the activity of Module-1 genes following PTZ exposure *in vivo*. We observed significant reduction in the PTZ-induced mRNA expression of Module-1 genes in the *Sesn3* morphant as compared with control morphant larvae (Fig. 5d), and we also found that transient overexpression of *Sesn3* in zebrafish larvae increased expression of Module-1 genes independently of PTZ treatment (Fig. 5e). Taken together, these data show that *Sesn3* knockdown attenuates both PTZ-induced locomotor convulsive behaviour and the transcriptional responses of *c-fos* and Module-1 genes to treatment with PTZ. These findings in the zebrafish model support the evidence from our studies of human and mouse epileptic hippocampus and primary murine neurons that *SESN3* positively regulates expression of proconvulsive molecules (Module-1 genes).

Discussion

Deciphering the complex regulatory processes of pathophysiological pathways in human brain remains a challenge due to the inaccessibility of ante-mortem tissue but can have important mechanistic and therapeutic implications³⁹. In this study, we have used surgical hippocampal tissue samples and employed systems genetics approaches¹⁷ to investigate transcriptional networks for epilepsy and their genetic regulation. We identified a large gene co-expression network in the human epileptic hippocampus that was conserved in mouse epileptic hippocampus and was enriched for GWAS genetic signals of focal epilepsy. In keeping with similar network-based studies of complex disease such as type-1 diabetes⁴⁰ and autism spectrum disorder^{41,42}, our approach leverages the combined evidence from genetic susceptibility variants across multiple genes¹⁵ to link the TLE-hippocampus network with susceptibility to focal epilepsy. Within the TLE-network, we identified a functionally coherent and coordinated transcriptional programme (Module-1), which was overexpressed in the hippocampus of TLE patients, and which encoded epileptogenic IL-1 (refs 2,3,43) and TLR-signalling pathways¹. We confirmed the upregulation TLR-signalling genes and proinflammatory cytokines in chronic epilepsy by RNA-Seq analysis in 200 mouse hippocampi. Preclinical studies in experimental models of epilepsy have consistently shown that individual proinflammatory cytokines such as IL-1 β or tumor necrosis factor (TNF)- α are overexpressed in brain areas of seizure generation and propagation⁴⁴. Therefore, targeting TLR and IL-1 signalling has been proposed as a possible avenue for therapeutic intervention in epilepsy and antiepileptogenesis^{1,3}, including reduction of acute seizures⁴⁵ and drug-resistant chronic epileptic activity⁴⁶. The identification of upstream genetic regulators of these pathways in the human epileptic brain might suggest opportunities for novel targets for disease modification. To investigate the genetic regulation of the TLE-network and the proinflammatory module therein, we employed Bayesian expression QTL mapping approaches¹⁸, which identified *SESN3* as a *trans*-acting genetic regulator of a proinflammatory transcriptional programme in the epileptic human hippocampus. The positive regulation of this network by *SESN3* was confirmed *in vitro* across different cell types by gene silencing (resulting in ~50% reduction of Module-1 gene expression) and overexpression experiments (resulting in approximately two- to sevenfold activation of Module-1 genes, Fig. 4), and *in vivo* using a zebrafish model of chemically induced seizures (Fig. 5e).

SESN3 is a member of the Sestrin family of proteins that have been shown to decrease intracellular reactive oxygen species and to confer resistance to oxidative stress¹⁹. Intrinsic antioxidant defenses are important for neuronal longevity and the genes that regulate these processes might well influence pathological processes associated with oxidative damage in the brain, a common feature of many neurodegenerative diseases including epilepsy^{47,48}. Therefore, we hypothesize that *SESN3* might regulate neuro-inflammatory molecules, previously implicated in epilepsy^{1,33,43,49}, through modulation of oxidative stress in the brain.

Our systems genetics analysis in the human hippocampus, combined with *in vitro* and *in vivo* data, revealed *SESN3*-dependent regulation of epileptogenic IL-1 β and TLR-signalling genes¹. The upstream genetic control of the proconvulsant transcriptional programme by *SESN3* in human TLE-hippocampus suggested a role for this gene in modulating seizures. To test the potential functional role of *SESN3* *in vivo*, we used an experimental model of acute epileptic seizures^{34,37} and found that knockdown of *Sesn3* attenuated chemical convulsant-induced locomotor activity and *c-fos* expression, as well as modulating Module-1 gene expression (Fig. 5). Our *in vitro* data in macrophages, BV2 microglial cells and primary neurons showed that *SESN3* is a positive regulator of proinflammatory molecules (Fig. 4), including IL-1 β and TNF- α , major mediators of inflammation, which are capable of inducing changes in neuronal excitability⁵⁰. The finding of reduced severity of PTZ-induced seizures upon knockdown of *Sesn3* in the zebrafish model is consistent with previous studies in rodents describing the effects of proinflammatory cytokines on seizures. In the context of pre-existing brain inflammation, antibody-mediated antagonism of TNF- α function inhibited susceptibility to PTZ-induced seizures in rats⁵¹, whereas administration of exogenous TNF- α increased susceptibility to PTZ-induced seizures⁵². Our findings in zebrafish are therefore in keeping with a role for *SESN3* in regulating proinflammatory cytokines and their downstream effect on CNS excitability and seizure susceptibility.

Taken together, our data provide the first evidence of a function for *SESN3* in regulating proconvulsant agents (for example, TNF- α , IL-1 and TLR-signalling genes) in human epileptic hippocampus, and suggest *SESN3* as a new potential target for modulating brain inflammation^{3,44} and CNS excitability⁵³. Our systems genetics approach builds on and extends previous methods correlating individual genetic variation with disease susceptibility by identifying disease-associated gene networks, pathophysiological pathways and their upstream genetic regulators in human brain. More generally, the systems genetics framework described here can be employed to identify genes and regulatory networks across diverse neuropsychiatric disorders where genetic factors can perturb underlying molecular pathways in the brain.

Methods

Gene expression profiling in the human hippocampus. All 129 patients considered in this study had mesial TLE and all tissue samples were from indistinguishable hippocampal tissue portions. Sample preparation and microarray analysis of human hippocampi are detailed in Supplementary Methods. Expression data were analysed using Illumina's GenomeStudio Gene Expression Module and normalized by quantile normalization with background subtraction. Microarray probes were annotated using either the Human HT-12 v3 annotation file or Ensembl (release 72). All patients gave informed consent for use of their tissue and all procedures were conducted in accordance with the Declaration of Helsinki and approved by the Ethics Committee of the University of Bonn Medical Center.

Gene co-expression network analysis. Gene co-expression networks were reconstructed using GGMs, which use partial correlations to infer co-expression relationships between any microarray probe pair in the data set, removing the

effect of other probes²³. We used the empirical Bayes local FDR statistics⁵⁴ to extract significant partial correlations (Supplementary Fig. 13), and which identified a large set of 2,124 inter-connected nodes belonging to the same connected component (TLE-network, Supplementary Data 2). Network extraction and identification of transcriptional modules are described in the Supplementary Methods.

Mapping the genetic control of networks. We used Bayesian variable selection models^{18,29} to identify the genetic control points (regulatory ‘hotspots’) of transcriptional modules in the TLE patient cohort. First, we combined PC analysis⁵⁵ with multivariate regression approaches to prioritize genome-wide genomic regions associated with the module expression. We then analysed all genes of the module with all SNPs in the regulatory region using the hierarchical evolutionary stochastic search algorithm¹⁸, where the module genes’ expression are jointly considered. Further details are reported in Supplementary Methods.

Genetic association of the TLE-network with epilepsy. To test if TLE-network genes are likely to be causally involved in the disease process, we assessed whether network genes are enriched for SNP variants associated to focal epilepsy by GWAS^{6,25}. Full details on the GWAS of focal epilepsy are reported in Supplementary Methods. Briefly, in the GWAS-enrichment analysis each gene of the TLE-network was assigned a GWAS significance value consisting of the smallest *P*-value of all SNPs mapped to it. We used the hypergeometric distribution test to assess whether SNPs close to (< 100 kb from) any network gene were more likely to associate with epilepsy by GWAS than SNPs close to genes not in the TLE-network. Empirical GWAS-enrichment *P*-values were generated by 1,000,000 randomly selected gene-sets and are reported in Supplementary Table 2 (see Supplementary Methods for additional details).

RNA-Seq analysis in the mouse hippocampus. RNA-Seq analysis in whole hippocampus from 100 epileptic (pilocarpine model)²⁷ and 100 control naïve mice (NMRI) is detailed in Supplementary Methods. Briefly, raw reads were mapped to the reference mouse genome (mm10) using TopHat version 2.0.8 (ref. 56) and read counts per gene were normalized across all samples using the ‘trimmed mean of *M*-value’ approach⁵⁷. Differential expression analysis was performed using the edgeR⁵⁷ and a threshold of 5% FDR was used to identify significant gene expression changes. Experimental animals were used only once for each study. All experimental procedures complied with the guidelines of the European Union Directive 2010/63/EU. A local ethical committee approved the experimental protocol.

In vitro studies. Details on all cell cultures used in these studies are reported in Supplementary Methods. siRNA knockdown experiments were performed in murine BMDMs and BV2 microglia cell lines using a mouse *Sesn3* ON-TARGETplus SMARTpool siRNA (100 nM, ThermoFisher Scientific) and Dharmafect 1 (ThermoFisher Scientific) as transfection reagent, according to the manufacturer’s recommendations. For LPS stimulation experiments, the transfected cells were washed twice in DMEM and stimulated with LPS (Sigma, 100 ng ml⁻¹) for an hour. For overexpression experiments, a third-generation LV was used to transduce murine primary hippocampal neuronal culture. Additional information and details on *Sesn3* siRNA target sequences, the real-time quantitative PCR for Module-1 genes and primer sequences are given in Supplementary Methods and Supplementary Table 4. The relative expression levels normalized to *Beta-actin* (or *Gapdh* as indicated) gene expression were then determined by the 2^{-ΔΔCt} method.

In vivo studies. To study the function of sestrin 3 in response to PTZ-induced seizures, two different morpholinos were designed to block the normal splicing of the zebrafish *Sesn3* primary transcript (see Supplementary Fig. 12 and Supplementary Methods). Embryos that were to be analysed by whole-mount *in situ* hybridization were first treated with 1-phenyl-2 thiourea at 23 h post fertilization (h.p.f.) to inhibit melanogenesis. At 3 d.p.f., larvae were treated for 1 h with 20 mM PTZ or left untreated, and all larvae were then fixed with paraformaldehyde immediately after the treatment period. RNA *in situ* hybridization analysis was carried out using a *c-fos* digoxigenin-labelled probe, which was prepared as recommended by the manufacturer of the *in situ* hybridization reagents (Roche). Whole-mount *in situ* hybridization was performed using standard procedures⁵⁸. Analysis of zebrafish locomotor activity was carried out using the Viewpoint Zebrafish system (Viewpoint) as previously reported in ref. 34. Briefly, 3 d.p.f. larvae were incubated in E3 medium with or without 20 mM PTZ in microtitre plates, with one larva per well, and larval movements were recorded with the Viewpoint Zebrafish over a recording period of 60 min, using a light cycle of 2 min: 100% light; 2 min: 0% light. The distance swam by each larva was measured for every 10-min period during the recording period, and the cumulative distance swam over the recording period was calculated. Rescue experiments were performed by co-injection of synthetic *sesn3* RNA into one-cell stage AB wild-type zebrafish embryos alone (2 nl of 0.3 ng ml⁻¹ *sesn3* mRNA) or in combination with *Sesn3* morpholinos. Additional details, including the quantitative PCR analyses of

c-fos and Module-1 genes, primer sequences are reported in Supplementary Methods. All experimental procedures involving zebrafish were performed in compliance with the UK Animal (Scientific Procedures) Act and approved by the University of Sheffield Animal Welfare Ethical Review Board.

References

- Maroso, M. *et al.* Toll-like receptor 4 and high-mobility group box-1 are involved in ictogenesis and can be targeted to reduce seizures. *Nature Med.* **16**, 413–419 (2010).
- Vezzani, A. *et al.* Powerful anticonvulsant action of IL-1 receptor antagonist on intracerebral injection and astrocytic overexpression in mice. *Proc. Natl Acad. Sci. USA* **97**, 11534–11539 (2000).
- Maroso, M. *et al.* Interleukin-1beta biosynthesis inhibition reduces acute seizures and drug resistant chronic epileptic activity in mice. *Neurotherapeutics* **8**, 304–315 (2011).
- Miller, L. L., Pellock, J. M., DeLorenzo, R. J., Meyer, J. M. & Corey, L. A. Univariate genetic analyses of epilepsy and seizures in a population-based twin study: the Virginia Twin Registry. *Genet. Epidemiol.* **15**, 33–49 (1998).
- Kjeldsen, M. J., Kyvik, K. O., Christensen, K. & Friis, M. L. Genetic and environmental factors in epilepsy: a population-based study of 11900 Danish twin pairs. *Epilepsy Res.* **44**, 167–178 (2001).
- Speed, D. *et al.* Describing the genetic architecture of epilepsy through heritability analysis. *Brain* **137**, 2680–2689 (2014).
- Kasperaviciute, D. *et al.* Common genetic variation and susceptibility to partial epilepsies: a genome-wide association study. *Brain* **133**, 2136–2147 (2010).
- Guo, Y. *et al.* Two-stage genome-wide association study identifies variants in CAMSAP1L1 as susceptibility loci for epilepsy in Chinese. *Hum. Mol. Genet.* **21**, 1184–1189 (2012).
- EPICURE Consortium *et al.* Genome-wide association analysis of genetic generalized epilepsies implicates susceptibility loci at 1q43, 2p16.1, 2q22.3 and 17q21.32. *Hum. Mol. Genet.* **21**, 5359–5372 (2012).
- Allen, A. S. *et al.* De novo mutations in epileptic encephalopathies. *Nature* **501**, 217–221 (2013).
- International League Against Epilepsy Consortium on Complex Epilepsies. Genetic determinants of common epilepsies: a meta-analysis of genome-wide association studies. *Lancet Neurol.* **13**, 893–903 (2014).
- Sullivan, P. F., Daly, M. J. & O’Donovan, M. Genetic architectures of psychiatric disorders: the emerging picture and its implications. *Nat. Rev. Genet.* **13**, 537–551 (2012).
- Guan, Y. *et al.* Tissue-specific functional networks for prioritizing phenotype and disease genes. *PLoS Comput. Biol.* **8**, e1002694 (2012).
- Piro, R. M. *et al.* An atlas of tissue-specific conserved coexpression for functional annotation and disease gene prediction. *Eur. J. Hum. Genet.* **19**, 1173–1180 (2011).
- Califano, A., Butte, A. J., Friend, S., Ideker, T. & Schadt, E. Leveraging models of cell regulation and GWAS data in integrative network-based association studies. *Nature Genet.* **44**, 841–847 (2012).
- Bartolomei, F., Chauvel, P. & Wendling, F. Epileptogenicity of brain structures in human temporal lobe epilepsy: a quantified study from intracerebral EEG. *Brain* **131**, 1818–1830 (2008).
- Civelek, M. & Lusi, A. J. Systems genetics approaches to understand complex traits. *Nat. Rev. Genet.* **15**, 34–48 (2014).
- Bottolo, L. *et al.* Bayesian detection of expression quantitative trait loci hot spots. *Genetics* **189**, 1449–1459 (2011).
- Budanov, A. V., Sablina, A. A., Feinstein, E., Koonin, E. V. & Chumakov, P. M. Regeneration of peroxiredoxins by p53-regulated sestrins, homologs of bacterial AhpD. *Science* **304**, 596–600 (2004).
- Nogueira, V. *et al.* Akt determines replicative senescence and oxidative or oncogenic premature senescence and sensitizes cells to oxidative apoptosis. *Cancer Cell* **14**, 458–470 (2008).
- Zamkova, M., Khromova, N., Kopnin, B. P. & Kopnin, P. Ras-induced ROS upregulation affecting cell proliferation is connected with cell type-specific alterations of HSF1/SESN3/p21Cip1/WAF1 pathways. *Cell Cycle* **12**, 826–836 (2013).
- Hagenbuchner, J. *et al.* FOXO3-induced reactive oxygen species are regulated by BCL2L1 (Bim) and SESN3. *J. Cell Sci.* **125**, 1191–1203 (2012).
- Schaefer, J. & Strimmer, K. An empirical Bayes approach to inferring large-scale gene association networks. *Bioinformatics* **21**, 754–764 (2005).
- Rossin, E. J. *et al.* Proteins encoded in genomic regions associated with immune-mediated disease physically interact and suggest underlying biology. *PLoS Genet.* **7**, e1001273 (2011).
- Speed, D. *et al.* A genome-wide association study and biological pathway analysis of epilepsy prognosis in a prospective cohort of newly treated epilepsy. *Hum. Mol. Genet.* **23**, 247–258 (2014).
- Ravizza, T. *et al.* The IL-1beta system in epilepsy-associated malformations of cortical development. *Neurobiol. Dis.* **24**, 128–143 (2006).
- Mazufferi, M., Kumar, G., Rospo, C. & Kaminski, R. M. Rapid epileptogenesis in the mouse pilocarpine model: video-EEG, pharmacokinetic and histopathological characterization. *Exp. Neurol.* **238**, 156–167 (2012).

28. Subramanian, A. *et al.* Gene set enrichment analysis: a knowledge-based approach for interpreting genome-wide expression profiles. *Proc. Natl Acad. Sci. USA* **102**, 15545–15550 (2005).
29. Bottolo, L. *et al.* ESS + +: a C + + objected-oriented algorithm for Bayesian stochastic search model exploration. *Bioinformatics* **27**, 587–588 (2011).
30. Gilchrist, M. *et al.* Systems biology approaches identify ATF3 as a negative regulator of Toll-like receptor 4. *Nature* **441**, 173–178 (2006).
31. Cao, D. L. *et al.* Chemokine CXCL1 enhances inflammatory pain and increases NMDA receptor activity and COX-2 expression in spinal cord neurons via activation of CXCR2. *Exp. Neurol.* **261C**, 328–336 (2014).
32. Ravizza, T. & Vezzani, A. Status epilepticus induces time-dependent neuronal and astrocytic expression of interleukin-1 receptor type I in the rat limbic system. *Neuroscience* **137**, 301–308 (2006).
33. Xanthos, D. N. & Sandkühler, J. Neurogenic neuroinflammation: inflammatory CNS reactions in response to neuronal activity. *Nat. Rev. Neurosci.* **15**, 43–53 (2014).
34. Baxendale, S. *et al.* Identification of compounds with novel anti-convulsant properties in a zebrafish model of epileptic seizures. *Dis. Models Mech.* **5**, 773–784 (2012).
35. Baraban, S. C., Taylor, M. R., Castro, P. A. & Baier, H. Pentylentetrazole induced changes in zebrafish behavior, neural activity and c-fos expression. *Neuroscience* **131**, 759–768 (2005).
36. Afrikanova, T. *et al.* Validation of the zebrafish pentylentetrazole seizure model: locomotor versus electrographic responses to antiepileptic drugs. *PLoS One* **8**, e54166 (2013).
37. Baraban, S. C., Dinday, M. T. & Hortopan, G. A. Drug screening in Scn1a zebrafish mutant identifies clemizole as a potential Dravet syndrome treatment. *Nat. Commun.* **4**, 2410 (2013).
38. Zhang, J. *et al.* c-fos regulates neuronal excitability and survival. *Nature Genet.* **30**, 416–420 (2002).
39. Zhang, B. *et al.* Integrated systems approach identifies genetic nodes and networks in late-onset Alzheimer's disease. *Cell* **153**, 707–720 (2013).
40. Heinig, M. *et al.* A trans-acting locus regulates an anti-viral expression network and type 1 diabetes risk. *Nature* **467**, 460–464 (2010).
41. Voineagu, I. *et al.* Transcriptomic analysis of autistic brain reveals convergent molecular pathology. *Nature* **474**, 380–384 (2011).
42. Parikshak, N. N. *et al.* Integrative functional genomic analyses implicate specific molecular pathways and circuits in autism. *Cell* **155**, 1008–1021 (2013).
43. Vezzani, A., Balosso, S. & Ravizza, T. The role of cytokines in the pathophysiology of epilepsy. *Brain. Behav. Immun.* **22**, 797–803 (2008).
44. Vezzani, A. & Granata, T. Brain inflammation in epilepsy: experimental and clinical evidence. *Epilepsia* **46**, 1724–1743 (2005).
45. Marchi, N. *et al.* Efficacy of anti-inflammatory therapy in a model of acute seizures and in a population of pediatric drug resistant epileptics. *PLoS One* **6**, e18200 (2011).
46. Bahcekapili, N. *et al.* Erythropoietin pretreatment suppresses seizures and prevents the increase in inflammatory mediators during pentylentetrazole-induced generalized seizures. *Int. J. Neurosci.* **124**, 762–770 (2014).
47. Papadia, S. *et al.* Synaptic NMDA receptor activity boosts intrinsic antioxidant defenses. *Nat. Neurosci.* **11**, 476–487 (2008).
48. Chuang, Y. C. *et al.* Upregulation of nitric oxide synthase II contributes to apoptotic cell death in the hippocampal CA3 subfield via a cytochrome c/caspase-3 signaling cascade following induction of experimental temporal lobe status epilepticus in the rat. *Neuropharmacology* **52**, 1263–1273 (2007).
49. Vezzani, A., French, J., Bartfai, T. & Baram, T. Z. The role of inflammation in epilepsy. *Nat. Rev. Neurol.* **7**, 31–40 (2011).
50. Balosso, S. *et al.* Molecular and functional interactions between tumor necrosis factor- α receptors and the glutamatergic system in the mouse hippocampus: implications for seizure susceptibility. *Neuroscience* **161**, 293–300 (2009).
51. Galic, M. A. *et al.* Postnatal inflammation increases seizure susceptibility in adult rats. *J. Neurosci.* **28**, 6904–6913 (2008).
52. Riazi, K. *et al.* Microglial activation and TNF α production mediate altered CNS excitability following peripheral inflammation. *Proc. Natl Acad. Sci. USA* **105**, 17151–17156 (2008).
53. Baram, T. Z. & Hatalski, C. G. Neuropeptide-mediated excitability: a key triggering mechanism for seizure generation in the developing brain. *Trends Neurosci.* **21**, 471–476 (1998).
54. Efron, B. Large-scale simultaneous hypothesis testing: the choice of a null hypothesis. *J. Am. Statist. Assoc.* **99**, 96–104 (2004).
55. Mardia, K. V., Kent, J. T. & Bibby, J. M. *Multivariate Analysis* (Academic, 1979).
56. Kim, D. *et al.* TopHat2: accurate alignment of transcriptomes in the presence of insertions, deletions and gene fusions. *Genome Biol.* **14**, R36 (2013).
57. Robinson, M. D., McCarthy, D. J. & Smyth, G. K. edgeR: a Bioconductor package for differential expression analysis of digital gene expression data. *Bioinformatics* **26**, 139–140 (2010).
58. Oxtoby, E. & Jowett, T. Cloning of the zebrafish krox-20 gene (krox-20) and its expression during hindbrain development. *Nucleic Acids Res.* **21**, 1087–1095 (1993).

Acknowledgements

We acknowledge funding from Imperial NIHR Biomedical Research Centre/Imperial Innovations (E.P., J.B., M.R.J.), National Genome Research Network (NGFNplus: EMINet, grant 01GS08122; S.S., A.J.B.), DFG (SFB1089; A.J.B.), DFG (KFO177/SFB-1089; A.J.B., S.S.), BMBF (01GQ0806, S.S.), GIF (A.J.B.), ESF EuroEpinomics (A.J.B.), Else-Kröner Fresenius Foundation (A.J.B.), Wellcome Trust (J.B.), Imperial College Junior research fellowship (J.B.) and BONFOR (S.S., A.J.B.), UCB Pharma (M.R.J., E.P., R.K.), Medical Research Council UK (E.P.), CONACYT, Mexico (P.L.M.S., V.T.C.), Imperial College/Imperial College Healthcare, who received a proportion of funding from the Department of Health's NIHR Biomedical Research Centres (BRC) funding scheme (M.R.J., E.P.). DNA collection for GWAS was part funded by the Wellcome Trust (M.R.J., Grant Reference WT066056). The research leading to these results has received funding from the European Union's Seventh Framework Programme (FP7/2007-2013) under grant agreement no. 602102 (EPITARGET; M.R.J., S.S., M.S., A.J.B., E.P.). The research was supported by the National Institute for Health Research (NIHR) Imperial Biomedical Research Centre (M.R.J., E.P.). The views expressed are those of the author(s) and not necessarily those of the NHS, the NIHR or the Department of Health. We thank Mario Falchi and Philippe Froguel for providing critical comments on the first version of the manuscript.

Author contributions

A.J.B. initiated and coordinated the hippocampus sample collection including related clinical data and gene expression data generation. E.P. and M.R.J. designed, implemented and coordinated systems genetics and functional studies. J.B. designed and performed functional studies in BMDM and BV2 cells, with assistance from B.R. and A.D. T.R. performed functional studies in neurons with assistance from A.S., S.K., K.W., F.W.G., B.R. and V.D.P. L.B. designed and developed the Bayesian methodology and performed genetic mapping analyses, with assistance from M.C.-H. M.L.K. performed gene expression, correlation and network analyses, with assistance from S.R.L. and T.D. K.P., P.N. and S.S. prepared human brain samples and probes, performed hybridizations, real-time quantitative PCR experiments and contributed data and clinical information in the TLE cohort. P.H., M.Mattheisen and S.C. carried out microarray experiments, SNP genotyping and raw data analyses in the TLE cohort. M.v.L. contributed hippocampal tissue microdissections and clinical data analyses in the TLE cohort. M.R.J., T.J.O'B., J.E., S.P. and A.J.C. coordinated sample collection and/or provided genotype and clinical data for the GWAS analysis of focal epilepsy. M.W., M.S. and P.R. contributed reagents and materials. M.R.J. and D.S. performed the GWAS analysis of focal epilepsy. E.P., M.R.J., M.L.K., D.S. and S.R.L. designed and carried out GWAS-enrichment analyses. E.P. and P.K.S. carried out TFBS motifs sequence analysis. R.M.K., P.F., B.D. and M.Mazzuferi generated the mouse RNA-seq data. E.P., M.R., K.S. and P.K.S. carried out comparative network analyses. A.S. provided primary hippocampal neurons and N.H. and A.D. provided BV2 cell lines and participated in functional studies. V.T.C. and P.L.M.S. designed and carried out experiments in zebrafish. E.P. and M.R.J. wrote the manuscript with input from A.B., J.B., L.B., V.T.C., V.D.P. and R.M.K. E.P., A.J.B. and M.R.J. were the joint senior authors of the study.

Additional information

Supplementary Information accompanies this paper at <http://www.nature.com/naturecommunications>

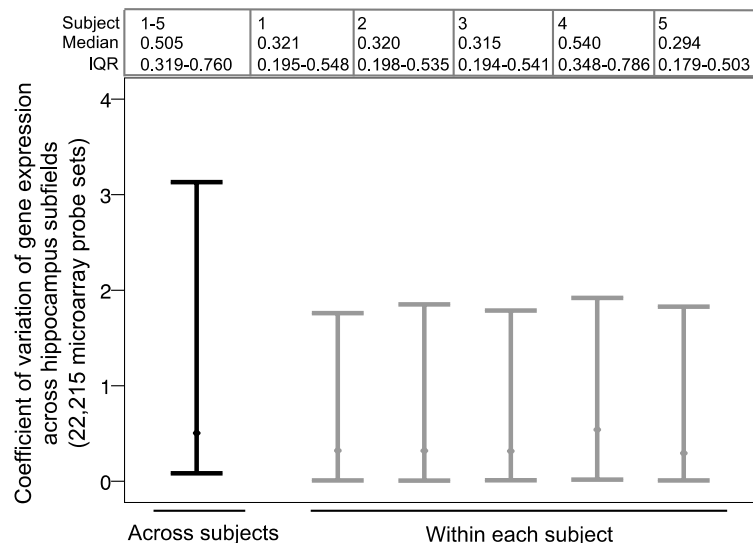
Competing financial interests: The authors declare no competing financial interests.

Reprints and permission information is available online at <http://npg.nature.com/reprintsandpermissions/>

How to cite this article: Johnson, M. R. *et al.* Systems genetics identifies Sestrin 3 as a regulator of a proconvulsant gene network in human epileptic hippocampus. *Nat. Commun.* **6**:6031 doi: 10.1038/ncomms7031 (2015).

Supplementary Figure 1: Inter-individual vs inter-hippocampus subfields variation in gene expression.

A



B

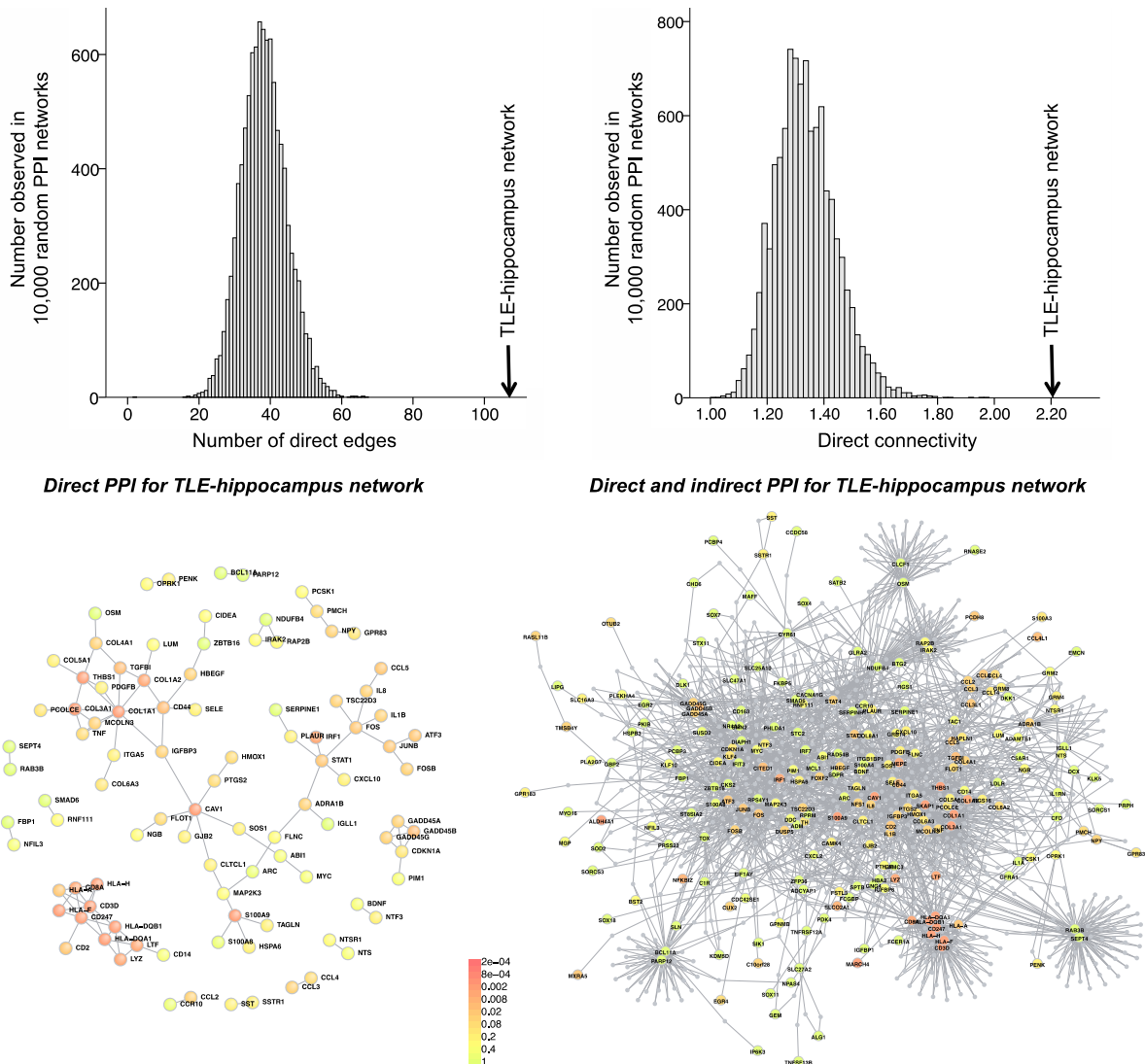
Functional annotation (GO terms, top and KEGG pathways, bottom) for the 518 annotated genes that were differentially expressed between the subjects ($n=5$)

Top significant GO terms	Genes	Fold Enrichment	P-value	FDR
Defense response	56	7.7	4.1E-08	1.7E-04
Immune response	57	7.8	8.2E-07	3.1E-03
Behavior	43	5.9	1.4E-06	5.8E-03
Metal ion homeostasis	24	3.3	5.9E-06	3.2E-02
Response to wounding	44	6	1.4E-05	5.2E-02
Activation of phospholipase C activity	12	1.6	1.5E-05	1.4E-01
Positive regulation of phospholipase activity	12	1.6	1.5E-05	1.4E-01

Top significant KEGG pathways	Genes	Fold Enrichment	P-value	FDR
Neuroactive ligand-receptor interaction	34	2.6	1.2E-07	<0.1
Metabolism of xenobiotics by cytochrome P450	12	4	3.4E-05	0.19
Drug metabolism	12	3.8	4.8E-05	0.26
Cytokine-cytokine receptor interaction	28	2.1	1.1E-04	0.30
Retinol metabolism	11	4	6.1E-05	0.35
Drug metabolism	9	4.1	2.3E-04	1.40
Linoleic acid metabolism	7	4.9	3.7E-04	2.70

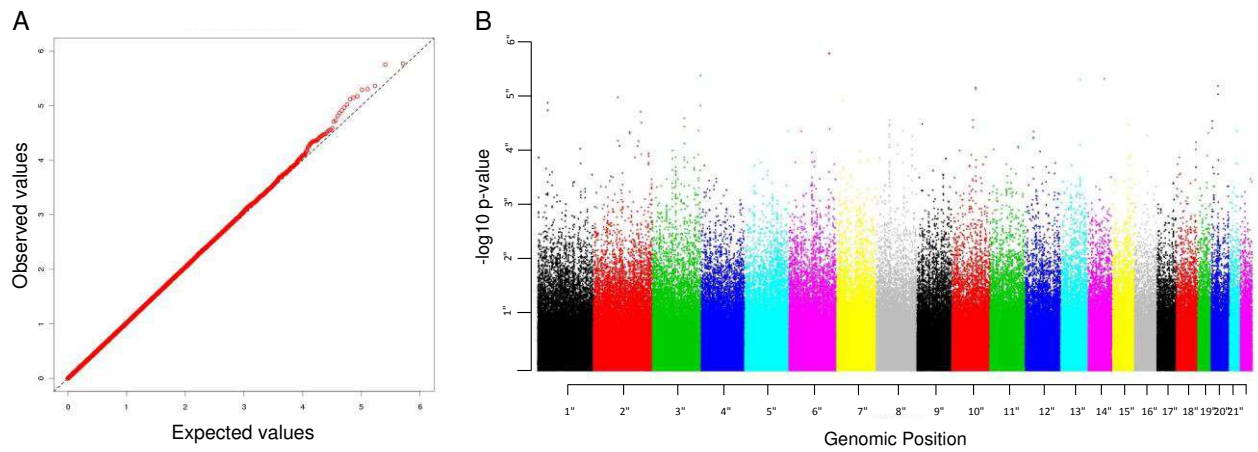
(A) We utilized surgical hippocampus samples from 5 patients with mesial temporal lobe epilepsy (MTLE) with hippocampus sclerosis (HS) of uniform pathology. For each subject, 4 hippocampus subfields were laser micro-dissected (dentate gyrus, CA1, CA3, CA4) and genome-wide expression profiles were generated for each subfield using Affymetrix HU 133A microarray. We use the coefficient of variation ($CV = \text{standard deviation}/\text{mean} * 100$) to quantify the degree of variation in gene expression across subfields in each subject and, after pooling together data from all subjects, the variation across subfields *and* across subjects. In each case, CV was calculated using 22,215 Affymetrix probe sets. We observed significantly bigger range of CV across subjects (black bar) than within each subject separately (grey bars). With the exception of subject 4, median and IQR of CV was higher across subjects than within each individual subject. Bars, range of the CVs; diamond, median CV. (B) We carried out differential expression (DE) analysis using Significance Analysis of Microarrays¹ to identify DE genes associated with (i) inter-individual variation and between hippocampus subfields and (ii) variation across hippocampus subfields only. False discovery rate (FDR) was assessed by 1,000 permutations. At 5% FDR we identified 518 DE annotated coding genes between the 5 subjects and subfields, while only 12 genes were found DE between hippocampus subfields. Functional annotation of the 518 DE genes was carried out by DAVID² and showed enrichment for GO terms and KEGG pathways. The results of the pilot microarray study of the hippocampus transcriptome showed higher inter-individual variability in gene expression than between hippocampus subfields within the same subject, and inform the use of whole hippocampus for subsequent genome-wide network analysis in the TLE cohort.

Supplementary Figure 2: TLE-network genes have significant interconnectivity as compared to random Protein-Protein-Interaction (PPI) networks.



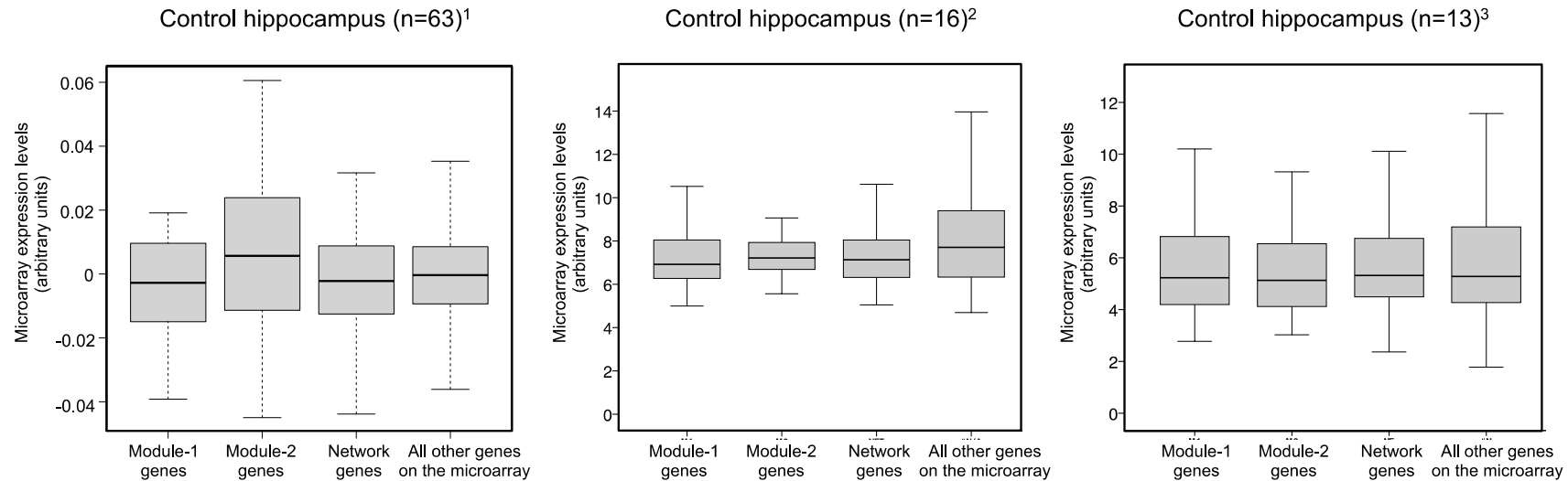
We used the DAPPLE algorithm³ to interrogate high-confidence PPI (from InWeb database, which contains 428,430 reported interactions, 169,810 of which are deemed high-confidence, non-self interactions across 12,793 proteins) and investigated to which extent the co-regulation pattern observed at the transcriptional level (i.e., co-expression network) was conserved at the protein level (i.e., PPI). We assessed physical connections among proteins encoded for by the genes in the network identified in the hippocampus of TLE patients (TLE-hippocampus network) and tested whether these PPI are likely to be observed by chance. Looking at 10,000 random PPI networks, we found that TLE-hippocampus network genes have significantly high interconnectivity at the protein level ($P = 9.9 \times 10^{-5}$). Histograms were plotted to represent random expectation for number of directed edges (left) and degree of direct connectivity (right); arrows indicate the number of directed edges (left) and direct connectivity (right) for the TLE-hippocampus network. The resultant PPI networks built from the TLE-hippocampus network are reported below the histograms: left, high confidence direct PPI interactions; right, global PPI network where other (indirect) PPI connected to the direct TLE-hippocampus network genes are included (grey dots). Color scale indicates the significance (P-value) of each PPI.

Supplementary Figure 3: GWAS of susceptibility to focal epilepsy.



(A) QQ plot for focal epilepsy meta-analysis. Cases: 1,429 patients with focal epilepsy (1,013 (71%) of these had a clinical diagnosis of temporal lobe epilepsy); controls: 7,358 healthy subjects from the WTCCC2. (B) Manhattan plot for GWAS of focal epilepsy. All SNPs associations are reported for each chromosome, indicated by different colors. See Supplementary Methods for additional details.

Supplementary Figure 4: Comparison with gene expression from the hippocampus of healthy subjects.



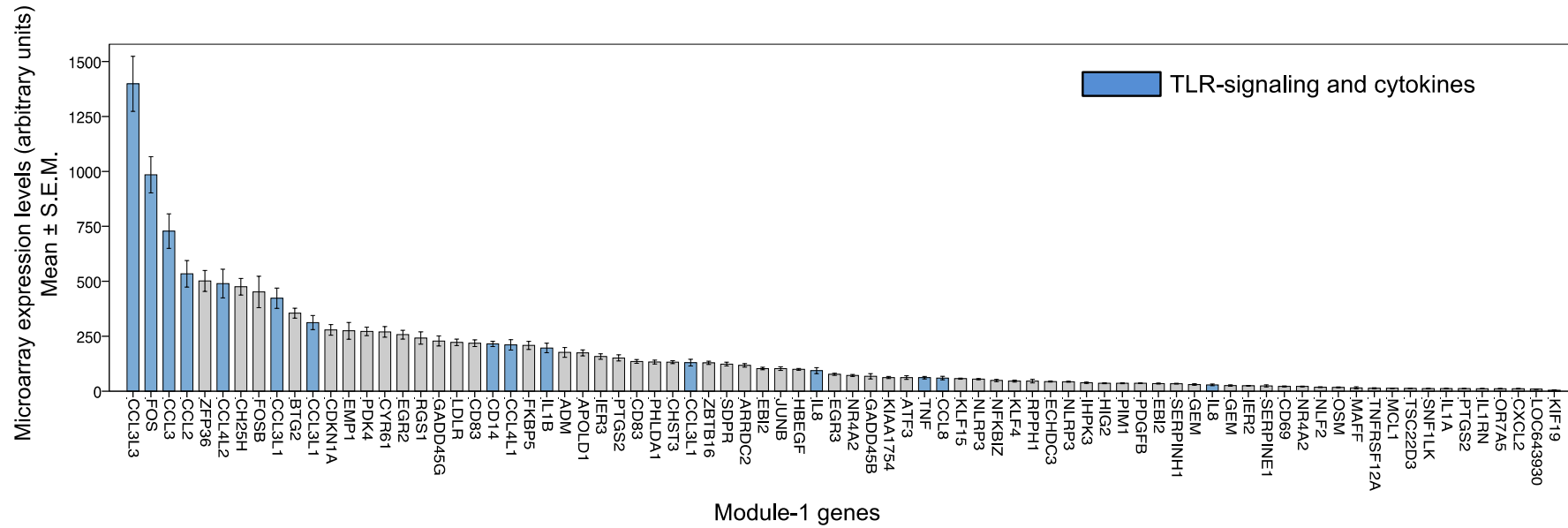
We used three separate, publicly available gene expression datasets from the hippocampus of healthy subjects and investigated whether Module-1 genes are up-regulated as compared with Module-2, the larger network or all other genes profiled by microarray. This analysis showed no significant differences between Module-1 expression and the rest of the genes analyzed, indicating that the observed up-regulation of Module-1 genes (when compared with the rest of genes analyzed, see Fig. 1e) is specific to the TLE patient cohort and it is not observed in subjects that lacked TLE (i.e., control hippocampus). A box plot-based representation of the distribution of gene expression levels for Module-1, Module-2, TLE-network and all other genes on the microarray in control hippocampi is shown below. The median, first quartile, third quartile and range in the distribution are shown.

(1) *Left panel*, hippocampal microarray expression data was obtained for 63 healthy post-mortem human brains from the Pritzker Neuropsychiatric Disorders Research Consortium; GEO accession number: GSE45642. From the whole set of gene expression data (n=670) in GSE45642, we used only 63 control samples, which had no psychiatric or neurological disorders, substance abuse, or any first-degree relative with a psychiatric disorder⁴.

(2) *Middle panel*, microarray expression data from hippocampi from left and right sides of four late mid-fetal human healthy brains (18, 19, 21, and 23 weeks of gestation); GEO accession number: GSE13344.

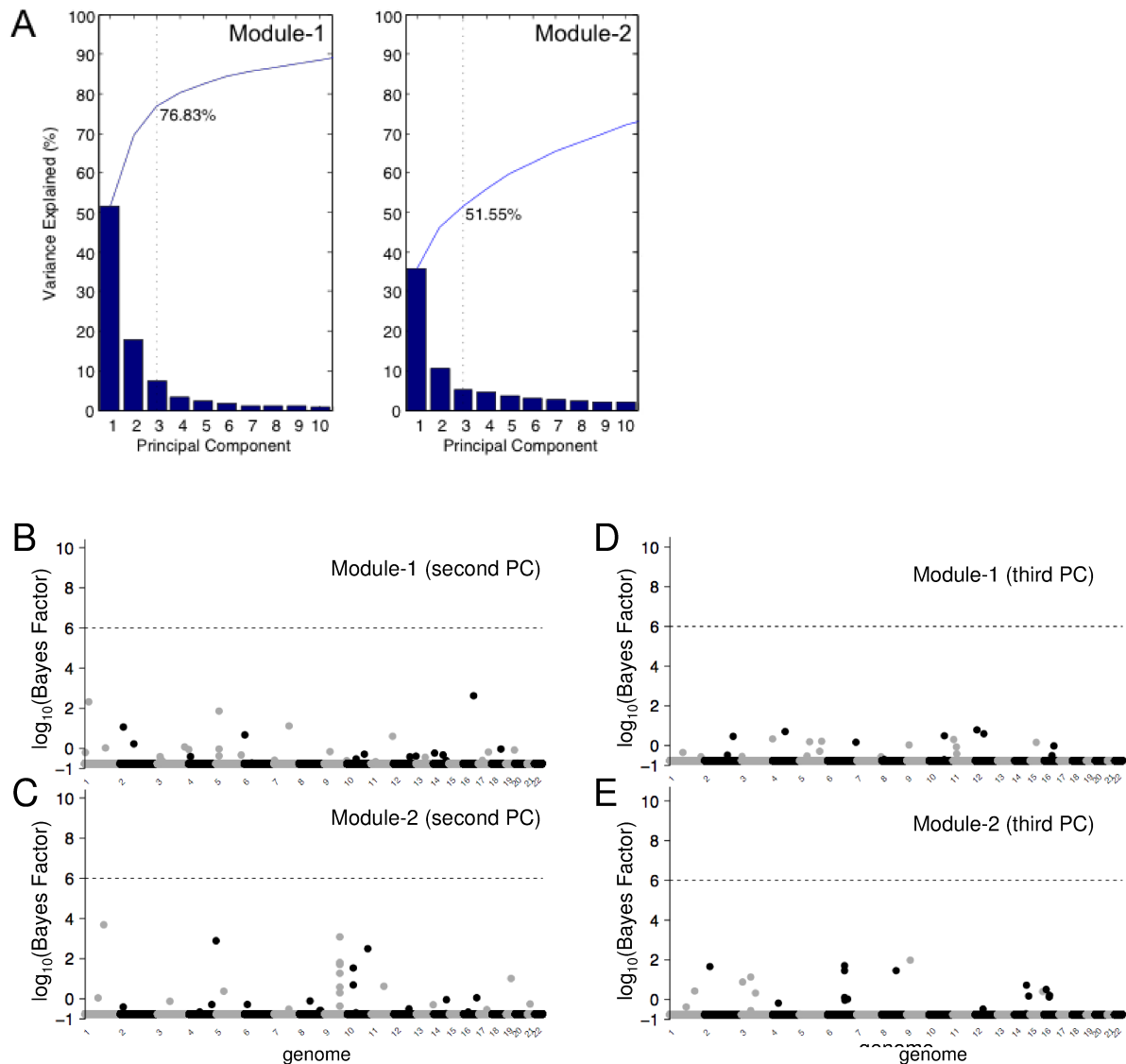
(3) *Right panel*, microarray expression data from human hippocampal samples were collected from individuals clinically classified as neurologically normal (mean age of 79.8 ± 9.1 yr); GEO accession number: GSE5281.

Supplementary Figure 5: Module-1 is enriched for TLR-signaling and cytokines.



mRNA expression of Module-1 genes, showing high expression for TLR-signaling genes and cytokines (highlighted in blue). In Module-1 we found 16 fold enrichment for inflammatory cytokines ($P = 6.6 \times 10^{-13}$), many of which belong to the IL-1 signaling cascade (*IL-1 β* , *IL-1RN*, *IL-1 α* , *TNF α*), and the TLR-signaling pathway (11 fold enrichment, $P = 1.4 \times 10^{-6}$). Average gene expression levels (and s.e.m.) were calculated across the 129 TLE patients.

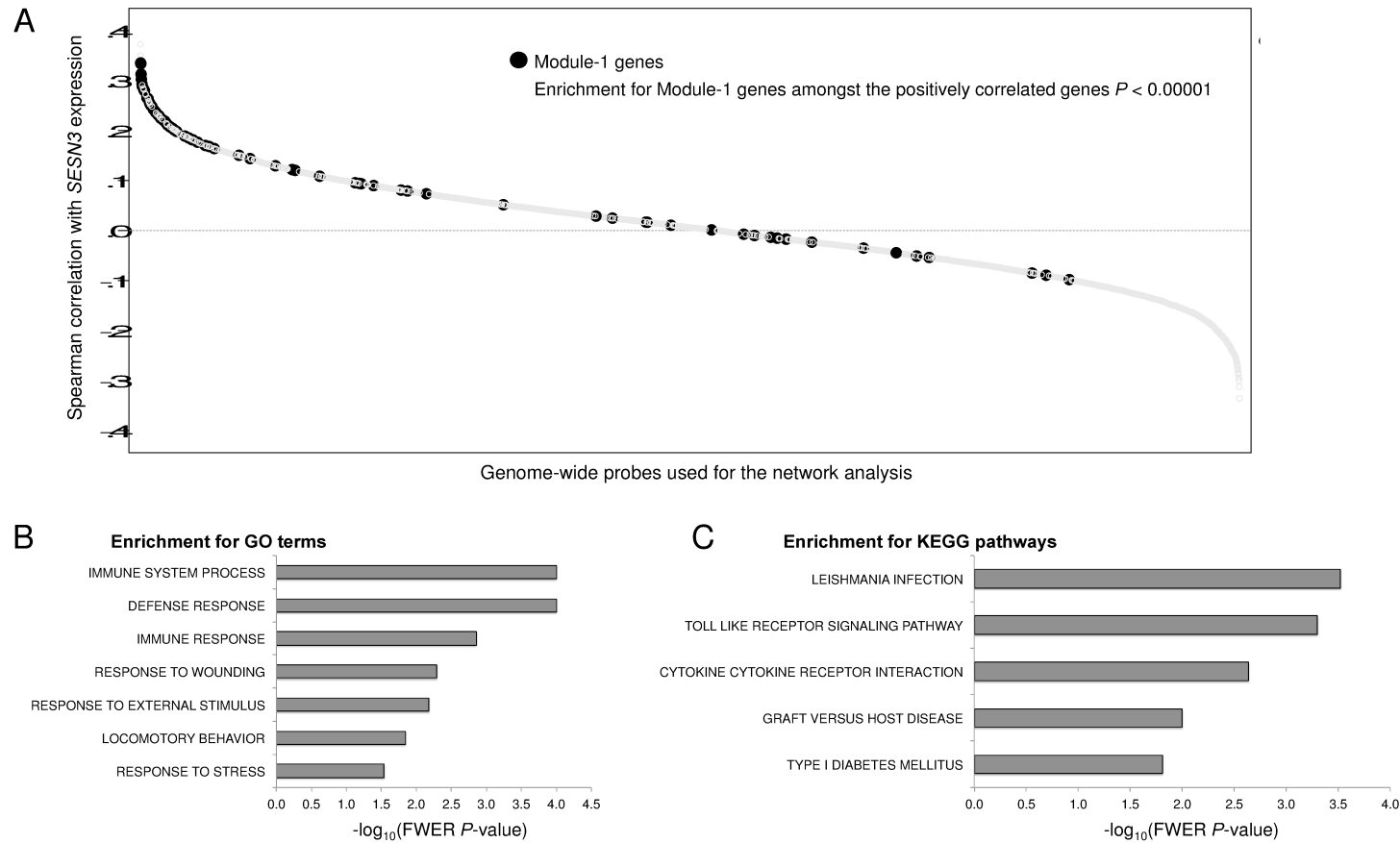
Supplementary Figure 6: Principal Component and genetic mapping analysis for Module-1 and Module-2 expression.



(A) Percentage of variance in gene expression explained by the Principal Components (PCs) for Module-1 and Module-2. For Module-1, the first three PCs accounted for ~77% of variance in gene expression, with the first PC accounting for more than half of the total variance in gene expression. For Module-2, the percentage of variance in gene expression explained the first three PCs is ~52%. Results of the genetic mapping for the second and third PC of Module-1 (B, D) and Module-2 (C, E) expression, respectively, showing no significant genetic control at local FDR<5% (i.e., $\log_{10}(\text{Bayes Factor}) > 6$). Dotted line, $\log_{10}(\text{Bayes Factor}) = 6$.

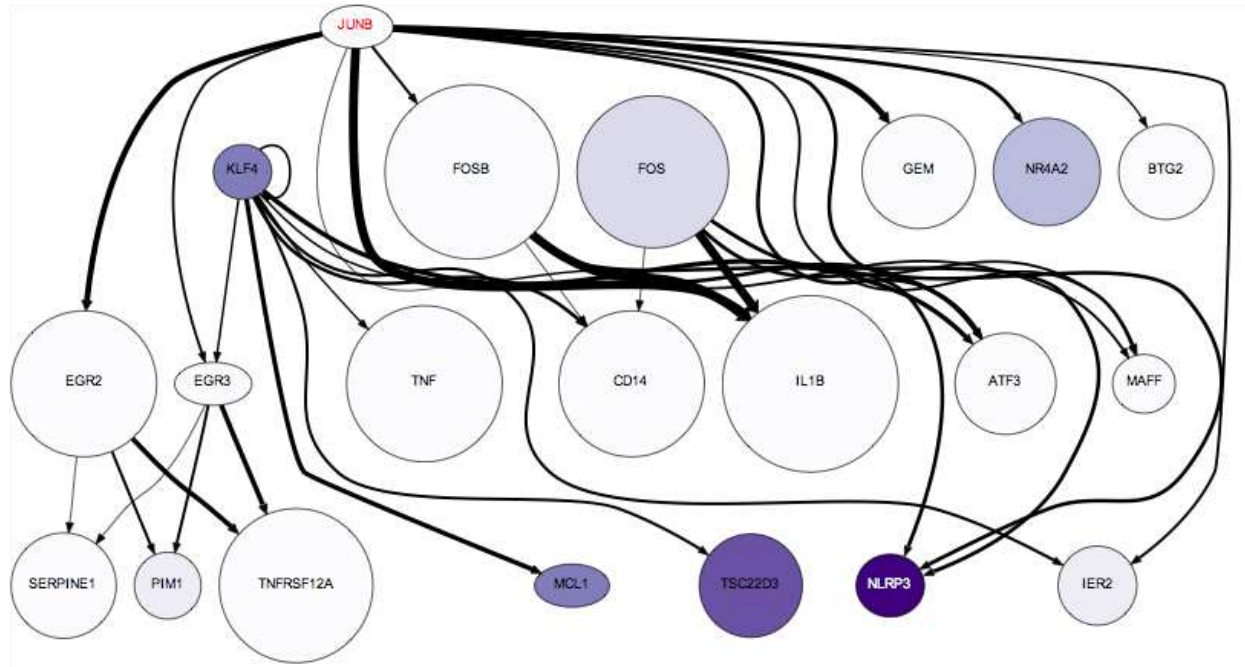
Genetic mapping results for the first PC of Module-1 expression are reported in the main text, Fig. 3a.

Supplementary Figure 7: Genome-wide correlation between *SESN3* mRNA expression and all microarray probes used for the network analysis (n=7,149).



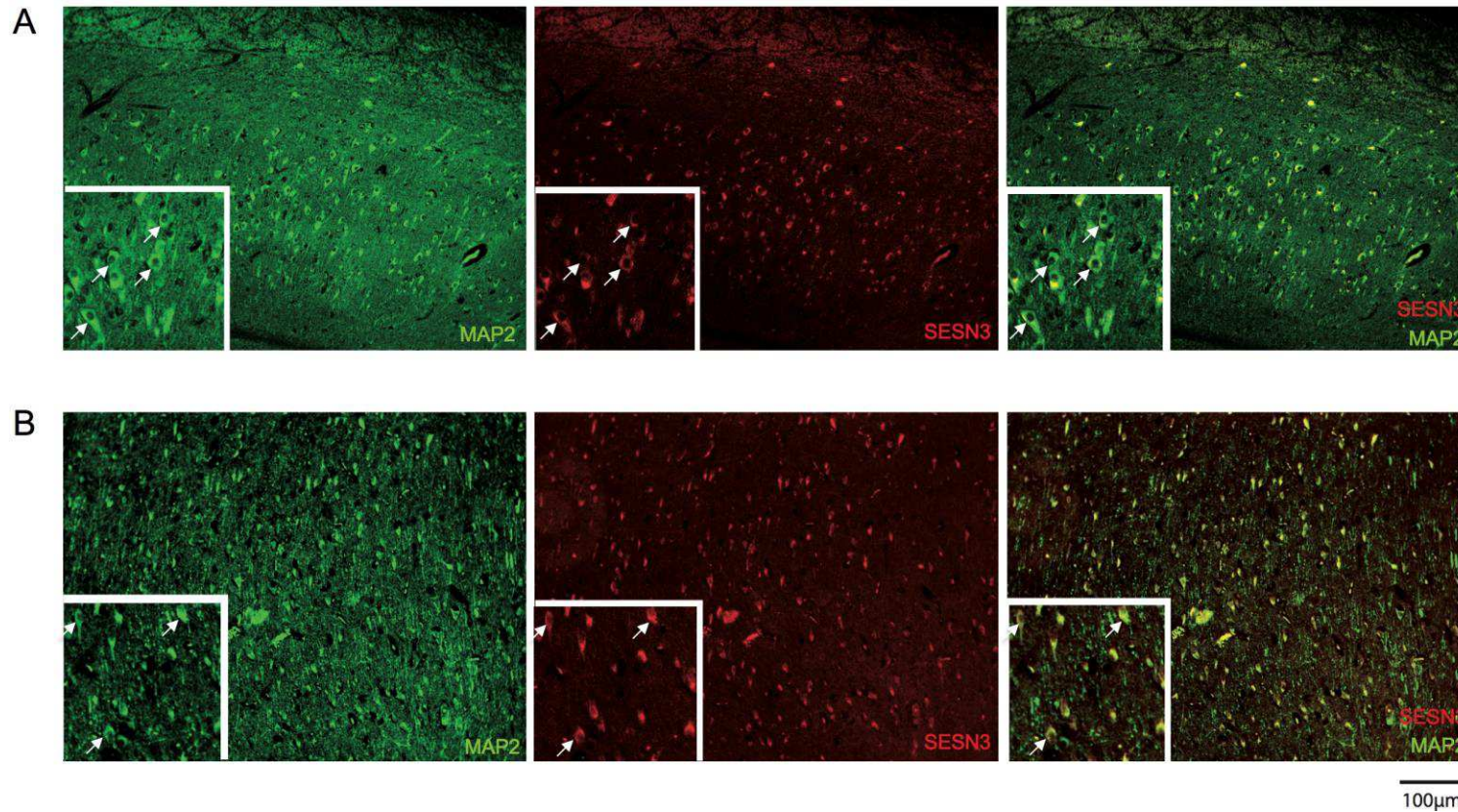
(A) Non-parametric Spearman correlation between *SESN3* and genome-wide probes was calculated and probe-correlations (y-axes) were ranked according to the magnitude of the correlation coefficient. The probes representing Module-1 genes are highlighted (black circles) and are significantly over-represented amongst the strongest positive correlated genes with *SESN3* expression (gene set enrichment analysis, $P < 0.00001$). (B) GO terms and (C) KEGG pathways enrichment analysis for the most highly correlated genes with *SESN3* expression genome-wide. FWER P -value, family wise error rate corrected P -value (calculated by 10,000 permutations).

Supplementary Figure 8: Predicted regulation of Module-1 genes by activator protein 1 (AP1) transcription factor.



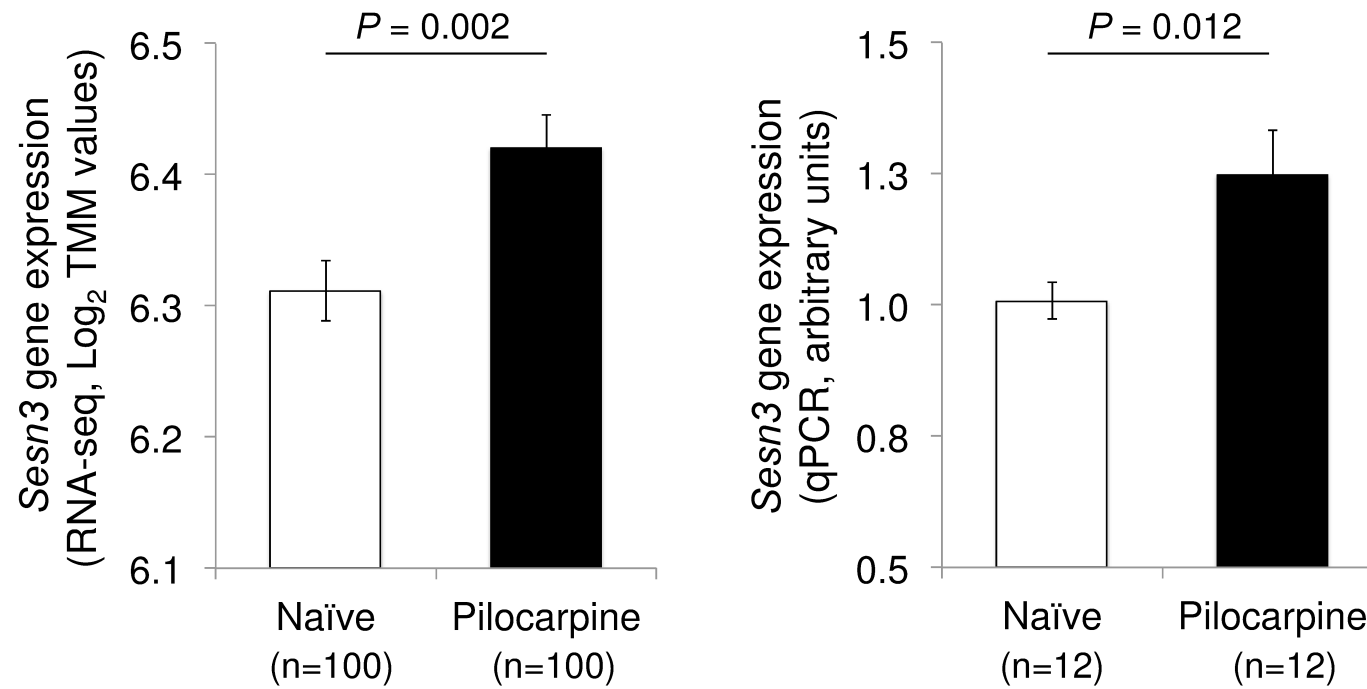
Module-1 regulation by AP1 (i.e., JUNB) was confirmed by robust transcription factor binding site (TFBS) predictions (indicated by arrowed edges in the network), which integrate physical protein-protein interaction among TFs measured using the Mammalian Two Hybrid (M2H) system and quantitative TF expression levels measured using qRT-PCR across tissues, and account for evolutionary conservation between mouse and humans (FANTOM4)⁵. AP1 is predicted to regulate, directly or indirectly, 20 genes of Module-1, and the TFBS are conserved between mouse and human. Evolutionarily conserved TFBS were predicted using the MotEvo algorithm with a set of non-redundant matrices (combining JASPAR, TRANSFAC and a small set of de-novo motifs trained on ChIP-chip datasets) and are represented as TFBS edges in the network. The weights of the TFBS edges are proportional to the “response values”, which represent how well the expression of each promoter responds to the motif activity for that TF. The diameter of each node is scaled to indicate the 'dynamics' of the gene and it is calculated by mapping to $\log(\max(\text{detected expression})/\min(\text{detected expression}))$ within the time course; highly dynamic nodes are larger than statically expressed nodes. The color of the node is mapped to a relative scale for each node between white for $\min(\text{detected expression})$ and purple $\max(\text{detected expression})$. Arrowheads indicate activating relationship.

Supplementary Figure 9: Immunohistochemical analyses of SESN3 in human hippocampal tissue.



Representative images of co-immunoreactions against MAP2 (green) antibody showed that SESN3 (red) is localized in neurons in human hippocampal tissue from an autopsy specimen (**A**) and a biopsy TLE hippocampus (**B**). While several factors (e.g., time interval between tissue harvesting and fixation, post-harvesting delay, etc.) might have affected the preservation and quality of tissues samples used for immunohistochemical analyses, we observed that the number of well-defined neuronal cell bodies (MAP2 positive with central round nucleus, indicated by the white arrows below) in (**B**) is reduced, probably due to epilepsy-associated neuronal degeneration in the TLE hippocampus. Although the number of viable neurons is reduced in the TLE hippocampus, more elements showed robust expression of SESN3 – insert in the overlay (insert = 50µm). Please refer to Fig. 4e for quantification of SESN3 expression in human hippocampal tissue by immunofluorescence analysis.

Supplementary Figure 10: Up-regulation of *Sesn3* gene expression in the mouse hippocampus after pilocarpine-induced status epilepticus.



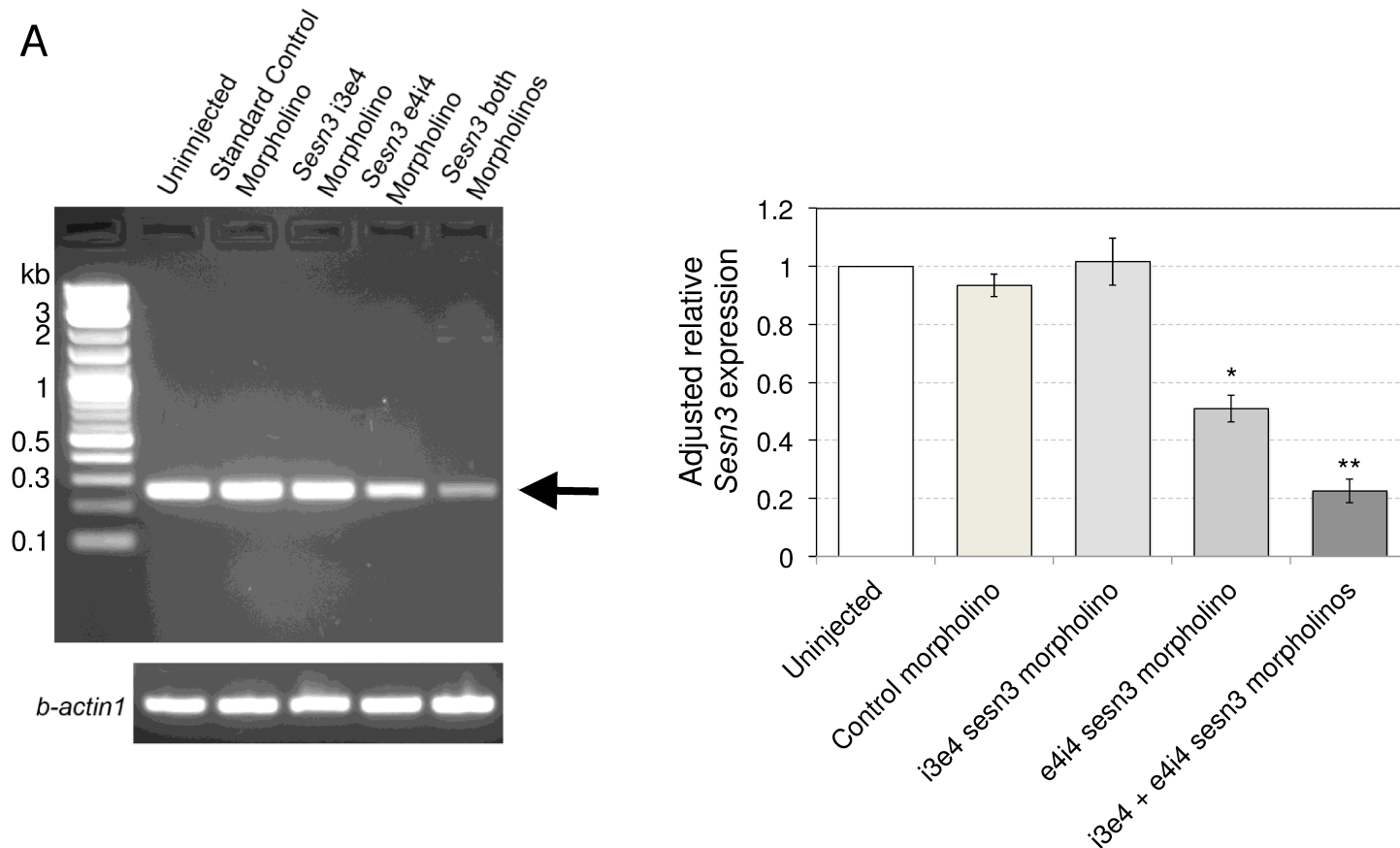
Sesn3 gene expression is increased in the mouse hippocampus after pilocarpine treatment vs naïve mice by RNA-Seq (left) and by qPCR (right) analysis. Non-parametric Mann-Whitney test (2-tailed) was used to assess differences between mean *Sesn3* mRNA expression in pilocarpine-treated vs naïve mice. TMM, trimmed mean of M-values. In the qPCR analysis *Sesn3* expression levels were normalized to *Gapdh* (endogenous control). All data are reported as mean gene expression \pm S.E.M and sample sizes are indicated in the figure.

Supplementary Figure 11: Expression of *sesn3* mRNA in the zebrafish larval brain.

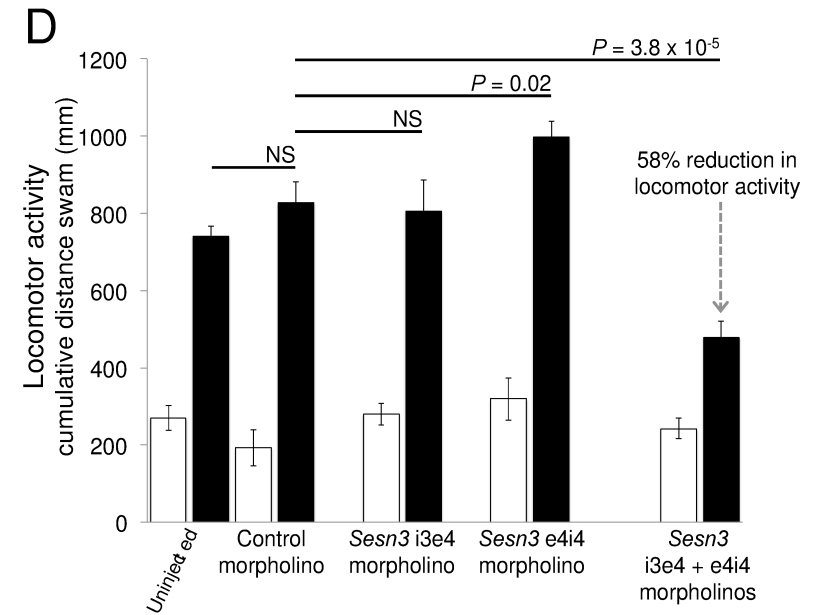
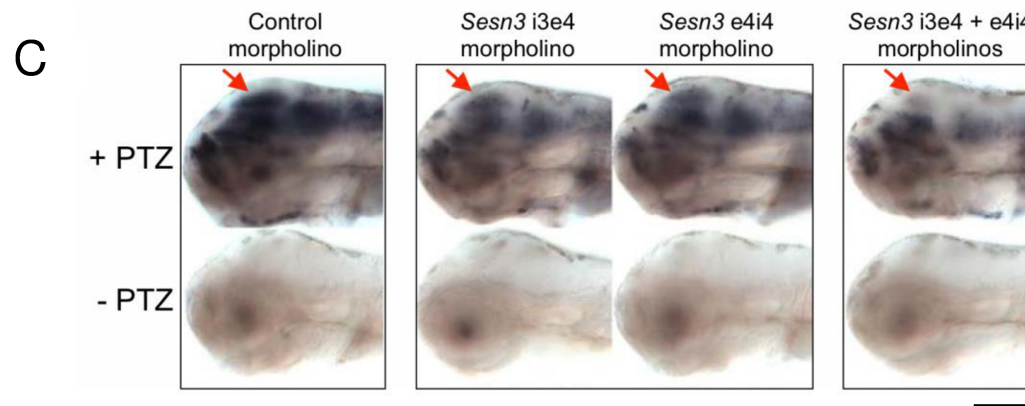
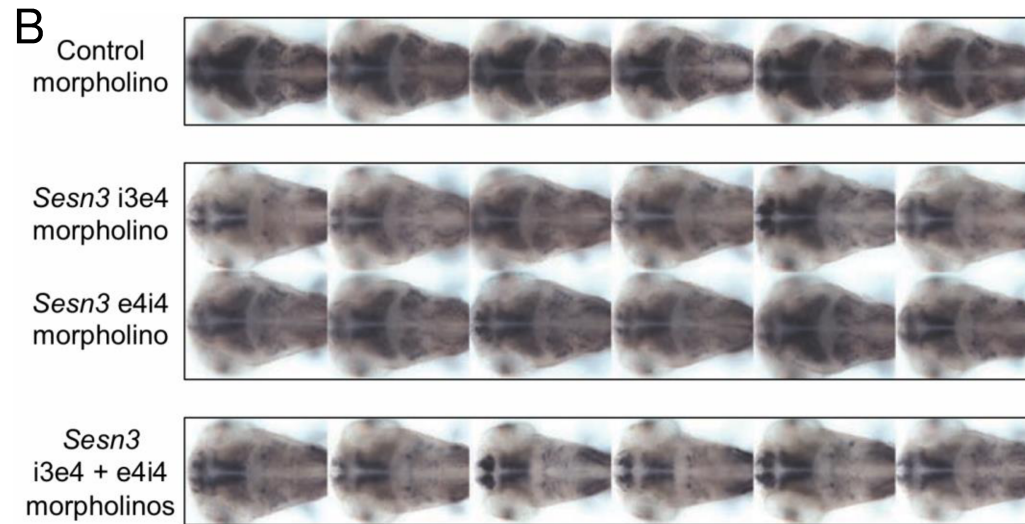


In situ hybridization analysis of *sesn3* mRNA expression in 3 dpf and 4 dpf zebrafish larvae. Lateral views of larvae (left panels) showing widespread expression of *sesn3* in larval brain. Transverse sections through the hindbrain (right panels) reveal extensive expression of *sesn3* in brain tissue, which is increased in 4 dpf larvae compared to 3 dpf larvae. dpf, days post fertilization. Probe specificity was tested and validated in independent experiments using *sesn3* antisense and *sesn3* sense (control) probes. Scale bar in left panels = 200 μm; scale bar in right panels = 100 μm.

Supplementary Figure 12: Microinjection of *sesn3* morpholinos into zebrafish embryos.



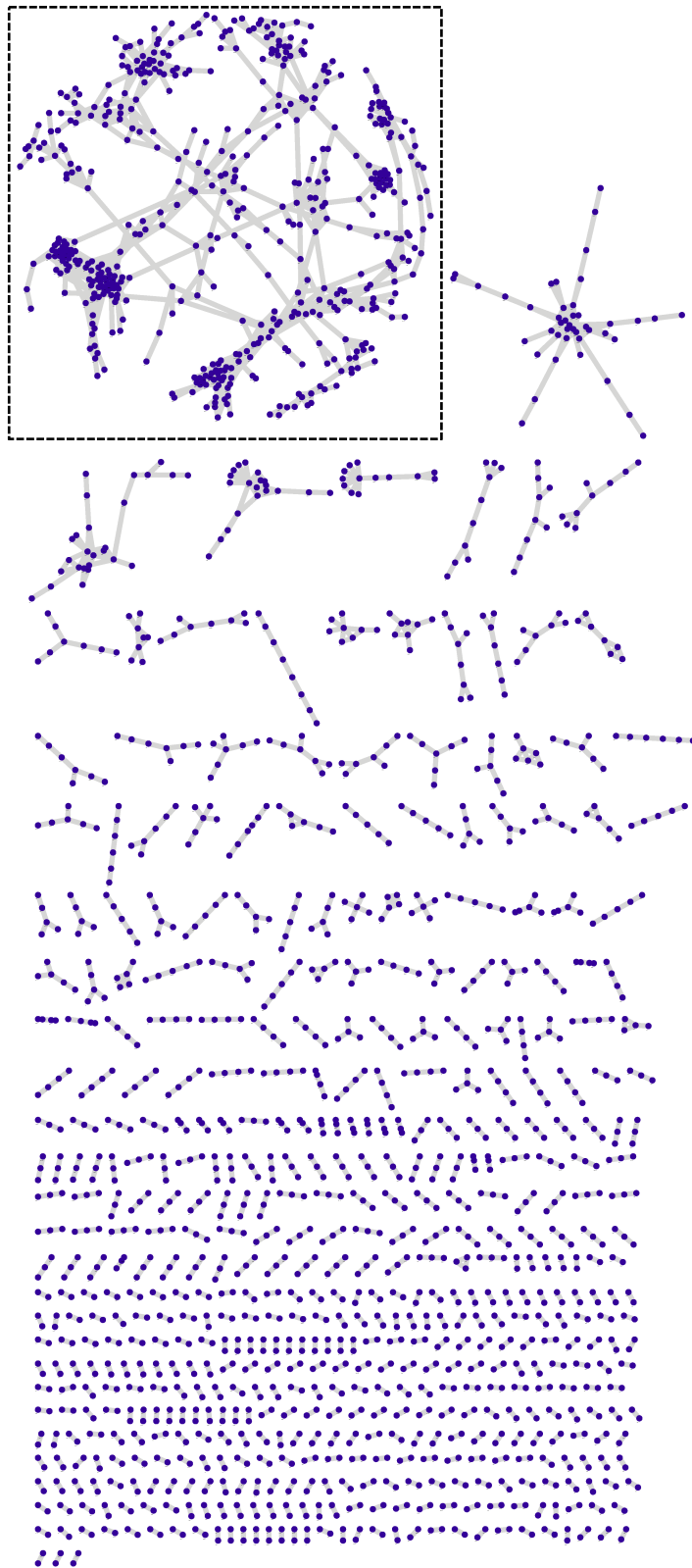
(A) Morpholino-mediated knock-down of *sesn3* mRNA levels in zebrafish embryos. RT-PCR analysis of *sesn3* mRNA expression in uninjected embryos and embryos injected with standard control, *sesn3 i3e4*, *sesn3 e4i4*, or *sesn3 i3e4* plus *sesn3e4i4* morpholinos. Injection of both *sesn3 i3e4* and *e4i4* morpholinos reduced the level of processed *sesn3* mRNA (arrowhead) to a much greater extent than did injection of either morpholino alone. The histogram on the right shows that injection of both morpholinos causes an ~80% reduction of *sesn3* mRNA relative to the *sesn3* mRNA level in uninjected embryos (100%). Separate quantitative qPCR data confirmed the significant reduction of *sesn3* mRNA relative to the *sesn3* mRNA level in uninjected embryos. Values were normalized with beta-actin loading controls and are represented as mean \pm s.e.m (n=3 in each group). *, $P = 0.001$; **, $P = 2 \times 10^{-5}$ (Mann-Whitney t-test, 2-tailed).



(B) Upper row shows PTZ-induced *c-fos* expression in the brain of 6 different 3 dpf sibling larvae microinjected with a control morpholino. Middle two rows show the effect of each morpholino (either i3e4 or e4i4) on PTZ-induced *c-fos* expression in the brain of 6 different sibling larvae. Lower row shows *c-fos* expression in the brain of 6 different larvae microinjected with the combination of the two *sesn3* morpholinos. Combined microinjection of *sesn3* i3e4 and *e4i4* morpholinos inhibited PTZ-induced *c-fos* expression more robustly than microinjection of either morpholino individually. Scale bar = 200 μm . **(C)** Upper row: lateral views of representative larvae from panel (A), showing effect of *sesn3* morpholinos (i3e4 and e4i4) on PTZ-induced *c-fos* expression. Red arrows

indicate optic tectum, where reduction in *c-fos* expression due to morpholino injection is most pronounced. Lower row shows individuals from the same pools of morpholino-injected embryos that were not treated with PTZ, and consequently no *c-fos* expression is detectable. Scale bar = 200 μm . **(D)** PTZ-induced locomotor activity of larvae injected with the combination of *sesn3* morpholinos (i3e4 + e4i4) is much lower than that observed in controls and larvae injected with either *sesn3* morpholino individually. Following PTZ treatment, injection of the combination of two *sesn3* morpholinos yields a 58% reduction in the cumulative distance swam as compared with the control morpholino ($P = 3.8 \times 10^{-5}$). Notably, microinjection of either morpholinos singly showed no significant effect or slightly increased locomotor activity as compared to larvae injected with control morpholino, after PTZ treatment. Black bars, cumulative locomotor activity in zebrafish exposed to 20mM PTZ. White bars, cumulative basal locomotor activity in larvae not treated with PTZ. Data are reported as mean \pm s.e.m. NS, not significant ($P > 0.05$).

Supplementary Figure 13: Partial correlations between gene expression profiles in the human hippocampus of TLE patients.



Significant partial correlations identified at 5% False Discovery Rate (FDR). Each node represents an Illumina probe, and each edge connecting any two nodes represents a significant partial correlation between the genes' expression profiles. A total of 2,124 nodes (representing 1,383 annotated genes, reported in Supplementary Data 2) connected by 2,496 edges were identified. The majority of the correlated nodes belong to small components of less than 50 nodes. None of these smaller modules was individually enriched (FDR<5%) for specific GO terms or KEGG pathways.

One large inter-connected component was apparent (indicated by the dotted line square), which was then extracted using clustering algorithms. This component included the top twenty highly inter-connected genes (i.e., hub genes) and included 442 annotated genes (please refer to Fig. 1 and the main text).

The large extracted component ("TLE-network") was enriched for several KEGG pathways including the "Toll-like receptor signaling pathway", the "NOD-like receptor signaling pathway" and the "chemokine signaling pathway" (detailed functional annotation of the TLE-network is reported in Fig. 1b and discussed in the main text).

Supplementary Table 1. Clinical Samples.

Genome-wide expression data were generated from whole human hippocampus samples from 131 patients who had undergone selective amygdalahippocampectomy for mesial temporal epilepsy (mTLE) with hippocampus sclerosis (HS). Clinical data recorded from each patient included: date of birth, sex, handedness, age at epilepsy onset, laterality of TLE (right/left), operation date, age at operation, pre-operative seizure type/s and frequency, antiepilepsy drug (AED) therapy at time of surgery, pathology. Pre-operative seizure frequency was estimated by a retrospective review of the hospital case records for the immediate pre-operative period defined by an absence of change in AED type or dose and expressed as seizures per month. Full clinical and gene expression data were available for 129 out of 131 samples, which were used for the network and genetic analyses. Simple partial seizures were not counted.

Total number of hippocampus samples	131
Number of subjects with HS ¹ alone	97 (74%)
Number subjects with dual pathology	34 (26%)
Average age at surgery [range, median]	33 years 4 months [1-64 years, 35 years]
Female	59 (45%)
Male	72 (55%)
Number of subjects with CPS ² alone	122
Number of subjects with PSG ³	9
Average number of seizures (CPS + PSG) per month [range, median]	15.1 [150, 5]

¹HS, hippocampus sclerosis;

²CPS, complex partial seizures;

³PSG, partial-onset secondary generalized seizures.

Supplementary Table 2. Association of network genes with susceptibility to focal epilepsy. Ensembl genes were mapped to all SNPs in a 100kb region around the gene transcription start site. Network genes were tested for over-representation in the GWAS data for focal epilepsy (Supplementary Figure 3) using the hypergeometric distribution test. The test significance (enrichment *P*-value) was estimated empirically by 1,000,000 permutations, with the size of the sample drawn equal to that of the set analysed. Enrichment analysis was performed for three SNP sets: intragenic SNPs; SNPs within a 10kb window and SNPs within a 100kb window around the gene transcription start site.

SNP set tested	Enrichment <i>P</i>-value	Number of genes with SNP having GWAS <i>P</i>-value <0.05
Intragenic SNPs	2.0×10^{-7}	83
SNPs <10kb window	2.2×10^{-7}	24
SNPs <100kb window	2.1×10^{-7}	42

Supplementary Table 3. Results of the Gene Ontology (GO) enrichment analysis for the genes in Module-1 and Module-2, respectively. The enrichment analysis was carried out using DAVID². Only GO terms showing significant enrichment are reported (false discovery rate (FDR) < 5%).

Module-1

GO Term	Count	%	P-value	Fold Enrichment	FDR
Response to wounding	20	29.4	3.40E-14	8.7	<0.01
Inflammatory response	15	22.1	5.70E-12	10.6	<0.01
Response to glucocorticoid stimulus	9	13.2	4.40E-11	26.5	<0.01
Behavior	16	23.5	9.40E-11	7.8	<0.01
Response to organic substance	19	27.9	9.50E-11	6	<0.01
Response to corticosteroid stimulus	9	13.2	9.60E-11	24.3	<0.01
Immune response	18	26.5	4.00E-10	6	<0.01
Response to steroid hormone stimulus	11	16.2	5.50E-10	13.1	<0.01
Response to endogenous stimulus	14	20.6	1.40E-09	7.9	<0.01
Taxis	10	14.7	1.50E-09	14.3	<0.01
Chemotaxis	10	14.7	1.50E-09	14.3	<0.01
Response to hormone stimulus	13	19.1	4.60E-09	8.1	<0.01
Defense response	16	23.5	4.90E-09	6	<0.01
Regulation of cell proliferation	17	25	2.30E-08	5	<0.01
Locomotory behavior	11	16.2	2.30E-08	9.2	<0.01
Negative regulation of cell proliferation	12	17.6	3.90E-08	7.6	<0.01
Regulation of cell cycle	11	16.2	1.60E-07	7.6	<0.01
Apoptosis	14	20.6	2.10E-07	5.3	<0.01
Programmed cell death	14	20.6	2.60E-07	5.3	<0.01
Death	15	22.1	3.20E-07	4.8	<0.01
Cell motion	12	17.6	7.60E-07	5.8	0.01
Response to organic cyclic substance	7	10.3	8.90E-07	13.3	0.02
Response to lipopolysaccharide	6	8.8	9.90E-07	17.9	0.03
Positive regulation of multicellular organismal process	9	13.2	1.00E-06	8.5	0.01
Regulation of smooth muscle cell proliferation	5	7.4	1.60E-06	24.9	0.07
Cell death	14	20.6	1.80E-06	4.5	0.01
Response to molecule of bacterial origin	6	8.8	1.90E-06	16	0.05
Positive regulation of cytokine production	6	8.8	2.50E-06	15.3	0.07

GO Term	Count	%	P-value	Fold Enrichment	FDR
Negative regulation of apoptosis	10	14.7	2.70E-06	6.5	0.03
Negative regulation of programmed cell death	10	14.7	3.00E-06	6.4	0.03
Negative regulation of cell death	10	14.7	3.10E-06	6.4	0.03
Response to mechanical stimulus	5	7.4	4.30E-06	20.5	0.15
Response to extracellular stimulus	8	11.8	4.70E-06	8.3	0.07
Leukocyte migration	5	7.4	4.70E-06	20.1	0.16
Regulation of apoptosis	14	20.6	6.60E-06	4	0.04
Regulation of programmed cell death	14	20.6	7.40E-06	4	0.05
Response to organic nitrogen	5	7.4	7.70E-06	18.2	0.24
Regulation of cell death	14	20.6	7.80E-06	3.9	0.05
Positive regulation of smooth muscle cell proliferation	4	5.9	9.40E-06	29.6	0.50
Positive regulation of cell proliferation	10	14.7	1.10E-05	5.5	0.10
Regeneration	5	7.4	1.20E-05	16.6	0.34
Leukocyte chemotaxis	4	5.9	1.90E-05	24.8	0.84
Response to bacterium	7	10.3	2.00E-05	8.3	0.27
Cell migration	8	11.8	2.40E-05	6.6	0.27
Positive regulation of cell division	4	5.9	2.40E-05	23.5	0.98
Cell chemotaxis	4	5.9	2.40E-05	23.5	0.98
Response to abiotic stimulus	9	13.2	2.80E-05	5.6	0.26
Regulation of viral genome replication	3	4.4	2.80E-05	49.1	2.50
Response to temperature stimulus	5	7.4	3.00E-05	13.8	0.70
Response to oxygen levels	6	8.8	3.30E-05	9.8	0.54
Response to corticosterone stimulus	3	4.4	4.20E-05	43	3.30
Regulation of cell division	4	5.9	5.10E-05	19.5	1.70
Localization of cell	8	11.8	5.20E-05	6	0.52
Cell motility	8	11.8	5.20E-05	6	0.52
Neutrophil chemotaxis	3	4.4	6.10E-05	38.2	4.20
Regulation of response to external stimulus	6	8.8	6.50E-05	8.7	0.94
Negative regulation of multicellular organismal process	6	8.8	7.70E-05	8.4	1.10
Positive regulation of macromolecule biosynthetic process	11	16.2	1.00E-04	3.9	0.66
Female pregnancy	5	7.4	1.10E-04	10.4	2.00
Positive regulation of cell cycle	4	5.9	1.10E-04	16.1	2.90
Regulation of cytokine production	6	8.8	1.30E-04	7.6	1.70
Positive regulation of cellular biosynthetic process	11	16.2	1.60E-04	3.7	0.95

GO Term	Count	%	P-value	Fold Enrichment	FDR
Positive regulation of biosynthetic process	11	16.2	1.80E-04	3.6	1.10
Protein kinase cascade	8	11.8	1.90E-04	5	1.60
Response to vitamin	4	5.9	1.90E-04	13.9	4.50
Positive regulation of protein transport	4	5.9	2.00E-04	13.7	4.60
Anti-apoptosis	6	8.8	2.70E-04	6.7	2.90
Response to hypoxia	5	7.4	2.90E-04	8.6	4.10
Blood vessel morphogenesis	6	8.8	3.00E-04	6.5	3.30
Negative regulation of transport	5	7.4	3.00E-04	8.5	4.20
Response to drug	6	8.8	3.40E-04	6.4	3.60
Regulation of system process	7	10.3	3.70E-04	5.2	3.20
Positive regulation of protein kinase activity	6	8.8	4.10E-04	6.2	4.10
Positive regulation of nitrogen compound metabolic process	10	14.7	4.20E-04	3.6	2.50
Positive regulation of kinase activity	6	8.8	4.90E-04	6	4.80
Protein amino acid phosphorylation	10	14.7	5.60E-04	3.4	3.20
Negative regulation of molecular function	7	10.3	5.90E-04	4.8	4.70

Module-2

GO term	Count	%	P-value	Fold Enrichment	FDR
Collagen fibril organization	4	7.4	1.10E-06	50.4	0.09
Extracellular matrix organization	5	9.3	8.70E-06	17.6	0.24
Blood vessel development	6	11.1	4.80E-05	9	0.66
Vasculature development	6	11.1	5.50E-05	8.7	0.74
Extracellular structure organization	5	9.3	7.60E-05	11.2	1.30
Response to nutrient levels	5	9.3	1.90E-04	9.3	2.60
Response to inorganic substance	5	9.3	2.20E-04	8.9	3.00
Response to extracellular stimulus	5	9.3	3.10E-04	8.3	3.90

Supplementary Table 4. Primer sequences used in the mouse qRT-PCR experiments and *Sesn3* siRNA target sequences.

Primer sequences		
Gene	Forward sequence	Reverse sequence
<i>IL-1b</i>	GGGCCTCAAAGGAAAGAATC	TACCAGTTGGGGAACCTCTGC
<i>IL-1a</i>	CCCGTCCTTAAAGCTGTCTG	AATTGGAATCCAGGGGAAAC
<i>ILRN</i>	TAGCAAATGAGCCACAGACG	ACATGGCAAACAACACAGGA
<i>Nlrp3</i>	ATGCTGCTTCGACATCTCCT	AACCAATGCGAGATCCTGAC
<i>Atf3</i>	TTTTCCGGGAGTTTCATCAG	GGTGTCGTCCATCCTCTGTT
<i>Ccl4</i>	AGCCAGCTGTGGTATTCCTG	GAGGAGGCCTCTCCTGAAGT
<i>Cd69</i>	TGGTGAACCTGGAACATTGGA	CTCACAGTCCACAGCGGTAA
<i>Egr2</i>	TTTGATGTGCACTGCTCTCC	TCACACAAGGCACAGAGGAC
<i>Egr3</i>	AGACGTGGAGGCCATGTATC	GGGAAAAGATTGCTGTCCAA
<i>Fos</i>	CTCCCGTGGTCACCTGTACT	TTGCCTTCTCTGACTGCTCA
<i>Fosb</i>	AGAGGTGCGAGGCAATTTTCA	GGAGGGAAGGGACAGAACTC
<i>Gadd45B</i>	CACCCTGATCCAGTCGTTCT	TGACAGTTCGTGACCAGGAG
<i>Junb</i>	CCATCAGCTACCTCCCACAT	GCTTTCGCTCCACTTTGATG
<i>Sesn3</i>	GCGAGGAGAAGAACATTTGC	TGTGGTTCGTGTCAACATCCT
<i>Tnfa</i>	TATGGCTCAGGGTCCAACCTC	CTCCCTTTGCAGAACTCAGG
<i>Hprt</i>	AAGCTTGCTGGTGAAAAGGA	TTGCGCTCATCTTAGGCTTT
<i>Gapdh</i>	GGGTGTGAACCACGAGAAAT	GTCTTCTGGGTGGCAGTGAT
<i>Sesn3</i> siRNA target sequences		
Target sequence 1:	GCAUCAAUCCAGAGAGAGA	
Target sequence 2:	GGCUGAAUGGCUUGGAAUA	
Target sequence 3:	AGUUCUACAUGCUGCGUAU	
Target sequence 4:	AAGCAAAUACGGCGGAUGA	

SUPPLEMENTARY METHODS

Pilot study using surgical hippocampus samples

We first assessed the extent of differences in gene expression between hippocampus subfields and between whole hippocampus between individuals using surgical hippocampus samples from five patients with mesial temporal lobe epilepsy (mTLE). For each hippocampus sample, four hippocampus subfields were laser micro-dissected (dentate gyrus, CA1, CA3 and CA4) and genome-wide expression profiles were generated for each subfield using Affymetrix microarray (n=22,215 probe sets) as described before in detail⁶. We found substantially higher inter-individual variability in whole-hippocampus gene expression than between hippocampal subfields (see Supplementary Figure 1), indicating that inter-individual variability in gene expression from whole hippocampus can be used to correlate with variation in phenotype, and informing the use of expression data from whole hippocampus in our subsequent expression analyses.

Clinical material

One hundred and forty seven patients with pharmacoresistant temporal lobe epilepsy (TLE) were studied, who underwent surgical treatment in the Epilepsy Surgery Program at the University of Bonn Medical Center. All patients had undergone a detailed pre-surgical evaluation using a combination of non-invasive and invasive procedures to establish that their seizures originated in the mesial temporal lobe⁷. Surgical removal of the hippocampus was clinically indicated in every case. All procedures were conducted in accordance with the Declaration of Helsinki and approved by the ethics committee of the University of Bonn Medical Center. Informed written consent was obtained from all patients. For the individual patients, the frequency of partial seizures occurring with impairment of consciousness (corresponding to the concept of a complex partial seizure) and partial seizures involving into bilateral tonic, clonic or tonic-clonic components (corresponding to the concept of a secondary generalized seizure) were assessed in the immediate pre-surgical period defined by an absence of change in drug therapy. Subjective sensory or psychic phenomena (simple partial seizures or auras) were not counted. Complex partial and secondary generalized seizures were each counted as

one event, and the combined total expressed as seizures per month. Clinical assessment was by review of the hospital case records from the single centre in the pre-surgical assessment period. Additional clinical variables recorded include: age and sex, handedness, laterality of TLE (determined by standard pre-surgical electro-clinical assessment including high quality structural magnetic resonance imaging), age at manifestation of epilepsy, antiepileptic drug (AED) therapy during the period of seizure frequency assessment (including type and dose for each AED), outcome of surgery and hippocampal pathology. For AED therapy, we grouped patients into one of the following three categories; (A) sodium channel blocker/s alone (B) combination therapy including an SV2A AED (C) combination therapy not including an SV2A AED (overview on clinical data in Supplementary Table 1 and⁸).

Effect of antiepileptic drug therapy, laterality and pathology on gene expression in the hippocampus of temporal lobe epilepsy patients

Genome-wide differential expression analyses were carried out to assess the extent to which each clinical cofactors affect variation in gene expression. No or limited effect of these clinical cofactors was found on gene expression in the hippocampus as detailed below.

Effect of AED therapy: The AED therapies at the time of surgery were classified into three main groups: Category A, patients taking a sodium channel blocker only (n=27), Category B, combination AED therapy that included levetiracetam (n=49) and Category C, combination AED therapy not including levetiracetam (n=52). Differential expression analysis using Significance Analysis of Microarrays (SAM)¹ followed by multiple testing correction did not identify significant differences between the three categories (false discovery rate (FDR) < 5%).

Effect of laterality of temporal lobe epilepsy: Differential expression analysis did not show any significant variation (FDR < 5%) in gene expression due laterality in the study sample.

Effect of pathology: SAM analysis showed a small set of genes that were differentially expressed between the 98 subjects with hippocampal sclerosis as a single pathology and 33 subjects associated

with dual pathology (i.e., hippocampal sclerosis plus an additional adjacent brain lesion)(see Supplementary Table 1). At 5% FDR, 3,151 protein coding genes were identified as differentially expressed. Of these, only 10 genes were also found in the network and significantly associated with seizure frequency (empirical P -value <5%).

Sample preparation and microarray analysis in human hippocampus

All 129 patients used in the present study had mesial temporal lobe epilepsy (mTLE) and all tissue samples were from indistinguishable hippocampal tissue portions. Fresh frozen sections were neuropathologically analyzed according to international standards and carefully matched for excellent anatomical preservation by experienced neuropathologists of the Dept. of Neuropathology Bonn. Up to 8 sections of 50.0 μm were used for genomic DNA and total RNA isolation. Total RNA was isolated from hippocampal tissue samples using AllPrep DNA/RNA Mini Kit (Qiagen, Hilden) according manufacturer's protocol. Tissue lysate was passed through an AllPrep RNeasy spin column to selectively isolate RNA. For all cases the RIN-range was from 6,5 to 10. In order to synthesize cDNA from total RNA and in vitro transcription to biotin-labeled cRNA, Illumina TotalPrep-96 RNA Amplification Kit (Life Technologies Corporation, Darmstadt) was used according to the manufacturer's protocol. Briefly, a reverse transcription procedure was applied to synthesize first strand cDNA from 50.0 ng total RNA. Second strand synthesis to convert the single-stranded cDNA to double-stranded DNA was carried out. After cDNA purification, *in vitro* transcription was performed for biotin-labeling and following purification of the resulted cRNA. A total amount of 750.0 ng cRNA was used for hybridization on Human HT-12 v3 Expression Bead Chips with Illumina Direct Hybridization Assay Kit (Illumina, San Diego, CA). Preparation of cRNA samples and BeadChips was done separately in BeadChip Hyb Chambers and the incubation was carried out overnight to hybridize the labeled cRNA strand to the beads containing respective complementary gene-specific sequences. BeadChips from overnight hybridization were cleaned in several washing steps. To detect the differential signals on the BeadChip, Cy3-Streptavidin was incorporated to bind to the hybridized probes. The Illumina BeadArray Reader was used to scan the excited fluorescent signals of the hybridized single-stranded product on the BeadChips. The data were further analyzed using Illumina's

GenomeStudio Gene Expression Module and were normalized by means of quantile normalization with background subtraction. The microarray probes were annotated using either the Human HT-12 v3 annotation file from Illumina or Ensembl (Human release 72).

Gene co-expression network analysis in the human hippocampus

For each probe, we first removed the effect of “age” and “gender” covariates from the expression data using linear model in R (<http://www.r-project.org/>). The residuals obtained from the linear regression were used as the input for the network analyses, which was carried out at the level of microarray probes. Gene co-expression networks were inferred using Graphical Gaussian Models (GGMs), which use partial correlations to assess co-expression relationships between any microarray probe pair in the dataset, removing the effect of other probes⁹. To maximize power to detect significant and sizeable partial correlations and co-expression networks, we prioritized probes showing both robust expression (i.e., probes expressed with a detection p-value < 0.05 in at least 20% of the samples) and the highest variation in gene expression (i.e., probes having a coefficient of variation (CV) of gene expression greater than the median CV calculated across all probes in the set). This delineated an informative set of 7,150 probes that were used in the GGM analysis, which was carried out using the package “*GeneNet*”^{9,10} in R (<http://www.r-project.org/>). For each pair of probes, partial correlations were estimated using a shrinkage estimator implemented in “*GeneNet*” package (for details about the shrinkage procedure refer to the original paper⁹). We then used the empirical Bayes local FDR statistic¹¹ to extract significant edges from the set of partial correlations (Supplementary Figure 13), which delineated a set of 2,124 inter-connected nodes (Supplementary Data 2).

Network extraction: We employed the Heinz algorithm¹², implemented in the R package *BioNet*¹³, to extract the largest connected component of 511 nodes (i.e., probes) from the set of partial correlations encompassing 2,124 nodes (Supplementary Data 2), which were detected at FDR 5%. This defined a co-expression network of 511 nodes, representing 442 annotated unique genes (Supplementary Data 1), which we called TLE-hippocampus derived transcriptional network (TLE-network).

Identification of transcriptional modules: The *ClusterViz* package on the Cytoscape platform¹⁴ was used to investigate and extract clusters within the large connected component of 511 nodes. This is based on the fast agglomerative algorithm based on edge clustering coefficients (FAG-EC) developed by¹⁵, which is a modification of the k-means algorithm, was used to extract discrete modules from the large connected component of 511 nodes. Briefly, an undirected simple graph G is created from the list of nodes and edges in the large component, and the clustering coefficients ($C_{i,j}$) of all edges in the graph are calculated according to

$$C_{i,j} = \frac{|N_i \cap N_j| + 1}{\min(k_i, k_j)} \quad \text{Equation (1)}$$

where k_i and k_j are the degrees of node i and node j . The edges are sorted in decreasing order of edge clustering coefficient. The higher the clustering coefficient of an edge, the more likely that it is an edge to be found inside the same module. All the nodes in graph G are initialized as singleton sub-graphs, which are mergeable. Edges are gradually added to clusters by working down the ordered list of edges. This procedure yielded two large modules comprising 80 nodes (representing 69 unique annotated genes) with 584 edges (Module-1) and 60 nodes (representing 54 unique annotated genes) with 247 edges (Module-2), respectively.

Mapping the genetic control of gene co-expression networks

Here we illustrate the strategy we used to map the genetic control points of the transcriptional modules in the TLE patient cohort. After preprocessing of the genotype data, we performed the following steps: *i*) Principal Components Bayesian GWA study (PCBGWAs) and *ii*) refinement of genetic mapping results provided by PCBGWAs.

Data preprocessing: imputation of missing values, Minor Allele Frequency (MAF) thresholding and tagging: Genotype data was available for 122 TLE samples. Missing values in the genotype data for each of the 22 autosomal chromosomes were imputed using FastPhase¹⁶, allowing 20 random starts of the EM algorithm (-T20), 100 iterations of the EM algorithm for each random start (-C100), no haplotype estimation (-H-4), without the determination of the number of clusters (-K1). We removed

SNPs with Minor Allele Frequency (MAF) < 0.05 and performed tagging at $D' > 0.80$ level¹⁷. The original data set consisting of 527,684 SNPs was reduced to 478,290 SNPs after MAF thresholding (19% reduction) and further shrunk to 346,408 SNP after tagging (34% reduction). This set of SNPs was used for all following analyses.

Step 1: Principal Components Bayesian GWA study (PCBGWAs)

We performed Principal Component (PC) analysis¹⁸ on Module-1 ($n=122$ and $q=80$) and Module-2 ($n=122$ and $q=60$) expression separately. The first three PCs (each explaining a proportion of variance $> 5\%$) accounted in total for 76.83% and 51.55% of the variability of Module-1 and Module-2, respectively (Supplementary Figure 6) and were used for the Bayesian GWA study.

We used PC-based multivariate regression approaches¹⁹ to prioritize genomic regions associated with Modules' expression. For each module, the first three PCs were associated to the set of predictors (~350K SNPs) using ESS++ (Evolutionary Stochastic Search)^{20,21}. Given the relatively small number of subjects ($n=122$), in order to detect important signals we imposed very strong sparsity with $E(p_\gamma) = 2$ and $V(p_\gamma) = 2$ (i.e., the *a priori* expected model size (expected number of true genetic associations) and variance of the model size), meaning the prior model size is likely to range from 0 to 6. In this set-up, given the level of sparsity and the number of predictors ($p=346,408$), the average prior probability π that a SNP is truly associated with the phenotype is 5.77×10^{-6} . ESS++, the Bayesian variable selection algorithm, was run for 110,000 sweeps, with 10,000 sweeps as burn-in, with three chains run in parallel and a hyper-prior on the selection coefficient τ . Diagnostic tests for convergence were performed similarly to²². Output from the algorithm enabled us to calculate the Best Model visited (which defines the best set of predictors visited, i.e. SNPs) as well as the Marginal Posterior Probability of Inclusion (MPPI) and the associated (local) FDR for each SNP²³. Following²⁴, for each predictor (SNP), we derived the Bayes Factor (BF) as the ratio between the Posterior Odds and the Prior Odds. Detailed discussion and the benefits of reporting BF over the more traditional critical level (*P*-value) of a test of association can be found in²⁵. Since in our set-up π is very small, the BF has to be

large ($\log_{10}(\text{BF}) > 6$) to provide strong evidence for phenotype-SNP association (with MPPI close to 1 and (local) $\text{FDR} < 0.05$).

Step 2: Refinement of genetic mapping results provided by PCBGWAs

For the locus on chromosome 11q21 detected by PCBGWAs for Module-1, we refined the association by defining a 1Mbp region centered on the significant SNP. We then linked all genes of the Module to all SNPs in the selected region using HESS²⁴, the extension of ESS++²¹ where a large number of traits (i.e., Module-1 genes' expression) are jointly considered. Sparsity was imposed setting $E(p_i) = 2$ and $V(p_i) = 2$ for each gene with the prior probability π that a SNP at the locus is truly associated equal to 0.0112 for Module-1. The algorithm was run for 110,000 sweeps, with 10,000 sweeps as burn-in, with three chains run in parallel. Convergence diagnostics of the Monte Carlo Markov Chain output showed no evidence of irregular behavior. The Best Model Visited is the most supported multivariate model ranked according to the Model Posterior Probability. For each multivariate model (i.e., any combination gene(s)-SNP(s)) visited during the Markov Chain Monte Carlo, the log-Posterior (\log marginal likelihood \times log prior on the model space) is available and, for each unique model visited, the Model Posterior Probability is equal to the renormalized log-Posterior probability. Finally the proportion of genes associated with each SNP is defined as the average number of genes that are predicted in the Best Models Visited by each SNP. This measure helps prioritizing SNPs that influence multiple genes at the same time and allows the discovery of so-called regulatory hot-spots, i.e., genetic loci that are associated with a large number of gene expression traits²⁴.

Genetic association of TLE-network genes with epilepsy susceptibility

To test whether co-expression networks are likely to be causal, we tested whether network genes are enriched for SNP variants genetically associated to epilepsy; since genotypes do not vary with disease status, genetic association of a network to disease susceptibility provides independent evidence for a causal relationship with the disease.

Genome-wide association study (GWAS) of susceptibility to focal epilepsy: To test whether networks show enrichment for epilepsy genetic association signals we undertook an epilepsy GWAS comprising 1,429 patients with focal epilepsy and 7,358 healthy controls. Three epilepsy cohorts of “UK, Swiss or Finnish ancestry” and matched healthy controls were combined via meta-analysis.

Patients: The diagnosis of focal epilepsy was made and/or reviewed by a consultant neurologist according to the International League Against Epilepsy (ILAE) definition of focal epilepsy²⁶. All causes of focal epilepsy (genetic, structural and unknown) according to the ILAE Revised Terminology and Concepts for Organisation of Seizures and Epilepsies²⁷ were included except patients with a progressive brain lesion who were excluded. The 1,429 cases with focal epilepsy available post-filtering (see below) were derived as follows: (a) 806 UK Ancestry cases; (b) 213 Swiss Ancestry cases provided by GSK; (c) 410 Finnish Ancestry cases also provided by GSK. Of the 1,429 patients, 1,013 (71%) had a clinical diagnosis of temporal lobe epilepsy (TLE).

Controls: Post filtering (see below), the 7,358 healthy controls were divided as follows: (a) 5,184 UK controls from the Wellcome Trust Case Control Consortium Phase 2 (WTCCC2), consisting of the 58 Birth Cohort (58 BC; 2,692 controls) and the National Blood Service (NBS; 2,492 controls); (b) 232 Swiss controls provided by GSK; (c) 1,942 Finnish Controls from either the Helsinki Birth Cohort (HBC; 1,671 controls) or GSK (271 controls).

Genotyping, Quality Control and Population Stratification: UK cases were genotyped on Illumina 660-Quad; WT controls were genotyped on Illumina 1.2M. Samples provided by GSK were genotyped on Illumina 610-Quad, HBC samples were genotyped on 660-Quad.

Identification of Close Relatives and Population Structure: For each ancestry band, we first estimated pairwise identity by descent (IBD) by calculating identity by state across a subset of roughly 50,000 of the highest quality SNPs, pruned to ensure approximate linkage disequilibrium. These pairwise IBD values enabled us to remove one of each pair of very close relatives (IBD>0.25) and identify population outliers. For the association analyses, we included covariates representative of population structure across the ancestry band as a whole (e.g. all UK ancestry samples) as well as covariates

specific to a particular set of samples (e.g. just 58 BC controls). We derived these covariates using the top eigenvectors calculated from (a subset of) the IBD estimate matrix. We determined the number of significant axes to include using the Tracy-Widom test implemented in EIGENSTRAT software²⁸.

Association Analysis: For the association testing across each ancestry band, we retained autosomal SNPs which satisfied the following criteria: MAF > 0.05, Call Rate (CR) > 0.99, p-value from test for Hardy-Weinberg equilibrium (HWE) > 0.0001; additionally SNPs with $0.01 < \text{MAF} < 0.05$ were retained if CR > 0.995 and HWE > 0.01. We utilized the logistic regression function implemented in PLINK²⁹. This fits a linear model to the log odds for susceptibility to focal epilepsy, which is made up of an intercept term, contributions from sex and from the population covariates and for the SNP in question. From the three GWASs, we had p-values for 512,450 SNPs (UK Study) 488,214 SNPs (Swiss Study) and 498,721 SNPs (Finnish Study). This meant that for 487,682/11,571/13,197 SNPs we had 3/2/1 p-values. Association p-values were combined using PLINK's meta-analysis function, which invokes a standard inverse variance weighting²⁹. We discovered no single SNP with a genome-wide significant association with susceptibility; all p-values were greater than 10^{-7} (see Supplementary Figure 3), consistent with the hypothesis that focal epilepsy is a highly polygenic trait with no common variants with strong effect sizes³⁰.

Enrichment analysis of network genes with epilepsy: To examine whether genes in the network were associated with susceptibility to focal epilepsy we first compared the genomic locations of each SNP genotyped in the focal epilepsy GWAS with the Ensembl gene annotations using the GRCh37.p5 build of the Ensembl database (www.ensembl.org). We then divided all SNPs into three major categories: (A) SNPs within any Ensembl gene in the network; (B) SNPs within 10kb region around any Ensembl gene in the network (excluding any in A); (C) SNPs within 100kb region around any Ensembl gene in the network (excluding any in A or B). Each gene was then assigned a GWAS significance value consisting of the lowest P-value of all SNPs mapped to it. We tested whether SNPs close to (<100kb from) any network genes were significantly more likely to associate with epilepsy in GWASs than SNPs close to genes not in the network. We used the hypergeometric distribution test to determine the degree of overrepresentation of significant genetic associations (i.e., GWAS P -value < 0.05) within

the network gene set. For each SNP category the null distribution of the hypergeometric test was generated by 1,000,000 randomly selected gene sets, where the size of the sample drawn was equal to that of the set analyzed³¹. This yielded the empirical enrichment *P*-values for the network genes within each SNP category, which are reported in Supplementary Table 2 and show that the distance between the SNPs and the network genes did not affect the reported enrichment results for the network.

RNA-sequencing analysis in the mouse hippocampus

Mouse pilocarpine model: A single injection of pilocarpine was used to trigger status epilepticus (SE) in male NMRI mice (Charles River, France) 28–32 g at the beginning of the study. As previously described³², animals were injected intraperitoneally (i.p.) with 1 mg/kg of Nmethylscopolamine bromide 30 min prior to pilocarpine treatment (300 mg/kg; i.p.). Within 10 to 45 min after pilocarpine treatment, animals displayed generalized clonic-tonic seizures that progressed to continuous convulsive activity, i.e. status epilepticus. The SE lasted 3 h and was interrupted by i.p. injection of diazepam (10 mg/kg) to limit the extent of brain damage. The mice surviving SE typically show spontaneous recurrent seizures within few days and continue to display them for several weeks³². In the present study all mice were continuously video monitored for a period of 2 weeks starting the recordings 4 weeks after pilocarpine-induced SE to document the presence of spontaneous recurrent seizures. The mice were then sacrificed 6 weeks after SE induction to collect brain samples.

RNA-Seq analysis: We carried out high-throughput sequencing of mRNA (RNA-Seq) in whole hippocampus from 100 epileptic (pilocarpine model where spontaneous recurrent seizures were documented by video monitoring of each individual animal)³² and 100 control naïve mice. Total RNA was isolated from 200 mouse hippocampi and cDNA and sample preparation for RNA sequencing was done according to the protocols recommended by the manufacturers (TruSeq RNA kit, Illumina). Samples were sequenced on an Illumina HiSeq 2000 sequencer as paired-end 75-nucleotide reads according to the protocol recommended by the vendor. Raw reads were mapped to the reference mouse genome (mm10) using TopHat version 2.0.8³³. Read counts per gene were calculated for each sample using HTseq version 0.5.3. Read counts per gene were further normalised across all samples

using the “trimmed mean of M-value” (TMM) approach as discussed in³⁴. Differential expression analysis was performed using the Bioconductor R package *edgeR*³⁴ version 3.2.4, and a threshold of 5% FDR was used to identify significant gene expression changes.

Cell culture and *in vitro* experiments

Bone-marrow-derived macrophages (BMDMs) from C57BL/6J mice were cultured in L929 conditioned media as previously described³⁵. Briefly femurs and tibias from each mouse were flushed out in HBSS (Life Technologies) with the use of a syringe. Total bone marrow-derived cells were plated in 6-well plates (Nunc) and cultured for 5 days in DMEM (Life Technologies) that contained 25 mM HEPES (Sigma), 25% L929 conditioned medium, 25% FBS (Biosera), penicillin (100 U/ml; Life Technologies), streptomycin (100 µg/ml; Life Technologies), and l-glutamine (2 mM; Life Technologies). Following 5 days of differentiation, these cells were characterized as macrophages by CD68 staining.

Murine microglial cell line (BV2) was kindly provided by Dr Joseph Bertrand (Karolinska institute, Sweden). BV2 cells were cultured and maintained in DMEM (Life Technologies) media and supplemented with 10% FBS (Biosera), 2 mM L-glutamine, penicillin (100 U/ml, Life Technologies) and streptomycin (100 mg/ml, Life Technologies).

Hippocampal neurons were derived from embryonic mice³⁶. Embryonic day 19 mice were harvested by cesarean section after culling the pregnant dams by cervical dislocation (strain GFPm-high, bred in our facility). The animal protocol was approved by the local ethics committee and performed under UK Home Office License. Brains were removed from the embryos and hippocampi were isolated from each brain hemisphere after removing meninges. Hippocampal tissue was then dissociated by 2.5% (wt/vol) trypsin digestion and trituration with a Pasteur pipette and a fine 1000 µl bore pipette. Low-density cultures (5×10^4 cells/ml) were plated onto 18 mm glass cover-slips introduced into 12-well (3 cm²) culture dishes. Tissue culture dishes were coated with (0.01mg/ml) poly-L-lysine. The cells were plated in Neurobasal medium (Life Technologies) supplemented with B27 (Life Technologies), 200mM glutamine (Life Technologies), 14.3M β-mercaptoethanol and streptomycin/amphotericin B

(Life Technologies). Hippocampal tissue preparations were incubated in the cell culture incubator at 37°C, 5% CO₂. Two days after plating, the medium was top up with 30% of the initial volume and after 3 more days 50% of the medium was changed. Subsequently every 4-5 days 50% of the medium was replaced. Hippocampal cultures were maintained for up to 10 days *in vitro*.

SESN3 silencing and assessment of Module-1 gene expression by qRT-PCR: siRNA knockdown experiments were performed in BMDMs or BV2 microglia cell lines by using a mouse *Sesn3* ON-TARGETplus SMARTpool siRNA (100nM, ThermoFisher Scientific) and Dharmafect 1 (1:50, ThermoFisher Scientific) a transfection reagent, according to manufacturer's recommendations. Briefly, cells cultured in 6-well plates were incubated in serum and antibiotic free DMEM for 10 h and transfected for 48 h with *SESN3* siRNA, which consists of a pool of four unique siRNA molecules against mouse *SESN3*, using Dharmafect 1 in OPTIMEM medium (Life Technologies). Control cells were transfected in the same conditions with non-targeting scrambled siRNA (100 nM). For lipopolysaccharide (LPS) stimulation experiments, the transfected BMDM cells were washed twice in DMEM and stimulated with LPS (Sigma, 100 ng/ml) for an hour. Cells (basal or LPS-stimulated) were then harvested in TriZOL (Life Technologies) and total RNA was extracted according to manufacturer's instructions. Real-time one step RT-PCR for Module-1 genes was performed on an ABI 7500 Sequence Detection System (Applied Biosystems, Warrington, UK) using SYBR Green (Stratagene, Cambridge, UK) with 100 ng of total RNA and gene-specific primer sets. Results were then exported to 7500 Fast system SDS software (ABS), and Ct values were determined for all of the genes analysed.

Lentivirus production and assessment of Module-1 gene expression by qRT-PCR: A third generation Lentiviral Vectors (LV) was used to transduce murine primary hippocampal neuronal culture. The LV was prepared by Calcium Phosphate transfection. Briefly, co-transfection of packaging plasmids (pMDLg/pRRE, 12.5 µg, pMD2.VSV-G, 6.25 µg, pRSV-REV, 7 µg) and transfer plasmid (pLCMV-Sesn3-1-Flag, 32 µg) was made in Hek 293T cells. Media was replaced at 18 hours and the harvesting was performed at 36 and 72 hours. The purification was obtained by over-night centrifugation at 4°C and 4,000 rpm. The LV transduction was performed by replacing the media with 33 µl of vector

(4.98×10^{17} IU/ml) and, to improve the vector penetration 8 μ g/ml of polybrene were supplemented to the cells. Three days after the LV transduction the RNA was extracted and the cDNA was synthesized. Real-time one step RT-PCR for Module-1 genes was performed as described above. The relative expression levels normalized to *Beta-actin* or *Gapdh* gene expression (as indicated) were then determined by using the $2^{-\Delta\Delta Ct}$ method.

Zebrafish studies

Microinjection of morpholino antisense oligonucleotides: To study the function of sestrin3 in response to Pentylentetrazole-induced (PTZ-induced) seizures, two different morpholinos (MOs) were designed to block the normal splicing of the zebrafish *sesn3* primary transcript. *Sesn3* i3e4MO targets the splice acceptor site between intron3 and exon 4 of the gene (5'-TGCAGCCTGGAAGACATGGAAAAA -3') whereas *Sesn3* e4i4MO targets the splice donor site between exon 4 and intron 4 (5'-GACTCCAACCTAATGGGTTTACTTGT-3'). We assessed the morpholinos efficacy and found that PTZ-induced locomotor activity of larvae injected with the combination of *sesn3* morpholinos (i3e4MO + e4i4MO) was much lower than that of controls and larvae injected with either *sesn3* morpholino individually (Supplementary Figure 12). *Sesn3* i3e4MO and *Sesn3* e4i4MO were co-injected into AB wildtype zebrafish embryos at the one- or two-cell stage, at a concentration of 0.05mM of each morpholino (total MO concentration 0.1mM) in water. *Sesn3* i3e4 + *Sesn3* e4i4 MO solution was microinjected in a final volume of approximately 2nl. The standard control morpholino (Gene Tools) was microinjected at a concentration of 0.1mM into one- or two-cell stage AB zebrafish embryos, in a volume of 2nl per embryo. Standard Control Morpholino sequence: 5'-CCTCTTACCTCAGTTACAATTTATA- 3' (Gene Tools). Embryos that were to be analysed by whole mount in situ hybridisation were first treated with 1-phenyl-2 thiourea (PTU) at 23 hours post-fertilization (hpf) to inhibit melanogenesis. At 3 days post-fertilisation (dpf), larvae were treated for one hour with 20mM PTZ or left untreated, and all larvae were then fixed with paraformaldehyde immediately after the treatment period.

RNA in situ hybridisation: A *c-fos* digoxigenin-labelled probe was prepared as recommended by the manufacturer of the in situ hybridisation reagents (Roche). Whole-mount in situ hybridisation was performed using standard procedures; details of the probe used are available on request (Vincent T. Cunliffe, MRC Centre for Developmental and Biomedical Genetics, Department of Biomedical Science, University of Sheffield, UK).

qPCR analysis of c-fos and Module-1 genes: Between 15 and 20 *sesn3* morphant larvae and control larvae were decapitated at 3dpf after 1hr of 20mM PTZ treatment and only the heads were processed for RNA extraction. The heads were treated with 200µl RNAlater (Ambion) and stored at 4°C. The RNA later was discarded and RNA was extracted using 1ml of TRIzol (Invitrogen). The RNA was then treated with 1µl DNase I (Invitrogen) and after a 30 minute incubation at 37°C, the RNA was precipitated with sodium acetate and ethanol. cDNA was synthesized using SuperScript® II First-Strand Synthesis System for RT-PCR kit (Invitrogen). The qPCR reactions were carried out using SYBR Green (Sigma) and 10ng of cDNA final concentration. The reactions were prepared in Hard-Shell® Low-Profile Thin-Wall 96-Well Skirted PCR Plates (BioRad) and the PCR machine used for the analyses was BioRad CFX96 Touch™ Real-Time PCR Detection System. The efficiency of the primers was assayed at 300ng concentration. The relative expression levels normalized to the housekeeping gene *beta-actin* gene expression were then determined by using the $2^{-\Delta\Delta Ct}$ method.

qPCR analysis of Module-1 genes after injection of synthetic sesn3 mRNA in zebrafish embryos: In vitro-synthesized *sesn3* RNA was injected into 1 cell-stage zebrafish embryos (~ 1ng *sesn3* RNA per embryo). At 28hpf, *sesn3* RNA-injected and control uninjected embryos were collected and frozen at -80°C. Total RNA was extracted using TRIzol (Invitrogen) and isopropanol. The extracted RNA was cleaned up using the RNeasy mini kit (QIAGEN) before first stand cDNA synthesis was performed using Superscript II Kit (Invitrogen). For the qPCR analyses the reactions were prepared in Hard-Shell® Low-Profile Thin-Wall 96-Well Skirted PCR Plates (Biorad). Each qPCR reaction contained 5µl Sybr green (Sigma), 0.6 µl 5µM forward primer (300ng final concentration), 0.6 µl 5µM reverse primer (300ng final concentration), 1 µl 1:10 cDNA dilution (10ng cDNA final concentration), and 2.8 µl RNase free water. The PCR machine used for the analyses was BioRad CFX96 Touch™ Real-Time

PCR Detection System. The efficiency of the primers was assayed at 300ng concentration. The relative expression levels normalized to the housekeeping gene *beta-actin* were then determined by using the $2^{-\Delta\Delta C_t}$ method.

Primers sequences used for the PCR: *Atf3* forward primer 5'-GAGACCCACCGAACTACCTG, reverse primer 5'-TGCTGCTGCAATTTGTTTC; *beta-actin1* forward primer 5'-CAACAACCTGCTGGGCAAA, reverse primer 5'-GCGTCGATGTCGAAGGTCA (Keegan et al., 2002); *cfos* forward primer 5'-TCGACGTGAACTCACCGATA, reverse primer 5'-CTTGCAGATGGGTTTGTGTG; *egr2b* forward primer 5'-CTGCCAGCCTCTGTGACTAT, reverse primer 5'-GCTTCTCCGTGCTCATATCC; *fosB* forward primer 5'-CCAGTGCCTCAGTCTCGAAG, reverse primer 5'-CGGCAGCCAGTTTATTCTC; *gapdh* forward primer 5'-GTGGAGTCTACTGGTGTCTT, reverse primer 5'-GTGCAGGAGGCATTGCTTAC.

Analysis of zebrafish locomotor activity using the Viewpoint Zebrabox system: The distance moved by larvae over a 1 hour period of PTZ treatment was recorded using the Zebrabox system (Viewpoint, France). AB larvae aged 3 dpf were transferred to a 48-well microlitre plate, one larva per well containing 500ul (for un-treated larvae) or 450ul (for PTZ-treated larvae) of E3 medium. Then 50ul of 200mM PTZ were added into the wells containing 450ul of E3 media to achieve a final concentration of 20mM PTZ. The locomotor behaviour of the larvae was then recorded for 1 hour using the Zebrabox equipment. The recording started immediately after PTZ was added and the Viewpoint software was set to integrate the data for the distance moved every 10 minutes. Locomotor activity of larvae was recorded with the Zebrabox using a light cycle of 2 minutes: 100% light; 2 minutes: 0% light.

Rescue experiments: To investigate if the phenotype observed in *sesn3* morphant larvae was caused by the decreased expression of *sestrin3*, synthetic *sesn3* messenger RNA was co-injected along with *sesn3* morpholinos into zebrafish embryos to determine whether the morphant phenotype could be rescued. A full-length zebrafish *sestrin3* cDNA clone (IMAGE:2601412) was subcloned into the pCS2+ expression vector to create pCS2+.sestrin3. A linearized template of pCS2+.sestrin3 was used

to synthesize *sesn3* RNA using the mMessage mMachine Kit (Ambion). The synthetic *sesn3* RNA was injected into one-cell stage AB wild type zebrafish embryos alone (2nl of 0.3ng/nl *sesn3* mRNA) or in combination with *sesn3* morpholinos (2nl of 0.3ng/nl *sesn3* mRNA + 0.05mM *sesn3* i3e4 MO + 0.05mM *sesn3* e4i4 MO). In addition, some embryos were injected with *sesn3* morpholinos alone (2nl of 0.05mM *sesn3* i3e4 MO + 0.05mM *sesn3* e4i4 MO). The locomotor activity in response to PTZ exposure was analyzed using the Viewpoint zebabox, as described above.

Immunohistochemistry analysis in human hippocampus from TLE patients

For immunohistochemistry, human hippocampal sections obtained from paraffin blocks were deparaffinized in xylene and rehydrated in a graded alcohol series. After a short step washing in phosphate-buffered saline (PBS), the slides were microwaved in citric acid buffer (10mM, pH 6.0) for 10 min and then washed in PBS. All washing steps were carried out for 2 x 5 min in PBS at room temperature (RT). Slides were blocked for 2 h at 37°C in PBS-blocking buffer (10% fetal calf serum (FCS) and 1% normal goat serum in PBS) to inhibit non-specific antibody binding. Antibodies targeted against polyclonal anti-rabbit antibody SESN3 (1:300; Novus Biologicals, Cambridge), neuronal nuclear protein (NeuN) antibody (1:500; Millipore, Billerica, MA USA) and monoclonal anti-mouse antibody HLA-DR (1:1200; Dako, Hamburg, Germany) were incubated over night at 4°C in PBS including 10% FCS. After washing, both secondary antibodies anti-rabbit Cy3 (1:400; Jackson Research, New Market UK) and anti-mouse FITC (1:400; Jackson Research, New Market UK) were applied, diluted in PBS including 10% FCS for 2h in the dark. After washing, respective slides were covered with VectaShield HardSet Mounting Medium for Fluorescence (Vector Laboratories, Burlingame, CA). Sections were then analyzed with the Axio Observer.A1 microscope (Carl Zeiss, Göttingen, Germany) with HXP 120 fluorescence light system.

Immunohistochemical staining: Human hippocampal paraffin slices were stained with antibodies against SESN3 (1:300; Novus Biologicals, Cambridge UK; NBP1-82717) and MAP2 (1:200; Millipore, Billerica, MA USA; MAB3418).

Quantification of cell fluorescence: Z-stacks of confocal images were generated to obtain maximum

intensity projections. Quantification of cell fluorescence intensity of SESN3 expressing cells in the conserved CA2 region of the hippocampus in both TLE patients samples (n = 7) and autopsy samples without known neurological disorders (n = 8) was carried out using ImageJ software by calculating: total cell fluorescence = integrated density – (area of selected cell x mean fluorescence of background readings). Average background was calculated based on three random regions in the vicinity of the cell count region per section. For each section a region of $167,772 \text{ px}^2 \approx 40,000 \mu\text{m}^2$ was selected and the cellular elements were counted, i.e., corresponding to approximately 20 cellular elements per section. All images were independently and blindly quantified.

REFERENCES

- 1 Tusher, V. G., Tibshirani, R. & Chu, G. Significance analysis of microarrays applied to the ionizing radiation response. *Proc Natl Acad Sci U S A* 98, 5116-5121 (2001).
- 2 Huang, D.W., Sherman, B.T. & Lempicki, R.A.. Systematic and integrative analysis of large gene lists using DAVID Bioinformatics Resources. *Nature Protoc.* 4, 44-57 (2009).
- 3 Rossin, E. J. *et al.* Proteins encoded in genomic regions associated with immune-mediated disease physically interact and suggest underlying biology. *PLoS Genetics* 7, e1001273, doi:10.1371/journal.pgen.1001273 (2011).
- 4 Li, J.Z., Bunney, B.G., Meng, F., Hagenauer, M.H. *et al.* Circadian patterns of gene expression in the human brain and disruption in major depressive disorder. *Proc Natl Acad Sci U S A* 110(24), 9950-5 (2013).
- 5 Ravasi, T., Suzuki, H., Cannistraci, C.V., *et al.* *Cell* 140, 744-753, doi: 10.1016/j.cell.2010.01.044 (2010).
- 6 Becker, A. J. *et al.* Correlated stage- and subfield-associated hippocampal gene expression patterns in experimental and human temporal lobe epilepsy. *The European journal of neuroscience* 18, 2792-2802 (2003).
- 7 Kral, T. *et al.* Preoperative evaluation for epilepsy surgery (Bonn Algorithm). *Zentralblatt fur Neurochirurgie* 63, 106-110, doi:10.1055/s-2002-35826 (2002).
- 8 Pernhorst, K. *et al.* Promoter variants determine gamma-aminobutyric acid homeostasis-related gene transcription in human epileptic hippocampi. *Journal of neuropathology and experimental neurology* 70, 1080-1088, doi:10.1097/NEN.0b013e318238b9af (2011).
- 9 Schafer, J. & Strimmer, K. An empirical Bayes approach to inferring large-scale gene association networks. *Bioinformatics* 21, 754-764, doi:bti062 [pii] 10.1093/bioinformatics/bti062 (2005).
- 10 Opgen-Rhein, R. & Strimmer, K. From correlation to causation networks: a simple approximate learning algorithm and its application to high-dimensional plant gene expression data. *BMC Syst Biol* 1, 37, doi:10.1186/1752-0509-1-37 (2007).
- 11 Efron, B. Large-scale simultaneous hypothesis testing: the choice of a null hypothesis. *J. Am. Statist. Assoc* 99, 96-104 (2004).
- 12 Dittrich, M. T., Klau, G. W., Rosenwald, A., Dandekar, T. & Muller, T. Identifying functional modules in protein-protein interaction networks: an integrated exact approach. *Bioinformatics* 24, i223-231, doi:10.1093/bioinformatics/btn161 (2008).

- 13 Beisser, D., Klau, G. W., Dandekar, T., Muller, T. & Dittrich, M. T. BioNet: an R-Package for the functional analysis of biological networks. *Bioinformatics* 26, 1129-1130, doi:10.1093/bioinformatics/btq089 (2010).
- 14 Cline, M. S. *et al.* Integration of biological networks and gene expression data using Cytoscape. *Nat Protoc* 2, 2366-2382, doi:10.1038/nprot.2007.324 (2007).
- 15 Li, M., Wang, J. & Chen, J. A fast agglomerate algorithm for mining functional modules in protein interaction networks. in *International Conference on BioMedical Engineering and Informatics*. Sanya, Hainan, China, Vol. I, pp 3-7 (2008)
- 16 Scheet, P. & Stephens, M. A fast and flexible statistical model for large-scale population genotype data: applications to inferring missing genotypes and haplotypic phase. *Am J Hum Genet* 78, 629-644, doi:10.1086/502802 (2006).
- 17 Carlson, C. S. *et al.* Selecting a maximally informative set of single-nucleotide polymorphisms for association analyses using linkage disequilibrium. *Am J Hum Genet* 74, 106-120, doi:10.1086/381000 (2004).
- 18 Mardia, K. V., Kent, J. T. & Bibby, J. M. *Multivariate Analysis*. (Academic Press, London, 1979).
- 19 Mei, H. *et al.* Principal-component-based multivariate regression for genetic association studies of metabolic syndrome components. *BMC genetics* 11, 100, doi:10.1186/1471-2156-11-100 (2010).
- 20 Bottolo, L. & Richardson, S. Evolutionary Stochastic Search for Bayesian model exploration. (2010).
- 21 Bottolo, L. *et al.* ESS++: a C++ objected-oriented algorithm for Bayesian stochastic search model exploration. *Bioinformatics* 27, 587-588, doi:10.1093/bioinformatics/btq684 (2011).
- 22 Petretto, E. *et al.* New insights into the genetic control of gene expression using a Bayesian multi-tissue approach. *PLoS Comput Biol* 6, e1000737, doi:10.1371/journal.pcbi.1000737 (2010).
- 23 Chen, W., Ghosh, D., Raghunathan, T. E. & Sargent, D. J. A false-discovery-rate-based loss framework for selection of interactions. *Statistics in medicine* 27, 2004-2021, doi:10.1002/sim.3118 (2008).
- 24 Bottolo, L. *et al.* Bayesian detection of expression quantitative trait Loci hot spots. *Genetics* 189, 1449-1459, doi:10.1534/genetics.111.131425 (2011).
- 25 Stephens, M. & Balding, D. J. Bayesian statistical methods for genetic association studies. *Nat Rev Genet* 10, 681-690, doi:10.1038/nrg2615 (2009).

- 26 Proposal for revised classification of epilepsies and epileptic syndromes. Commission on Classification and Terminology of the International League Against Epilepsy. *Epilepsia* 30, 389-399 (1989).
- 27 Berg, A. T. *et al.* Revised terminology and concepts for organization of seizures and epilepsies: report of the ILAE Commission on Classification and Terminology, 2005-2009. *Epilepsia* 51, 676-685, doi:10.1111/j.1528-1167.2010.02522.x (2010).
- 28 Patterson, N., Price, A. L. & Reich, D. Population structure and eigenanalysis. *PLoS Genet* 2, e190, doi:10.1371/journal.pgen.0020190 (2006).
- 29 Purcell, S. *et al.* PLINK: a tool set for whole-genome association and population-based linkage analyses. *Am J Hum Genet* 81, 559-575, doi:10.1086/519795 (2007).
- 30 Kasperaviciute, D. *et al.* Common genetic variation and susceptibility to partial epilepsies: a genome-wide association study. *Brain : a journal of neurology* 133, 2136-2147, doi:10.1093/brain/awq130 (2010).
- 31 Good, P. I. *Permutation, Parametric, and Bootstrap Tests of Hypotheses*. 3rd edn, (Springer, 2005).
- 32 Mazzuferi, M., Kumar, G., Rospo, C. & Kaminski, R. M. Rapid epileptogenesis in the mouse pilocarpine model: video-EEG, pharmacokinetic and histopathological characterization. *Exp Neurol* 238, 156-167, doi:10.1016/j.expneurol.2012.08.022 (2012).
- 33 Kim, D. *et al.* TopHat2: accurate alignment of transcriptomes in the presence of insertions, deletions and gene fusions. *Genome Biol* 14, R36, doi:10.1186/gb-2013-14-4-r36 (2013).
- 34 Robinson, M. D., McCarthy, D. J. & Smyth, G. K. edgeR: a Bioconductor package for differential expression analysis of digital gene expression data. *Bioinformatics* 26, 139-140, doi:10.1093/bioinformatics/btp616 (2010).
- 35 Behmoaras, J. *et al.* Genetic loci modulate macrophage activity and glomerular damage in experimental glomerulonephritis. *J Am Soc Nephrol* 21, 1136-1144, doi:10.1681/ASN.2009090968 (2010).
- 36 Seibenhener, M. L. & Wooten, M. W. Isolation and culture of hippocampal neurons from prenatal mice. *J Vis Exp*, doi:10.3791/3634 (2012).

Sestrin 3 as a regulator of a proconvulsant gene network: characterization of a rat knock out model

Paolo Roncon^{1*}, Silvia Zucchini^{1*}, Marie Soukupova¹, Giovanna Paolone¹, Marilyne Labasque¹, Anna Binaschi¹, Chiara Falcicchia¹, Tiziana Rossetti², Enrico Petretto³, Michael R Johnson⁴, Michele Simonato¹

¹ Department of Medical Sciences, Section of Pharmacology and Neuroscience Center, University of Ferrara, 44121 Ferrara, Italy;

² Medical Research Council (MRC) Clinical Sciences Centre, Imperial College London, Hammersmith Hospital, Du Cane Road, London W12 0NN, UK;

³ Duke-NUS Graduate Medical School, 8 College Road, Singapore 169857, Singapore;

⁴ Division of Brain Sciences, Imperial College London, Hammersmith Hospital Campus, Burlington Danes Building, London W12 0NN, UK;

* These authors equally contributed to this work.

Epilepsy is a serious neurological disorder that affects 1% of the world population. Several studies have implicated release of proconvulsant inflammatory molecules (i.e. interleukine 1 β) and Toll-like receptor (TLR) signaling in both epileptogenesis and seizure generation. A gene-regulatory network that contains a specialized, highly expressed transcriptional module encoding proconvulsive cytokines and TLR signaling genes has been recently identified in the hippocampus of drug-resistant epileptic patients and mice. Unsupervised computational analyses pinpointed sestrin 3 (Sesn3) as a key regulator of this proconvulsant gene network.

In vitro experiments demonstrated that Sesn3 positively regulates the module in macrophages, microglia and neurons; moreover, morpholino-mediated Sesn3 knockdown in zebrafish confirmed the regulation of the transcriptional module, and attenuated chemically induced behavioral seizures. This study aimed at expanding these finding by exploring the functional implications of Sesn3 in mammals. To this aim, Sesn3 knock out rats have been created from the Sprague-Dawley strain and their epileptic phenotype has been investigated using the pilocarpine model. Severity of epilepsy co-morbidities (cognitive impairment, anxiety,

depression) was also examined using multiple behavioral tests, including elevated plus maze, novel object recognition, open field and forced swimming. We found that *Sesn3* silencing increases the dose of pilocarpine and the time needed to enter status epilepticus (SE).

Behavioral analysis revealed that *Sesn3* KO rats are less anxious and less prone to develop depression compared to control Sprague Dawley rats. Taken together, these findings confirm that *Sesn3* may favor occurrence and/or exacerbate seizures. Moreover, the knocking down of the *Sesn3* gene in rats revealed a phenotype less prone to develop anxiety and depression.

Thus, *Sesn3* seems may be viewed as a master regulator of the expression of molecules that are involved not only in the generation of seizures, but also in epilepsy comorbidities.

1
2 **Silencing status epilepticus-induced BDNF expression with**
3 **Herpes Simplex Virus type-1 based amplicon vectors**

4
5 Chiara Falcicchia,^{1,2*} Pascal Trempat,^{1,2} Anna Binaschi,¹ Coline Perrier-
6 Biollay,² Paolo Roncon,¹ Marie Soukupova,¹ Hervé Berthommé² and Michele
7 Simonato^{1,3}
8

9 ¹ Department of Medical Science, Section of Pharmacology, Neuroscience Center, University
10 of Ferrara and National Institute of Neuroscience, Ferrara, Italy

11 ² Bioviron, Université Claude Bernard Lyon 1, Villeurbanne, France

12 ³ Laboratory of Technologies for Advanced Therapy (LTTA), Technopole of Ferrara, Ferrara,
13 Italy
14
15
16
17
18

19 * Corresponding author:

20
21 E-mail: chiara.falcicchia@unife.it (CF)
22

under second revision

23 **Abstract**

24 Brain-derived neurotrophic factor (BDNF) has been found to produce pro- but also anti-
25 epileptic effects. Thus, its validity as a therapeutic target must be verified using advanced
26 tools designed to block or to enhance its signal. The aim of this study was to develop tools to
27 silence the BDNF signal. We generated Herpes simplex virus type 1 (HSV-1) derived
28 amplicon vectors, i.e. viral particles containing a genome of 152 kb constituted of
29 concatameric repetitions of an expression cassette, enabling the expression of the gene of
30 interest in multiple copies. HSV-1 based amplicon vectors are non-pathogenic and have been
31 successfully employed in the past for gene delivery into the brain of living animals.
32 Therefore, amplicon vectors should represent a logical choice for expressing a silencing
33 cassette, which, in multiple copies, is expected to lead to an efficient knock-down of the
34 target gene expression. Here, we employed two amplicon-based BDNF silencing strategies.
35 The first, antisense, has been chosen to target and degrade the cytoplasmic mRNA pool of
36 BDNF, whereas the second, based on the convergent transcription technology, has been
37 chosen to repress transcription at the *BDNF* gene. Both these amplicon vectors proved to be
38 effective in down-regulating *BDNF* expression *in vitro*, in BDNF-expressing mesoangioblast
39 cells. However, only the antisense strategy was effective *in vivo*, after inoculation in the
40 hippocampus in a model of status epilepticus in which BDNF mRNA levels are strongly
41 increased. Interestingly, the knocking down of BDNF levels induced with BDNF-antisense
42 was sufficient to produce significant behavioral effects, in spite of the fact that it was
43 produced only in a part of a single hippocampus. In conclusion, this study demonstrates a
44 reliable effect of amplicon vectors in knocking down gene expression *in vitro* and *in vivo*.
45 Therefore, this approach may find broad applications in neurobiological studies.

46

47

48 **Keywords**

49 BDNF, gene silencing, hippocampus, epilepsy, convergent transcription, HSV-1 based

50 amplicon vectors

51

under second revision

52 Introduction

53

54 The neurotrophin brain-derived neurotrophic factor (BDNF) is widely expressed in the brain,
55 where it exerts a key role in neuronal survival, differentiation, and plasticity [1,2]. BDNF is
56 therefore viewed as a promising therapeutic target for central nervous system disorders, for
57 example in the transformation of a normal brain in epileptic, a phenomenon in which cell
58 death, neurogenesis and morphological and functional changes are thought to be involved
59 [3,4]. However, an important issue that has limited development of therapies that target the
60 BDNF system has been the difficulty in delivering it to a specific and restricted brain region
61 and thereby locally modulating its levels. Here, we present novel tools to pursue this aim:
62 amplicon vectors derived from Herpes simplex virus type 1 (HSV-1) capable to down-
63 regulate *BDNF* expression *in vitro* and *in vivo*.

64 Amplicon vectors are HSV-1 particles identical to wild type HSV-1 from the
65 structural and host-range points of view, but which carry a concatemeric form of a DNA
66 plasmid, named amplicon plasmid, instead of the 152 Kb viral genome. HSV-1 amplicon
67 vectors hold considerable promise as gene-transfer vehicles because of their very high
68 capacity to host foreign DNA with high number of repeats of the transgene [5], a feature that,
69 in principle, makes them particularly suited to efficiently knock-down a target gene.

70 Two silencing strategies have been pursued in this study. The first, called “antisense”,
71 has been chosen to target and degrade the cytoplasmic messenger RNA (mRNA) pool of
72 BDNF via an RNA interference (RNAi) mechanism [6]. In RNAi, antisense RNA molecules
73 inhibit gene expression by causing the destruction of complementary mRNA molecules in a
74 sequence-specific manner [7]. A natural antisense BDNF mRNA has been recently identified
75 in the mouse brain [8].

76 The second strategy, based on the “convergent transcription technology” [9],
77 represses the *BDNF* gene through chromatin remodeling. The convergent transcription
78 approach is based on co-expression of the sense and antisense RNA strands from independent
79 expression cassettes or a divergent cassette in which a full-length complementary DNA
80 (cDNA) sequence is positioned between two identical promoters [10,11], such that
81 independent transcription from each promoter produces a pool of sense and antisense RNAs
82 capable of forming long dsRNAs and undergoing processing to the effector siRNAs [9]. The
83 use of convergent transcription from opposing promoters to induce gene silencing has been
84 reported in trypanosomes and *Drosophila* [12,13], as well as in yeast and mammalian cells
85 [14]. It has been predicted that the expression of up to 8% of human genes may be influenced
86 by antisense RNA or antisense transcription [15,16], suggesting that convergent transcription
87 does occur with high frequency in the human genome [9].

88 In the present study, the silencing effect of amplicon vectors has been assessed by
89 examining their efficiency in down-regulating BDNF levels *in vitro*, in BDNF-expressing
90 mesoangioblast cells, and *in vivo*, using a rat model of status epilepticus in which BDNF
91 mRNA levels are strongly increased in the hippocampus.

92
93

94 **Materials and Methods**

95

96 **Amplicon vectors**

97 **Amplicon plasmids.** For construction of the plasmid containing antisense BDNF
98 (plasmid pAM2-BDNF-antisense-GFP), the XbaI-BamHI fragment containing the
99 cytomegalovirus (CMV) promoter was cut from the pMA-RQ-CMV plasmid and cloned in

100 the XbaI-BamHI sites of pAM-GFP, a plasmid expressing the green fluorescent protein
101 (GFP) under control of the IE4/5 promoter, to obtain the pAM-GFP-CMV plasmid. The
102 BDNF fragment was cut from the plasmid pBSK-BDNF using EcoRI blunted-end sites by
103 Klenow and cloned in the polylinker NheI blunted-end sites of pAM2-GFP-CMV, flanked by
104 the CMV promoter and a Simian Virus 40 (SV40) polyadenylation signal (Fig 1A). To
105 discriminate between cloning in sense and antisense orientation, 12 starter cultures, obtained
106 after transformation of *E. Coli* high efficiency transformation competent bacteria, were
107 digested with ScaI, PvuII and PstI, and run on agarose gel electrophoresis.

108 For construction of the BDNF convergent transcription plasmid (pAM-CT-BDNF-
109 GFP), a new CMV fragment (HindIII/PmeI) was subcloned into the HindIII/EcoRV site of
110 pAM-GFP-CMV, in the opposite direction compared to the other CMV promoter, obtaining
111 the pAM-CT-GFP plasmid. The pAM-CT-BDNF-GFP plasmid was then obtained by cloning
112 the EcoRI blunted-end sites by Klenow BDNF fragment of pBSK-BDNF plasmid in the
113 EcoRV-digested pAM-CT-GFP plasmid, in order to put the BDNF sequence between the two
114 CMV promoters (Fig 1B). The pAM2-GFP plasmid was used as control amplicon (Fig 1C).

115 **Cell lines and virus.** The cell lines employed in this study were the following:
116 genetically modified mesoangioblasts producing BDNF and GFP (MABs-BDNF; [17]),
117 Gli36 cells (a human glioblastoma cell line), Vero cells (African green monkey kidney
118 epithelial cell line), trans-complementing Vero cells for amplification and purification of
119 HSV-1 based amplicon vectors. All cell lines were propagated in Dulbecco's minimum
120 essential medium (DMEM, Lonza, Switzerland) supplemented with 10% fetal bovine serum
121 (FBS, Invitrogen Gibco, USA), 100 U/ml penicillin and 100 mg/ml streptomycin
122 (Invitrogen). Cells were maintained at 37°C in a humidified incubator containing 5% CO₂.
123 All cell lines were provided by Bioviron (France).

124 **Amplicon production.** Amplicon vectors were produced by transfecting 10 µg of

125 each amplicon plasmid (pAM2-BDNF-antisense-GFP, pAM-CT-BDNF-GFP and pAM2-
126 GFP) into trans-complementing-producing-Vero cells using the jetPRIME reagent (Polyplus-
127 transfection, France). Cells were superinfected the following day with the LaLΔJ helper virus
128 at a multiplicity of infection (MOI) of 0.5 plaque forming units (pfu)/cell in medium M199
129 (Gibco) supplemented with 1% FBS and 1% penicillin/streptomycin. Three days later, cells
130 were harvested and amplicon viral particles were extracted by several rounds of freeze/thaw
131 and sonication. To calculate purity of the production, amplicon and helper particles were
132 titrated to obtain transduction units (tu)/ml (using cell number counting assay on Gli36 cells)
133 and pfu/ml (on trans-complementing Vero cells). Several successive rounds of infections and
134 productions were performed to obtain high quantity of amplicon particles and a final
135 infection-production step was performed on a trans-complementing-purifying-Vero cell to
136 obtain a final high purity working stock of amplicon vectors over the helper. The degree of
137 purity was greater than 99% for all amplicon vectors. All virus stocks were checked for no
138 revertant helper viruses on Vero cells.

139 **Cell infection.** Confluent MABs-BDNF cells seeded in 6-well plates were infected
140 with the GFP-control, BDNF-antisense or BDNF-CT amplicon at MOI 5, and maintained at
141 34°C in DMEM with 10% FBS for 24, 48, 72 or 96 h. At each time point, cells were washed
142 twice in PBS, then scraped and resuspended in 50 µl of lysis buffer (50 mM Tris-HCL pH 8,
143 150 mM NaCl, 1% NP-40) containing a protease inhibitor cocktail (Roche, Germany). Lysate
144 was used for western blot analysis. The protein content of the lysates was evaluated by the
145 Bradford method using the Bio-Rad protein assay kit (Bio-Rad Laboratories, CA, USA).

146

147 **Animals**

148 Male Sprague-Dawley rats (240-260 g; Harlan, Italy) were used for *in vivo* experiments.
149 They were housed under standard conditions: constant temperature (22-24°C) and humidity

150 (55-65%), 12 h light/dark cycle, free access to food and water. Experiments involving
151 animals were conducted in accordance with European Community (EU Directive
152 2010/63/EU), national and local laws and policies. The IACUC of the University of Ferrara
153 approved this research, that was authorized by the Italian Ministry for Health (D.M.
154 246/2012-B). All efforts were made to minimize animal suffering.

155 **Amplicon infusion.** Under ketamine and xylazine (43 and 7 mg/kg, intra-
156 peritoneal, i.p.) anesthesia, a glass needle connected to a perfusion pump was implanted in
157 the right dorsal hippocampus using a stereotaxic apparatus for small animals, with the
158 following coordinates: A -1.7; L -1.5; D +3.7 [18]. Anesthesia was then maintained using
159 isoflurane (1.4% in air, 1.2 ml/min). Two different doses of amplicon vector, 1×10^4 tu and
160 5×10^5 tu, were injected in a volume of 1 μ l at a flow rate of 0.1 μ l/min. Amplicon vectors
161 (GFP-control, BDNF-antisense and BDNF-CT) were injected 5 days before pilocarpine
162 administration.

163 **Status Epilepticus.** Pilocarpine was administered i.p. (340 mg/kg), 30 min after a
164 single subcutaneous injection of methyl-scopolamine (1 mg/kg, to prevent peripheral effects
165 of pilocarpine), and the rats' behavior was monitored for several hours thereafter, using the
166 scale of Racine [19]: 1, chewing or mouth and facial movements; 2, head nodding; 3,
167 forelimb clonus; 4, generalized seizures with rearing; 5, generalized seizures with rearing and
168 falling. Within the first hour after injection, all animals developed seizures evolving into
169 recurrent generalized (stage 4 and higher) convulsions (status epilepticus, SE). SE was
170 interrupted 3 h after onset by administration of diazepam (10 mg/kg i.p.). Even if it is known
171 that long durations of pilocarpine SE lead to increased damage [20] and may even lead to
172 lower degrees of BDNF induction [21], we chose this experimental conditions because, in our
173 previous studies, they were associated with strong increases in BDNF levels in the
174 hippocampus [22,23], with peak of mRNA levels at 3 h and peak of BDNF protein at 6 h

175 after SE. Rats were therefore killed by decapitation under isofluorane anesthesia at three
176 different time points: 3 h, 6 h and 24 h after onset of SE. Brains were rapidly frozen in 2-
177 methylbutane.

178

179 **Histology**

180 Brains were removed, immersed in 10% formalin for 48 h and then paraffin embedded. Serial
181 sections of 6 µm were cut with a Microtome (Leica RM2125RT, Germany). In all
182 experiments, adjacent sections were used for different staining procedures.

183 **Immunohistochemistry.** Sections were dewaxed (2 washes in xylol, 10 min
184 each; 5 min in 100% ethanol, 5 min in 95% ethanol, 5 min in 80% ethanol) and re-hydrated
185 in distilled water for 5 min. All antigens were unmasked using a commercially available kit
186 (Unmasker, Diapath), according to the manufacturer's instructions. After washing in
187 phosphate buffered saline (PBS), sections were incubated with Triton x-100 (Sigma; 0.3% in
188 PBS 1×, room temperature, 10 min), washed twice in PBS 1×, and incubated with 5% bovine
189 serum albumin (BSA) and 5% serum of the species in which the secondary antibody was
190 produced, for 30 min. They were incubated overnight at 4°C in humid atmosphere with a
191 primary antibody specific for different cellular markers: glial fibrillary acid protein (GFAP;
192 mouse polyclonal, Sigma) 1:100; ionized calcium binding adaptor molecule 1 (IBA-1; rabbit
193 monoclonal, AbCam MA, USA) 1:200; GFP (rabbit polyclonal, Santa Cruz, Texas) 1:50.
194 After 5-min rinses in PBS, sections were incubated with Triton (as above, 30 min), washed in
195 PBS and incubated with a goat anti-mouse Alexa 594 secondary antibody (1:250, Invitrogen)
196 for mouse primary antibodies, or with a goat anti-rabbit, Alexa 488 secondary antibody
197 (1:250; Invitrogen) for rabbit primary antibodies, at room temperature for 3.5 hours.
198 NeuroTrace (1:150) was included in the secondary antibody incubation. After staining,
199 sections were washed in PBS, counterstained with 0.0001% 4'-6-diamidino-2-phenylindole

200 (DAPI) for 15 min, and washed again. Coverslips were mounted using anti fading, water
201 based Gel/Mount (Sigma).

202 For interferon-beta ($\square\square\square$ - β)immunohistochemistry, we employed the Dako
203 Cytomation EnVision[®] + Dual Link System-HRP (DAB+) kit. Adjacent sections were
204 unmasked as described above and, after washing in PBS, were incubated for 10 min at room
205 temperature with Endogenous Enzyme Block to quench endogenous peroxidase activity.
206 Subsequently, they were incubated overnight at 4°C in humid atmosphere with the primary
207 antibody (rabbit polyclonal anti-IFN- β , 1:50 dilution, MyBioSource, CA, USA). After 5-min
208 rinses in PBS, sections were incubated for 30 min with Labeled Polymer-HRP [Dako
209 Cytomation EnVision[®] + Dual Link System-HRP (DAB+)]. Staining was completed by a 5
210 min incubation with 3,3'-diaminobenzidine (DAB) substrated-chromogen, resulting in a
211 brown staining of the antigen-antibody complex. Finally, coverslips were mounted using a
212 water-based mounting medium (Gel Mount[™], Sigma).

213

214 **Quantitative analysis**

215 **Tissue sample extraction.** The left and right dorsal hippocampi were dissected
216 by cutting the brain coronally using a metallic matrix (Zivic Instruments, PA, USA) up to a
217 level corresponding to plate 38-57 of the rat brain atlas [18] and processed to extract total
218 RNA, genomic DNA and proteins using the RNeasy Lipid Tissue Mini kit (Qiagen,
219 Germany). RNA extraction was performed following the manufacturer instructions. Proteins
220 and genomic DNA were isolated after RNA extraction using the phenol phase. Briefly,
221 genomic DNA was precipitated from the phenol phase with ethanol and pellets were washed
222 with sodium citrate ethanol solution and stored in 75% ethanol at -80°C. After DNA
223 precipitation, proteins were isolated from the supernatant ethanol-phenol by isopropanol
224 precipitation. Proteins were then washed several times with 0.3 M guanidine HCl-95%

225 ethanol solution before being air-dried and resuspended in a rehydration buffer (62 mM Tris-
226 HCl pH 6.8; 2% SDS; 10% glycerol; 12.5 mM EDTA; 50 mM DTT; β -mercaptoethanol;
227 protease inhibitor cocktail) by a 20 min incubation at 95°C and 3 rounds of 30 sec sonication.
228 The protein content of the lysates was evaluated by the Bradford method using the Bio-Rad
229 protein assay kit (Bio-Rad Laboratories).

230 **Western Blot analysis and quantification.** Infected MABs and dissected
231 dorsal hippocampal extracts, corresponding to 20 and 30 μ g total proteins respectively, were
232 analyzed by Western blotting. Proteins were quantified using the Bradford method using the
233 Bio-Rad protein assay kit (Bio-Rad Laboratories, CA, USA) and a Bio-spectrometer
234 (Eppendorf, Germany). Each sample was diluted in sodium dodecyl sulfate (SDS)-gel
235 loading buffer, boiled for 10 min and centrifuged before loading. Samples were then
236 electrophoretically separated onto a 12% SDS-polyacrylamide gel and transferred to
237 nitrocellulose membranes. After blocking in a buffer (PBS-Tween20) containing 5% dried
238 milk, membranes were incubated with the primary antibody in a buffer containing 2.5% dried
239 milk overnight at 4°C. After three washings, incubations were performed with the secondary
240 antibody in buffer/dried milk at room temperature for 1 h. The pro-BDNF protein was
241 revealed using a rabbit anti-proBDNF monoclonal antibody (AbCam, dilution 1:1000) that is
242 specific for pro-BDNF and does not detect mature BDNF; GFP using a mouse anti-GFP
243 monoclonal antibody (Roche; 1:1000); actin using a rabbit anti-actin monoclonal antibody
244 (Sigma, MO, USA; 1:1000). Mouse monoclonal antibodies were revealed using a goat anti-
245 mouse horseradish peroxidase (HRP)-conjugated secondary antibody (Dako, Denmark;
246 dilution 1:1000) and rabbit monoclonal antibodies by a swine anti-rabbit HRP-conjugated
247 secondary antibody (Dako; dilution 1:3000). The immunocomplexes were detected using the
248 ECL Western blot detection kit (GE Healthcare, NJ, USA) and ChemiDoc XRS (Bio-rad)
249 for electronic blot pictures. Quantification was performed using the Image Lab software (Bio-

250 rad).

251 **Real-time quantitative polymerase chain reaction (qRT-PCR).** RNA
252 concentration was determined using a Bio-spectrometer (Eppendorf, Germany). Strand-
253 specific cDNA was synthesized using the cDNA first Strand Superscript III kit (Invitrogen,
254 USA) according to the manufacturer's instructions, with minor modifications. Following
255 incubation at 65°C for 5 min in ice, 500 ng total RNA from the tissue samples were reverse-
256 transcribed with specific BDNF-antisense (AS-RT) and GAPDH primers (GAPDH-RT) at a
257 final concentration of 0.1 µM, using the SuperScript III reverse transcriptase, at 55°C for 50
258 min. The AS-RT primer was designed to be specific to the amplicon sequence of the BDNF
259 antisense mRNA and not to the endogenous BDNF or to the natural antisense BDNF
260 sequence (Fig. 2). The reaction was terminated by inactivation of the SuperScript III reverse
261 transcriptase at 85°C for 5 min. For removing the excess of RT primers, 10 U of exonuclease
262 I was added and the solution was incubated at 37°C for 30 min, then at 80°C for 30 min for
263 inactivation. Next, RNase H was added and finally, following manufacturer's instructions,
264 each reaction was diluted to a final volume of 200 µL and cDNA stored at -20°C until use.
265 Several controls were used, including reactions lacking RNA, reactions with RNA but
266 lacking the reverse transcriptase enzyme and reactions lacking primers, to assess self-priming
267 from secondary structure or genomic DNA contamination. The primers we used are listed in
268 Table 1 and were designed using the Multiplex2 Software (<http://bioinfo.ut.ee/multiplex/>).

269

270 **Table 1. Primers and sequences.**

	Primers	Sequences
Reverse Transcription	AS-RT	AATAGCATCACAAATTTACAA
	GAPDH-RT	TGGTCCAGGGTTTCTTACTC
qPCR	qPCR AS For	AATTCACGCGTGGTACCTCTA

	qPCR AS Rev	CACTGCATTCTAGTTGTGGTTTG
	qPCR ratGAPDH For	GGGTGTGAACCACGAGAAAT
	qPCR ratGAPDH Rev	ACTGTGGTCATGAGCCCTTC

271

272

273

274

275

276

277

278

279

280

281

282

283

284

285

286

287

288

289

290

291

292

BDNF-antisense was assessed by qRT-PCR on a Bio-Rad CFX96 Real-Time PCR Detection System (Bio-rad) using SSoAdvanced Universal SYBR Green Supermix (Bio-Rad Laboratories). Primers were designed using the Primer3 Plus Software (<http://www.bioinformatics.nl/cgi-bin/primer3plus/primer3plus.cgi>) according to Bio-Rad instructions. Their sequences are described in Table 1. The BDNF antisense qPCR primers amplify specifically the amplicon sequence of the antisense BDNF mRNA. Two μ L of the first-strand cDNA sample or reverse transcription controls described above were used in the reaction, and water was used for negative control reaction. Each qPCR experiment was performed in triplicate for both controls and test samples. The qPCR reactions contained the SsoAdvanced universal SYBR Green supermix, plus 250 nM or 500 nM of forward and reverse primers for GAPDH or BDNF-antisense, respectively. The qPCR conditions for all targets were as follows: 95°C for 30 s, then 95°C for 10 s and 64°C for 20 s repeated 40 times. At the end of the run, the Melting curve analysis was 60°C to 95°C with 0.5°C increment and 2-5 s per step. Data analyses were done with CFX Manager (Bio-Rad) and real-time data quantification was achieved using the Δ Ct values using GAPDH as reference gene. Each RNA sample was run in a separate assay: 14 samples of dorsal hippocampi injected with the BDNF-antisense-GFP amplicon vector, 15 injected with the control vector and 3 not treated at all (naïve).

Statistical analysis

Statistical comparisons of the data were performed using ANOVA and *post-hoc* the

293 Dunnett's test for *in vitro* validation of amplicon vectors, to compare pro-BDNF expression
294 in the right and left hippocampus, and to determine whether the time to enter convulsive SE
295 differed significantly between rats injected with the different amplicon vectors.

296

297

298 **Results**

299

300 **HSV-1 amplicon plasmid generation**

301 We developed two silencing strategies to down-regulate BDNF protein level. The antisense
302 strategy targets and degrades the cytoplasmic mRNA pool of BDNF. For this purpose, we
303 generated an amplicon plasmid, pAM2-BDNF-antisense-GFP, that expresses both the mRNA
304 for GFP and the synthetic antisense rat BDNF mRNA (Fig 1A). The second strategy, based
305 on the Convergent Transcription (CT) technology, represses the *BDNF* gene at the level of
306 transcription. For this purpose, we generated a plasmid (pAM2-CT-BDNF-GFP) in which the
307 BDNF cDNA is inserted between two cytomegalovirus (CMV) promoters oriented in
308 opposing directions (Fig 1B), such that the resulting convergent transcription could elicit
309 down-regulation of the *BDNF* gene transcription through chromatin remodeling associated
310 with epigenetic silencing marks [14]. We also generated a control amplicon plasmid and
311 vector (named GFP amplicon vector), which possesses only the GFP reporter cassette (Fig
312 1C).

313 Following the cloning steps, large purified stocks of 3 corresponding amplicon
314 vectors were produced. The titer of each stock was 9.4×10^8 t.u./ml, 1.05×10^9 t.u./ml and
315 1.05×10^7 t.u./ml, respectively for BDNF-antisense-GFP, BDNF-CT-GFP and control GFP
316 amplicon vectors. The BDNF-antisense-GFP and BDNF-CT-GFP amplicon vectors contain

317 more than 20 copies of the silencing cassette. As described, we produced each amplicon
318 vector with a GFP expression cassette for monitoring the infection in cells and animals.

319

320

321 ***In vitro* validation**

322 The next step was to evaluate the effect of each amplicon vector against BDNF *in vitro*. In
323 order to study efficiency to repress BDNF expression, we infected BDNF-expressing
324 mesoangioblast (MABs) cells with BDNF-antisense-GFP or BDNF-CT-GFP amplicon
325 vectors at a multiplicity of infection (MOI) of 5. Control conditions were MAB cells infected
326 with the control GFP amplicon vector at MOI 5 or not infected. The infection of cells with
327 BDNF-antisense-GFP or BDNF-CT-GFP amplicon vectors was confirmed by a strong GFP
328 fluorescence, as shown in Figs 2A and 2E. As an outcome measure to assess effectiveness of
329 the vectors, we examined levels of the precursor protein for BDNF, i.e. pro-BDNF, for 96
330 hours after infection using western blot analysis. MAB cells infected with the BDNF-
331 antisense-GFP amplicon vector displayed a strong reduction of pro-BDNF levels beginning
332 as soon as 24 h post infection as compared with uninfected cells or cells infected with the
333 control GFP amplicon vector. The decrease of pro-BDNF protein levels was even more
334 prominent at the following time-points, and became essentially complete 96 h after infection
335 (Fig 2D). These data indicate a fast and very efficient silencing activity for the BDNF-
336 antisense-GFP amplicon vector *in vitro*.

337 The same experiment was performed using the BDNF-CT-GFP amplicon vector and,
338 again, we observed a nearly complete cancellation of pro-BDNF expression from MAB cells
339 at 96 h after the injection (Fig 2G). However, the time-course differed in that the decline in
340 pro-BDNF protein levels occurred more slowly than with BDNF-antisense-GFP (Fig 2H).

341 These results indicate that, *in vitro*, both amplicon vectors, BDNF-antisense-GFP and BDNF-

342 CT-GFP, produce a highly efficient knock-down of pro-BDNF levels. Thus, both vectors
343 were elected for *in vivo* testing.

344

345

346 ***In vivo* validation**

347 We first explored the toxicity of the amplicon vectors after direct injection in the rat
348 hippocampus. To this aim, we injected 5×10^5 t.u. of either vector in a volume of 1 μ l in the
349 right hippocampus dentate gyrus area of naïve rats and, 5 days after injection, examined
350 gliosis, microcytosis and neuronal loss using GFAP, IBA-1 immunofluorescence and
351 NeuroTrace staining, respectively. Administration of the BDNF-antisense-GFP or of the
352 BDNF-CT-GFP amplicon vectors did not alter the morphology of the hippocampus (Fig 3
353 shows the dentate gyrus; S1 Fig shows the whole hippocampus). The density of GFAP-
354 positive cells in the injected hippocampus was similar to that of the non-injected,
355 contralateral one, i.e. there was no indication of reactive astrocytosis (Fig 3 and S1 Fig).
356 Similar to GFAP cells, the density of IBA-1 positive cells was comparable in both the
357 ipsilateral and the contralateral hippocampus, indicating absence of reactive microgliosis (Fig
358 3 and S1 Fig). Finally, neuronal density, as measured using the NeuroTrace staining, was also
359 not altered after injection of either amplicon vector (Fig 3 and S1 Fig). Taken together, these
360 data suggest that treatment with amplicon vectors do not induce an overt damage when
361 directly injected in the brain.

362 We also evaluated the interferon response by using IFN- β immunohistochemistry.
363 IFN- β positive cells were detected at the site of injection of BDNF-antisense-GFP, and the
364 majority of these cells appeared to be microglial based on IBA-1 immunofluorescence (S2A
365 Fig). This finding is in line with previous literature reports [24,25]. IFN- β positive cells were
366 also detected after injection of the BDNF-CT-GFP amplicon vector and, interestingly, the

367 IFN response seemed greater than with BDNF-antisense-GFP (S2B Fig). This finding may
368 be due to higher levels of double stranded RNA generated with the CT technology, as
369 compared with the antisense approach.

370 Next, we tested the biological efficiency for down-regulation of BDNF protein levels.
371 To this aim, we decided to employ the pilocarpine model. Intra-peritoneal injection of
372 pilocarpine in rodents provokes generalized seizures leading to a status epilepticus (SE),
373 which drives a massive increase in BDNF levels in the hippocampus [26,22]. To test the
374 efficiency of amplicon vectors, we injected them in the right dorsal hippocampus, 5 days
375 before pilocarpine administration, and animals were then killed at 3 different time points: 3 h
376 (peak of pilocarpine-induced increase in BDNF mRNA levels; [27,26]), 6 h (peak of
377 pilocarpine-induced increase in BDNF protein levels; [28,22]) and 24 h after onset of SE.
378 Rats were injected either with the control GFP, the BDNF-antisense-GFP or the BDNF-CT-
379 GFP vector at 2 doses, 1×10^4 or 5×10^5 t.u., i.e. the high dose that did not cause overt toxicity
380 (see above) and a >1 log lower dose. Amplicon vector injections into the dorsal hippocampus
381 produced expression of GFP in infected cells (Fig 4A for BDNF-antisense-GFP) at the site of
382 injection, whereas a negligible number of positive cells were observed contralateral to
383 injection under these experimental conditions. We therefore decided to use the contralateral
384 dorsal hippocampus as an internal control. First, we quantified synthetic antisense BDNF
385 mRNA levels in the ipsilateral and contralateral hippocampi injected with the BDNF-
386 antisense-GFP amplicon vector, using the real-time quantitative polymerase chain reaction
387 (qRT-PCR) method and primers specific to the amplicon cassette for the synthetic BDNF
388 antisense mRNA but absent in the endogenous sense and natural antisense BDNF mRNA (S3
389 Fig). Amplicon-derived synthetic antisense BDNF mRNA was detected in dorsal hippocampi
390 injected with the BDNF-antisense-GFP amplicon vector (mean ΔCT 1.4 ± 0.7 ; $n=14$), but not
391 in the contralateral, non-injected side (no detectable signal). In addition, the synthetic

392 antisense BDNF mRNA was neither detectable in animals injected with the control vector
393 (n=15) nor in naïve animals (n=3).

394 Pro-BDNF expression was then measured by western blot in the hippocampus at 3
395 different time points after SE, and the signal was normalized to α -actin before calculating the
396 ratio between the ipsilateral (right) and contralateral (left) hippocampus. The control GFP
397 amplicon vector did not produce any effect, whereas the low dose (1×10^4 t.u.) of the BDNF-
398 antisense-GFP amplicon vector exhibited a robust reduction of pro-BDNF protein levels at all
399 time points (Fig 4B). This effect may be dose-dependent, because the high dose led to a
400 greater (even if not significantly greater) effect. Different from the antisense strategy, only a
401 small, non-significant reduction (about 10%) in pro-BDNF protein levels was observed in
402 low (1×10^4 t.u.) or high (5×10^5 t.u.) dose BDNF-CT-GFP injected hippocampi (low dose
403 effect at 3 h after SE shown in S4 Fig). Thus, the BDNF-CT-GFP amplicon vector cannot
404 induce sufficiently robust and/or prolonged heterochromatin changes to prevent SE-related
405 *BDNF* transactivation *in vivo*, whereas the BDNF-antisense amplicon vector proves effective
406 in knocking down efficiently pro-BDNF protein levels.

407 The model system we employed for analysis of *BDNF* knock down permits an initial
408 evaluation of the behavioral implications. Knocking down *BDNF* overexpression only in a
409 part of a single hippocampus cannot be expected to produce robust behavioral effects in a
410 model in which a pro-convulsant agent is administered systemically. However, we observed
411 that animals treated with BDNF-antisense-GFP entered convulsive SE later than those treated
412 with the control GFP amplicon vector (Fig 5A). Moreover, whereas the infusion of both
413 BDNF-antisense-GFP and BDNF-CT-GFP amplicon vectors per se did not produce overt
414 signs of behavioral toxicity, because all animals were apparently well after the surgery and in
415 the following days, the percentage of animals that died after pilocarpine administration was
416 higher in the high dose BDNF-antisense group (Fig 5B). Thus, even knocking down *BDNF*

417 expression in a portion of a single hippocampus seems sufficient to elicit significant
418 behavioral effects.

419

420

421 **Discussion**

422

423 In this study, we generated two types of amplicon vectors to locally knock down the levels of
424 BDNF: a classical antisense approach and an approach based on convergent transcription.
425 The latter technology was used for the first time in combination with a viral vector, both *in*
426 *vitro* and *in vivo*. Whereas both approaches proved highly efficient *in vitro* with a nearly
427 complete knock down of BDNF protein, only the former (antisense) provided robust results
428 in the *in vivo* settings of SE-induced *BDNF* overexpression in the hippocampus.

429 HSV-1-based amplicon particles were generated following a recently described
430 method that produces relatively high titers of vector stocks with reduced amounts of helper
431 virus [29]. Although this helper virus is completely defective, cannot replicate in cells nor it
432 can disseminate in organisms, it was important to highly purify the amplicon vectors so to
433 prevent all potential residual cytotoxicity. Here, we produced amplicon vectors with very low
434 helper contamination (less than 1%) and provided evidence that these vectors were not
435 cytotoxic and produced no overt cell damage when injected *in vivo*, although subtle apoptotic
436 cell death cannot be ruled out. Other advantages of the amplicon approach are also
437 significant. In particular, worth of note is the fact that the amplicon genomes are free of
438 HSV-1 genes and replication functions, offering the opportunity to package very large
439 transgenic sequences: it is thus possible to transduce more than 110 kb of foreign DNA in a
440 single particle [30]. Since this amount of space (152 kbp total) must all be filled to produce
441 stable particles, small transgenes are repeated in concatamers, with a number of repeats that

442 will depend on the size of the original amplicon plasmid [5,31]. In the present study, the
443 produced BDNF-antisense-GFP and BDNF-CT-GFP amplicon vectors contained more than
444 20 copies of the BDNF silencing cassette and therefore were expected to ensure a particularly
445 efficient knock down of the protein of interest.

446 HSV-1 based amplicon vectors also share many useful features of the HSV-1 parent
447 virus [32], like the ability to infect a broad range of dividing and non-dividing host cells,
448 including neurons. HSV-1 based amplicon vectors allow efficient infection of many neuronal
449 types, with transgene expression over an extended period of time without demonstrable side
450 effects [33].

451 The two strategies for knocking down *BDNF* gene expression, the classical antisense
452 strategy and the convergent transcription strategy, are conceptually different. The former is
453 based on the technique of RNA interference (RNAi) that was first discovered in
454 *Caenorhabditis elegans* [6]. RNAi is a gene silencing mechanism in which a double-stranded
455 RNA (dsRNA) molecule is generated that directs the specific degradation of the
456 corresponding target mRNA [34]. The BDNF-antisense-GFP amplicon targets and degrades
457 the cytoplasmic mRNA pool of BDNF through the mechanism of RNA interference:
458 expression of the transgene leads to formation of sense RNA-RNA hybrids in the cytosol and
459 thereby degrades and/or prevents translation of pro-BDNF mRNA. The second strategy that
460 we tested is based on the convergent transcription (CT) technology [9] that acts through
461 nuclear transcriptional gene silencing. The CT technology seemed particularly attractive
462 since it has been reported to induce locally restricted heterochromatin spreading at the target
463 gene and a silencing with long-lasting effects compared to the transient siRNA or shRNA
464 methods [14]. The *in vitro* experiments demonstrated a reliable and very strong effect of both
465 amplicon vectors in knocking down pro-BDNF levels and, therefore, both were elected for *in*

466 *vivo* studies. Noteworthy, the kinetics of BDNF reduction seemed slower with the CT
467 compared with the antisense strategy.

468 To study the effects of amplicon *in vivo*, we decided to employ a status epilepticus
469 model. Epileptogenic stimuli are known to affect the expression of BDNF transcripts in the
470 hippocampus [35,23]. Under the experimental conditions employed in this study, pilocarpine
471 leads to increased BDNF mRNA and protein levels peaking respectively 3 and 6 h after onset
472 of status epilepticus [22,28]. It is thought that increased BDNF levels play a role in the
473 transformation of a normal brain in epileptic, i.e. in a brain that can spontaneously generate
474 seizures. Indeed, spontaneous seizures begin to occur a few days after pilocarpine status
475 epilepticus, and this latency period is associated with plastic changes in the epileptogenic
476 area, including increased neurogenesis, cell death, plastic modifications of synaptic contacts
477 [36]. BDNF exerts relevant effects upon all of these phenomena. However, it is still unclear
478 what the implications of its increased biosynthesis could be. Strategies to down-regulate the
479 BDNF signal have been reported by many to retard epileptogenesis [37-40], and bath-applied
480 BDNF exacerbates seizure activity in the epileptic hippocampus *in vitro* [41,42]. In contrast,
481 the combined supplementation of BDNF and fibroblast growth factor 2 (FGF-2) has been
482 reported to attenuate cellular alterations associated with epileptogenesis and to highly
483 significantly reduce the frequency and severity of spontaneous recurrent seizures [43-45]. To
484 dissect out these mechanisms there is a need to develop tools to locally modulate the BDNF
485 signal *in vivo*, in particular to block it.

486 Therefore, we decided to test the ability of our vectors to down-regulate BDNF expression in
487 the pilocarpine model system. First, in keeping with previous reports [33], we found that *in*
488 *vivo* injection of amplicon vectors did not cause obvious toxic effects (cell death) nor
489 significant activation of astrocytes or microglia. Second, and more important, we found that
490 the silencing activity mediated by the BDNF-antisense-GFP amplicon vector was highly

491 significant, even at relatively low doses, whereas the BDNF-CT-GFP amplicon vector did not
492 produce significant reductions in pro-BDNF levels. Why the efficiency of *in vivo* silencing
493 was so different between the two strategies, in spite of the fact that both were equally
494 effective *in vitro*, is difficult to understand. One hypothesis could be that CT cannot induce
495 sufficiently strong and/or prolonged heterochromatin changes on the genome to prevent
496 pilocarpine-induced transactivation of the *BDNF* gene. On the contrary, antisense RNAi-
497 based mechanisms would be more efficient and rapid at degrading a pool of cytoplasmic
498 BDNF mRNA, thus leading to a stronger and a more prolonged effect on BDNF synthesis.

499 Importantly, the knock-down of BDNF levels induced with BDNF-antisense-GFP
500 was sufficient to produce significant behavioral effects, in spite of the fact that it was
501 produced in a part of a single hippocampus and not in the entire epileptogenic area.
502 Moreover, the kind of behavioral results that were obtained are also worth noting, in that they
503 reflect the double-edge pattern of BDNF effects in epileptogenesis. On one hand, consistent
504 with the pro-epileptic effects of BDNF [37-40] we observed an increased latency to onset of
505 status epilepticus in BDNF-antisense-GFP-injected animals. On the other hand, consistent
506 with the neuroprotective role of BDNF [45] we observed an increased mortality of animals
507 injected with BDNF-antisense-GFP. These initial data must be verified and extended using
508 multiple, bilateral injections ensuring a robust and widespread knock down of *BDNF* gene
509 expression in the epileptogenic region.

510 In conclusion, this study demonstrates a reliable effect of amplicon vectors in
511 knocking down gene expression. At variance with the CT strategy, which is effective only *in*
512 *vitro*, the BDNF-antisense-GFP amplicon vector proves effective both *in vitro* and *in vivo*,
513 knocking down efficiently BDNF protein levels in the injected hippocampus at different time
514 points. Therefore, the antisense strategy seems a better choice for silencing BDNF expression
515 *in vivo*, at least in our model. This is further supported by the observation that even knocking

516 down BDNF expression in a portion of a single hippocampus is sufficient to elicit significant
517 behavioral effects. Taken together, these data illustrate the broad potential of HSV-1 based
518 amplicon vectors as gene transfer tools for effectively silencing gene expression.

519

520

521 **Acknowledgements**

522 This work has been supported by a grant from the European Community [FP7-PEOPLE-
523 2011-IAPP project 285827 (EPIXCHANGE)] to MS and HB.

524

under second revision

525 **References**

526

527 1. Cohen-Cory S, Kidane AH, Shirkey NJ, Marshak S. Brain- derived neurotrophic factor and
528 the development of structural neuronal connectivity. *Dev Neurobiol.* 2010;70:271–288.

529 2. Yoshii A, Constantine-Paton M. Postsynaptic BDNF-TrkB sig- naling in synapse
530 maturation, plasticity, and disease. *Dev Neurobiol.* 2010;70:304–322.

531 3. Simonato M, Tongiorgi E, Kokaia M. Angels and demons: neurotrophic factors and
532 epilepsy. *Trends Pharmacol Sci.* 2006;27: 631-638.

533 4. Simonato M, Zucchini S. Are the neurotrophic factors a suitable therapeutic target for the
534 prevention of epileptogenesis? *Epilepsia.* 2010;51(Suppl 3): 48-51.

535 5. Kwong AD, Frenkel N. Herpes simplex virus amplicon: effect of size on replication of
536 constructed defective genomes containing eucaryotic DNA sequences. *J Virol.* 1984;51:
537 595-603.

538 6. Wang J, Barr MM. RNA interference in *Caenorhabditis elegans*. *Methods Enzymol.*
539 2005;392:36-55.

540 7. Fire A, Xu S, Montgomery MK, Kostas SA, Driver SE, Mello CC. Potent and specific
541 genetic interference by double-stranded RNA in *Caenorhabditis elegans*. *Nature.*
542 1998;391: 806–811.

543 8. Modarresi F, Faghihi MA, Lopez-Toledano MA, Fatemi RP, Magistri M, Brothers SP, et
544 al. Inhibition of natural antisense transcripts *in vivo* results in gene-specific transcriptional
545 upregulation. *Nat Biotechnol.* 2012;30: 453-459.

546 9. Tran N, Cairns MJ, Dawes IW, Arndt GM. Expressing functional siRNAs in mammalian
547 cells using convergent transcription. *BMC Biotech.* 2003;3:21.

- 548 10. Wang J, Tekle E, Oubrahim H, Mieyal JJ, Stadtman ER and Chock PB. Stable and
549 controllable RNA interference: Investigating the physiological function of
550 glutathionylated actin. *Proc Natl Acad Sci U S A*. 2003;100:5103-5106.
- 551 11. Lee NS, Dohjima T, Bauer G, Li H, Li MJ, Ehsani A, et al. Expression of small
552 interfering RNAs targeted against HIV-1 rev transcripts in human cells. *Nat Biotechnol*.
553 2002;20: 500-505.
- 554 12. Shi H, Djikeng A, Mark T, Wirtz E, Tschudi C and Ullu E. Genetic interference in
555 *Trypanosoma brucei* by heritable and inducible double-stranded RNA. *Rna*.
556 2000;6:1069-1076.
- 557 13. Giordano E, Rendina R, Peluso I and Furia M. RNAi Triggered by Symmetrically
558 Transcribed Transgenes in *Drosophila melanogaster*. *Genetics*. 2002;160:637-648.
- 559 14. Gullerova M, Proudfoot NJ. Convergent transcription induces transcriptional gene
560 silencing in fission yeast and mammalian cells. *Nat Struct Mol Biol*. 2012;19: 1193-201.
- 561 15. Chao-Chung YS and Becker KG. A genome-wide view of antisense. *Nat Biotechnol*.
562 2003;21:492.
- 563 16. Shendure J and Church GM. Computational discovery of sense- antisense transcription in
564 the human and mouse genomes. *Genome Biol*. 2002;3:RESEARCH0044.
- 565 17. Su T, Scardigli R, Fasulo L, Paradiso B, Barbieri M, Binaschi A, et al. Bystander Effect
566 on Brain Tissue of Mesoangioblasts Producing Neurotrophins. *Cell Transplant*. 2012;21:
567 1613-1627.
- 568 18. Pellegrino LJ, Pellegrino AS, Cushman AJ. A stereotaxic atlas of the rat brain. New York
569 and London: Plenum Press. 1979.
- 570 19. Racine RJ. Modification of seizure activity by electrical stimulation. II. Motor seizure.
571 *Electroencephalogr. Clin Neurophysiol*. 1972;32: 281-294.

- 572 20. Curia G, Longo D, Biagini G, Jones SG, Avoli M. The pilocarpine model of temporal
573 lobe epilepsy. *Journal of Neuroscience Methods*. 2008; 172:143–157.
- 574 21. Biagini G, Avoli M, Marcinkiewicz J and Marcinkiewicz M. Brain-derived neurotrophic
575 factor superinduction parallels anti-epileptic neuroprotective treatment in the pilocarpine
576 epilepsy model. *J of Neurochemistry*. 2001; 76:1814-1822.
- 577 22. Tongiorgi E, Armellin M, Giulianini PG, Bregola G, Zucchini S, Paradiso B, et al. Brain-
578 derived neurotrophic factor mRNA and protein are targeted to discrete dendritic laminae
579 by events that trigger epileptogenesis. *J Neurosci*. 2004; 24:6842–6852.
- 580 23. Chiaruttini C, Sonogo M, Baj G, Simonato M, Tongiorgi E. BDNF mRNA splice variants
581 display activity-dependent targeting to distinct hippocampal laminae. *Mol Cell Neurosci*.
582 2008;37:11–19.
- 583 24. Tsitoura E, Thomas J, Cuchet D, Thoinet K, Mavromara P, Epstein AL. Infection with
584 herpes simplex type 1-based amplicon vectors results in an IRF3/7-dependent, TLR-
585 independent activation of the innate antiviral response in primary human fibroblasts.
586 *Journal of General Virology*. 2009; 90:2209-2220.
- 587 25. Khorrooshi R, Morch MT, Holm TH, Berg CT, Dieu RT, Draeby D, et al. Induction of
588 endogenous Type I interferon within the central nervous system plays a protective role in
589 experimental autoimmune encephalomyelitis. *Acta Neuropathol*. 2015; 130:107-118.
- 590 26. Simonato M, Molteni R, Bregola G, Muzzolini A, Piffanelli M, Beani L, et al. Different
591 patterns of induction of FGF-2, FGF-1 and BDNF mRNAs during kindling
592 epileptogenesis in the rat. *Eur J Neurosci*. 1998;10: 955-965.
- 593 27. Mudò G, Jiang XH, Timmusk T, Bindoni M, Belluardo N. Change in Neurotrophins and
594 Their Receptor mRNAs in the Rat Forebrain After Status Epilepticus Induced by
595 Pilocarpine. *Epilepsia*. 1996;37: 198-207.

- 596 28. Elmer E, Kokaia K, Kokaia M, Carnahan J, Nawa H, Lindvall O. Dynamic changes of
597 brain-derived neurotrophic factor protein levels in the rat forebrain after single and
598 recurring kindling-induced seizures. *Neurosci.* 1998; 83: 351-362.
- 599 29. Epstein A. HSV-1-derived amplicon vectors: recent technological improvements and
600 remaining difficulties. *Mem Inst Osw Cruz.* 2009;104: 399-410.
- 601 30. Epstein A. HSV-1-based amplicon vectors: design and applications. *Gene Therapy.*
602 2005;12: 154-158.
- 603 31. Boehmer PE, Lehman IR. Herpes simplex virus DNA replication. *Annu Rev Biochem.*
604 1997;66: 347-384.
- 605 32. Wang S, Fraefel C, Breakefield X. HSV-1 amplicon vectors. *Methods Enzymol.*
606 2002;346:593-603.
- 607 33. Oehmig A, Fraefel C, Xandra O, Breakefield. Update on Herpesvirus Amplicon Vectors.
608 *Molecular Therapy.* 2004;10: 630-643.
- 609 34. Kavi HH, Fernandez H, Xie W, Birchler JA. Genetics and biochemistry of RNAi in
610 *Drosophila.* *Curr Top Microbiol Immunol.* 2008;320: 37-75.
- 611 35. Timmusk T, Palm K, Metsis M, Reintam T, Paalme V, Saarma M, et al. Multiple
612 promoters direct tissue-specific expression of the rat BDNF gene. *Neuron.* 1993;10:475-
613 489.
- 614 36. Pitkänen A, Sutula TP. Is epilepsy a progressive disorder? Prospects for new therapeutic
615 approaches in temporal-lobe epilepsy. *Lancet Neurol.* 2002;1: 173-81.
- 616 37. Kokaia M, Ernfors P, Kokaia Z, Elmer E, Jaenisch R, Lindvall O. Suppressed
617 epileptogenesis in BDNF mutant mice. *Exp. Neurol.* 1995;33: 215-224.
- 618 38. Binder DK, Routbort MJ, McNamara JO. Immunohistochemical evidence of seizure-
619 induced activation of trk receptors in the mossy fiber pathway of adult rat hippocampus. *J.*
620 *Neurosci.* 1999;19: 4616-4626.

- 621 39. He XP, Kotloski R, Nef S, Luikart BW, Parada LF, McNamara JO. Conditional deletion
622 of TrkB but not BDNF prevents epileptogenesis in the kindling model. *Neuron*. 2004;43:
623 31–42.
- 624 40. Liu G, Gu B, He XP, Joshi RB, Wackerle HD, Rodriguiz RM, et al. Transient inhibition
625 of TrkB kinase after status epilepticus prevents development of temporal lobe epilepsy.
626 *Neuron*. 2013;79: 31-38.
- 627 41. Scharfman HE. Hyperexcitability in combined entorhinal/hippocampal slices of adult rat
628 after exposure to brain-derived neurotrophic factor. *J Neurophysiol*. 1997;78: 1082–1095.
- 629 42. Scharfman HE, Goodman JH, Sollas AL. Actions of brain-derived neurotrophic factor in
630 slices from rats with spontaneous seizures and mossy fiber sprouting in the dentate gyrus.
631 *J Neurosci*. 1999;19: 5619–5631.
- 632 43. Paradiso B, Marconi P, Zucchini S, Berto E, Binaschi A, Bozac A, et al. Localized
633 delivery of fibroblast growth factor-2 and brain-derived neurotrophic factor reduces
634 spontaneous seizures in an epilepsy model. *Proc Natl Acad Sci U S A*. 2009;106: 7191-6.
- 635 44. Bovolenta R, Zucchini S, Paradiso B, Rodi D, Merigo F, Navarro Mora G, et al.
636 Hippocampal FGF-2 and BDNF overexpression attenuates epileptogenesis-associated
637 neuroinflammation and reduces spontaneous recurrent seizures. *J Neuroinflammation*.
638 2010;7:81.
- 639 45. Paradiso B, Zucchini S, Su T, Bovolenta R, Berto E, Marconi P, et al. Localized
640 overexpression of FGF-2 and BDNF in hippocampus reduces mossy fiber sprouting and
641 spontaneous seizures up to 4 weeks after pilocarpine-induced status epilepticus. *Epilepsia*.
642 2011;52: 572-8.
- 643

644 **Figure legends**

645

646 **Fig 1. Structure of the amplicon plasmids.** (A) The pAM2-BDNF-antisense-GFP plasmid
647 (6.84 Kb) results by insertion in antisense orientation of a fragment (1.1 Kb) containing the
648 BDNF sequence and a poly-A tail. (B) In the pAM-CT-BDNF-GFP plasmid (7.07 Kb), the
649 BDNF sequence (1.1 Kb) is inserted in convergent transcription, between two CMV
650 promoters. (C) The control plasmid, pAM2-GFP plasmid (5.70 Kb). These 3 plasmids were
651 used to produce stocks of amplicon vectors at high purities (see text).

652

653 **Fig 2. In vitro validation of the amplicon vectors.** (A to D) Infection of mesoangioblast cells
654 (MABs) constitutively expressing BDNF with the BDNF-antisense-GFP amplicon vector at
655 MOI 5. Infection of the cells with amplicon vectors was confirmed by GFP fluorescence (A)
656 and GFP detection on western blot (C). Pro-BDNF expression was analyzed by western blot
657 in the 4 days following infection and pro-BDNF signal was normalized to α -actin for
658 quantification (D). (E to H) Infection of MABs with the BDNF-CT-GFP amplicon vector at
659 MOI 5. Infection of the cells was confirmed by GFP fluorescence (E) and GFP detection on
660 western blot (G). Pro-BDNF expression was analyzed by western blot in the 4 days following
661 infection and pro-BDNF signal was normalized to α -actin for quantification (H). Data in D
662 and H are the mean \pm SEM of 6 experiments. * $p < 0.05$, ** $p < 0.01$, *** $p < 0.001$: ANOVA and
663 post-hoc Dunnett test. Horizontal bars in panels A, B, E and F = 25 μ m.

664

665 **Fig 3. Absence of overt amplicon vector-induced toxicity after injection in the dorsal**
666 **hippocampus.** Dentate gyrus (DG) of the dorsal hippocampus injected (ipsilateral) and non-
667 injected (controlateral) with BDNF-antisense-GFP or with BDNF-CT-GFP amplicon vector.

668 Nuclei are marked by DAPI in blue, GFAP-positive astrocytes in red, IBA-1-positive
669 microglia in green and neuronal nuclei are labeled by NeuroTrace in magenta. Horizontal
670 bars = 100 μ m.

671

672 **Fig 4. Transgene expression following injection of amplicon vectors in the right and left**
673 **hippocampus at different time points after pilocarpine-induced status epilepticus.** (A)

674 Representative GFP immunofluorescence in the dorsal hippocampus of a rat at 5 days post
675 injection with the BDNF-antisense-GFP amplicon vector. (B) Quantification of the pro-
676 BDNF signal, normalized to α -actin, 3, 6 and 24 h after pilocarpine status epilepticus induced
677 5 days after injection of the amplicon vectors in the right dorsal hippocampus. Data in B are
678 the mean \pm SEM of 4-5 rats per group. * $p < 0.05$, ANOVA and post-hoc Dunnett test.

679 Horizontal bar in A = 250 μ m.

680

681 **Fig 5. Behavioral effects.** (A) Time to enter convulsive status epilepticus following
682 administration of the different doses of BDNF-antisense-GFP vector. * $p < 0.05$, ANOVA and
683 post-hoc Dunnett test. (B) Mortality of pilocarpine-treated animals injected with the different
684 doses of BDNF-antisense-GFP amplicon vector. Data in are the mean \pm SEM of 10-14
685 animals.

686

687

688

689

690

691

692

Supporting Information

693

694

695 **S1 Fig. *Absence of overt amplicon vector-induced toxicity after injection in the dorsal***

696 ***hippocampus.*** Dorsal hippocampus injected (ipsilateral) and non injected (contralateral) with

697 BDNF-antisense-GFP or with BDNF-CT-GFP amplicon vector. Nuclei are marked by DAPI

698 in blue, GFAP-positive astrocytes in red, IBA-1-positive microglia in green and neuronal

699 nuclei are labeled by NeuroTrace in magenta. Horizontal bars = 200 μm (12,5 μm in

700 CA1/CA3 boxes).

701

702 **S2 Fig. *Interferon β response.*** Representative sections showing IFN- β

703 immunohistochemistry in the dorsal hippocampus injected with the BDNF-antisense-GFP

704 (left panel, A) or with the BDNF-CT-GFP amplicon vector (right panel, B). In the insert,

705 nuclei are marked in blue by DAPI and IBA-1-positive cells (microglia) are in red.

706 Horizontal bar = 25 μm .

707

708 **S3 Fig. *Structure of the qRT-PCR primers.*** (A) Synthetic antisense BDNF mRNA. (B)

709 Endogenous BDNF mRNA. CDS: coding DNA sequence. UTR: untranslated region. Rev:

710 reverse. For: forward.

711

712 **S4 Fig. *Transgene expression following injection of amplicon vectors in the right and left***

713 ***hippocampus at 3h after pilocarpine-induced status epilepticus.*** (A) Representative GFP

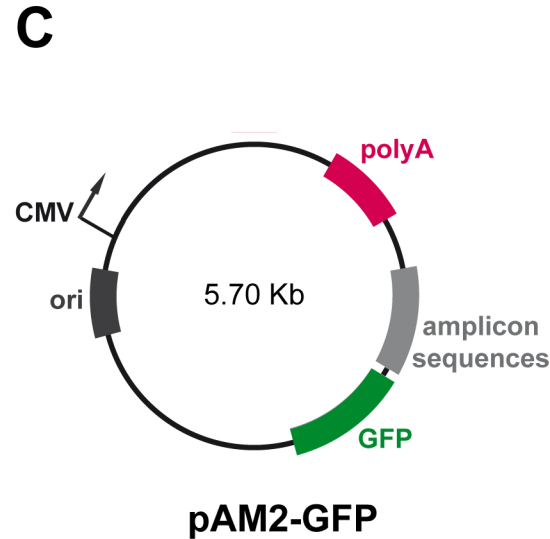
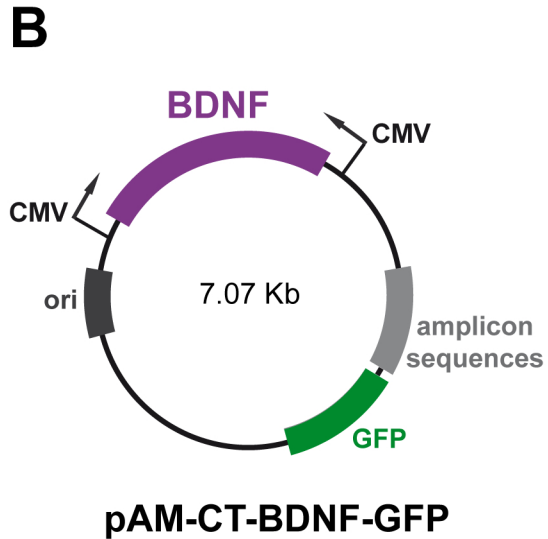
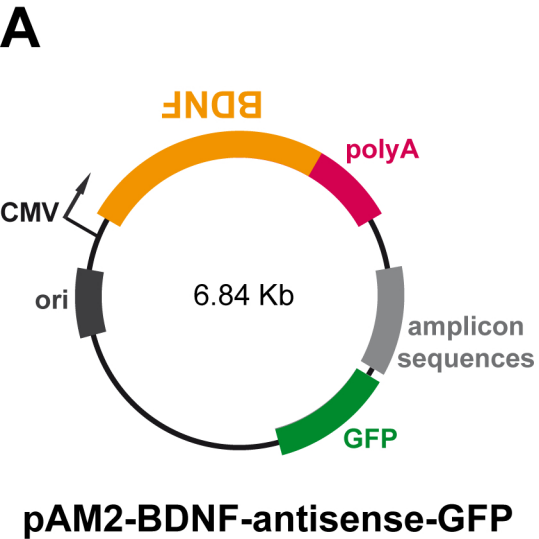
714 immunofluorescence in the dorsal hippocampus of a rat at 5 days post injection with the

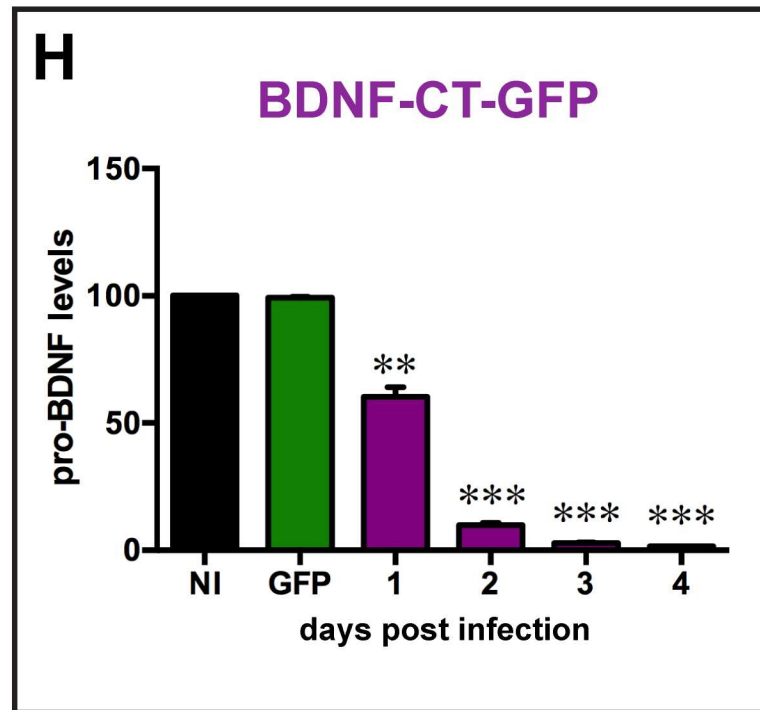
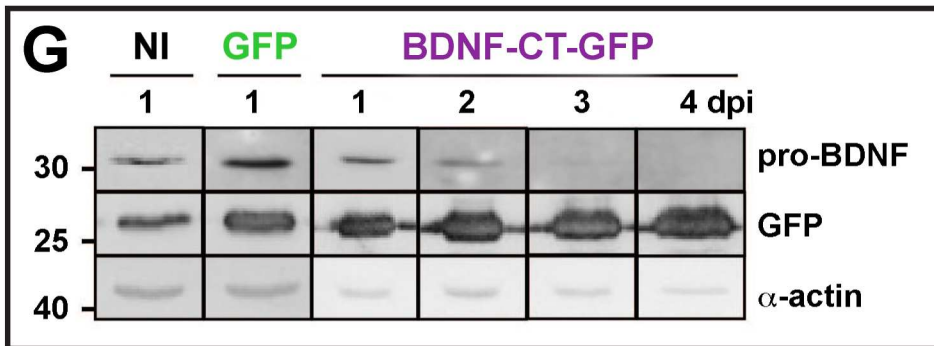
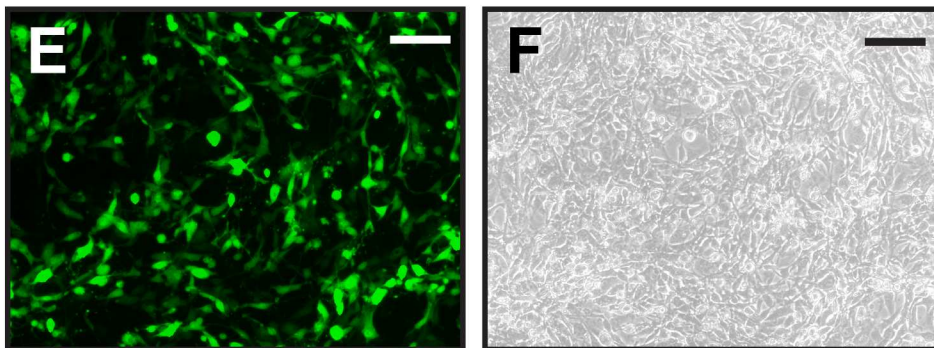
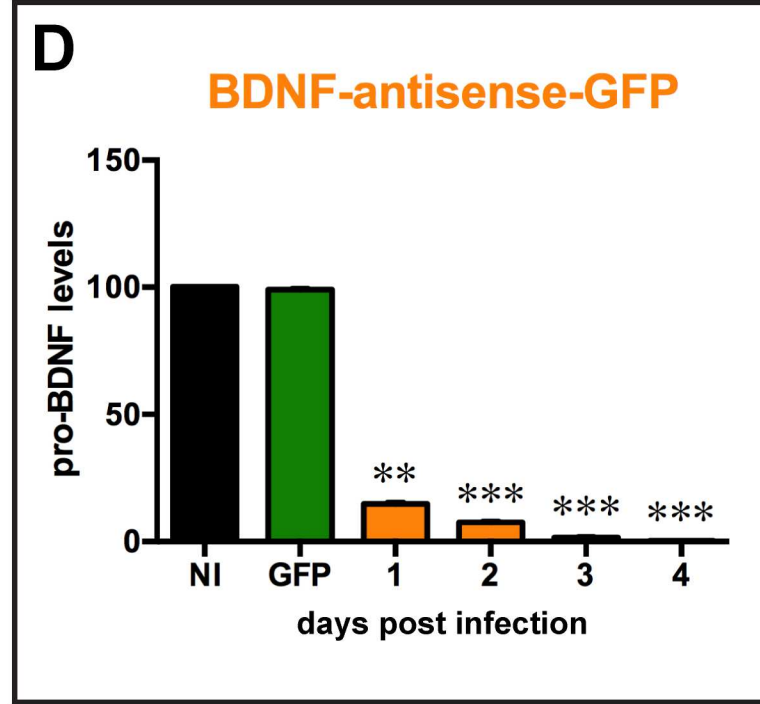
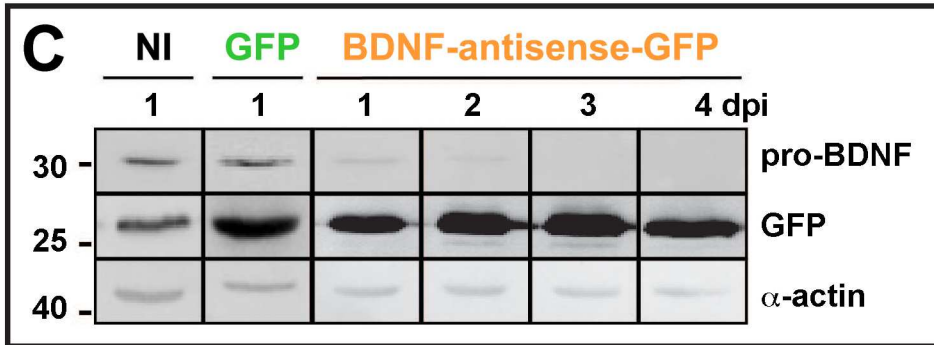
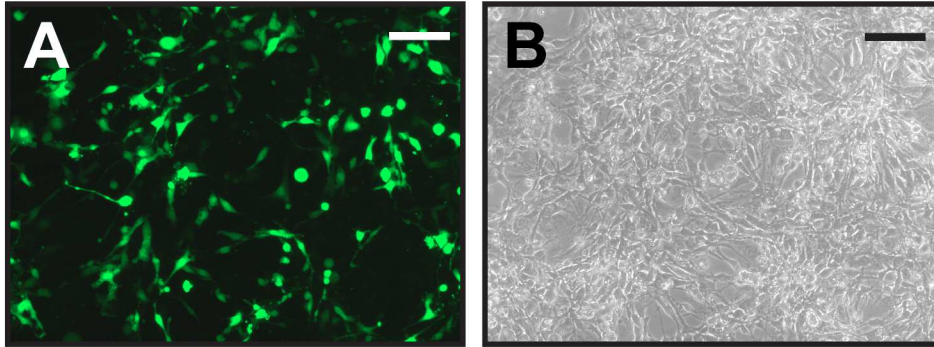
715 BDNF-CT-GFP amplicon vector. (B) Quantification of the pro-BDNF signal, normalized to

716 α -actin, 3 h after pilocarpine status epilepticus induced 5 days after injection of the amplicon

717 vectors in the right dorsal hippocampus. (n = 5 animals per group). Horizontal bar in A = 250
718 μm .

under second revision

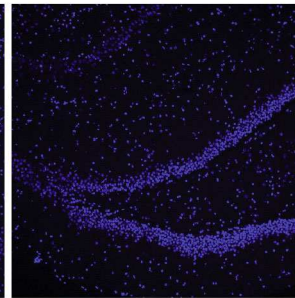
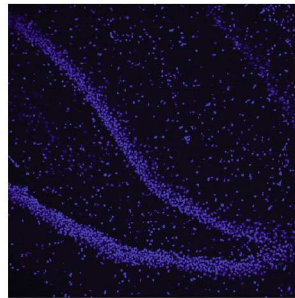
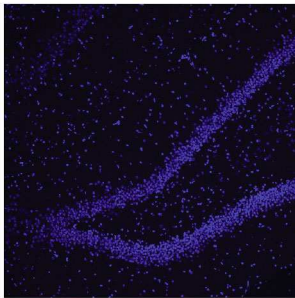
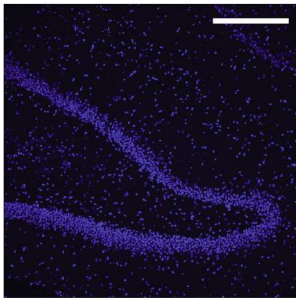




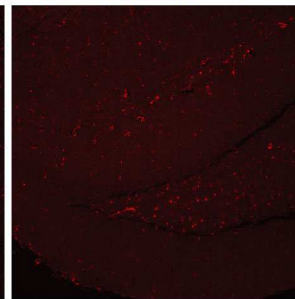
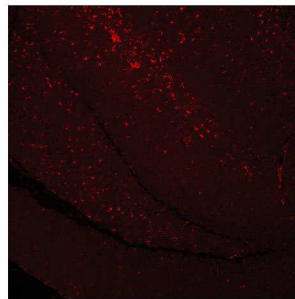
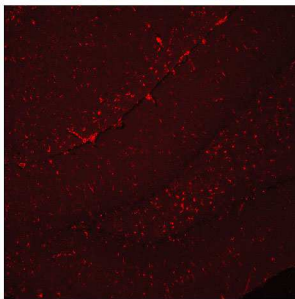
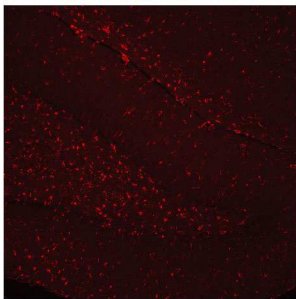
BDNF-antisense-GFP

BDNF-CT-GFP

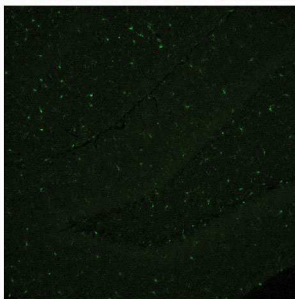
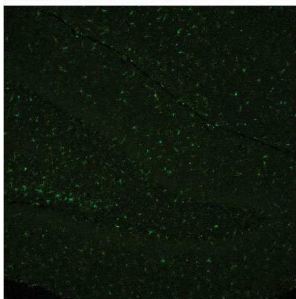
DAPI



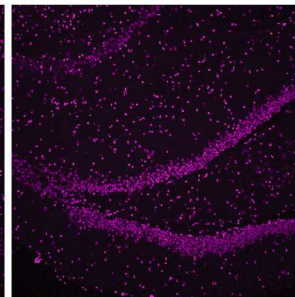
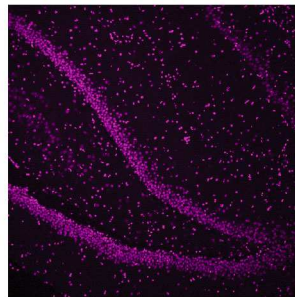
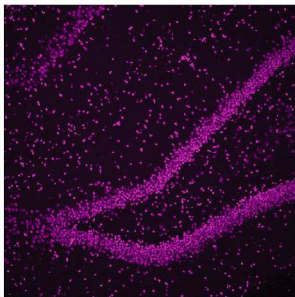
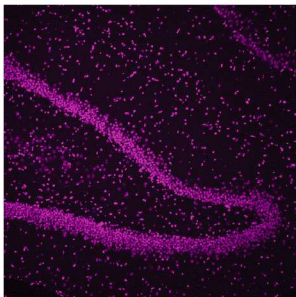
GFAP



IBA1



NeuroTrace

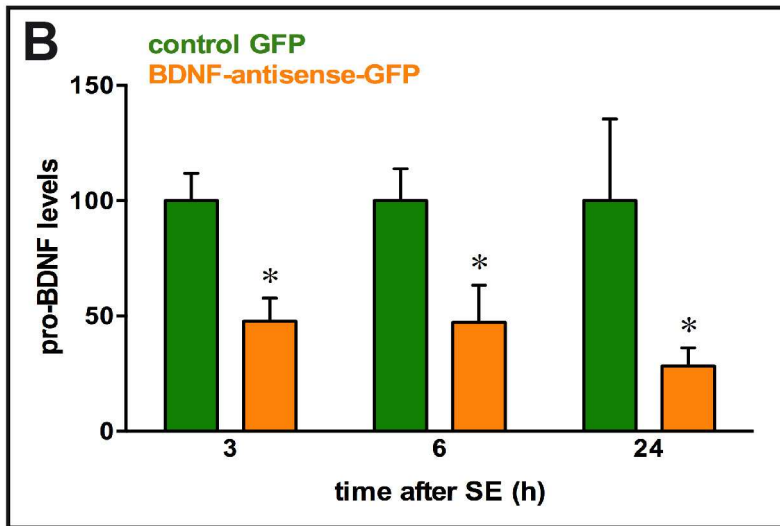
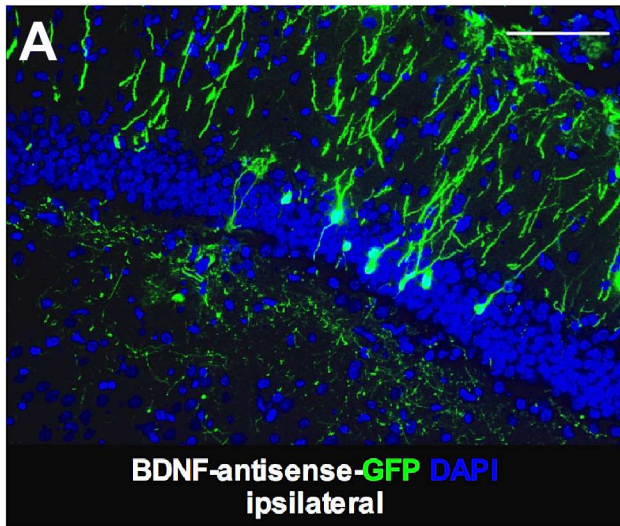


ipsilateral

contralateral

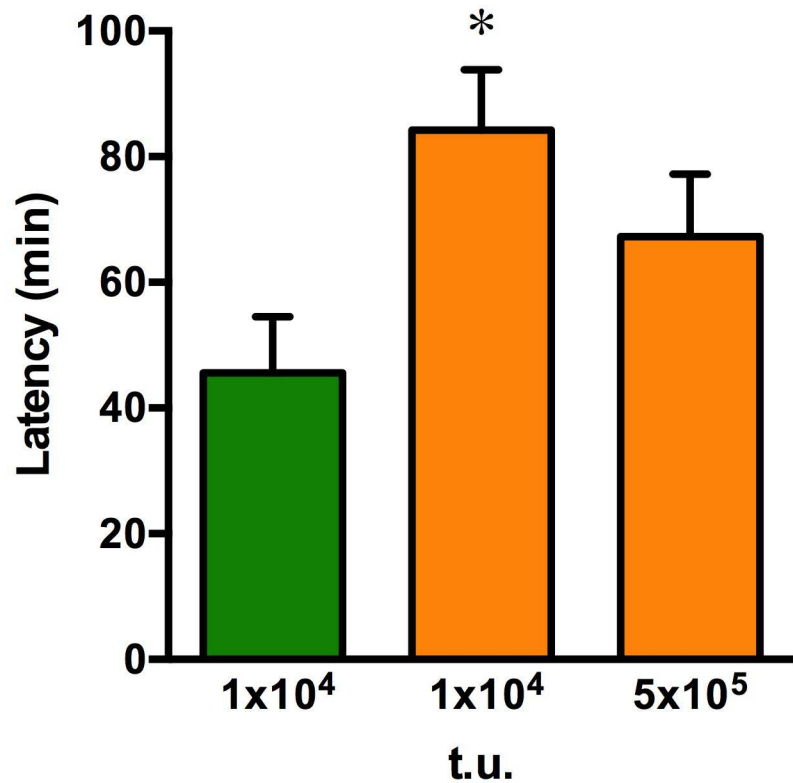
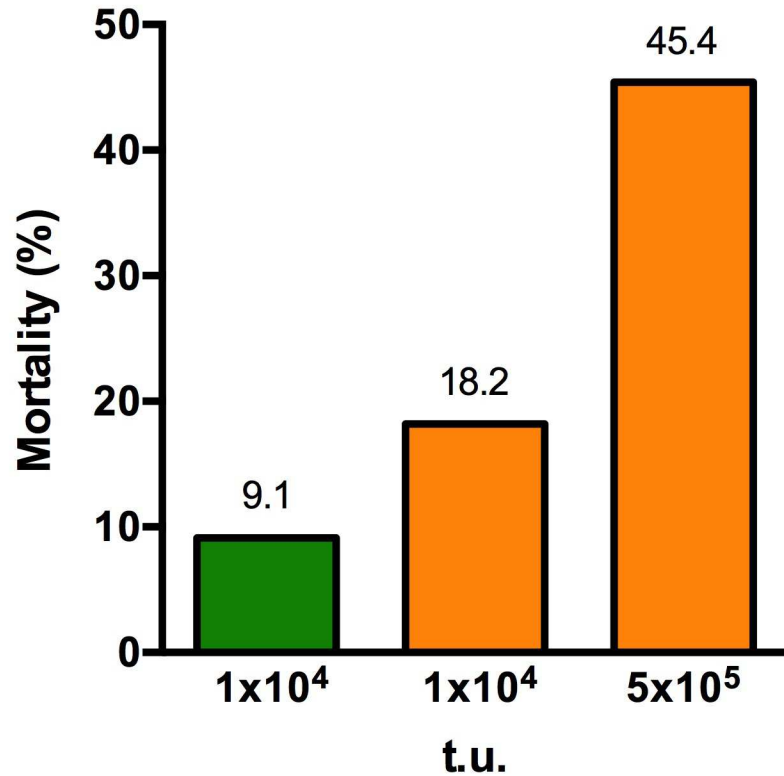
ipsilateral

contralateral



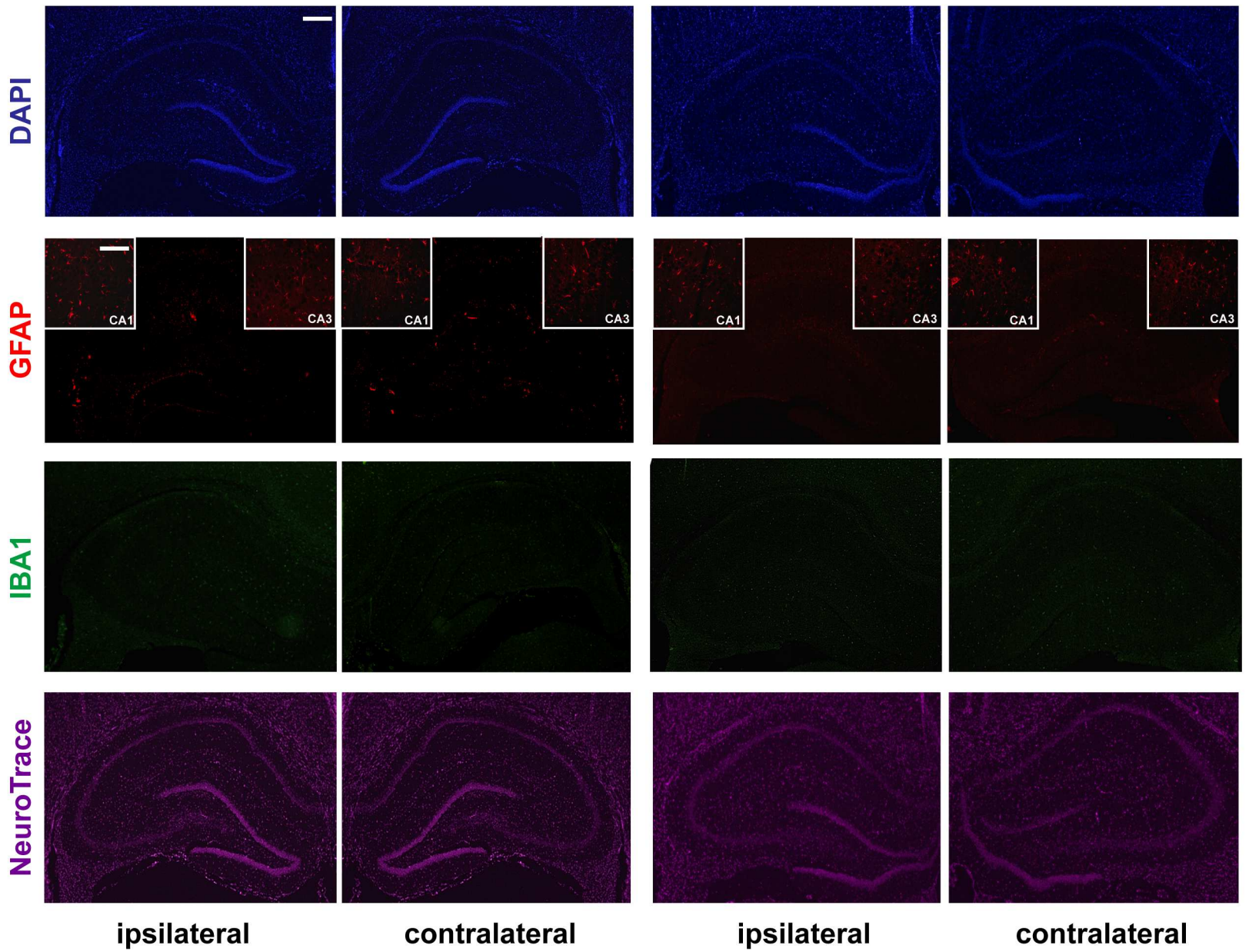
A

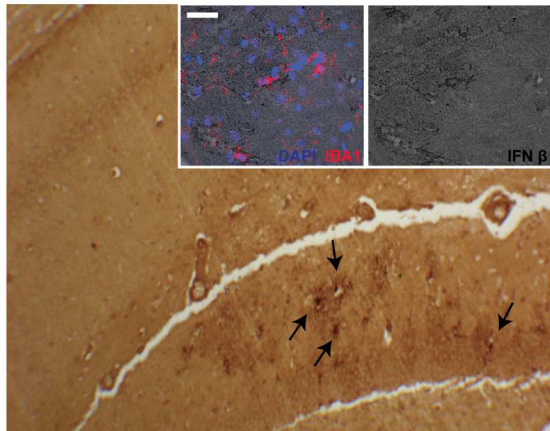
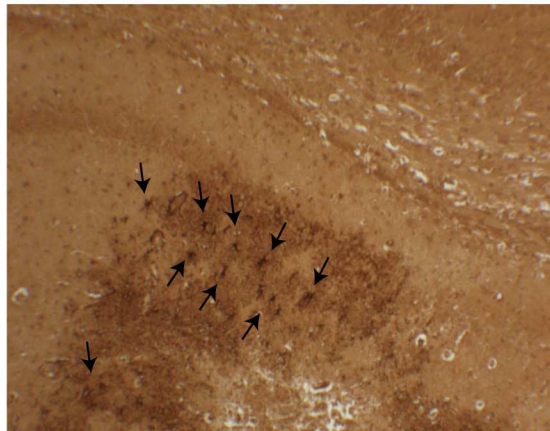
control GFP
BDNF-antisense-GFP

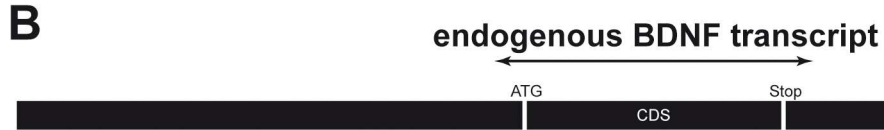
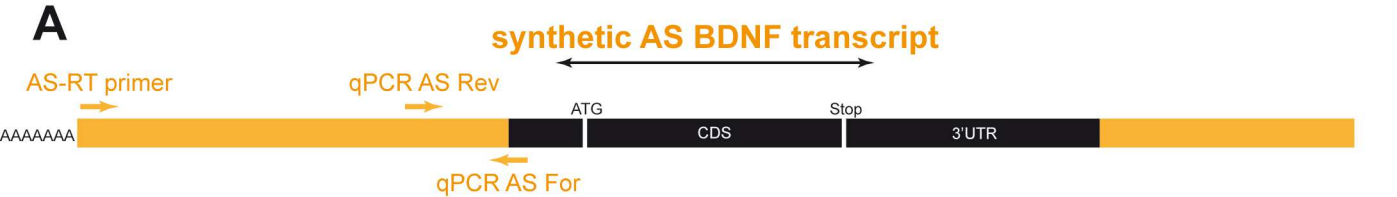
**B**

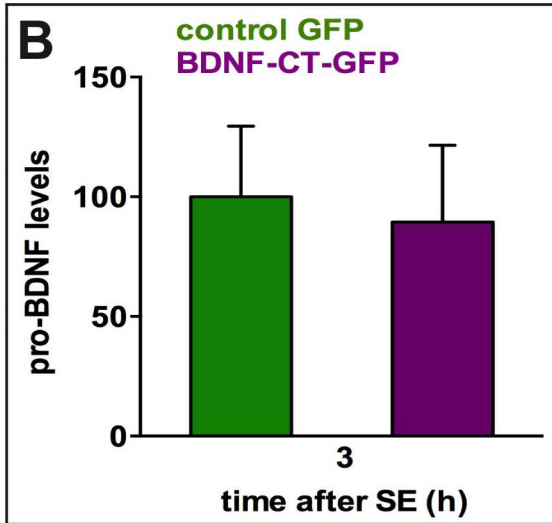
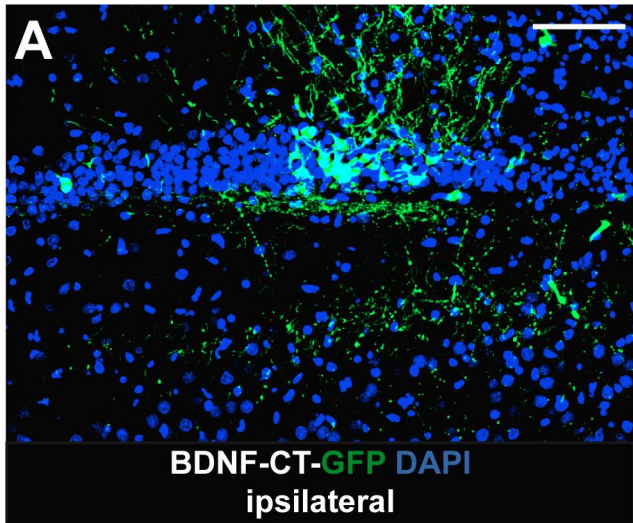
BDNF-AS-GFP

BDNF-CT-GFP



A**BDNF-antisense-GFP****Interferon β** **ipsilateral****B****BDNF-CT-GFP****ipsilateral**





Chapter 5

**Excitatory/inhibitory unbalance
in epilepsy**

5.1 Neurotransmitter systems involved in epileptic hyperactivity

The involvement of various neurotransmitter systems (especially of excitatory and inhibitory amino acids) in the generation of epileptic hyperactivity as well as in the initiation and spread of seizures has been well documented by many authors (Ben-Ari, 2006; Bradford, 1995; Werner and Covenas, 2011). Accordingly, the augmented activity of the excitatory amino acid glutamate together with aspartate, once a front-runner, now trailing behind (Louvel et al., 1992), may be responsible for seizure generation. However, it remains controversial if this exaggerated excitatory input is amplified by a reduction in inhibition in epileptic foci due to loss of GABAergic neurons, or a reduction of GABA release, or a reduction of GABA effectiveness at its receptors (Sierra-Paredes and Sierra-Marcuno, 2007).

5.2 Role of the glutamatergic system in seizure activity

A disorder in glutamate-mediated excitatory neurotransmission has long been a candidate as a central factor in the etiology of at least some forms of human and experimental epilepsy. Thus, glutamate itself and its receptor agonists (e.g. N-methyl D-aspartate acid, NMDA) cause seizures when injected directly in the brain. Moreover, glutamate itself is present in most neuronal cells at an average concentration of 10 mM, much higher than any other excitatory agent. Experimental evidence shown that the high intracellular concentration of glutamate provides a very high concentration gradient, causing the continuous outward diffusion of a potent excitatory molecule. This appears to be balanced by a very effective continuous inward transport back into the neuron and into glial cells due to the high-affinity uptake system (Bradford, 1995). Functional alterations associated with tissue damage, gliosis and scarring, all phenomena associated with epileptogenesis, might well lead to reduced rates of glutamate re-uptake and its consequent accumulation associated to the seizures onset.

5.3 Human and animal studies evidencing the role of glutamate in epilepsy

The excitatory glutamatergic system may be centrally involved in epileptic changes at three levels. Namely, (i) in the chronic sub-convulsive hyperactivity, which occurs in the epileptic focus and is detectable by EEG; (ii) in the amplified excitatory activity which leads to initiation of seizures and recruitment of excitatory neurons situated adjacent to the focus; thus (iii) the spread and generalization of the hyperactivity.

Human studies mostly focused on neurochemical analysis of tissue levels of amino acids in surgically removed brain samples or on the measurement of amino acid levels in the cerebrospinal fluid (CSF). These studies are relatively rare, probably because of the difficulties associated with obtaining consent of suitable epileptic patients and with obtaining focal epileptic brain tissue and appropriate control tissue. However, most of these studies reported an higher glutamate and also aspartate concentration in epileptic hippocampi and their increase before seizure onset reaching potentially excitotoxic levels (Cavus et al., 2005; Sherwin, 1999).

Data from animal studies confirm the observations made in the human brain. An increase in glutamate release has been reported during seizures (Kanamori and Ross, 2011; Meurs et al., 2008; Ronne et al., 2001) and even in the interictal (between seizures) period (Ueda et al., 2001) in different animal models of epilepsy. A paradoxical decrease of glutamate release during seizures has been described only after intrahippocampal perfusion of picrotoxin in rats (Sierra-Paredes et al., 1998).

5.4 Role of the GABAergic system in seizure activity

As mentioned above, the control of excitability in the mammalian brain, including epileptic hyper-excitability, is largely dependent on the main inhibitory neurotransmitter, γ -aminobutyric acid (GABA). Indeed, many drugs potentiating GABA transmission are effective antiseizure agents (Treiman, 2001). Unfortunately, however, little is known on the dynamic changes in the GABAergic system in natural course of TLE and in its progression towards pharmaco-resistance. Only some aspects of the alterations specifically affecting the

GABA system have been identified. For example, a substantial loss of glutamic acid decarboxylase (GAD) mRNA-containing (i.e. GABAergic) neurons has been found in the hilus of dentate gyrus (Obenaus et al., 1993) and in the stratum oriens of CA1 (Houser and Esclapez, 1996). Moreover, a reduced density of specific GABAergic neurons, including parvalbumin- (Drexel et al., 2011; Kuruba et al., 2011; Pavlov et al., 2011) and somatostatin-positive interneurons (Paradiso et al., 2009; Sperk et al., 1992; Sun et al., 2007), has been found in the epileptic hippocampus.

Another interesting alteration is that repetitive activation leads to profound post-synaptic GABA_A receptor desensitization (run-down) in the human epileptic tissue (Ragozzino et al., 2005) and in chronically epileptic rats (Mazuferi et al., 2010; Palma et al., 2007). The pre-synaptic counterpart of these alterations in GABA_A receptor response has not been systematically studied yet. Microdialysis studies in pharmaco-resistant epileptic patients undergoing depth electrode investigation prior to surgery have shown an increased outflow of GABA in the hippocampus in response to seizures, even if this increase was not as dramatic as that of the excitatory neurotransmitters glutamate and aspartate (During and Spencer, 1993; Thomas et al., 2005; Wilson et al., 1996), whereas the basal, interictal GABA outflow was non significantly reduced in the epileptogenic hippocampus (Pan et al., 2008). For obvious reasons, these works lack stringent controls apart from the apparently non-epileptogenic contralateral hippocampus (During and Spencer, 1993; Thomas et al., 2005) or hippocampus of patients with neo-cortical epilepsy (Pan et al., 2008). Unfortunately, studies in animal models also did not provide insight on this issue, because they revealed transient or non-significant increases in hippocampal GABA outflow during pilocarpine-induced SE (Khongsombat et al., 2008; Meurs et al., 2008; Smolders et al., 1997), but did not yet explore the possible subsequent adaptive changes in GABA neurotransmission.

5.5 References

Ben-Ari Y (2006) Seizures beget seizures: the quest for GABA as a key player. *Crit Rev Neurobiol*, 18:135-144.

Bradford HF (1995) Glutamate, GABA and epilepsy. *Prog Neurobiol* 47:477-511.

Werner FM, Covenas R (2011) Classical neurotransmitters and neuropeptides involved in generalized epilepsy: a focus on antiepileptic drugs. *Curr Med Chem* 18:4933-4948.

Louvel J, Pumain R, Roux FX, Chodkiewicz JP (1992) Recent advances in understanding epileptogenesis in animal models and in humans. *Adv Neurol* 57:517-523.

Sierra-Paredes G, Sierra-Marcuno G (2007) Extrasynaptic GABA and glutamate receptors in epilepsy. *CNS Neurol Disord Drug Targets* 6:288-300.

Cavus I, Kasoff WS, Cassaday MP, Jacob R, Gueorguieva R, Sherwin RS, Krystal JH, Spencer DD, Abi-Saab WM (2005) Extracellular metabolites in the cortex and hippocampus of epileptic patients. *Ann Neurol* 57:226-235.

Sherwin AL (1999) Neuroactive amino acids in focally epileptic human brain: a review. *Neurochem Res* 24:1387-1395.

Kanamori K, Ross BD (2011) Chronic electrographic seizure reduces glutamine and elevates glutamate in the extracellular fluid of rat brain. *Brain Res* 1371:180-191.

Meurs A, Clinckers R, Ebinger G, Michotte Y, Smolders I (2008) Seizure activity and changes in hippocampal extracellular glutamate, GABA, dopamine and serotonin. *Epilepsy Res* 78:50-59.

Ronne EE, Hillered L, Flink R, Kihlstrom L, Lindquist C, Nie JX, Olsson Y, Silander HC (2001), Extracellular amino acid levels measured with intracerebral microdialysis in the model of posttraumatic epilepsy induced by intracortical iron injection. *Epilepsy Res* 43:135-144.

Ueda Y, Doi T, Tokumaru J, Yokoyama H, Nakajima A, Mitsuyama Y, Ohya-Nishiguchi H, Kamada H, Willmore LJ (2001), Collapse of extracellular glutamate regulation during epileptogenesis: down-regulation and functional failure of glutamate transporter function in rats with chronic seizures induced by kainic acid. *J Neurochem* 76:892-900.

Sierra-Paredes G, Galan-Valiente J, Vazquez-Illanes MD, Aguilar-Veiga E, Soto-Otero R, Mendez-Alvarez E, Sierra-Marcuno G (1998) Extracellular amino acids in the rat hippocampus during picrotoxin threshold seizures in chronic microdialysis experiments. *Neurosci Lett* 248:53-56.

Treiman DM, (2001), GABAergic mechanisms in epilepsy. *Epilepsia* 42 Suppl 3, 8-12.

Obenaus A, Esclapez M, Houser CR (1993), Loss of glutamate decarboxylase mRNA-containing neurons in the rat dentate gyrus following pilocarpine-induced seizures. *J. Neurosci*, 13: 4470-4485.

Houser CR, Esclapez M (1996), Vulnerability and plasticity of the GABA system in the pilocarpine model of spontaneous recurrent seizures. *Epilepsy Res*, 26: 207-218.

Drexel M, Preidt AP, Kirchmair E, Sperk G (2011), Parvalbumin interneurons and calretinin fibers arising from the thalamic nucleus reuniens degenerate in the subiculum after kainic acid-induced seizures. *Neuroscience*, 189: 316-329.

Kuruba R, Hattiangady B, Parihar VK, Shuai B, Shetty AK (2011), Differential susceptibility of interneurons expressing neuropeptide Y or parvalbumin in the aged hippocampus to acute seizure activity. *PLoS. One*, 6:e24493.

Pavlov I, Huusko N, Drexel M, Kirchmair E, Sperk G, Pitkanen A, Walker MC (2011), Progressive loss of phasic, but not tonic, GABAA receptor-mediated inhibition in dentate granule cells in a model of post-traumatic epilepsy in rats. *Neuroscience*, 194: 208-219.

Paradiso B, Marconi P, Zucchini S, Berto E, Binaschi A, Bozac A, Buzzi A, Mazzuferi M, Magri E, Navarro MG, Rodi D, Su T, Volpi I, Zanetti L, Marzola A, Manservigi R, Fabene PF, Simonato M (2009), Localized delivery of fibroblast growth factor-2 and brain-derived neurotrophic factor reduces spontaneous seizures in an epilepsy model. *Proc Natl Acad Sci USA*, 106:7191-7196.

Sperk G, Marksteiner J, Gruber B, Bellmann R, Mahata M, Ortler M (1992), Functional changes in neuropeptide Y- and somatostatin-containing neurons induced by limbic seizures in the rat. *Neuroscience*, 50: 831-846.

Sun C, Mtchedlishvili Z, Bertram EH, Erisir A, Kapur J (2007), Selective loss of dentate hilar interneurons contributes to reduced synaptic inhibition of granule cells in an electrical stimulation-based animal model of temporal lobe epilepsy. *J. Comp Neurol*, 500: 876-893.

Ragozzino D, Palma E, Di AS, Amici M, Mascia A, Arcella A, Giangaspero F, Cantore G, Di GG, Manfredi M, Esposito V, Quarato PP, Miledi R, Eusebi F (2005), Rundown of GABA type A receptors is a dysfunction associated with human drug-resistant mesial temporal lobe epilepsy. *Proc Natl Acad Sci USA*, 102: 15219-15223.

Mazzuferi M, Palma E, Martinello K, Maiolino F, Roseti C, Fucile S, Fabene PF, Schio F, Pellitteri M, Sperk G, Miledi R, Eusebi F, Simonato M (2010), Enhancement of GABA(A)-current run-down in the hippocampus occurs at the first spontaneous seizure in a model of temporal lobe epilepsy. *Proc Natl Acad Sci USA*, 107:3180-3185.

Palma E, Roseti C, Maiolino F, Fucile S, Martinello K, Mazzuferi M, Aronica E, Manfredi M, Esposito V, Cantore G, Miledi R, Simonato M, Eusebi F (2007), GABA(A)-current rundown of temporal lobe epilepsy is associated with repetitive activation of GABA(A) "phasic" receptors. *Proc Natl Acad Sci USA*, 104: 20944-20948.

Pan JW, Cavus I, Kim J, Hetherington HP, Spencer DD (2008), Hippocampal extracellular GABA correlates with metabolism in human epilepsy. *Metab. Brain Dis*, 23:457-468.

During MJ, Spencer DD (1993), Extracellular hippocampal glutamate and spontaneous seizure in the conscious human brain. *Lancet*, 341:1607-1610.

Wilson CL, Maidment NT, Shomer MH, Behnke EJ, Ackerson L, Fried I, Engel JJr (1996), Comparison of seizure related amino acid release in human epileptic hippocampus versus a chronic, kainate rat model of hippocampal epilepsy. *Epilepsy Res*. 26:245-254.

Thomas PM, Phillips JP, O'Connor WT (2005), Microdialysis of the lateral and medial temporal lobe during temporal lobe epilepsy surgery. *Surg. Neurol*, 63:70-79.

Khongsombat O, Watanabe H, Tantisira B, Patarapanich C, Tantisira MH (2008), Acute effects of N-(2-propylpentanoyl)urea on hippocampal amino acid neurotransmitters in pilocarpine-induced seizure in rats. *Epilepsy Res*, 79:151-157.

Smolders I, Lindekens H, Clinckers R, Meurs A, O'Neill MJ, Lodge D, Ebinger G, Michotte Y (2004), In vivo modulation of extracellular hippocampal glutamate and GABA levels and limbic seizures by group I and II metabotropic glutamate receptor ligands. *J. Neurochem*, 88:1068-1077.



Impairment of GABA release in the hippocampus at the time of the first spontaneous seizure in the pilocarpine model of temporal lobe epilepsy



Marie Soukupová^{a,b,*}, Anna Binaschi^{a,b}, Chiara Falcicchia^{a,b}, Silvia Zucchini^{a,b,c}, Paolo Roncon^{a,b}, Eleonora Palma^{d,e}, Eros Magri^f, Enrico Grandi^f, Michele Simonato^{a,b,c}

^a Department of Medical Sciences, Section of Pharmacology, Neuroscience Center, University of Ferrara, Italy

^b National Institute of Neuroscience, Italy

^c Laboratory of Technologies for Advanced Therapy (LTITA), Technopole of Ferrara, Italy

^d Department of Physiology and Pharmacology University of Roma "Sapienza", Italy

^e IRCCS San Raffaele Pisana, Roma, Italy

^f Department of Morphology, Surgery and Experimental Medicine, Section of Pathology, University of Ferrara, Italy

ARTICLE INFO

Article history:

Received 20 January 2014

Revised 27 March 2014

Accepted 16 April 2014

Available online 21 April 2014

Keywords:

Temporal lobe epilepsy

Pilocarpine

GABA release

Parvalbumin

Somatostatin

ABSTRACT

The alterations in GABA release have not yet been systematically measured along the natural course of temporal lobe epilepsy. In this work, we analyzed GABA extracellular concentrations (using in vivo microdialysis under basal and high K⁺-evoked conditions) and loss of two GABA interneuron populations (parvalbumin and somatostatin neurons) in the ventral hippocampus at different time-points after pilocarpine-induced status epilepticus in the rat, i.e. during development and progression of epilepsy. We found that (i) during the latent period between the epileptogenic insult, status epilepticus, and the first spontaneous seizure, basal GABA outflow was reduced to about one third of control values while the number of parvalbumin-positive cells was reduced by about 50% and that of somatostatin-positive cells by about 25%; nonetheless, high K⁺ stimulation increased extracellular GABA in a proportionally greater manner during latency than under control conditions; (ii) at the time of the first spontaneous seizure (i.e., when the diagnosis of epilepsy is made in humans) this increased responsiveness to stimulation disappeared, i.e. there was no longer any compensation for GABA cell loss; (iii) thereafter, this dysfunction remained constant until a late phase of the disease. These data suggest that a GABAergic hyperresponsiveness can compensate for GABA cell loss and protect from occurrence of seizures during latency, whereas impaired extracellular GABA levels can favor the occurrence of spontaneous recurrent seizures and the maintenance of an epileptic state.

© 2014 Elsevier Inc. All rights reserved.

Introduction

In temporal lobe epilepsy (TLE), the most frequent epilepsy syndrome in adults, the hippocampal formation often displays distinct neuropathological features, such as neuronal death, neurogenesis, gliosis, axonal sprouting and reorganization of neuronal interconnections. These abnormalities develop in a previously healthy tissue, often after an initial "epileptogenic" event that can produce damage, for example an episode of prolonged, uncontrolled seizures (status epilepticus, SE). Only after a latent period of weeks to years epileptogenic events may be followed by spontaneous recurrent seizures, i.e. by the diagnosis of epilepsy (Pitkanen and Sutula, 2002).

The control of excitability in the mammalian brain, including epileptic hyper-excitability, is largely dependent on the main inhibitory

neurotransmitter, γ -aminobutyric acid (GABA). Indeed, many drugs potentiating GABA transmission are effective antiseizure agents (Treiman, 2001). Unfortunately, however, little is known on the dynamic changes in the GABAergic system in natural course of TLE and in its progression toward pharmaco-resistance. In the epileptic tissue, seizures are not generated in a normal circuit but in a profoundly rewired network (Cossart et al., 2005). Only some aspects of the alterations specifically affecting the GABA system have been identified. For example, a substantial loss of glutamic acid decarboxylase (GAD) mRNA-containing (i.e. GABAergic) neurons has been found in the hilus of dentate gyrus (Obenaus et al., 1993) and in the stratum oriens of CA1 (Houser and Esclapez, 1996). Moreover, reduced number of specific GABAergic neurons, including parvalbumin- (Drexel et al., 2011; Kuruba et al., 2011; Pavlov et al., 2011) and somatostatin-positive interneurons (Paradiso et al., 2009; Sperk et al., 1992; Sun et al., 2007), has been found in the epileptic hippocampus. Another interesting alteration is that repetitive activation leads to profound post-synaptic GABA_A receptor desensitization (run-down) in the human epileptic tissue (Ragozzino et al., 2005) and in chronically epileptic rats (Mazzuferi et al., 2010; Palma et al., 2007).

* Corresponding author at: Department of Medical Sciences, Section of Pharmacology, University of Ferrara, Via Fossato di Mortara 17-19, 44121 Ferrara, Italy. Fax: +39 0532 455205.

E-mail address: marie.soukupova@unife.it (M. Soukupová).

The pre-synaptic counterpart of these alterations in the GABA system has not been systematically studied yet. Microdialysis studies in pharmacoresistant epileptic patients undergoing depth electrode investigation prior to surgery have shown an increased outflow of GABA in the hippocampus in response to seizures, even if this increase was not as dramatic as that of the excitatory neurotransmitters glutamate and aspartate (During and Spencer, 1993; Thomas et al., 2005; Wilson et al., 1996), whereas the basal, interictal GABA outflow was non-significantly reduced in the epileptogenic hippocampus (Pan et al., 2008). For obvious reasons, these works lack stringent controls apart from the apparently non-epileptogenic contralateral hippocampus (During and Spencer, 1993; Thomas et al., 2005) or hippocampus of patients with neo-cortical epilepsy (Pan et al., 2008). Unfortunately, studies in animal models also did not provide insight on this issue, because they revealed transient or non-significant increases in hippocampal GABA outflow during pilocarpine-induced SE (Khongsombat et al., 2008; Meurs et al., 2008; Smolders et al., 1997), but did not yet explore the possible subsequent adaptive changes in GABA neurotransmission.

Here, we used microdialysis to analyze the basal and potassium stimulated GABA outflow in the ventral hippocampus at different time-points after pilocarpine induced SE in the rat. In parallel, we measured the loss of parvalbumin- and somatostatin-expressing GABA interneurons. We found that the loss of GABA neurons is compensated by hyper-responsiveness of the system in the latency period, whereas GABA outflow is dramatically reduced when spontaneous seizures begin to occur.

Materials and methods

Animals

Male Sprague–Dawley rats (250–350 g; Harlan, Italy) were used for all experiments. They were housed under standard conditions: constant temperature (22–24 °C) and humidity (55–65%), 12 h light/dark cycle, free access to food and water. Procedures involving animals and their care were carried out in accordance with European Community (EU Directive 2010/63/EU), national and local laws and polices (authorization: D.M. 83/2009-B and D.M. 246/2012-B). All animals were acclimatized to the microdialysis laboratory conditions for at least 1 h before each experiment and euthanized immediately after the last day of microdialysis by an anesthetic overdose. Rats were killed by decapitation under 1.4% isoflurane anesthesia. The number of animals was kept as small as possible.

Pilocarpine

Rats were randomly assigned to groups that received a single injection of methyl-scopolamine (1 mg/kg, s.c.) 30 min prior to pilocarpine (370 mg/kg, i.p.) or a single injection of methyl-scopolamine 30 min prior to vehicle (0.9% NaCl solution; control animals), and their behavior was observed by experienced researchers for at least 6 h thereafter. Within the first 20–25 min after pilocarpine injection, 83% of the animals developed seizures evolving into recurrent generalized convulsions (status epilepticus, SE). SE was interrupted 3 h after onset by administration of diazepam (20 mg/kg, i.p.). One fourth of the animals that entered SE (i.e. 21% of those administered pilocarpine) died during SE or within 1–2 days. Test and interspersed control animals were then randomly assigned to five experimental groups representing different phases of the natural history of the disease (Fig. 1A): acute phase (24 h after SE), latency (7–9 days after SE), first spontaneous seizure (11 ± 1 days after SE), early chronic (22–24 days after SE, i.e. about 10 days after the first seizure) and late chronic (2 months after SE, i.e. about 50 days after the first seizure). Animals that did not fully recover (i.e. no increase in body weight within the first week) after pilocarpine SE were excluded from the study. Data were collected and processed only from those animals in which the probe was correctly placed, as estimated using a

hematoxylin-eosin staining (see below). Experiments were considered completed only when the number of animals in the various groups achieved five or more. In summary: inclusion/exclusion criteria were development of convulsive SE within 1 h after pilocarpine administration; weight gain in the first week after SE; correct positioning of the microdialysis probe.

Analysis and statistics

Convulsive seizures were assessed by 24/24-h video monitoring, performed using a digital video surveillance system DSS1000 (V4.7.0041FD, AverMedia Technologies, USA). Video monitoring was started approximately 6 h after pilocarpine administration (i.e. at the end of direct observation by the researchers – see above) and continued until day 5. For proper identification of the first spontaneous seizure, continuous video-EEG monitoring was started from day 5 after SE until the day of the first spontaneous seizure (Fig. 1A). Video-EEG monitoring (hardware system MP150 and software AcqKnowledge 4.3, all from Biopac, USA) was started at day 5 because, as previously reported (Mazzuferi et al., 2010; Paradiso et al., 2009), we do not observe spontaneous seizures earlier than 8–9 days after pilocarpine administration under the experimental conditions employed in this study. Video-EEG was also performed in the course of microdialysis for assessment of absence of seizures in the 3 h prior to microdialysis and of seizures evoked by high K^+ ; video-monitoring was also performed in two 2-weeks epochs in the early (days 11–24) and late (days 49–62) chronic phase for assessment of generalized seizure progression (Fig. 1A).

EEG seizures were categorized and measured as periods of paroxysmal activity of high frequency (>5 Hz) characterized by a >3-fold amplitude increment over baseline with progression of the spike frequency that lasted for a minimum of 3 s (Williams et al., 2009). Seizure severity was scored using the scale of Racine (Racine, 1972): 1, chewing or mouth and facial movements; 2, head nodding; 3, forelimb clonus; 4, generalized seizure with rearing; 5, generalized seizure with rearing and falling. Video-EEG analysis was performed by two independent investigators that were blind for the group to which the rats belonged. In case of differential evaluation, data were reviewed together to reach a consensus (Paradiso et al., 2011). In the early and late chronic period, animals were continuously video recorded for two weeks before and during microdialysis, to identify frequency and duration of generalized seizures (class 4 or 5), which were statistically examined using the Student's t-test for unpaired data. The Kruskal-Wallis and post hoc the Dunn's multiple comparison test were used for evaluation of high K^+ -evoked seizures.

Microdialysis

Surgery

Under initial ketamine/xylazine (43 and 7 mg/kg, i.p.) anesthesia, rats were secured to a stereotaxic apparatus with the nose bar positioned at +5 mm. Anesthesia was then maintained using isoflurane (1.4% in air; 1.2 ml/min). A 15 mm long guide cannula (MAB 4.15.iC; Agn Tho's, Lidingö, Sweden, outer diameter 500 ± 5 µm) equipped with a dummy cannula (Plastics One, Roanoke, Virginia, USA) and with a recording electrode glued at its outside (0.5 mm longer than the cannula, 0.3 mm in diameter) was implanted into the right ventral hippocampus (A –3.4 mm; L +4.5 mm; P +6.5 mm to bregma; Fig. 1B). A reference electrode was placed on the skull. The guide cannula was fixed to the skull with four stainless screws and methacrylic cement. Rats were allowed 7 days to recover.

In vitro recovery

To optimize the experimental conditions of microdialysis, we estimated the in vitro recovery of GABA when using two perfusion rates and five different home-made or manufactured probes, all of them of 1 mm membrane length. We compared two home-made probes endowed with a polyacrylonitrile membrane (molecular weight cut-

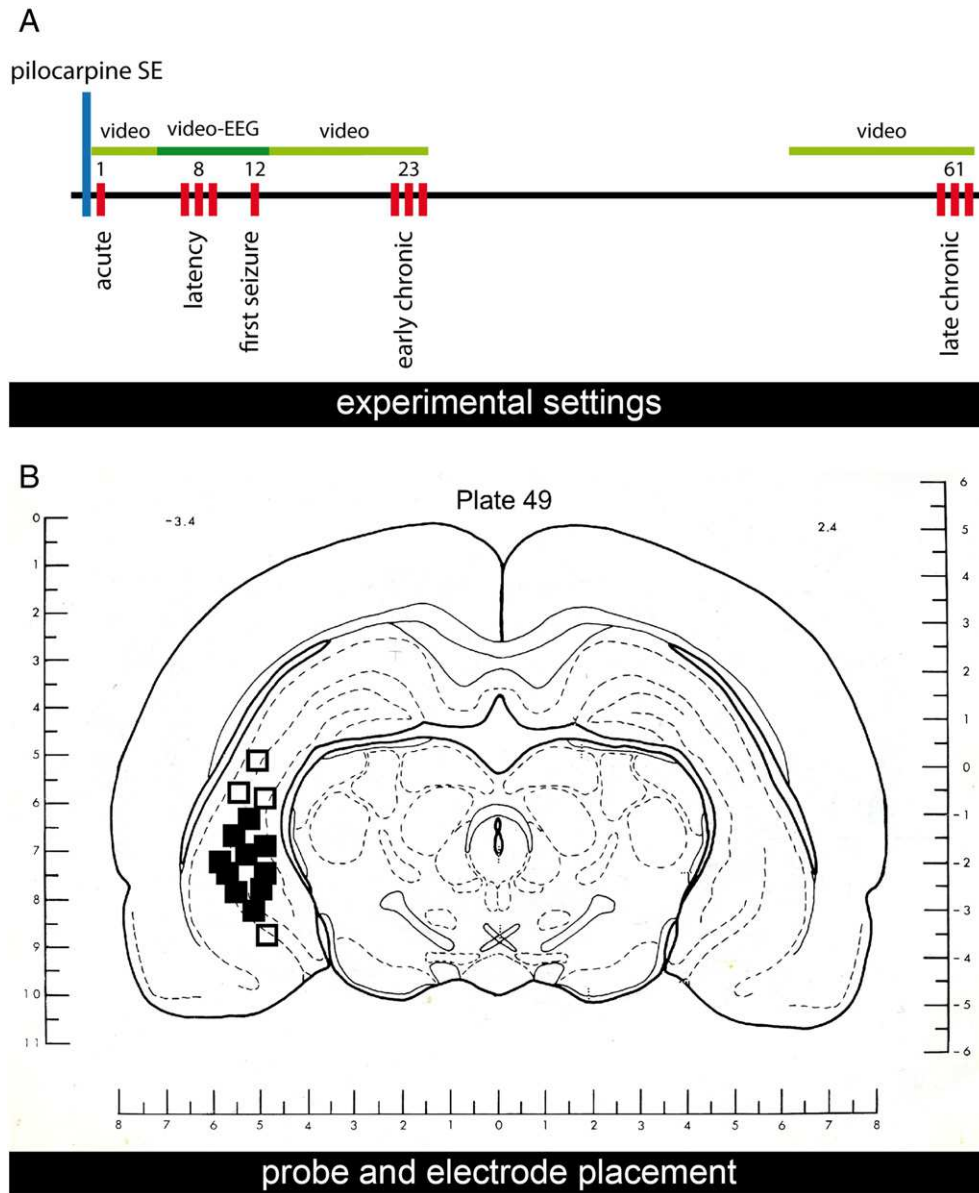


Fig. 1. (A) Schematic diagram of the experiments. Numbers refer to days after SE. The time points of microdialysis experiments are indicated by red bars. See text for details. (B) Schematic illustration of the microdialysis probe positions within the ventral hippocampus. The solid squares (some overlapping) indicate correctly localized probe-electrode tips ($n = 25$). Open squares indicate incorrectly localized probe-electrode tips in animals not included in the study ($n = 4$). Coronal brain slices containing the microdialysis probes and recording sites were processed after the experiment for histological analysis. The numbers above the illustration show the distance from bregma (Pellegriano et al. 1979).

off 40 kDa; AN-69, Hospal, Bologna, Italy) or cuprophane membrane (molecular weight cut-off 10 kDa; Hospal) and three manufactured probes endowed either with cuprophane membrane: MAB 4.15.1.Cu (Agn Tho's) and CMA11Cu (CMA, Sweden) or with polyestersulfone membrane: MAB 4.15.1.PES (Microbiotech/se AB, Sweden). The probes were perfused at rates 2 $\mu\text{l}/\text{min}$ or 3 $\mu\text{l}/\text{min}$ with a Ringer solution (see the composition below) while placed in a vial containing 2 nmol/ml γ -[2,3- $^3\text{H}(\text{N})$]-aminobutyric acid (^3H -GABA; PerkinElmer) in Ringer solution. After a 30 min washout period, three 30 min perfusate samples and three equal volume samples of the solution in the vial were collected; 2.5 ml scintillation fluid (Ultima Gold TM, Packard Bioscience) were added and ^3H -GABA content was analyzed using a liquid scintillation spectrophotometer (Tri-Carb 2500TR, Packard, Goringhen, Netherlands). The mean recovery (i.e. the mean ^3H -GABA content in the perfusate as a percentage of the content in an equal volume of the vial solution) was $10.11 \pm 0.67\%$ at a flow rate of 2 $\mu\text{l}/\text{min}$ and $4.87 \pm 0.22\%$ at 3 $\mu\text{l}/\text{min}$ when using the MAB 4.15.1.Cu probe; $9.52 \pm 0.68\%$ at a flow rate of 2 $\mu\text{l}/\text{min}$ and $4.26 \pm 0.62\%$ at 3 $\mu\text{l}/\text{min}$ when using the CMA11Cu probe;

6.39 ± 0.22 at a flow rate of 2 $\mu\text{l}/\text{min}$ and $6.32 \pm 0.84\%$ at 3 $\mu\text{l}/\text{min}$ when using the polyacrylonitrile home-made probe; $5.06 \pm 0.21\%$ at a flow rate of 2 $\mu\text{l}/\text{min}$ and 4.73 ± 0.33 at 3 $\mu\text{l}/\text{min}$ when using the MAB 4.15.1.PES probe; and $4.36 \pm 0.33\%$ at a flow rate of 2 $\mu\text{l}/\text{min}$ and 2.30 ± 0.47 at 3 $\mu\text{l}/\text{min}$ when using the home-made cuprophane probe. Therefore, we chose to use the MAB 4.15.1.Cu probes perfused at a flow rate 2 $\mu\text{l}/\text{min}$.

Microdialysis procedure

Twenty-four h before the experiment, rats were briefly anesthetized with isoflurane and a vertical microdialysis probe, endowed with the 1 mm cuprophane dialyzing membrane (MAB 4.15.1.Cu; cut-off 6 kDa; outer diameter $300 \pm 5 \mu\text{m}$) was inserted in the guide cannula and fixed with modeling clay to the guide cannula support. At the day of the experiment, animals were EEG-monitored to verify absence of seizures for the 3 h preceding the initiation of sample collection. The animals were attached to an EEG hard-wire system and, at the same time, to the microdialysis pump (Univentor, model 864, Malta). The

microdialysis probe was perfused at a flow rate 2 $\mu\text{l}/\text{min}$ with a Ringer solution (composition, in mM: MgCl_2 0.85, KCl 2.7, NaCl 148, CaCl_2 1.2) with 0.3% BSA. Starting 1 h after the onset of perfusion, 5 basal samples were collected every 30 min. Stimulation was then applied as a 10 min perfusion with a modified Ringer solution containing 100 mM K^+ (equimolar compensation with Na^+ ; composition, in mM: MgCl_2 0.85, KCl 100, NaCl 50.7, CaCl_2 1.2, 0.3% BSA). From the onset of stimulation, dialysate samples were collected every 10 min. This stimulation procedure is known to produce a slight elevation in extracellular K^+ concentration near the dialyzing membrane (Largo et al., 1996) and, as a consequence to increase the efflux of several neurotransmitters, including GABA (Aparicio et al., 2004; Marti et al., 2000; Mazzuferi et al., 2005; Takeda et al., 2003). Perfusion of a hippocampal probe with high K^+ is known to evoke seizures in epilepsy models like kindling (Aparicio et al., 2004; Marti et al., 2000; Mazzuferi et al., 2005), thus EEG and behavior were recorded during the all microdialysis session. Routinely, the experiments were repeated for 3 days in 8 h microdialysis sessions, except for the acute phase and first seizure groups, in which a single microdialysis session was performed, respectively 24 h after SE or within 24 h after the first spontaneous seizure (Fig. 1A).

For determination of Ca^{2+} dependency and tetrodotoxin sensitivity of GABA outflow, we used naïve and early chronic rats. In separate microdialysis sessions, all rats were either continuously perfused with a normal Ringer solution; shifted to a perfusion buffer without Ca^{2+} after the third 30-min collection period; or shifted to a perfusion buffer containing 1 μM tetrodotoxin (TTX) after the third 30-min collection period. For characterization of the Ca^{2+} dependency and TTX sensitivity of high K^+ -evoked GABA outflow, the animals were perfused with normal Ringer solution, Ringer solution without Ca^{2+} or Ringer with 1 μM TTX during a 10-min stimulation with 100 mM K^+ (as described above).

Chromatography

GABA levels in the dialysate were measured with a high performance liquid chromatograph (HPLC) system comprising a Smartline Pump 1000 solvent delivery module (Knauer, Berlin, Germany), a HT300L autosampler (HTA, Brescia, Italy) and a Smartline Manager 5000 degasser plus system controller unit (Knauer, Berlin, Germany). HPLC was coupled with a RF-551 spectrofluorimetric detector (Shimadzu, Kyoto, Japan). GABA and interfering compounds were separated on a 250×4.6 mm, 5 μm particles, EUROSIL bioselect 300A column (LabService Analytica, Italy). The column was protected by a 5×4 mm precolumn containing the same packing. The mobile phase was a binary gradient between solution A (0.1 M sodium phosphate, pH 3.0) and solution B (40% 0.1 M sodium phosphate, 30% methanol, 30% acetonitrile, pH 4.0). Precolumn autoderivatization (2 min) and injection were done by the addition of 20 μl of the derivatization mixture containing phthalaldehyde (Sigma) and 5-mercaptoethanol (Merck), 20:1 (v/v) to 20 μl of dialysate. Elution was carried out at a rate of 0.9 ml/min at a temperature of 22 °C. Chromatograms were recorded 25 min at 345 nm excitation and 455 nm emission wavelengths. GABA retention time was 17.06 min. The method was validated and calibration was performed using standard samples prepared by spiking the Ringer solution and modified Ringer solution with GABA and amino acid standard solution for calibrating amino acid analyzers (Sigma). The sensitivity of the method was 0.16 pmol/20 μl sample according to the ICH Harmonised Tripartite Guideline (2005).

Quantification and statistics

The amounts of GABA in perfusates have been expressed either as absolute values (pmol/10 min) or as percent of basal outflow, as previously described (Mazzuferi et al., 2005). Basal values have been calculated as the mean amount of GABA measured in the last 3 spontaneous (basal) fractions collected before stimulus application. In animals in which multiple microdialysis sessions were performed (i.e. the latency and the two chronic groups), data from the 3 days were averaged to obtain a single estimate for each animal. Time-course curves were

expressed in absolute values (pmol/10 min) or as percent of basal values. High K^+ -evoked GABA overflow was calculated by subtracting the presumed basal outflow from the total outflow in the samples taken upon stimulus application and in the following 4 samples (5 collection periods, i.e. 50 min). The presumed basal outflow was obtained by interpolation between the samples preceding and following the above-mentioned 5 collection periods containing high K^+ -evoked overflow. The % high K^+ -evoked outflow was estimated by dividing the sum of the outflow in the samples taken upon stimulus application and in the following 4 by the presumed basal outflow, obtained as described above, and multiplying by 100. To analyze the data, one-way ANOVA and post hoc Dunnett's test ($p < 0.05$ and $p < 0.001$) or Mann-Whitney test (statistical significance at $p < 0.05$) were used, as indicated in the figure legends.

Immunohistochemistry and immunofluorescence

Tissue preparation

Rats were killed 1 h after completion of the microdialysis procedure by decapitation after an anesthetic overdose. Their brains were rapidly removed, immersed in 10% formalin, and paraffin embedded after 48 h. Coronal sections (6 μm thick) were cut across the entire hippocampus, plates 48–52 (Pellegrino et al., 1979) and mounted onto polarized slides (Superfrost slides, Diapath). To standardize the cutting level and to verify the correct probe placement, one section every 10 was used for hematoxylin-eosin staining. These sections were dewaxed (two washes in xylol for 10 min, 5 min in ethanol 100%, 5 min in ethanol 95%, 5 min in ethanol 80%), incubated in Mayer's hematoxylin solution 0.1% (Fluka, 5 min), washed in water (5 min), incubated in alcohol eosin solution 0.5% (Diapath, 2 min) and dehydrated; coverslips were mounted using DPX Mountant for histology (Fluka).

Procedure

Sections were dewaxed and rehydrated as described above. All antigens were unmasked using a commercially available kit (Unmasker, Diapath), according to the manufacturer's instructions. After washing in phosphate buffered saline (PBS), sections were incubated with Triton x-100 (Sigma; 0.3% in PBS 1 \times , room temperature, 10 min), washed twice in PBS 1 \times , and incubated with 5% BSA and 5% serum of the species in which the secondary antibody was produced for 30 min. They were incubated in humid atmosphere with the primary antibodies overnight at 4 °C, as follows: parvalbumin 1:100 (mouse monoclonal, Swant), somatostatin-14 1:250 (rabbit polyclonal, Peninsula Laboratories). Detection of parvalbumin was obtained using the biotin-streptavidin system associated with a 3,3'-diamino-benzidine tetrahydrochloride (DAB) substrate kit for peroxidase (Dako EnVision Dual Link System HRP, Dako). Somatostatin-14 was detected using a goat anti-rabbit, Alexa Fluor 594-conjugated, secondary antibody (1:1000, Invitrogen) at room temperature for 3 h. After staining the somatostatin-14 sections were washed in PBS, counterstained with 0.0001% 4',6-diamidino-2-phenylindole (DAPI, Sigma) for 10 min, and washed again. Coverslips were mounted using Shur/Mount (TBS).

Quantification and statistics

The number of parvalbumin or somatostatin positive cells was counted in 500,000 μm^2 frames, in three hippocampal subareas (CA1 including stratum oriens, pyramidale and radiatum; CA3 including stratum oriens, pyramidale, lucidum and radiatum; dentate gyrus, DG, including hilus, stratum granulare and moleculare), every 50th section (that is, one 6 μm thick section every 300 μm) of the left hippocampus, in the region contralateral to the one used for microdialysis. In this way, three sections spanning 0.9 mm of the central part of the hippocampus were evaluated in each animal. Images were acquired using a Leica DFC300 FX video camera mounted on a Leica DMRA2 microscope, captured with a 10 \times objective, and analyzed in a blinded manner by four investigators, using the program Leica FW 4000. Data obtained from

the multiple sections examined for each rat by the 4 investigators were averaged to obtain a single estimate for each animal. The counts of parvalbumin or somatostatin positive cells have been expressed first as absolute values (number of cells/frame), then as percent of cells in control animals. Data were analyzed using one-way ANOVA and post hoc the Dunnett's test.

Chemicals and solutions

Pilocarpine hydrochloride, scopolamine methylnitrate and xylazine hydrochloride were purchased from Sigma. TTX was purchased from Tocris. All drugs were freshly dissolved in isoosmotic saline solution just before use. Diazepam (Valium®, Roche), ketamine (Ketavet®, InterVet) and isoflurane (IsoFlo®, Esteve Farma) were used in their original fabricated form. 4-Aminobutyric acid, used as standard for chromatography, was from Fluka. Acetonitrile (HPLC grade) and methanol (HPLC grade) were purchased from Sigma. Sodium phosphate dibasic anhydrous (analytical grade) was from Fluka.

Results

Video-EEG

To verify that the animals employed in this study present the characteristics of epilepsy development and progression as extensively reported for the pilocarpine model, we performed behavioral and EEG monitoring at specific time points (Fig. 1A). Pilocarpine (370 mg/kg, i.p. 30 min after methyl-scopolamine 1 mg/kg) induced a robust convulsive SE (latency: 25 ± 5 min), which was interrupted after 3 h using diazepam (20 mg/kg, i.p.). For 2–3 days after SE, the animals experienced some occasional, self-limiting generalized seizures (less than 1 min duration) and then entered a latency state in which they were apparently well (Curia et al., 2008; Mazzuferi et al., 2010; Paradiso et al., 2009). Animals that were not killed in the acute group (24 h after SE), after being video-monitored for 5 days, were continuously video-EEG monitored for verification that no spontaneous seizures occurred in the first 9 days, for the latency group, or identification of the first spontaneous seizure, for the first seizure group. The first spontaneous seizure occurred 11.1 ± 0.6 days after SE (mean \pm SEM, $n = 18$). Thereafter, seizures occurred in clusters, as previously described (Goffin et al., 2007; Mazzuferi et al., 2010; Williams et al., 2009), and aggravated in time. In early chronic rats (from 18 to 24 days after SE) the mean daily frequency of generalized (classes 4 and 5) seizures was 1.0 ± 0.2 and the mean forelimb clonus duration was 7.4 ± 1.3 s (mean \pm SEM, $n = 10$), while in late chronic rats (days 55–62 after SE) the mean daily generalized seizure frequency was 2.5 ± 0.5 and the mean forelimb clonus duration 24 ± 3 s (mean \pm SEM, $n = 6$), indicating a progression of the disease (Fig. 2).

During the course of microdialysis experiments, rats were video-EEG monitored to evaluate the response to perfusion of high K^+ in the hippocampus. As shown in Fig. 3, animals in the control, acute and latency groups exhibited partial seizures of class 1 or 2, only rarely severe seizures. More severe seizures appeared to occur with the first spontaneous seizure and in the subsequent stages (time points) of the disease that we examined, but this phenomenon was not statistically significant. It is worth reporting, however, that the response in those animals was apparently distributed in a bi-modal fashion, with a subgroup exhibiting generalized seizures (stage 4 or 5) during high K^+ perfusion, and another subgroup responding with no seizures or non-convulsive seizures only (Fig. 3B). This bi-modal distribution may correlate with the variable vicinity between a cluster of spontaneous seizures and the microdialysis session. Interestingly, the duration of high K^+ evoked seizures was non-significantly reduced in the acute period, i.e. in the post-ictal phase after SE, and then progressively increased in the course of the disease (Fig. 3C).

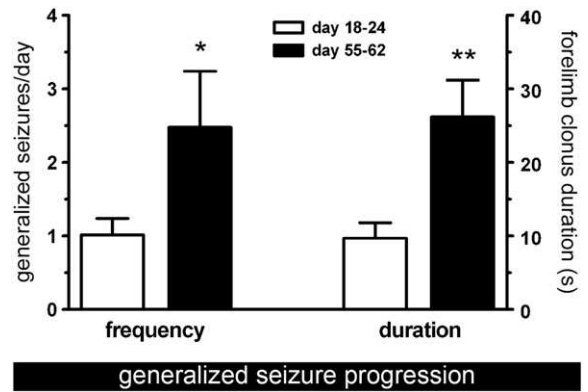


Fig. 2. Behavioral analysis. Average frequency (left Y axis) and forelimb clonus duration (right Y axis) of spontaneous generalized seizures (classes 4 and 5) in the early and late chronic period after pilocarpine induced-SE. Data are the mean \pm SEM of 10 (early chronic – open columns) and 6 (late chronic – solid columns) animals per group. * $p < 0.05$ and ** $p < 0.01$, Student's t-test for unpaired data.

GABA release

Basal, unstimulated GABA outflow was not significantly altered 24 h after SE, but progressively decreased thereafter, reaching a minimum at the time of the first seizure and then remaining constantly low (about 30% of control values) in the early and late chronic period (control group: 3.26 ± 0.12 pmol/10 min; acute: 2.65 ± 0.47 ; latency: 1.06 ± 0.19 ; first seizure: 0.83 ± 0.21 ; early chronic: 0.89 ± 0.15 ; late chronic: 0.86 ± 0.29 ; Fig. 4A). Perfusion with a solution containing high K^+ increased GABA outflow with peak 10 to 20 min after high K^+ perfusion, most likely due to the time needed for accumulation of K^+ in the extracellular spaces around the microdialysis probe (the time course of GABA outflow is shown in absolute values and in percent of basal values in Fig. 4B and C, respectively). Notably, whereas high K^+ perfusion led to a robust increase in GABA outflow in control and latency rats, its effect was very modest in chronic rats. In absolute values, in fact, the net high K^+ -evoked GABA overflow was significantly decreased at the time of the first seizure and in chronic animals (Fig. 4D). Probe perfusion with 100 mM K^+ in those animals achieved not even one third of the GABA overflow observed in control, acute and latency rats. However, because of the much lower basal outflow, the effect of high K^+ was proportionally greater during latency (Fig. 4C and E): when expressed as percent of basal levels, GABA overflow was the greatest in latency animals (up to $217 \pm 34\%$), robust in the control ($149 \pm 5\%$) and in the acute group ($179 \pm 12\%$), and much smaller, about 130%, in all other groups (1st seizure, early and late chronic). These data suggest that the reduced basal outflow of GABA during latency (Fig. 4A) is compensated by a relatively greater stimulus-evoked overflow (Fig. 4C and E), which was similar to the one observed under control conditions in absolute values (Fig. 4D). In contrast, GABA outflow reduction (i.e. impaired extracellular GABA concentrations) in the hippocampus occurs in conjunction with (and may therefore favor) the occurrence of spontaneous recurrent seizures. Importantly, GABA outflow was found reduced also in the subset of animals that responded to high K^+ perfusion with severe seizures (see above), i.e. extracellular GABA concentrations were equally impaired even under conditions when they were expected to be increased (During and Spencer, 1993; Thomas et al., 2005; Wilson et al., 1996). In fact, the high K^+ -evoked overflow in chronic animals experiencing generalized seizures was not significantly different ($p > 0.05$, Mann Whitney U test) from the one measured in animals that did not experienced generalized seizures (0.48 ± 0.16 vs. 0.63 ± 0.13 pmol in the convulsive vs. the non-convulsive seizure group).

These alterations in GABA extracellular concentrations were largely Ca^{2+} -dependent and TTX-sensitive. When Ca^{2+} was omitted from the perfusion buffer, the basal GABA outflow gradually declined to $41.3 \pm$

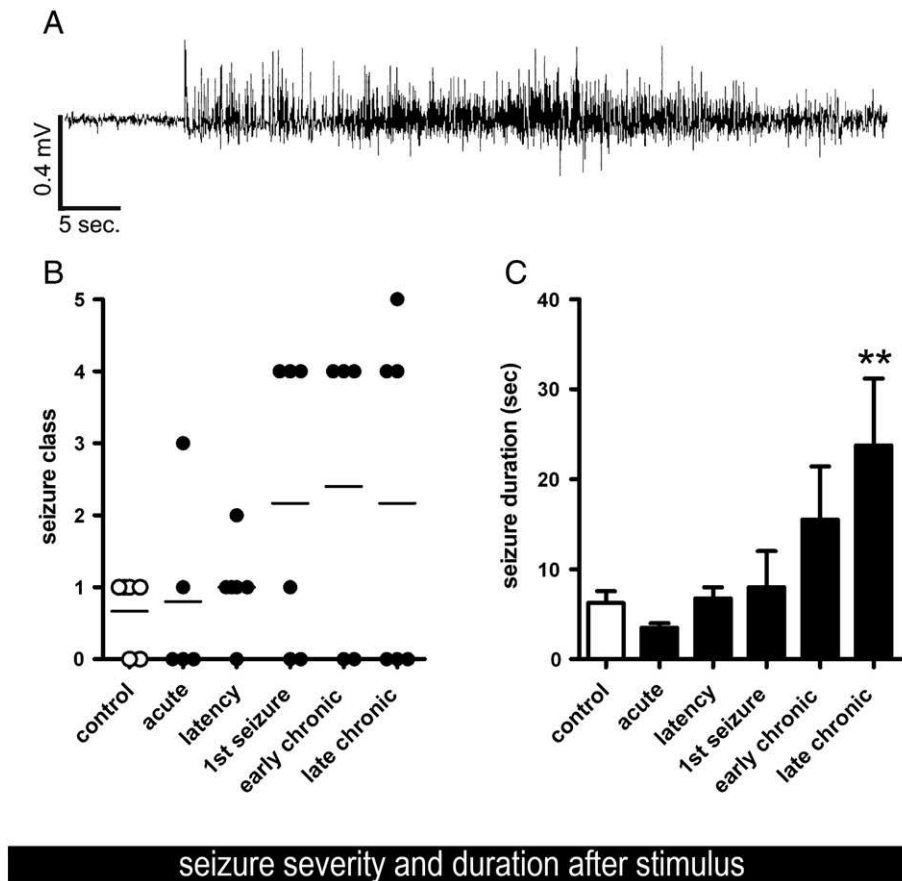


Fig. 3. Seizure activity in response to hippocampal perfusion with a 100 mM K^+ modified Ringer solution for 10 min. (A) Representative seizure evoked by high K^+ perfusion in a late chronic rat. (B) Seizure severity scored according to Racine (1972). (C) EEG-measured single seizure duration during the high K^+ stimulation. After the initial lack of response in rats 24 h after SE the duration of seizures progressively increases and reaches the maximum in late chronic animals. Data are the means \pm SEM of 5–6 animals per group. * $p < 0.05$, Kruskal–Wallis test and post hoc Dunn's test.

5.5% in control animals and to $51.8 \pm 6.8\%$ in early chronic rats (Fig. 5). TTX perfusion (1 μ M) also decreased the spontaneous efflux of GABA, in control rats to $21.7 \pm 5.4\%$ and in early chronic rats to $34.4 \pm 11.2\%$ of baseline levels (Fig. 5). Both omission of Ca^{2+} and TTX completely abolished the effect of the high K^+ stimulation (Fig. 5). These data suggest, even if not conclusively demonstrate, a significant contribution of neuronal exocytotic release to the observed epilepsy-associated alterations in GABA outflow.

Loss of GABA interneurons

The dramatic drop in basal, unstimulated GABA release observed beginning at the stage of latency might be caused by a loss of GABA neurons. To explore this possibility, immunohistochemistry and immunofluorescence experiments were performed on the brain of rats at the end of the microdialysis experiments, to estimate the number of parvalbumin and somatostatin-positive cells in the ventral hippocampus. These experiments revealed that the population of parvalbumin-positive cells decreased in the hippocampus of pilocarpine-treated animals. The loss of parvalbumin-positive cells was most rapid and dramatic in the hilus of the dentate gyrus, where it became significant already in the acute phase and further worsened until dropping to less than 10% of control values in the late chronic group (Fig. 6D). The loss of these cells was less dramatic and slower in CA3 (Fig. 6E) and especially in CA1, where it became significant only with the first seizures and did not drop below about 50% of control values (Fig. 6F). The loss of parvalbumin-positive cells that we observed in this study is in line with previously published reports (Andre et al., 2001; Chakir et al., 2006; Kuruba et al., 2011; Pavlov et al., 2011). Furthermore, we observed that the number of

somatostatin-positive cells in the hilus of the dentate gyrus also significantly decreased in pilocarpine-treated animals, reaching a minimum (about 50% of control values) in chronic animals (Fig. 7B). No significant variations were observed in the CA1 and CA3 region (data not shown).

Discussion

Main findings

Three key findings emerge from this study: (i) during the epileptogenesis (latent) period, loss of at least some sub-populations of GABA cells is already significant and basal GABA outflow is reduced but the response to high K^+ stimulation proportionally increases; (ii) at the time of the first spontaneous seizure this relatively increased responsiveness to stimulation disappeared; (iii) this dysfunction remains then constant until late phases of the disease.

These findings integrate previous observations, where an increased run-down of the $GABA_A$ current, a sign of impaired responsiveness of $GABA_A$ receptors to stimulation, began in the hippocampus at the time of the first spontaneous seizure (Mazzuferi et al., 2010). Thus, a dramatic impairment of GABA signal appears to take place exactly at the time of the first spontaneous seizure, when both reduced extracellular GABA levels and rapid receptor desensitization are observed. We propose that these phenomena represent a mechanism of transition from latency to spontaneous seizures, i.e., epilepsy. Once established, these maladaptive changes in the GABA system are constantly present in the chronic epileptic condition [see also (Mazzuferi et al., 2010)], arguing that they also underlie maintenance of the disease.

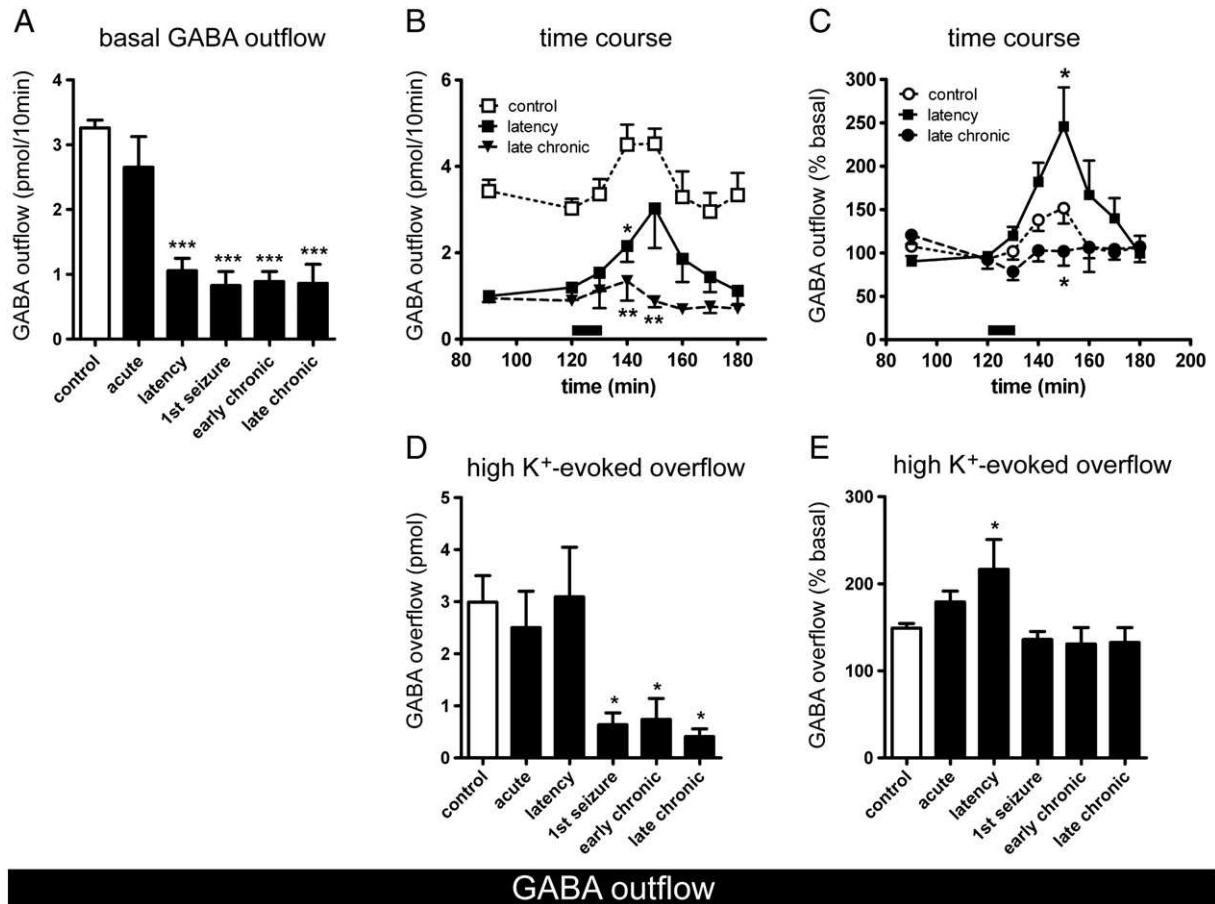


Fig. 4. (A) Spontaneous basal GABA outflow from the hippocampus of control (white column) and pilocarpine-treated (black columns) rats. Under basal conditions, extracellular GABA levels are significantly decreased in the hippocampus of pilocarpine rats, a phenomenon that starts during the latency period and continues at the time of the first spontaneous seizure and in the chronic state. (B) Time course of the effect of 10 min perfusion with 100 mM K⁺ (horizontal bar) on GABA outflow from the hippocampus of control (open squares), latency (filled squares) and late chronic rats (filled triangles). In control rats, GABA outflow increases from relatively high basal levels (3.46 ± 0.26 pmol/10 min) to reach 4.53 ± 0.35 pmol/10 min after the stimulus. Animals in the latency period respond to the high K⁺ increasing GABA outflow up to 3.03 ± 0.92 pmol/10 min, whereas animals in the late chronic phase react very moderately. For clarity, the profiles in acute, 1st seizure and early chronic animals are not shown. However, the one in acute animals was similar to that in controls and those in 1st seizure and in early chronic animals were similar to that in late chronic. (C) Time course of the effect of 10 min perfusion with 100 mM K⁺ (horizontal bar) on GABA outflow from the hippocampus of control (open circles), latency (filled squares) and late chronic (filled circles) rats. Animals in the latency period respond to the stimulus increasing GABA release up to about 246%, while animals in the late chronic phase do not react at all. For clarity, the profiles in acute, 1st seizure and early chronic animals are not shown. However, the one in acute animals was similar to that in controls and those in 1st seizure and in early chronic animals were similar to that in late chronic. (D) High (100 mM) K⁺-evoked GABA overflow from the hippocampus of control (white column) and pilocarpine-treated (black column) rats. Note the dramatic drop in GABA overflow beginning at the time of the first seizure. See [Materials and methods](#) for details on the quantification. (E) Effect of 100 mM K⁺ perfusion on GABA outflow, expressed as percent of basal release. Data are the means \pm SEM of 5–6 rats per group. * $p < 0.05$, *** $p < 0.001$; one-way ANOVA and post hoc Dunnett's test in (A, B and D); Mann–Whitney U test in (C, E).

GABA microdialysis

Microdialysis sampling can provide significant insights into brain function, but has some limitations that should be kept in mind. The first is that the dialysis membrane extends across a relatively wide area, in our case including different hippocampal subfields (not only dentate gyrus but also CA3 and CA1). Thus, the data are an estimate of the GABA extracellular concentrations in all these different subregions. Another relevant limitation is that microdialysis probes reside at distance from the synaptic gap and measure the extracellular concentrations of neurotransmitters, i.e. the result of molecules released into and removed from the extracellular space by neurons, glial cells and other non-neuronal cells. Therefore, measured neurotransmitter levels depend not only on release but also on reuptake. Other factors, like extracellular space volume (which diminishes with age), alterations in the extracellular matrix and environmental factors (for example, tissue damage associated with the probe's insertion and substances entering from the bloodstream) may also influence the measures. Moreover, the relative contribution of neurons and astrocytes to the dialyzed neurotransmitter may be modified by activity. A widely employed strategy

to stimulate neurotransmitter release is the elevation of K⁺ concentrations in the microdialysis perfusion fluid. Passive diffusion of K⁺ across the microdialysis membrane into the tissue will raise extracellular concentrations and induce neuronal depolarization and neurotransmitter release, in principle not only from neurons but also from glia (Stiller et al., 2003).

One way to estimate what part of the dialysate content is of neuronal origin is to establish if the signal fulfills the two classical criteria of neurotransmitter release, Na⁺- and Ca²⁺-dependency, by using TTX and abolishing Ca²⁺ from the perfusion medium. Data generated in this manner should nonetheless be interpreted with caution for GABA, since its release from astrocytes may be also, at least partly, Ca²⁺-dependent (Lee et al., 2010, 2011).

With specific reference to microdialysis measured GABA, action potential-dependent release from neuronal presynaptic vesicles has been shown to be a major source of the ambient transmitter (Glykys and Mody, 2007). The remaining GABA probably originates from astrocytes (Lee et al., 2010; Yoon et al., 2011) and is released in a non-vesicular manner by reversed plasma membrane transport (Rossi et al., 2003). Indeed, GAT-3, a GABA transporter specifically expressed

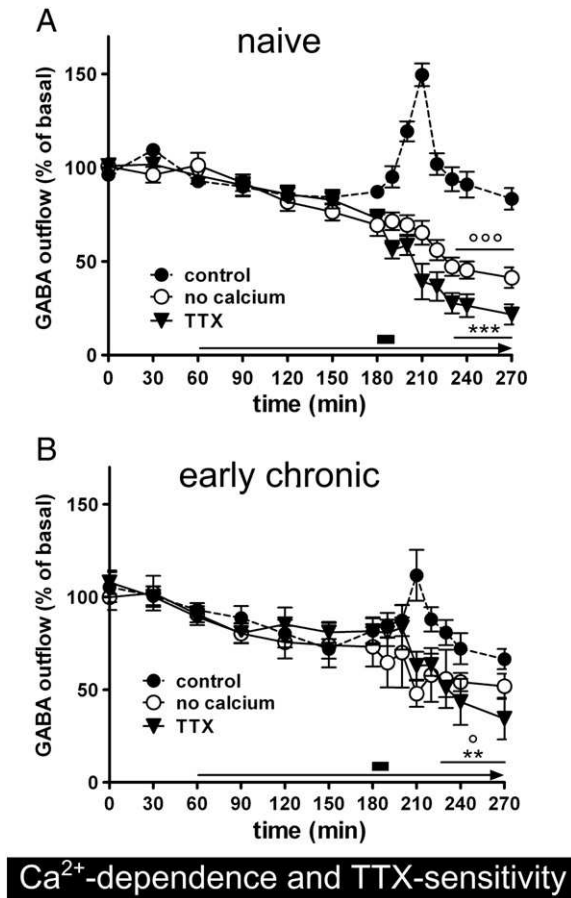


Fig. 5. Ca^{2+} -dependence and TTX-sensitivity of the spontaneous and stimulated GABA outflow from the hippocampus of naïve, non-epileptic rats (A) and early chronic rats (B) perfused with a normal Ringer solution (solid circles), Ringer without Ca^{2+} (open circles), or a Ringer solution containing $1 \mu\text{M}$ TTX (triangles). Perfusion of Ringer without Ca^{2+} or with TTX is indicated by an arrow. The 10 min perfusion with high K^+ (black bar) is indicated by a black box above the arrow. Data are presented as a percentage of basal values (average of the three samples preceding Ca^{2+} omission or TTX application) and are the mean \pm SEM of 5–6 animals. $^{\circ}p < 0.05$, $^{\circ\circ}p < 0.001$, no calcium vs. respective values in normal Ringer; $^{\circ\circ}p < 0.01$, $^{\circ\circ\circ}p < 0.001$ TTX vs. respective values in normal Ringer; Mann–Whitney U-test.

in astrocytes, has been shown to significantly contribute to the regulation of extracellular GABA levels (Kersante et al., 2013). In the present study, both the basal and the high K^+ -evoked GABA outflow from the hippocampus of naïve animals were in the range reported by others (de Groote and Linthorst, 2007; Lasley and Gilbert, 2002; Luna-Munguia et al., 2012; Portelli et al., 2009; Takeda et al., 2003; Tong et al., 2009; Wislowska-Stanek et al., 2008). About 50% of the basal outflow and almost all K^+ -evoked GABA overflow were Ca^{2+} -dependent, again in agreement with previous findings (Lasley and Gilbert, 2002). Finally, again similar with our data, the local administration of TTX decreased extracellular GABA to approximately 25% of baseline levels in earlier reports (de Groote and Linthorst, 2007; Kersante et al., 2013).

To our best knowledge, the spontaneous GABA outflow during the development of TLE has never been measured before. Thus far, the attempts to correlate the dynamic changes of extracellular GABA concentrations in the epileptic hippocampus with the occurrence of spontaneous seizures have been limited, and deal with the sole epileptogenic insult (SE). Pilocarpine has been reported to cause a short-lasting (2–3 h) elevation of extracellular GABA concentrations in the hippocampus (Khongsombat et al., 2008; Meurs et al., 2008; Smolders et al., 2004), and no changes were observed at 24 h (Goffin et al., 2007). Whereas previous studies limited measurement of extracellular GABA levels to

the first short period after pilocarpine-induced SE, we studied in detail the subsequent phases of the disease, and disclosed a progressive decrease of basal GABA outflow in epileptic animals, initiating during the latency period and reaching a minimum at the time of the first spontaneous seizure. We also observed that the basal GABA outflow then remained steadily low in chronic animals. Data from a microdialysis study in the kindling model support these findings, because a low interictal GABA release was revealed in fully kindled rats (Luna-Munguia et al., 2011). On the other hand, no changes in extracellular GABA levels were observed in chronic rats following intra-hippocampal injection of kainate (Liu et al., 2012). Differences in the epilepsy model (pilocarpine and kindling vs. intra-hippocampal kainate) may account for this discrepancy: one hypothesis could be that the loss of GABAergic cells is less pronounced with the intra-hippocampal kainate procedure employed by Liu et al. (2012).

We also found that GABA outflow from the hippocampus of chronic rats (unlike in control, acute and latency rats) was not significantly increased by high potassium stimulation, in spite of evoking relatively severe seizures. The impaired response to stimulation in epileptic animals begins at the time of the first spontaneous seizure, and is in sharp contrast with a highly increased response during latency. We speculate that this GABAergic hyper-responsiveness during latency contributes to maintain an appropriate inhibitory control and to prevent seizure occurrence despite the significant loss of GABA neurons. In keeping with this idea, (1) high K^+ perfusion evoked short partial seizures during latency but could evoke generalized seizures in chronic animals, i.e. the hippocampus seems less likely to develop seizures during latency; (2) we observed reduction of GABA outflow at the time of the first spontaneous seizure, and the exhaustion of pre-synaptic GABA release has been shown to herald the onset of ictal events in the hippocampal formation in mice (Zhang et al., 2012). Importantly, this exhaustion of pre-synaptic GABA release capacity seems to occur at the same time of the increased post-synaptic GABA_A current rundown, i.e. of GABA_A receptor desensitization (Mazzuferi et al., 2010). Together, these events are expected to lead to a severe impairment of GABA inhibitory control and to strongly favor the occurrence of spontaneous seizures, i.e. lead to the transition from latency to epilepsy.

GABA cell loss

The loss of GABA neurons has been extensively studied in the past and a detailed analysis was beyond the scope of this study. To guesstimate the contribution of cell loss to the observed changes in GABA outflow, however, we studied two classes of GABA interneurons that are known to be particularly vulnerable to epileptogenic insults (namely somatostatin- and parvalbumin-positive interneurons) in the hippocampi of the animals employed for microdialysis. Somatostatin- and parvalbumin-positive cells are estimated to account for about one third of GABA interneurons in the dentate gyrus (Buckmaster and Dudek, 1997).

These cells have been found to be damaged after SE in animal models (Chakir et al., 2006; Drexel et al., 2011; Paradiso et al., 2011). It has been estimated that about 80% of the missing GABAergic neurons in kainate treated rats are somatostatin-positive (Buckmaster and Jongen-Relo, 1999), and that nearly 80% of somatostatin-containing cell in the hilus die following pilocarpine SE in mice (Peng et al., 2013). More limited loss of somatostatin-immunoreactive cells was reported in other models (Buckmaster and Jongen-Relo, 1999; Dinocourt et al., 2003; Gorter et al., 2001). Parvalbumin-positive cells have also been reported to die in various epilepsy models, although in a maybe less dramatic manner compared with those somatostatin-positive (Andre et al., 2001; Gill et al., 2010; Gorter et al., 2001; Marx et al., 2013; Sun et al., 2007). In particular, a progressive reduction of parvalbumin-positive GABAergic neurons in dentate gyrus, CA1 and CA3 was described in the pilocarpine model (Drexel et al., 2011; Knopp et al., 2008; Kuruba et al., 2011; Pavlov et al., 2011).

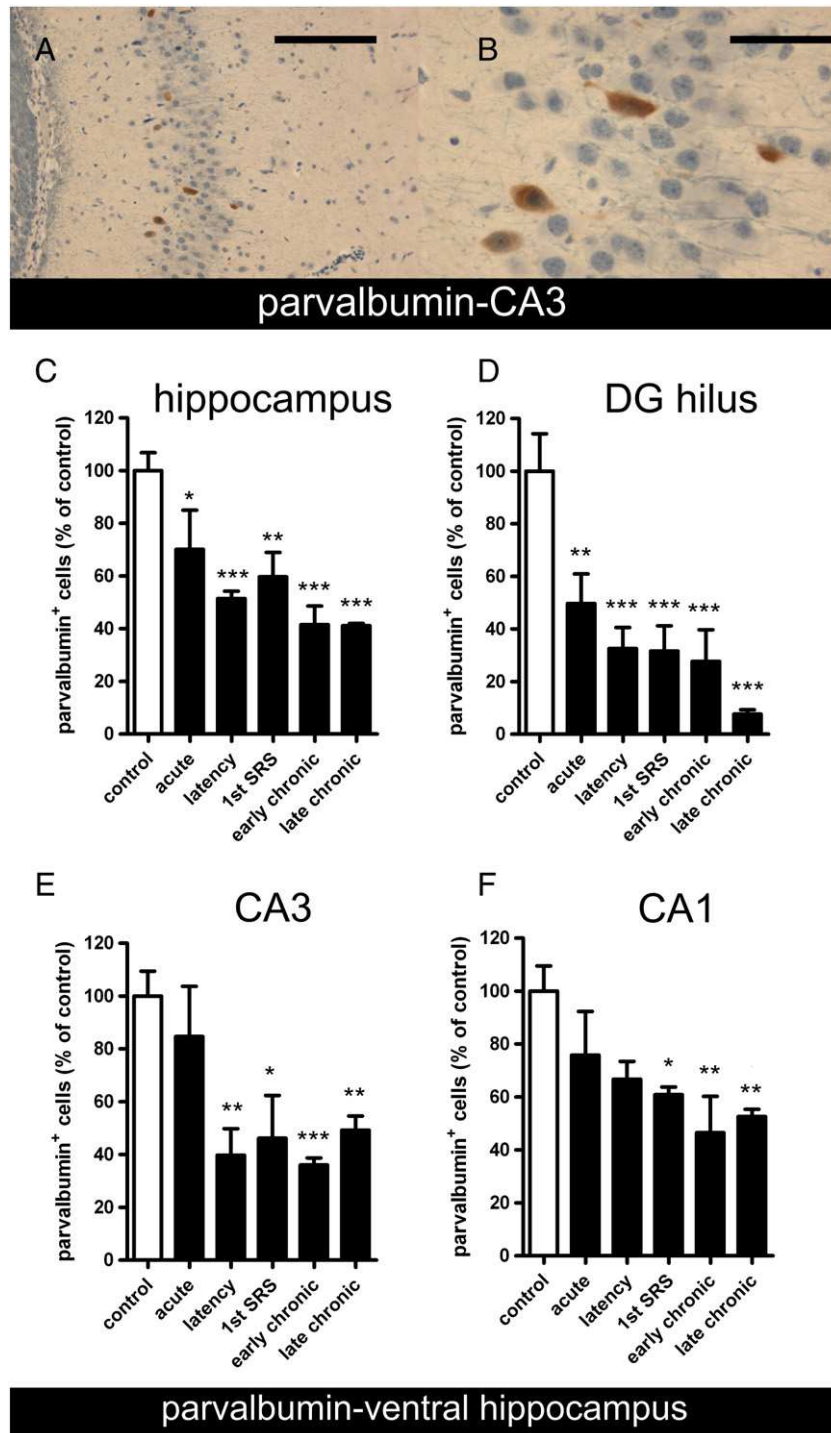


Fig. 6. Parvalbumin positive cell loss at various time points after pilocarpine induced SE. (A) and (B) Representative parvalbumin positive cells (brown – DAB; cell nuclei in blue – hematoxylin) in the CA3 area of a pilocarpine rat during the latency period, 9 days after SE. (B) is a higher magnification of (A). Horizontal bar: 1 mm in (A) and 75 μ m in (B). (C–F) Quantification of parvalbumin cells loss in the whole ventral hippocampus (C), hilus of DG (D), CA3 (E) and CA1 (F). Control values are in the white column, values in pilocarpine-treated rats in the black columns. See **Materials and methods** for details on calculations. Note the rapid loss of parvalbumin positive cells in the hilus of the dentate gyrus early after the SE and the massive loss in late chronic animals (D). The data are the means \pm SEM of 5–6 animals per group. * $p < 0.05$, ** $p < 0.01$, *** $p < 0.001$ vs. control; one-way ANOVA and post hoc Dunnett's test.

These findings were confirmed in human tissue. The density of parvalbumin- (Andrioli et al., 2007) and of somatostatin-positive interneurons (Sundstrom et al., 2001) in the hippocampal formation was significantly reduced in TLE patients compared with autopsy controls. As in the present study, all above mentioned works rely

on immunohistochemical localization of neurochemical markers, and therefore it is difficult to establish whether a loss of immunostaining is due to the actual loss of the particular cell type, or if the marker expression diminished below detection threshold while the cell was still functional. However, double labeling studies with the

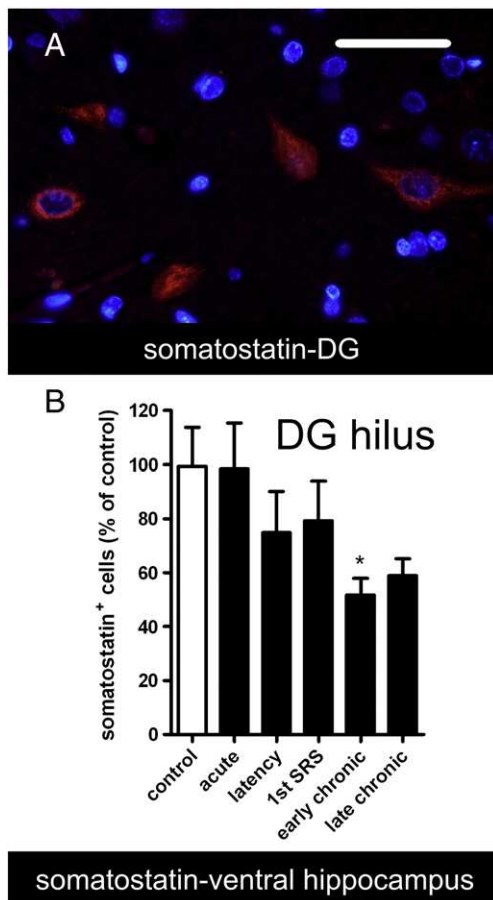


Fig. 7. Somatostatin positive cells loss at various time points after pilocarpine induced SE. (A) Representative somatostatin positive cell (red immunofluorescence) in the hilus of the dentate gyrus of a late chronic animal. Nuclei (DAPI labeled) in blue. Horizontal bar: 75 μ m. (B) Quantification of somatostatin-positive cells in the DG hilus. See **Materials and methods** for details on calculations. Note the significant loss of somatostatin positive interneurons in early chronic animals. No significant change in somatostatin-positive cells was observed in the CA1 and CA3 regions (data not shown). The data are the means \pm SEM of 5–6 animals per group. * $p < 0.05$; one-way ANOVA and post hoc Dunnett's test.

neuronal degeneration marker Fluoro-Jade B revealed loss of both somatostatin (Sun et al., 2007) and parvalbumin-expressing interneurons (Huusko et al., 2013) in epilepsy models.

Our findings are in line with those published previously. We found that the number of parvalbumin-positive cells in pilocarpine treated animals reduces gradually during the course of the disease, alongside the decrease in basal GABA outflow. In particular, the loss of parvalbumin-positive neurons was most rapid and advanced in the dentate gyrus, where it became significant already in the acute phase, whereas it was less dramatic and slower in the CA3 and especially in the CA1 region, where it became significant only with the first spontaneous seizure. We also observed that the number of GABAergic somatostatin-positive cells in the hilus of the dentate gyrus also decreased, reaching its minimum in the chronic period.

As mentioned above, however, it should be kept in mind that more than 20 different subtypes of GABA interneurons have been identified in the hippocampus (Tepper et al., 2010) and some of them, in particular calretinin and calbindin-positive interneurons, have been shown to degenerate or even disappear in animal models of TLE (Bouillere et al., 2000; van Vliet et al., 2004). These findings lend further support to the hypothesis that death of GABA neurons, and the consequently reduced GABA release, in the hippocampus favors (or rather sustains) epileptiform activity.

Conclusions

Speculatively, the present data suggest that a GABAergic hyper-responsiveness may protect from the occurrence of seizures during latency, while impaired GABA release in the hippocampus may favor the occurrence of spontaneous recurrent seizures and the maintenance of an epileptic state. Further studies will be needed to validate this hypothesis, in particular with reference to altered chloride regulation occurring in epilepsy that reduces GABA inhibitory efficacy (Pathak et al., 2007). A better understanding of the (mal)adaptive changes occurring in the GABA system in the natural course of the disease will be important to design rational therapeutic approaches.

Acknowledgments

This study was supported by a grant from the Italian Ministry for the University (Prin 2009, to EP and EG).

References

- Andre, V., Marescaux, C., Nehlig, A., Fritschy, J.M., 2001. Alterations of hippocampal GABAergic system contribute to development of spontaneous recurrent seizures in the rat lithium-pilocarpine model of temporal lobe epilepsy. *Hippocampus* 11, 452–468.
- Andrioli, A., Alonso-Nanclares, L., Arellano, J.I., DeFelipe, J., 2007. Quantitative analysis of parvalbumin-immunoreactive cells in the human epileptic hippocampus. *Neuroscience* 149, 131–143.
- Aparicio, L.C., Candeletti, S., Binaschi, A., Mazzuferi, M., Mantovani, S., Di Benedetto, M., Landuzzi, D., Lopetuso, G., Romualdi, P., Simonato, M., 2004. Kainate seizures increase nociceptin/orphanin FQ release in the rat hippocampus and thalamus: a microdialysis study. *J. Neurochem.* 91, 30–37.
- Bouillere, V., Loup, F., Kiener, T., Marescaux, C., Fritschy, J.M., 2000. Early loss of interneurons and delayed subunit-specific changes in GABA(A)-receptor expression in a mouse model of mesial temporal lobe epilepsy. *Hippocampus* 10, 305–324.
- Buckmaster, P.S., Dudek, F.E., 1997. Neuron loss, granule cell axon reorganization, and functional changes in the dentate gyrus of epileptic kainate-treated rats. *J. Comp. Neurol.* 385, 385–404.
- Buckmaster, P.S., Jongen-Reilo, A.L., 1999. Highly specific neuron loss preserves lateral inhibitory circuits in the dentate gyrus of kainate-induced epileptic rats. *J. Neurosci.* 19, 9519–9529.
- Chakir, A., Fabene, P.F., Ouazzani, R., Bentivoglio, M., 2006. Drug resistance and hippocampal damage after delayed treatment of pilocarpine-induced epilepsy in the rat. *Brain Res. Bull.* 71, 127–138.
- Cossart, R., Bernard, C., Ben-Ari, Y., 2005. Multiple facets of GABAergic neurons and synapses: multiple fates of GABA signalling in epilepsies. *Trends Neurosci.* 28, 108–115.
- Curia, G., Longo, D., Biagini, G., Jones, R.S., Avoli, M., 2008. The pilocarpine model of temporal lobe epilepsy. *J. Neurosci. Methods* 172, 143–157.
- de Groote, L., Linthorst, A.C., 2007. Exposure to novelty and forced swimming evoke stressor-dependent changes in extracellular GABA in the rat hippocampus. *Neuroscience* 148, 794–805.
- Dinocourt, C., Petanjek, Z., Freund, T.F., Ben-Ari, Y., Esclapez, M., 2003. Loss of interneurons innervating pyramidal cell dendrites and axon initial segments in the CA1 region of the hippocampus following pilocarpine-induced seizures. *J. Comp. Neurol.* 459, 407–425.
- Drexel, M., Preidt, A.P., Kirchmair, E., Sperk, G., 2011. Parvalbumin interneurons and calretinin fibers arising from the thalamic nucleus reuniens degenerate in the subiculum after kainic acid-induced seizures. *Neuroscience* 189, 316–329.
- During, M.J., Spencer, D.D., 1993. Extracellular hippocampal glutamate and spontaneous seizure in the conscious human brain. *Lancet* 341, 1607–1610.
- Gill, D.A., Ramsay, S.L., Tasker, R.A., 2010. Selective reductions in subpopulations of GABAergic neurons in a developmental rat model of epilepsy. *Brain Res.* 1331, 114–123.
- Glykys, J., Mody, I., 2007. The main source of ambient GABA responsible for tonic inhibition in the mouse hippocampus. *J. Physiol.* 582, 1163–1178.
- Goffin, K., Nissinen, J., Van, L.K., Pitkanen, A., 2007. Cyclicity of spontaneous recurrent seizures in pilocarpine model of temporal lobe epilepsy in rat. *Exp. Neurol.* 205, 501–505.
- Gorter, J.A., van Vliet, E.A., Aronica, E., Lopes da Silva, F.H., 2001. Progression of spontaneous seizures after status epilepticus is associated with mossy fibre sprouting and extensive bilateral loss of hilar parvalbumin and somatostatin-immunoreactive neurons. *Eur. J. Neurosci.* 13, 657–669.
- Houser, C.R., Esclapez, M., 1996. Vulnerability and plasticity of the GABA system in the pilocarpine model of spontaneous recurrent seizures. *Epilepsy Res.* 26, 207–218.
- Huusko, N., Romer, C., Ndode-Ekane, X.E., Lukasiuk, K., Pitkanen, A., 2013. Loss of hippocampal interneurons and epileptogenesis: a comparison of two animal models of acquired epilepsy. *Brain Struct. Funct.* <http://dx.doi.org/10.1007/s00429-013-0644-1>.
- ICH Harmonised Tripartite Guideline, 2005. Validation of analytical procedures: text and methodology Q2(R1). International Conference of Harmonization of Technical Requirements for Registration of Pharmaceuticals for Human Use. Inter. ICH Global Cooperation Group.

- Kersante, F., Rowley, S.C., Pavlov, I., Gutierrez-Mecinas, M., Semyanov, A., Reul, J.M., Walker, M.C., Linthorst, A.C., 2013. A functional role for both γ -aminobutyric acid (GABA) transporter-1 and GABA transporter-3 in the modulation of extracellular GABA and GABAergic tonic conductances in the rat hippocampus. *J. Physiol.* 591, 2429–2441.
- Khongsombot, O., Watanabe, H., Tantisira, B., Patarapanich, C., Tantisira, M.H., 2008. Acute effects of N-(2-propylpentanoyl)urea on hippocampal amino acid neurotransmitters in pilocarpine-induced seizure in rats. *Epilepsy Res.* 79, 151–157.
- Knopp, A., Frahm, C., Fidzinski, P., Witte, O.W., Behr, J., 2008. Loss of GABAergic neurons in the subiculum and its functional implications in temporal lobe epilepsy. *Brain* 131, 1516–1527.
- Kuruba, R., Hattiangady, B., Parihar, V.K., Shuai, B., Shetty, A.K., 2011. Differential susceptibility of interneurons expressing neuropeptide Y or parvalbumin in the aged hippocampus to acute seizure activity. *PLoS One* 6, e24493.
- Largo, C., Cuevas, P., Somjen, G.G., Martin, R.R., Herreras, O., 1996. The effect of depressing glial function in rat brain in situ on ion homeostasis, synaptic transmission, and neuron survival. *J. Neurosci.* 16, 1219–1229.
- Lasley, S.M., Gilbert, M.E., 2002. Rat hippocampal glutamate and GABA release exhibit biphasic effects as a function of chronic lead exposure level. *Toxicol. Sci.* 66, 139–147.
- Lee, S., Yoon, B.E., Berglund, K., Oh, S.J., Park, H., Shin, H.S., Augustine, G.J., Lee, C.J., 2010. Channel-mediated tonic GABA release from glia. *Science* 330, 790–796.
- Lee, M., McGeer, E.G., McGeer, P.L., 2011. Mechanisms of GABA release from human astrocytes. *Glia* 59, 1600–1611.
- Liu, H.G., Yang, A.C., Meng, D.W., Chen, N., Zhang, J.G., 2012. Stimulation of the anterior nucleus of the thalamus induces changes in amino acids in the hippocampi of epileptic rats. *Brain Res.* 1477, 37–44.
- Luna-Munguia, H., Orozco-Suarez, S., Rocha, L., 2011. Effects of high frequency electrical stimulation and R-verapamil on seizure susceptibility and glutamate and GABA release in a model of phenytoin-resistant seizures. *Neuropharmacology* 61, 807–814.
- Luna-Munguia, H., Meneses, A., Pena-Ortega, F., Gaona, A., Rocha, L., 2012. Effects of hippocampal high-frequency electrical stimulation in memory formation and their association with amino acid tissue content and release in normal rats. *Hippocampus* 22, 98–105.
- Marti, M., Bregola, G., Morari, M., Gemignani, A., Simonato, M., 2000. Somatostatin release in the hippocampus in the kindling model of epilepsy: a microdialysis study. *J. Neurochem.* 74, 2497–2503.
- Marx, M., Haas, C.A., Haussler, U., 2013. Differential vulnerability of interneurons in the epileptic hippocampus. *Front. Cell. Neurosci.* 7, 167.
- Mazzuferi, M., Binaschi, A., Rodi, D., Mantovani, S., Simonato, M., 2005. Induction of B1 bradykinin receptors in the kindled hippocampus increases extracellular glutamate levels: a microdialysis study. *Neuroscience* 135, 979–986.
- Mazzuferi, M., Palma, E., Martinello, K., Maiolino, F., Roseti, C., Fucile, S., Fabene, P.F., Schio, F., Pellitteri, M., Sperk, G., Miledi, R., Eusebi, F., Simonato, M., 2010. Enhancement of GABA(A)-current run-down in the hippocampus occurs at the first spontaneous seizure in a model of temporal lobe epilepsy. *Proc. Natl. Acad. Sci. U. S. A.* 107, 3180–3185.
- Meurs, A., Clinckers, R., Ebinger, G., Michotte, Y., Smolders, I., 2008. Seizure activity and changes in hippocampal extracellular glutamate, GABA, dopamine and serotonin. *Epilepsy Res.* 78, 50–59.
- Obenaus, A., Esclapez, M., Houser, C.R., 1993. Loss of glutamate decarboxylase mRNA-containing neurons in the rat dentate gyrus following pilocarpine-induced seizures. *J. Neurosci.* 13, 4470–4485.
- Palma, E., Roseti, C., Maiolino, F., Fucile, S., Martinello, K., Mazzuferi, M., Aronica, E., Manfredi, M., Esposito, V., Cantore, G., Miledi, R., Simonato, M., Eusebi, F., 2007. GABA(A)-current rundown of temporal lobe epilepsy is associated with repetitive activation of GABA(A) “phasic” receptors. *Proc. Natl. Acad. Sci. U. S. A.* 104, 20944–20948.
- Pan, J.W., Cavus, I., Kim, J., Hetherington, H.P., Spencer, D.D., 2008. Hippocampal extracellular GABA correlates with metabolism in human epilepsy. *Metab. Brain Dis.* 23, 457–468.
- Paradiso, B., Marconi, P., Zucchini, S., Berto, E., Binaschi, A., Bozac, A., Buzzi, A., Mazzuferi, M., Magri, E., Navarro, M.G., Rodi, D., Su, T., Volpi, I., Zanetti, L., Marzola, A., Manservigi, R., Fabene, P.F., Simonato, M., 2009. Localized delivery of fibroblast growth factor-2 and brain-derived neurotrophic factor reduces spontaneous seizures in an epilepsy model. *Proc. Natl. Acad. Sci. U. S. A.* 106, 7191–7196.
- Paradiso, B., Zucchini, S., Su, T., Bovolenta, R., Berto, E., Marconi, P., Marzola, A., Navarro, M. G., Fabene, P.F., Simonato, M., 2011. Localized overexpression of FGF-2 and BDNF in hippocampus reduces mossy fiber sprouting and spontaneous seizures up to 4 weeks after pilocarpine-induced status epilepticus. *Epilepsia* 52, 572–578.
- Pathak, H.R., Weissinger, F., Terunuma, M., Carlson, G.C., Hsu, F.C., Moss, S.J., Coulter, D.A., 2007. Disrupted dentate granule cell chloride regulation enhances synaptic excitability during development of temporal lobe epilepsy. *J. Neurosci.* 27, 14012–14022.
- Pavlov, I., Huusko, N., Drexel, M., Kirchmair, E., Sperk, G., Pitkanen, A., Walker, M.C., 2011. Progressive loss of phasic, but not tonic, GABA_A receptor-mediated inhibition in dentate granule cells in a model of post-traumatic epilepsy in rats. *Neuroscience* 194, 208–219.
- Pellegrino, L.J., Pellegrino, A.S., Cushman, A.J., 1979. *A Stereotaxic Atlas of the Rat Brain*. Plenum Press, New York and London.
- Peng, Z., Zhang, N., Wei, W., Huang, C.S., Cetina, Y., Otis, T.S., Houser, C.R., 2013. A reorganized GABAergic circuit in a model of epilepsy: evidence from optogenetic labeling and stimulation of somatostatin interneurons. *J. Neurosci.* 33, 14392–14405.
- Pitkanen, A., Sutula, T.P., 2002. Is epilepsy a progressive disorder? Prospects for new therapeutic approaches in temporal-lobe epilepsy. *Lancet Neurol.* 1, 173–181.
- Portelli, J., Aourz, N., De, B.D., Meurs, A., Smolders, I., Michotte, Y., Clinckers, R., 2009. Intrastrain differences in seizure susceptibility, pharmacological response and basal neurochemistry of Wistar rats. *Epilepsy Res.* 87, 234–246.
- Racine, R.J., 1972. Modification of seizure activity by electrical stimulation. II. Motor seizure. *Electroencephalogr. Clin. Neurophysiol.* 32, 281–294.
- Ragozzino, D., Palma, E., Di, A.S., Amici, M., Mascia, A., Arcella, A., Giangaspero, F., Cantore, G., Di, G.G., Manfredi, M., Esposito, V., Quarato, P.P., Miledi, R., Eusebi, F., 2005. Run-down of GABA type A receptors is a dysfunction associated with human drug-resistant mesial temporal lobe epilepsy. *Proc. Natl. Acad. Sci. U. S. A.* 102, 15219–15223.
- Rossi, D.J., Hamann, M., Attwell, D., 2003. Multiple modes of GABAergic inhibition of rat cerebellar granule cells. *J. Physiol.* 548, 97–110.
- Smolders, I., Van, B.K., Ebinger, G., Michotte, Y., 1997. Hippocampal and cerebellar extracellular amino acids during pilocarpine-induced seizures in freely moving rats. *Eur. J. Pharmacol.* 319, 21–29.
- Smolders, I., Lindekens, H., Clinckers, R., Meurs, A., O'Neill, M.J., Lodge, D., Ebinger, G., Michotte, Y., 2004. In vivo modulation of extracellular hippocampal glutamate and GABA levels and limbic seizures by group I and II metabotropic glutamate receptor ligands. *J. Neurochem.* 88, 1068–1077.
- Sperk, G., Marksteiner, J., Gruber, B., Bellmann, R., Mahata, M., Ortler, M., 1992. Functional changes in neuropeptide Y- and somatostatin-containing neurons induced by limbic seizures in the rat. *Neuroscience* 50, 831–846.
- Stiller, C.O., Taylor, B.K., Linderoth, B., Gustafsson, H., Warsame, A.A., Brodin, E., 2003. Microdialysis in pain research. *Adv. Drug Deliv. Rev.* 55, 1065–1079.
- Sun, C., Mchedlishvili, Z., Bertram, E.H., Erisir, A., Kapur, J., 2007. Selective loss of dentate hilar interneurons contributes to reduced synaptic inhibition of granule cells in an electrical stimulation-based animal model of temporal lobe epilepsy. *J. Comp. Neurol.* 500, 876–893.
- Sundstrom, L.E., Brana, C., Gatherer, M., Mephram, J., Rougier, A., 2001. Somatostatin- and neuropeptide Y-synthesizing neurones in the fascia dentata of humans with temporal lobe epilepsy. *Brain* 124, 688–697.
- Takeda, A., Hirate, M., Tamano, H., Oku, N., 2003. Release of glutamate and GABA in the hippocampus under zinc deficiency. *J. Neurosci. Res.* 72, 537–542.
- Tepper, J.M., Tecuapetla, F., Koos, T., Ibanez-Sandoval, O., 2010. Heterogeneity and diversity of striatal GABAergic interneurons. *Front. Neuroanat.* 4, 150.
- Thomas, P.M., Phillips, J.P., O'Connor, W.T., 2005. Microdialysis of the lateral and medial temporal lobe during temporal lobe epilepsy surgery. *Surg. Neurol.* 63, 70–79.
- Tong, X., Ratnaraj, N., Patsalos, P.N., 2009. Vigabatrin extracellular pharmacokinetics and concurrent gamma-aminobutyric acid neurotransmitter effects in rat frontal cortex and hippocampus using microdialysis. *Epilepsia* 50, 174–183.
- Treiman, D.M., 2001. GABAergic mechanisms in epilepsy. *Epilepsia* 42 (Suppl. 3), 8–12.
- van Vliet, E.A., Aronica, E., Tolner, E.A., Lopes da Silva, F.H., Gorter, J.A., 2004. Progression of temporal lobe epilepsy in the rat is associated with immunocytochemical changes in inhibitory interneurons in specific regions of the hippocampal formation. *Exp. Neurol.* 187, 367–379.
- Williams, P.A., White, A.M., Clark, S., Ferraro, D.J., Swiercz, W., Staley, K.J., Dudek, F.E., 2009. Development of spontaneous recurrent seizures after kainate-induced status epilepticus. *J. Neurosci.* 29, 2103–2112.
- Wilson, C.L., Maidment, N.T., Shomer, M.H., Behnke, E.J., Ackerson, L., Fried, I., Engel Jr., J., 1996. Comparison of seizure related amino acid release in human epileptic hippocampus versus a chronic kainate rat model of hippocampal epilepsy. *Epilepsy Res.* 26, 245–254.
- Wisłowska-Stanek, A., Hamed, A., Lehner, M., Bidzinski, A., Turzynska, D., Sobolewska, A., Walkowiak, J., Plaznik, A., 2008. Effects of midazolam and buspirone on in vivo concentration of amino acids and monoamine metabolites in the rat hippocampus. *Pharmacol. Rep.* 60, 209–218.
- Yoon, B.E., Jo, S., Woo, J., Lee, J.H., Kim, T., Kim, D., Lee, C.J., 2011. The amount of astrocytic GABA positively correlates with the degree of tonic inhibition in hippocampal CA1 and cerebellum. *Mol. Brain* 4, 42.
- Zhang, Z.J., Koifman, J., Shin, D.S., Ye, H., Florez, C.M., Zhang, L., Valiante, T.A., Carlen, P.L., 2012. Transition to seizure: ictal discharge is preceded by exhausted presynaptic GABA release in the hippocampal CA3 region. *J. Neurosci.* 32, 2499–2512.

INCREASED EXTRACELLULAR LEVELS OF GLUTAMATE IN THE HIPPOCAMPUS OF CHRONICALLY EPILEPTIC RATS

M. SOUKUPOVA,^{a,*} A. BINASCHI,^a C. FALCICCHIA,^a
E. PALMA,^{b,c} P. RONCON,^a S. ZUCCHINI^{a,d} AND
M. SIMONATO^{a,d}

^a Department of Medical Sciences, Section of Pharmacology, Neuroscience Center, University of Ferrara and National Institute of Neuroscience, Via Fossato di Mortara 17-19, Ferrara, Italy

^b Department of Physiology and Pharmacology, University of Roma "Sapienza", Piazzale Aldo Moro 5, Roma, Italy

^c IRCCS San Raffaele, Via della Pisana 235, Roma, Italy

^d Laboratory of Technologies for Advanced Therapy (LTTA), Technopole of Ferrara, Via Ludovico Ariosto 35, Ferrara, Italy

Abstract—An increase in the release of excitatory amino acids has consistently been observed in the hippocampus during seizures, both in humans and animals. However, very little or nothing is known about the extracellular levels of glutamate and aspartate during epileptogenesis and in the interictal chronic period of established epilepsy. The aim of this study was to systematically evaluate the relationship between seizure activity and changes in hippocampal glutamate and aspartate extracellular levels under basal and high K⁺-evoked conditions, at various time-points in the natural history of experimental temporal lobe epilepsy, using *in vivo* microdialysis. Hippocampal extracellular glutamate and aspartate levels were evaluated: 24 h after pilocarpine-induced status epilepticus (SE); during the latency period preceding spontaneous seizures; immediately after the first spontaneous seizure; in the chronic (epileptic) period. We found that (i) basal (spontaneous) glutamate outflow is increased in the interictal phases of the chronic period, whereas basal aspartate outflow remains stable for the entire course of the disease; (ii) high K⁺ perfusion increased glutamate and aspartate outflow in both control and pilocarpine-treated animals, and the overflow of glutamate was clearly increased in the chronic group. Our data suggest that the glutamatergic signaling is preserved and even potentiated in the hippocampus of epileptic rats, and thus may favor the occurrence of spontaneous recurrent

seizures. Together with an impairment of GABA signaling (Soukupova et al., 2014), these data suggest that a shift toward excitation occurs in the excitation/inhibition balance in the chronic epileptic state. © 2015 IBRO. Published by Elsevier Ltd. All rights reserved.

Key words: temporal lobe epilepsy, pilocarpine, glutamate, aspartate, microdialysis.

INTRODUCTION

A disorder in glutamate-mediated excitatory neurotransmission has long been a candidate as a central factor in the pathophysiology of at least some forms of human and experimental epilepsy. A number of studies have suggested that an abnormal amplification of glutamate signaling occurs during seizures (Bradford, 1995; Sherwin, 1999). Moreover, an impairment of inhibition due to reduction of GABA release (Soukupova et al., 2014), desensitization of GABA_A receptors (Palma et al., 2007; Mazzuferi et al., 2010) and/or loss of GABAergic interneurons (Huusko et al., 2015; Houser, 2014) may contribute to exaggerate excitatory signals. Altogether, studies carried out in the last two decades both in epileptic patients and in animal models support the notion that, during seizures, epileptic circuitries lack the necessary balance between inhibition and excitation in favor of the latter.

In humans, epilepsy has been found to be associated with increased extracellular levels of glutamate and aspartate. A highly significant increase in glutamate extracellular concentration was observed before and during partial seizures with secondary generalization in mesial temporal lobe epilepsy (mTLE) patients undergoing surgery, using bilateral intrahippocampal microdialysis and the non-epileptogenic hippocampus of each patient as control (During and Spencer, 1993). Microdialysis evidence supports the notion that not only glutamate but also aspartate extracellular concentrations are significantly increased in the epileptogenic brain tissue under basal conditions and during intense seizures in epilepsy surgery patients (Sherwin, 1999; Thomas et al., 2003). Moreover, the interictal extracellular glutamate levels in the non-epileptogenic human hippocampus were found to be much lower compared to those in the epileptogenic area (Cavus et al., 2008). Although these results indicate a strong association between higher glutamate (and maybe also aspartate) and epileptiform

*Corresponding author. Address: Department of Medical Sciences, Section of Pharmacology, University of Ferrara, Via Fossato di Mortara 17-19, 44121 Ferrara, Italy. Tel: +39-0532-455345; fax: +39-0532-455205.

E-mail addresses: marie.soukupova@unife.it (M. Soukupova), anna.binaschi@unife.it (A. Binaschi), chiara.falcicchia@unife.it (C. Falcicchia), eleonora.palma@uniroma1.it (E. Palma), paolo.roncon@unife.it (P. Roncon), silvia.zucchini@unife.it (S. Zucchini), michele.simonato@unife.it (M. Simonato).

Abbreviations: ANOVA, analysis of variance; EEG, electroencephalogram; HPLC, high-performance liquid chromatography; mTLE, mesial temporal lobe epilepsy; SE, status epilepticus.

activity, for obvious reasons all these human studies lack stringent controls and do not provide information on the dynamic changes occurring in the natural history of the disease.

Several animal studies support and integrate the observations made in humans. Increases in hippocampal or cortical extracellular glutamate and aspartate have been consistently observed during different types of chemically and electrically induced seizures in rats. An ictal increase in hippocampal glutamate levels has been described after microperfusion of various chemoconvulsants (namely pilocarpine, picrotoxin and 3,5-dihydrophenylglycine) into the hippocampus (Meurs et al., 2008) or during chronic-phase seizures following intrahippocampal kainate injection in rats (Wilson et al., 1996; Kanamori and Ross, 2011). Hippocampal extracellular aspartate levels were also found to increase during seizures (Wilson et al., 1996). A very small number of studies describe the interictal extracellular levels of glutamate (or aspartate) in chronic models of epilepsy. However, a significant increase in extracellular glutamate concentrations has been observed in the hippocampus of rats 60 days after intra-amygdala kainate injection (Ueda et al., 2001) and in fully kindled as compared with naïve rats (Mazzuferi et al., 2005; Maciejak et al., 2009). Similarly, significantly increased extracellular interictal levels of aspartate have been observed in a model of focal epilepsy induced by intracortical injection of ferrous chloride (Ronne Engstrom et al., 2001).

Altogether, human and animal studies suggest that glutamate and aspartate extracellular levels are increased in the chronically epileptic tissue (and further increased during seizures). Evidence in this respect needs to be strengthened under rigidly controlled conditions. Moreover, no data are available on the changes in these systems that may occur in the course of the disease, from the initial epileptogenic insult to the development and maintenance of spontaneous seizures. In a previous study (Soukupova et al., 2014) we have demonstrated that GABA release undergoes significant changes in the course of TLE development. Here, we used microdialysis to analyze, for the first time in detail, basal and stimulated glutamate and aspartate outflow in the hippocampus at different time-points of TLE.

EXPERIMENTAL PROCEDURES

Animals

Male Sprague–Dawley rats (250–350 g; Harlan, Milan, Italy) were housed under controlled illumination (12-h light/dark cycle; light on 06.00 am) and environmental conditions (ambient temperature 22–24 °C, humidity 55–65%) beginning at least one week before surgeries. Rat chow and tap water were available *ad libitum*. The experimental procedures were approved by the University of Ferrara Institutional Animal Care and Use Committee and by Italian Ministry of Health (authorization: D.M. 246/2012-B) in accordance with guidelines outlined in the European Communities Council Directive of 24 November 1986 (86/609/EEC). All animals

were acclimatized to the microdialysis laboratory conditions for at least 1 h before each experiment. After the last day of microdialysis, they were killed by decapitation under 1.4% isoflurane anesthesia. Dialysates from a subset of the animals employed in this study (two per group) had been also employed in another, previously published study (Soukupova et al., 2014) to measure GABA outflow. All efforts were made to reduce animal numbers and suffering during the experiments.

Pilocarpine protocol. The pilocarpine protocol was identical to one we previously described (Soukupova et al., 2014). Briefly, intraperitoneal injection of pilocarpine (350 mg/kg) 30 min after a single subcutaneous injection of methyl-scopolamine (1 mg/kg) induced in animals the typical behavior: early partial seizures (movements of vibrissae and head nods within 5 min after pilocarpine administration) evolving into recurrent generalized convulsions (status epilepticus, SE) within 25–30 min. Rats that did not develop SE within 30 min received an additional dose of pilocarpine (175 mg/kg, i.p.). SE was interrupted 3 h after onset by administration of diazepam (20 mg/kg, i.p.). Control animals received a single injection of methyl-scopolamine (1 mg/kg) 30 min prior to vehicle (0.9% NaCl solution, pH adjusted to 7.0). Recording of the seizure behavior began immediately after the pilocarpine injection and was continued for at least 6 h thereafter.

To favor recovery from the body weight loss that follows SE, animals were injected with saline (1 ml of 0.9% NaCl solution, pH adjusted to 7.0) and fed with a 10% sucrose solution for 2–3 days. Those animals that did not achieve the initial body weight within the first week after pilocarpine SE were excluded from the study. Rats were randomly assigned to four experimental groups: acute phase (24 h after SE), latency (7–9 days after SE), first spontaneous seizure (approximately 11 days after SE), and chronic period (22–24 days after SE, i.e., about 10 days after the first seizure). Data were collected and processed only from those animals in which the probe was correctly placed. In summary: inclusion/exclusion criteria were development of convulsive SE within 1 h after pilocarpine administration; weight gain in the first week after SE; correct positioning of the microdialysis probe. The number of valid animals per group was predetermined as five or more (Soukupova et al., 2014).

Identification of seizures and electroencephalogram (EEG) activity. EEG seizures were defined as periods of paroxysmal activity of high frequency (> 5 Hz) characterized by a > 3-fold amplitude increment over baseline with progression of the spike frequency that lasted for a minimum of 3 s (Williams et al., 2009; Paradiso et al., 2011). They were detected using a hard wire system MP150 and AcqKnowledge 4.3 software (both Biopac, Goleta, CA, USA). Severity of behavioral seizures was scored according to Racine (1972): class 1, chewing, lips and facial movements; class 2, head nods; class 3, forelimb clonus; class 4, generalized seizure with rearing; class 5, generalized seizure with rearing and falling.

As previously described (Soukupova et al., 2014), a 24/24-h video monitoring was started approximately 6 h after pilocarpine administration (i.e., at the end of direct observation by the researchers – see above) and continued until day 5, using a digital video surveillance system DSS1000 (V4.7.0041FD, AverMedia Technologies, Fremont, CA, USA). Beginning at day 5, rats were continuously video-EEG monitored to verify absence of spontaneous seizures (for the latency group) or to obtain proper identification of the first spontaneous seizure (for the first seizure group). Video-EEG monitoring was started at day 5 after SE because, under the experimental conditions employed in this study, we do not observe spontaneous seizures earlier than 8 days after pilocarpine administration (Paradiso et al., 2009; Mazzuferi et al., 2010).

Following occurrence of the first spontaneous seizure and until the microdialysis experiments, i.e. in the chronic period, animals were only video-monitored to determine frequency and duration of generalized seizures (class 4 or 5). Video-EEG was however performed during microdialysis sessions, to make sure that spontaneous seizures were not occurring before or during the experiment and to examine possible correlations between high K^+ -evoked EEG seizure activity and changes in extracellular glutamate and aspartate. All video-EEG analyses were conducted by two independent investigators that were blinded for the group of tested animals. In case of divergence, data were examined together to reach a consensus (Paradiso et al., 2011).

Statistical analysis. Kruskal–Wallis plus post hoc Dunn's test and a one-way analysis of variance (ANOVA) and post hoc Dunnett's test were used to determine whether respectively severity and duration of high K^+ -evoked seizures during microdialysis differed significantly from those in normal rats.

In vivo brain microdialysis

Microdialysis procedure. Brain microdialysis experiments were performed in awake and freely moving rats as previously described (Soukupova et al., 2014). In brief, rats were stereotaxically implanted with a guide cannula coupled with a recording electrode under general anesthesia induced with ketamine/xylazine (43 and 7 mg/kg, i.p.) and maintained with isoflurane 1.4% in air (flow 1.2 ml/min). A reference electrode was placed on the skull. Animals were given a post-operative analgesic treatment (ketoprofen 5 mg/kg, i.p.) for 2 days, and allowed to recover for at least 7 days.

Twenty-four hours before the experiment, rats were briefly anesthetized with isoflurane and a vertical microdialysis probe, endowed with a 1-mm cuprophane dialyzing membrane (MAB 4.15.1.Cu, Agn Tho's, Lidingö, Sweden; cut-off 6 kDa; outer diameter $300 \pm 5 \mu\text{m}$; mean glutamate recovery *in vitro* $15.49 \pm 0.42\%$; mean aspartate recovery *in vitro* $14.89 \pm 0.36\%$), was inserted and fixed to the guide cannula. *In vitro* recovery was measured by placing probes in a continuously stirred vial containing 2.5 μM

aspartate and 2.5 μM glutamate in Ringer solution (see composition of Ringer below) and maintained at 37 °C using a block heater (QBD2, Grant Instruments, Cambridge, England). Probes were perfused with Ringer at a flow rate of 2 $\mu\text{l}/\text{min}$. After a 30-min wash-out period, three 30-min perfusate samples and three equal volume samples of the solution in the vial were collected. The amounts of aspartate and glutamate in the samples were determined using the high-performance liquid chromatography (HPLC) method described below.

Probes were placed in the right ventral hippocampus, at the following stereotaxic coordinates: A –3.4 mm from bregma; L +4.8 mm; V +7.0 mm below the dura (Pellegrino et al., 1979). To verify absence of seizures for the 3 h preceding the initiation of sample collection and to monitor seizure activity during microdialysis, animals were attached to an EEG hard-wire system during the entire microdialysis session. Following an initial 60-min equilibration period, dialysis was started with Ringer solution (composition, in mM: MgCl_2 0.85, KCl 2.7, NaCl 148, CaCl_2 1.2, 0.3% BSA) at a flow rate of 2.0 $\mu\text{l}/\text{min}$ maintained using a Univentor infusion pump (mod. 864, Zejtun, Malta). Five consecutive 30 min dialysate samples were collected under baseline conditions (perfusion with normal Ringer), and stimulation was then applied as a 10-min perfusion with a modified Ringer solution containing 100 mM K^+ (equimolar compensation with Na^+ ; composition, in mM: MgCl_2 0.85, KCl 100, NaCl 50.7, CaCl_2 1.2, 0.3% BSA) after the collection of the fifth post-equilibration dialysate. From that moment, dialysates were collected every 10 min. The high potassium perfusion has been described to elevate an extracellular K^+ concentration near the dialyzing membrane (Largo et al., 1996) and thereby increase the efflux of several neurotransmitters, including glutamate (Takeda et al., 2003; Tanaka et al., 2003; Mazzuferi et al., 2005). Moreover, it has been shown (Timmerman and Westerink, 1997) that, under these experimental conditions, high K^+ -evoked glutamate overflow is almost entirely Ca^{2+} -dependent (indicating a prevalent origin from a vesicular pool), while basal glutamate efflux is essentially Ca^{2+} -independent and tetrodotoxin-insensitive (which questions its neuronal origin). Because perfusion of a hippocampal probe with high K^+ is known to provoke seizures in epilepsy models (Marti et al., 2000; Aparicio et al., 2004; Mazzuferi et al., 2005; Soukupova et al., 2014), as mentioned above EEG and behavior were recorded during the entire microdialysis session. Experiments were repeated for 3 consecutive days in 8-h microdialysis sessions, except for the acute (24 h) and first seizure groups, in which only one microdialysis session took place 24 h after SE or within 24 h after the first spontaneous seizure. On completion of each experiment, rats were euthanized with an anesthetic overdose and their brains removed, fixed in 10% formalin and paraffin-embedded. Coronal sections were cut in order to verify probe placement as described in precedence (Soukupova et al., 2014).

Dialysates were analyzed for glutamate and aspartate content using a modified HPLC method (Soukupova

et al., 2014), employing a Smartline manager 5000 degasser and system controller unit, a Smartline 1000 quaternary gradient pump (Knauer, Berlin, Germany), an HT300L auto-sampler with a 20- μ l sample loop (HTA, Brescia, Italy) and a RF-551 spectrofluorimetric detector (Shimadzu, Kyoto, Japan). A 250 \times 4.6 mm chromatographic column packed with an EUROSIL bios-elect 300A and a 5 \times 4 mm pre-column containing the same packing (LabService Analytica, Italy) were used. The mobile phase was a binary gradient between solution A (0.1 M sodium phosphate buffer, pH 6.0) and solution B (40% 0.1 M sodium phosphate buffer, 30% methanol, 30% acetonitrile, pH 6.5), pushed through the system at a flow rate of 0.8 ml/min. Amino acids were detected at $\lambda_{\text{excitation}}/\lambda_{\text{emission}} = 345/455$ nm after 2 min pre-column derivatization with 20 μ l orthophthaldialdehyde (OPA; Sigma, Milan, Italy) mixed with 5-mercaptoethanol (Sigma, Milan, Italy) 20:1 (v/v) added to 20 μ l of sample. Under these conditions, the mixture of amino acids containing aspartate (t_r 4.61 min), glutamate (t_r 6.07 min) and the internal standard L-homoserine (t_r 8.99 min), was separated within 20 min. The method was validated by spiking the Ringer solution and modified Ringer solution with aspartate, glutamate, L-homoserine and an amino acid standard solution (Sigma, Milan, Italy). The sensitivity of the method was 0.74 pmol/20 μ l sample for glutamate and 1.13 pmol/20 μ l sample for aspartate.

Quantification and statistics. The amounts of glutamate and aspartate in dialysates have been expressed either as absolute values (pmol/10 min), which represents the value in 20 μ l of sample, or as percent of basal outflow, as previously described (Mazzuferi et al., 2005; Soukupova et al., 2014). Briefly, basal values represent the mean amount of glutamate and aspartate measured in the last four spontaneous fractions collected before stimulus (when multiple microdialysis sessions were performed, i.e., latency and chronic group, data from the 3 days were averaged to obtain a single estimate per animal). Time-course curves were expressed in absolute values (pmol/10 min) or as percent of basal values. High K^+ -evoked glutamate and aspartate overflow was calculated by subtracting the presumed basal outflow from the total outflow in the samples taken upon stimulus application and in the following three samples. The presumed basal outflow was obtained by interpolation between the samples preceding and following the above-mentioned four collection periods. The %high K^+ -evoked overflow was then estimated by dividing the sum of the outflow in the four samples taken upon and after stimulus (above) by the presumed basal outflow, and multiplying by 100. The statistical comparisons were made using a one-way ANOVA followed by the Dunnett's test. The Holm–Sidak multiple comparison test was employed for an analysis of differences between amino acid concentrations in the time-course of the experiments.

Chemicals

Pilocarpine hydrochloride, scopolamine methylnitrate and xylazine hydrochloride (all from Sigma, Milano, Italy) were freshly dissolved in isoosmotic 0.9% NaCl (Sigma,

Milano, Italy) solution prior to use. Original medicinal products containing diazepam (Valium[®], Roche, Basel, Switzerland), ketamine (Ketavel[®], InterVet, Aprilia, Italy) and isoflurane (IsoFlo[®], Esteve Farma, Milano, Italy) were used to sedation and anesthesia. Standards for chromatography: L-aspartic acid, L-glutamic acid, L-homoserine and solvents acetonitrile (HPLC grade) and methanol (HPLC grade) were all from Sigma (Milano, Italy).

RESULTS

SE and seizure assessment

Animals were video-EEG recorded at specific time points to monitor the development and progression of epilepsy and to detect the onset of spontaneous seizures. A pilocarpine dose of 350 mg/kg (i.p.) was sufficient to induce SE (latency: 25 \pm 5 min) in most of the cases. About 75% of all rats (17 of 22) needed no further injections (the remaining 25% received one additional injection of pilocarpine). Typically, the animals experienced some occasional, self-limiting generalized seizures (less than 1 min duration) for 2–3 days after SE, then entered a latency state in which they were apparently well (Mazzuferi et al., 2010; Soukupova et al., 2014). Beginning 5 days after SE, animals were video-EEG monitored for verification that no spontaneous seizures occurred until day 9 after SE, for the latency group, or for identification of the first spontaneous seizure, for the first seizure group. The average seizure-free period was 11.3 \pm 0.5 days (mean \pm SEM, $n = 15$). After occurrence of the first spontaneous seizure, the remaining animals (i.e., those in the chronic group) were switched back to simple video-monitoring. In these animals, behavioral seizures occurred in clusters, as previously described (Goffin et al., 2007; Williams et al., 2009; Mazzuferi et al., 2010; Soukupova et al., 2014), and aggravated in time. During the last week of monitoring, the frequency of generalized (class 4 and 5) seizures per day was 1.5 \pm 0.4 (mean \pm SEM, $n = 12$).

Rats were video-EEG recorded starting 3 h before and during microdialysis experiments. No spontaneous seizure was recorded during perfusion with basal Ringer. During perfusion with high K^+ , in line with previous results (Soukupova et al., 2014) and as shown in Fig. 1, animals in the control group exhibited no behavioral seizure or partial seizures of class 1, and animals in the latency group exhibited predominantly seizures of class 1. Control and latency animals, however, also exhibited numerous wet-dog shakes when perfused with high K^+ . More severe seizures occurred in acute (24 h after SE), in first spontaneous seizure and in chronic animals, although this phenomenon reached statistical significance only in chronic animals. It is worth reporting that the response in first seizure and chronic animals was apparently distributed in a bi-modal fashion, with a subgroup exhibiting generalized seizures (class 4 or 5) during high K^+ perfusion, and another subgroup responding with non-generalized seizures only (class 1 or 2; Fig. 1A). This bi-modal distribution may correlate with the variable proximity between a cluster of spontaneous seizures

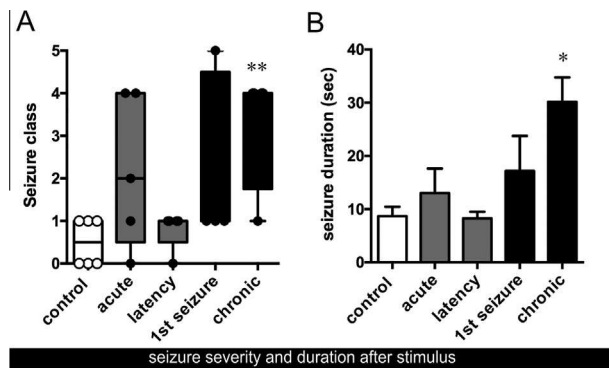


Fig. 1. Seizure activity in response to hippocampal perfusion with 100 mM K^+ for 10 min in control (white columns) and pilocarpine-treated (gray and black columns) rats. (A) Seizure severity scored according to Racine (1972). (B) EEG-measured single seizure duration during the high K^+ stimulation. Data are the means \pm SEM of 5–6 animals per group. * $p < 0.01$ Kruskal–Wallis and post hoc Dunn's test. ** $p < 0.05$, one-way ANOVA and post hoc Dunnett's test.

and the microdialysis session. The duration of high K^+ -evoked seizures was non-significantly reduced in the latency period, i.e., in the post-ictal phase after SE, and then progressively increased in the course of the disease (Fig. 1B).

Glutamate

Basal glutamate outflow was higher in epileptic animals with spontaneous seizures (i.e., first seizure and chronic group) than in control rats, but the increase was statistically significant only for the chronic animals group (Fig. 2; Table 1).

Perfusion with a solution containing high K^+ increased glutamate outflow in all experimental groups. The stimulation effect peaked 10–20 min after high K^+ perfusion, most likely due to the time needed for accumulation of K^+ in the extracellular spaces around the microdialysis probe. In control, acute and latency rats, glutamate outflow increased from relatively low basal levels preceding the stimulus to reach 17.57 ± 1.99 , 20.34 ± 6.46 and 18.75 ± 4.77 pmol/10 min, 10 min after high K^+ perfusion. In first seizure and chronic rats, glutamate outflow increased from relatively high basal levels to achieve 22.22 ± 3.28 and 20.76 ± 1.04 pmol/10 min, respectively, 10 min after the stimulus. The high K^+ -evoked glutamate outflow in chronic animals returned to basal values with a delay of about 30 min compared to all other experimental groups (Fig. 2B). Such protracted increase in outflow paralleled the increased severity and duration of high K^+ -evoked seizures (Fig. 1) and may reflect the impairment of compensating GABA release during this period (Soukupova et al., 2014). When expressed as percent of basal outflow, the response to high K^+ stimulation was approximately 150% in all experimental groups (Fig. 2C). The net high K^+ -evoked glutamate overflow was not significantly different from the one in control animals at the different time points (Fig. 2D). However, a clear tendency to an increased

overflow was observed in chronic period group, coherent with the prolonged response described above (Fig. 2D). When expressed as percent of basal outflow, however, no differences at all were observed because, as described above, basal glutamate outflow was also increased to a similar extent in the chronic group (Fig. 2E).

Aspartate

The basal aspartate outflow was lower (half or less) than glutamate outflow in all experimental groups (Table 1). No significant difference was detected in basal or high K^+ -evoked aspartate outflow between the different experimental groups (Table 1). The time course of high K^+ stimulated aspartate outflow was also similar in all groups.

DISCUSSION

The main findings of the present study must be discussed in conjunction with parallel findings on GABA outflow. We have previously demonstrated that, during the latent period, basal GABA outflow is reduced but the response to high K^+ stimulation increases whereas, beginning at the time of the first spontaneous seizure, this increased responsiveness to stimulation disappears and the system remains dysfunctional (Soukupova et al., 2014). In this study we have extended the analysis to the excitatory neurotransmitters glutamate and aspartate, and found that (i) basal (spontaneous) extracellular glutamate levels are not significantly different from control levels during latency but raise significantly in the chronic stage, whereas aspartate extracellular levels remain stable during the entire course of experimental TLE; (ii) stimulus-evoked (high K^+ stimulation) glutamate and aspartate outflow do not vary significantly in the course of the disease, even if a clear tendency to an increase is observed for glutamate in the chronic period. Therefore, contrary to GABA, the function of the excitatory glutamatergic and aspartatergic systems is maintained or even increased in TLE. Even if a significant part of the glutamatergic terminals in the hippocampus synapse on and activate inhibitory GABA neurons, this does not lead to increased GABA release (that is instead reduced, presumably due to the loss of GABA neurons; Soukupova et al., 2014) implicating a net shift in the inhibition to excitation balance toward excitation.

Before discussing these findings, the limitations of the microdialysis technique should be considered. First, the extracellular concentrations of glutamate, aspartate and GABA are not direct indices of synaptic activity. Changes in dialysate concentrations of these neurotransmitters should be regarded as a read-out of the activity of neuron–astrocyte units. It has been proposed that dialysate changes in principal neurotransmitters are an index of their volume transmission rather than of their synaptic release (Del Arco et al., 2003). The activity of neurons is functionally linked to that of astrocytes, which can also release and reuptake glutamate, aspartate or GABA, thereby contributing to the regulation of their amounts in the

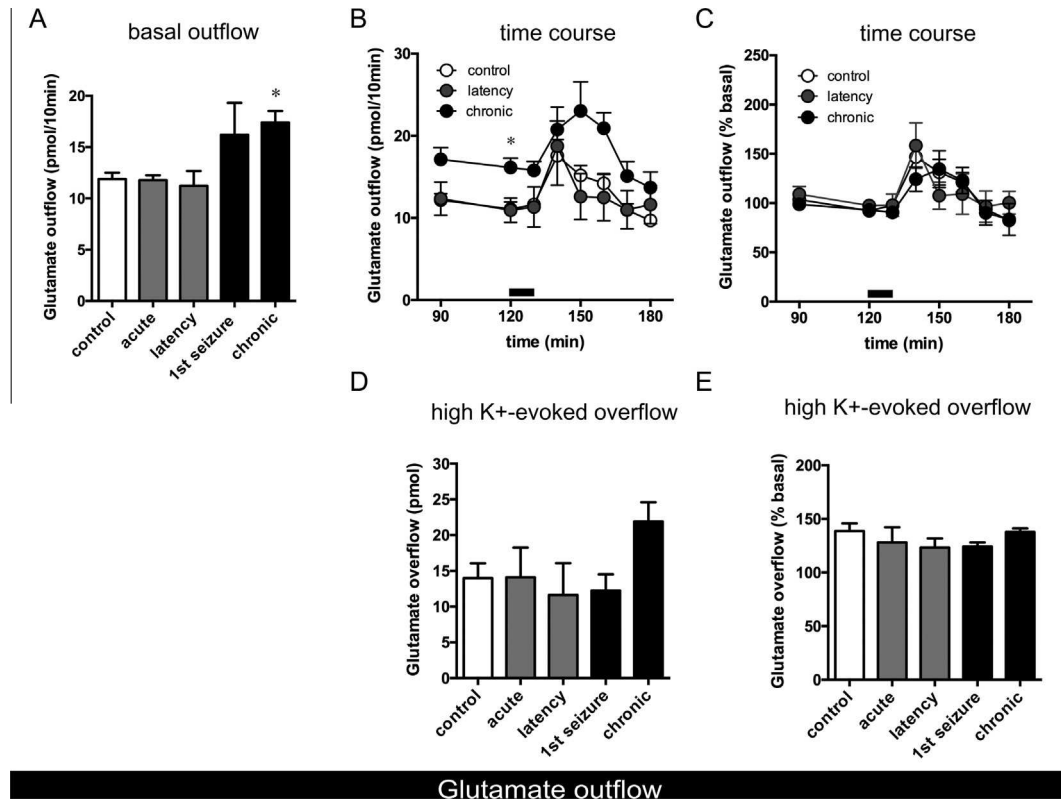


Fig. 2. (A) Spontaneous basal glutamate outflow from the hippocampus of control (white column) and pilocarpine-treated (gray and black columns) rats. Basal glutamate levels are significantly higher in the hippocampus of chronic pilocarpine-treated rats compared to controls. (B) Time course of the effect of 10 min perfusion with 100 mM K^+ (horizontal bar) on glutamate outflow from the hippocampus of control (open circles), latency (gray circles) and chronic rats (black circles). The time of high K^+ perfusion shown here and in (C) corresponds exactly to the time when high K^+ is in the probe (the switch to high K^+ solution was performed 17 min before, i.e., the time necessary to reach the brain via the tubing in our system). In control rats, glutamate outflow increases from 11.63 ± 0.69 pmol/10 min to reach 17.57 ± 1.99 pmol/10 min after the stimulus. Similarly, glutamate outflow increases from 11.33 ± 2.45 to 18.75 ± 4.77 pmol/10 min in the latency period group. In chronic rats, glutamate outflow raises from relatively high basal levels (15.79 ± 1.07) to reach 20.76 ± 1.04 pmol/10 min in the first 10 min after the stimulus and 23.03 ± 3.55 pmol/10 min 20 min after the stimulus. For clarity, the profiles in acute and first seizure animals are not shown. However, the one in acute animals was similar to that in latency animals and the one in first seizure animals was similar to that in chronic animals. (C) Time course of the effect of 10-min perfusion with the high K^+ (horizontal bar) on glutamate outflow from the hippocampus of control (open circles), latency (gray circles) and early chronic (black circles) rats. All animals respond to the stimulus with an increase in glutamate outflow to approximately 150% of basal values. For clarity, the profiles in acute and first seizure animals are not shown. However, the one in acute animals was similar to that in latency animals and the one in first seizure animals was similar to that in chronic animals. (D) High (100 mM) K^+ -evoked glutamate overflow from the hippocampus of control (white column) and pilocarpine-treated (gray and black columns) rats. See 'Quantification and statistics' for details. (E) Effect of 100 mM K^+ perfusion on glutamate overflow, expressed as percent of basal release. The glutamate percent overflow remains stable in all experimental groups. Data are the means \pm SEM of 5–6 animals per group. * $p < 0.05$, one-way ANOVA plus Dunnett's test (A) or Holm–Sidak t test (B).

Table 1. Basal and high K^+ -evoked glutamate and aspartate outflow from the hippocampus of control and pilocarpine-treated rats

	Control	Acute	Latency	1st seizure	Chronic
<i>Glutamate</i>					
Basal outflow (pmol/10 min)	11.87 ± 0.63	11.79 ± 0.45	11.23 ± 1.44	16.19 ± 3.13	$17.40 \pm 1.12^*$
High K^+ -evoked overflow (pmol)	15.69 ± 2.40	14.13 ± 5.38	11.63 ± 4.47	12.25 ± 2.26	21.92 ± 2.68
High K^+ -evoked overflow (% basal)	138.6 ± 7.3	128.0 ± 14.1	123.3 ± 8.6	124.3 ± 3.7	137.7 ± 3.5
<i>Aspartate</i>					
Basal outflow (pmol/10 min)	5.92 ± 0.89	6.58 ± 2.00	6.01 ± 0.15	7.17 ± 1.55	6.25 ± 0.78
High K^+ -evoked overflow (pmol)	7.19 ± 1.23	8.47 ± 1.29	10.89 ± 1.15	7.99 ± 3.86	9.32 ± 1.63
High K^+ -evoked overflow (% basal)	142.0 ± 8.3	137.6 ± 10.7	156.3 ± 17.0	122.3 ± 9.9	147.5 ± 10.2

Data are the means \pm SEM of 5–6 animals per group.

* $p < 0.05$ vs. Control; ANOVA and post hoc Dunnett's test.

extracellular space (Del Arco et al., 2003). Once released from neurons and astrocytes, glutamate, aspartate or GABA can be re-uptaken or spill-over from the synaptic

cleft to perisynaptic and extrasynaptic regions, where they reach the microdialysis probe (Watson et al., 2006). Thus, variations in the extracellular space volume

(that have been reported to occur in epilepsy; Lux et al., 1989), alterations in the extracellular matrix and environmental factors (like tissue damage associated with the probe's insertion and substances entering from the bloodstream) may also influence the measures.

Even with the above limitations, the present data suggest that the development of TLE sets a new equilibrium between excitatory and inhibitory neurotransmission in the hippocampus. We found here that the basal outflow of glutamate is increased in the chronic epileptic period in the pilocarpine model, and that of aspartate remains stable at all time-points. It should be emphasized that this increased glutamate outflow was detected in inter-seizure periods: because spontaneous seizures increase glutamate release (During and Spencer, 1993) and therefore represent a confounding factor under these experimental conditions, animals were video-EEG monitored beginning 3 h before microdialysis, and the experiment was interrupted if a spontaneous seizure occurred. These findings are in line with previous observations in humans, in which the microdialysis-measured outflow of glutamate was higher in the epileptogenic hippocampus of patients with medication-resistant complex partial seizures than in the contralateral, non-epileptogenic hippocampus (Cavus et al., 2008). Similarly, increased extracellular concentrations of glutamate have been reported in the hippocampus of chronically epileptic rats (Ronne Engstrom et al., 2001; Ueda et al., 2001; Mazzuferi et al., 2005; Maciejak et al., 2009). At variance with our findings, the spontaneous outflow of aspartate was found elevated in one study (Ronne Engstrom et al., 2001). Altogether, these data suggest that increased extracellular glutamate levels in the hippocampus may play a role in the maintenance of a chronic epileptic condition.

The absence of differences in the response to stimulation (high K^+ perfusion) at the different time points also supports preservation of function of excitatory networks. Indeed, with reference to basal levels, high K^+ -evoked the outflow of approximately an extra 50% glutamate and aspartate in controls as well as in all pilocarpine treated animals. If anything, the glutamate response to stimulation was increased in chronic animals, in which we observed a net tendency toward a prolonged response, with longer time needed to recover basal glutamate outflow levels and an overall tendency to increase the overflow generated by the stimulation. A similar phenomenon was described by others (Ueda et al., 2001). In our previous study (Soukupova et al., 2014) we observed a reduced basal GABA outflow and a strong impairment of the GABAergic response to potassium stimulation in the chronic phase, most likely caused by loss of GABA interneurons (Huusko et al., 2015; Houser, 2014; Soukupova et al., 2014). Together, these data support a dramatic unbalance of the excitation to inhibition ratio in favor of excitation, a phenomenon that greatly favors the spontaneous occurrence of seizures.

The maintenance of an apparently normal excitatory signal may seem surprising if considering that not only inhibitory interneurons, but also principal excitatory

neurons are lost in the epileptic tissue. Studies of the resected tissue from patients with intractable TLE and animals with SE-induced epilepsy have shown neuropathological modifications (Pitkanen and Sutula, 2002), including: (1) hippocampal neuronal loss, primarily of CA1 and CA3 pyramidal neurons, (2) sprouting and reorganization of the mossy fibers, the axons of dentate gyrus granule cells, (3) increased neurogenesis in the dentate gyrus and (4) hippocampal gliosis. It may be hypothesized that sprouted mossy fibers, newborn granule cells and gliosis may compensate for the extensive loss of excitatory neurons in the sclerotic hippocampus, maintaining unmodified (or not significantly modified) the extracellular levels of glutamate and aspartate.

Another puzzling observation is that the variations in glutamate levels are not paralleled by variations in aspartate. Glutamate and aspartate are located in the same excitatory terminals in the hippocampus, even if glutamate is more abundant than aspartate (Gundersen, 2008). However, aspartate vesicles are also co-expressed with GABA vesicles and, therefore, aspartate may be co-released with GABA in the hippocampus (Gundersen, 2008; Nadler, 2011). Altogether, while the co-release of aspartate at excitatory synapses may be increased in chronic epilepsy (like that of glutamate), the co-release of aspartate and GABA at inhibitory synapses may be decreased because of loss of GABA terminals (Soukupova et al., 2014). As a consequence, its outflow, as detected by microdialysis, could remain essentially unchanged.

CONCLUSION

Based on the data presented in this study and on the data from our previous work (Soukupova et al., 2014) we suggest that preserved glutamatergic and aspartatergic extracellular levels, together with an impairment of GABA release, favor the occurrence of spontaneous recurrent seizures and contribute to maintaining a chronic epileptic state. The present findings support the growing body of data implicating that the dampening excitatory neurotransmission may be a useful strategy to block epileptic seizures (Zwart et al., 2014).

Acknowledgments—This study was supported by a grant from the Italian Ministry for the University (Prin 2009, to E.P.) and AICE-Fire (to E.P.). The authors have no conflict of interest to declare.

REFERENCES

- Aparicio LC, Candeletti S, Binaschi A, Mazzuferi M, Mantovani S, Di Benedetto M, Landuzzi D, Lopetuso G, Romualdi P, Simonato M (2004) Kainate seizures increase nociceptin/orphanin FQ release in the rat hippocampus and thalamus: a microdialysis study. *J Neurochem* 91:30–37.
- Bradford HF (1995) Glutamate, GABA and epilepsy. *Prog Neurobiol* 47:477–511.
- Cavus I, Pan JW, Hetherington HP, Abi-Saab W, Zaveri HP, Vives KP, Krystal JH, Spencer SS, Spencer DD (2008) Decreased hippocampal volume on MRI is associated with increased extracellular glutamate in epilepsy patients. *Epilepsia* 49:1358–1366.

- Del Arco A, Segovia G, Fuxe K, Mora F (2003) Changes in dialysate concentrations of glutamate and GABA in the brain: an index of volume transmission mediated actions? *J Neurochem* 85:23–33.
- During MJ, Spencer DD (1993) Extracellular hippocampal glutamate and spontaneous seizure in the conscious human brain. *Lancet* 341:1607–1610.
- Goffin K, Nissinen J, Van Laere K, Pitkanen A (2007) Cyclicity of spontaneous recurrent seizures in pilocarpine model of temporal lobe epilepsy in rat. *Exp Neurol* 205:501–505.
- Gundersen V (2008) Co-localization of excitatory and inhibitory transmitters in the brain. *Acta Neurol Scand* 117(Suppl. 188):29–33.
- Houser CR (2014) Do structural changes in GABA neurons give rise to the epileptic state? *Adv Exp Med Biol* 813:151–160.
- Huusko N, Romer C, Ndode-Ekane XE, Lukasiuk K, Pitkanen A (2015) Loss of hippocampal interneurons and epileptogenesis: a comparison of two animal models of acquired epilepsy. *Brain Struct Funct* 220(1):153–191.
- Kanamori K, Ross BD (2011) Chronic electrographic seizure reduces glutamine and elevates glutamate in the extracellular fluid of rat brain. *Brain Res* 1371:180–191.
- Largo C, Cuevas P, Somjen GG, Martin del Rio R, Herreras O (1996) The effect of depressing glial function in rat brain in situ on ion homeostasis, synaptic transmission, and neuron survival. *J Neurosci* 16:1219–1229.
- Lux HD, Heinemann U, Dietzel I (1989) Ionic changes and alterations in the size of the extracellular space during epileptic activity. *Adv Neurol* 44:619–639.
- Maciejak P, Szyndler J, Turzynska D, Sobolewska A, Taracha E, Skorzewska A, Lehner M, Bidzinski A, Hamed A, Wislowska-Stanek A, Plaznik A (2009) The effects of group III mGluR ligands on pentylenetetrazol-induced kindling of seizures and hippocampal amino acids concentration. *Brain Res* 1282:20–27.
- Marti M, Bregola G, Morari M, Gemignani A, Simonato M (2000) Somatostatin release in the hippocampus in the kindling model of epilepsy: a microdialysis study. *J Neurochem* 74:2497–2503.
- Mazzuferi M, Binaschi A, Rodi D, Mantovani S, Simonato M (2005) Induction of B1 bradykinin receptors in the kindled hippocampus increases extracellular glutamate levels: a microdialysis study. *Neuroscience* 135:979–986.
- Mazzuferi M, Palma E, Martinello K, Maiolino F, Roseti C, Fucile S, Fabene PF, Schio F, Pellitteri M, Sperk G, Miledi R, Eusebi F, Simonato M (2010) Enhancement of GABA(A)-current run-down in the hippocampus occurs at the first spontaneous seizure in a model of temporal lobe epilepsy. *Proc Natl Acad Sci U S A* 107:3180–3185.
- Meurs A, Clinckers R, Ebinger G, Michotte Y, Smolders I (2008) Seizure activity and changes in hippocampal extracellular glutamate, GABA, dopamine and serotonin. *Epilepsy Res* 78:50–59.
- Nadler JV (2011) Aspartate release and signalling in the hippocampus. *Neurochem Res* 36:668–676.
- Palma E, Roseti C, Maiolino F, Fucile S, Martinello K, Mazzuferi M, Aronica E, Manfredi M, Esposito V, Cantore G, Miledi R, Simonato M, Eusebi F (2007) GABA(A)-current rundown of temporal lobe epilepsy is associated with repetitive activation of GABA(A) “phasic” receptors. *Proc Natl Acad Sci U S A* 104:20944–20948.
- Paradiso B, Marconi P, Zucchini S, Berto E, Binaschi A, Bozac A, Buzzi A, Mazzuferi M, Magri E, Navarro MG, Rodi D, Su T, Volpi I, Zanetti L, Marzola A, Manservigi R, Fabene PF, Simonato M (2009) Localized delivery of fibroblast growth factor-2 and brain-derived neurotrophic factor reduces spontaneous seizures in an epilepsy model. *Proc Natl Acad Sci U S A* 106:7191–7196.
- Paradiso B, Zucchini S, Su T, Bovolenta R, Berto E, Marconi P, Marzola A, Navarro MG, Fabene PF, Simonato M (2011) Localized overexpression of FGF-2 and BDNF in hippocampus reduces mossy fiber sprouting and spontaneous seizures up to 4 weeks after pilocarpine-induced status epilepticus. *Epilepsia* 52:572–578.
- Pellegrino LJ, Pellegrino AS, Cushman AJ (1979) A stereotaxic atlas of the rat brain. New York and London: Plenum Press.
- Pitkanen A, Sutula TP (2002) Is epilepsy a progressive disorder? Prospects for new therapeutic approaches in temporal-lobe epilepsy. *Lancet Neurol* 1:173–181.
- Racine RJ (1972) Modification of seizure activity by electrical stimulation. II. Motor seizure. *Electroencephalogr Clin Neurophysiol* 32:281–294.
- Ronne Engstrom E, Hillered L, Flink R, Kihlstrom L, Lindquist C, Nie JX, Olsson Y, Silander HC (2001) Extracellular amino acid levels measured with intracerebral microdialysis in the model of posttraumatic epilepsy induced by intracortical iron injection. *Epilepsy Res* 43:135–144.
- Sherwin AL (1999) Neuroactive amino acids in focally epileptic human brain: a review. *Neurochem Res* 24:1387–1395.
- Soukupova M, Binaschi A, Falcicchia C, Zucchini S, Roncon P, Palma E, Magri E, Grandi E, Simonato M (2014) Impairment of GABA release in the hippocampus at the time of the first spontaneous seizure in the pilocarpine model of temporal lobe epilepsy. *Exp Neurol* 257:39–49.
- Takeda A, Hirate M, Tamano H, Oku N (2003) Release of glutamate and GABA in the hippocampus under zinc deficiency. *J Neurosci Res* 72:537–542.
- Tanaka S, Tsuchida A, Kiuchi Y, Oguchi K, Numazawa S, Yoshida T (2003) GABAergic modulation of hippocampal glutamatergic neurons: an in vivo microdialysis study. *Eur J Pharmacol* 465:61–67.
- Thomas PM, Phillips JP, Delanty N, O’Connor WT (2003) Elevated extracellular levels of glutamate, aspartate and gamma-aminobutyric acid within the intraoperative, spontaneously epileptiform human hippocampus. *Epilepsy Res* 54:73–79.
- Timmerman W, Westerink BH (1997) Brain microdialysis of GABA and glutamate: what does it signify? *Synapse* 27:242–261.
- Ueda Y, Doi T, Tokumaru J, Yokoyama H, Nakajima A, Mitsuyama Y, Ohya-Nishiguchi H, Kamada H, Willmore LJ (2001) Collapse of extracellular glutamate regulation during epileptogenesis: down-regulation and functional failure of glutamate transporter function in rats with chronic seizures induced by kainic acid. *J Neurochem* 76:892–900.
- Watson CJ, Venton BJ, Kennedy RT (2006) In vivo measurements of neurotransmitters by microdialysis sampling. *Anal Chem* 78:1391–1399.
- Williams PA, White AM, Clark S, Ferraro DJ, Swiercz W, Staley KJ, Dudek FE (2009) Development of spontaneous recurrent seizures after kainate-induced status epilepticus. *J Neurosci* 29:2103–2112.
- Wilson CL, Maidment NT, Shomer MH, Behnke EJ, Ackerson L, Fried I, Engel Jr J (1996) Comparison of seizure related amino acid release in human epileptic hippocampus versus a chronic, kainate rat model of hippocampal epilepsy. *Epilepsy Res* 26:245–254.
- Zwart R, Sher E, Ping X, Jin X, Sims Jr JR, Chappell AS, Gleason SD, Hahn PJ, Gardinier K, Gernert DL, Hobbs J, Smith JL, Valli SN, Witkin JM (2014) Perampanel, an antagonist of alpha-amino-3-hydroxy-5-methyl-4-isoxazolepropionic acid receptors, for the treatment of epilepsy: studies in human epileptic brain and nonepileptic brain and in rodent models. *J Pharmacol Exp Ther* 351:124–133.

Chapter 6

Conclusions and future perspectives

6.1 Summary

In this thesis, I approached the study of TLE from different points of view, including (i) the investigation of miRNAs and other regulatory genes as new putative therapeutic targets, (ii) the study of circulating miRNAs as biomarkers of epilepsy, (iii) the regulations of molecular mechanisms that lead to the development of the disease and its comorbidities, and (iv) the significance of an excitation/inhibition unbalance in TLE development.

6.2 MiRNAs

Both the identification of new putative therapeutic targets for the cure of the disease and of biomarkers for the screening of patients at risk to develop epilepsy are important clinical needs. MicroRNAs seem to have the features to respond to these requests. The main question is whether these new putative therapeutic targets can be identified in an unbiased manner. The introduction of the “omics sciences” generated optimism towards the discovery of the molecular mechanisms of epileptogenesis, which should allow researchers to select the most appropriate targets for antiepileptogenic therapies (Pitkänen and Lukasiuk, 2011). Within these new sciences, the miRNomics is the one that attracted the most attention in the field of epilepsy. MicroRNAs are tiny genetic rheostats regulating the expression of messenger RNAs through different mechanisms, revealing a regulatory impact that is even more pervasive as a potential therapeutic tool (Ghosh et al, 2007).

In the field of epilepsy, a series of reports have recently profiled miRNAs expression both in brain human samples (Kan et al, 2012; McKiernan et al, 2012; Kaalund et al, 2014) and in various animal models (Hu et al, 2012; Jimenez-Mateos et al, 2011; Song et al, 2011; McKiernan et al, 2012; Risbud and Porter, 2013; Bot et al, 2013; Gorter et al, 2014; Kretschmann et al, 2015). All these studies, even if of great scientific impact, have some limitations. First, the brain tissue was the whole hippocampus or a mechanically-dissected hippocampal sub-region in most studies, which implicates not only heterogeneity in terms of cell composition, but also a different representation of different cell types in control and epileptic samples, as the epileptic hippocampus is characterized by cell loss and astrocytosis. Second, human studies lacked a proper control, in that the epileptic tissue was from surgeries

and the control from autopsies. Third, no detailed evaluation of the changes in the course of disease was performed. Forth, blood samples were not collected and microarray-analyzed.

In this thesis we focused on miRNAs changes occurring during the entire course of the disease in a single brain region, that is, the granule cell layer of the DG. This area is a compact layer of (almost) identical cells, considered to act as a “gate” to inhibit hippocampal over-excitation (Krook-Magnuson et al, 2015) and is involved in the seizures generation in patients – consequently, very often removed at surgery. Moreover, it has been shown that the DG undergoes important functional changes during epileptogenesis (Pitkänen and Lukasiuk, 2009). Finally, it has been well characterized from all points of view: developmental, neurochemical, morphological, physiological.

Our investigation in human samples (Zucchini et al., 2014; see Chapter 3) revealed a significant down-regulation of miR-487a in the laser-microdissected DG of those TLE-patients that were affected by GCP-2, suggesting its role in the histo-pathogenesis of the disease. In this particular study, the comparison was all between surgical samples, with or without GCP. In general, however, the problem of human studies is the lack of a proper control. In many microarray studied, autoptic tissue is used as control for surgery resected tissue (bioptic). We demonstrated that, at least for miRNA studies, this is not a valid approach. We included in the analysis 2 epileptic autoptic cases that did not died for “epilepsy causes”, revealing with hierarchical clustering analysis that these two segregated with the other autoptic cases and not with the bioptic epileptic cases. Thus, the tissue origin may influence the analysis more than the disease. A different methodological approach should therefore be used for identifying a miRNA signature in epilepsy patients, for example basing the clustering analysis on epileptic autoptic cases.

To study miRNAs changes through the different phases of TLE and not only in the chronic stage (as allowed in drug-resistant patients that underwent the surgical resection of the focus epilepticus), we performed a microarray analysis on the DG of epileptic rats killed at different time points in the natural history of the disease: early and late latency, at the time of the first spontaneous seizure and in the chronic stage (Roncon et al., 2015; see Chapter 3). This analysis gave great insights in the field of epileptogenesis, highlighting an overlap of several miRNAs, such as miR-21-5p, miR-23a-5p, miR-146a-5p and miR-181c-5p, with datasets obtained from other animal models (Bot et al, 2013; Gorter et al, 2014). However, the

question remains if the miRNAs identified with these studies were model- or epilepsy-specific. To pursue an answer, we performed a meta-analysis of miRNA datasets obtained from different studies. This meta-analysis, that is reported in the third chapter, highlighted the highly significant dysregulation of brain-enriched miRNAs such as miR-212-3p, miR-132-3p and miR-146a-5p and revealed their great potential as new therapeutic targets.

As stated above, the identification of patients that will develop epilepsy remains a major issue in the field of antiepileptogenic therapy. For the first time, we investigated changes in circulating miRNAs in the plasma of epileptic rats, in order to better understand their role as biomarkers of disease (Roncon et al., 2015). With a microarray analysis, we detected different groups of miRNAs that shown different patterns during the phases of TLE in the rat pilocarpine model. Rats were killed at different time points (early and late latency, at the time of the first spontaneous seizure and in the chronic stage) and blood was collected through an intracardiac puncture before the killing. Almost all rats that underwent the pilocarpine model became epileptic, i.e. displayed recurrent spontaneous seizures in the chronic stage (Curia et al, 2008). This allowed us to be confident in considering epileptic also those rats that were killed in the two latency phases. We detected and RT-PCR validated a miRNA, miR-9a-3p, which levels were significantly higher in plasma collected in the early latency phase compared to controls and the others disease phases. These results strongly suggest a potential of miRNAs as biomarkers of disease, although further investigation in refined models, in which not all animals develop epilepsy, will be necessary. Moreover, this has been demonstrated to be a proof of concept for microarray studies in different animal model of disease, which will be used for a new meta-analysis.

In conclusion, miRNAs generated a great interest in the scientific community investigating novel potential therapeutic targets and biomarkers in the field of epilepsy. They hold the important features to be translationally applicable in patients, providing an opportunity to approach the clinical needs for a really preventive, antiepileptogenic therapy, and not simply the mere suppression of symptoms.

6.3 Sestrin 3

Complex diseases, such as epilepsy, may be driven by molecular processes that affect multiple genes acting in concert to activate transcriptional networks and pathways relevant. In epilepsy, the introduction of methods to analyze gene expression at the whole transcriptome level did not yet permit to identify common epileptogenic mechanisms (Pitkanen and Lukasiuk, 2011). One alternative strategy has been to use systems-level approaches to investigate transcriptional networks and pathways within pathologically relevant cells and tissues. Indeed, we integrated the analysis of transcriptional networks with genetic susceptibility data and phenotypic information (Johnson et al., 2015, see Chapter 4). In this manner, specific transcriptional programs may be connected to disease states, leading to the identification of pathogenic pathways and of their genetic regulators as new targets for therapeutic intervention. We identified a gene-regulatory network that contains a specialized, highly expressed transcriptional module encoding proconvulsive cytokines and Toll-like receptor signaling genes. Using genome-wide Bayesian expression QTL mapping, we probed the genome for key genetic regulators of this network in the human brain, detecting the *Sesn3* gene as a trans-acting genetic regulator of this proconvulsant gene network. In vitro experiments demonstrated that *Sesn3* positively regulates the module in macrophages, microglia and neurons. Moreover, morpholino-mediated *Sesn3* knockdown in zebrafish confirmed the regulation of the transcriptional module, and attenuated chemically induced behavioral seizures in vivo.

To further assess the role of *Sesn3* in regulating epilepsy-associated gene networks, we investigated the phenotype of *Sesn3*-KO rats both in normal conditions and in the pilocarpine model of epilepsy. As expected, we found that these animals are less prone to pilocarpine seizures. Moreover, using behavioral tests like EPM, NOR, OF and FST, we found that *Sesn3* KO rats have an “adolescent” attitude that makes them less prone to develop anxiety and depression, i.e. established comorbid conditions in patients affected by epilepsy. These results suggest a role of the *Sesn3* gene as a regulator of pathways that lead not only to seizure onset but also to epilepsy comorbidities. These are promising insights that will have to be confirmed with a more detailed characterization of the *Sesn3*-KO strain in different model

of epilepsy. Moreover, a more refined silencing approach should be used. For example, amplicon-vectors may be used to silence the gene only in the hippocampus.

6.4 Excitatory and inhibitory unbalance in the epileptic brain

The balance between glutamate and GABA neurotransmitters is an established mechanism that can lead to the development of seizures in epilepsy. Many of currently available AEDs act modulating the glutamate and the GABA activities, thereby controlling the hyper-excitability that leads to seizure development. Unfortunately, little is known on the dynamic changes in the excitatory/inhibitory system in natural course of TLE and in its progression towards pharmaco-resistance. Through microdialytic probes implanted in the ventral hippocampus, we investigated GABA and glutamate release in the entire natural history of the disease (Soukoupova et al., 2014, see Chapter 5). We found that basal GABA outflow was reduced by 75% compared to the control value during the latency phase, while the number of parvalbumin-positive cells was reduced by about 50% and that of somatostatin-positive cells by about 25%. Nevertheless, high K^+ stimulation increased extracellular GABA in a greater manner in this period, ensuring preservation of phasic inhibitory responses. This responsiveness disappeared at the time of the first spontaneous seizure and all along the late chronic stage.

Glutamate and aspartate levels were evaluated at the same time points (Soukoupova et al., 2015, see Chapter 5). We found that basal glutamate outflow was increased in the interictal phases in the chronic period, whereas aspartate remained stable. The high K^+ stimulation increased glutamate and aspartate outflow in all experimental groups, including controls, but the overflow of glutamate was clearly increased in the chronic group.

These data suggest that a GABAergic hyper-responsiveness can compensate for GABA cell loss and protect from occurrence of seizures during latency. In contrast, impaired extracellular GABA levels can favor the occurrence of spontaneous recurrent seizures in the chronic stage, when glutamatergic signaling is preserved and even potentiated. These findings support the growing body of data suggesting that dampening excitatory neurotransmission may be a useful strategy to block epileptic seizures (Zwart et al., 2014).

6.5 References

Bot AM, Debski KJ, Lukasiuk K (2013), Alterations in miRNA levels in the dentate gyrus in epileptic rats. *PLoS ONE*8:e76051. doi: 10.1371/journal.pone.0076051.

Curia G, Longo D, Biagini G, Jones RS, Avoli M (2008), The pilocarpine model of temporal lobe epilepsy. *J Neurosci Methods*, 172(2):143-57.

Ghosh Z, Chakrabarti J, Mallick B (2007), miRNomics-The bioinformatics of microRNA genes. *Biochem Biophys Res Commun*, 363(1):6-11.

Gorter JA, Iyer A, White I, Colzi A, van Vliet EA, Sisodiya S, Aronica E (2014), Hippocampal subregion-specific microRNA expression during epileptogenesis in experimental temporal lobe epilepsy. *Neurobiol Dis*, 62:508-20.

Hu K, Xie YY, Zhang C, Ouyang DS, Long HY, Sun DN, Long LL, Feng L, Li Y, Xiao B (2012), MicroRNA expression profile of the hippocampus in a rat model of temporal lobe epilepsy and miR-34a-targeted neuroprotection against hippocampal neurone cell apoptosis post-status epilepticus. *BMC Neurosci*, 13:115. doi: 10.1186/1471-2202-13-115.

Jimenez-Mateos EM, Bray I, Sanz-Rodriguez A, Engel T, McKiernan RC, Mouri G, Tanaka K, Sano T, Saugstad JA, Simon RP, Stallings RL, Henshall DC (2011), MiRNA Expression profile after status epilepticus and hippocampal neuroprotection by targeting miR-132. *Am J Pathol*, 179(5):2519-32.

Kaalund SS, Venø MT, Bak M, Møller RS, Laursen H, Madsen F, Broholm H, Quistorff B, Uldall P, Tommerup N, Kauppinen S, Sabers A, Fluiter K, Møller LB, Nossent AY, Silahatoglu A, Kjems J, Aronica E, Tümer Z (2014), Aberrant expression of miR-218 and miR-204 in human mesial temporal lobe epilepsy and hippocampal sclerosis-convergence on axonal guidance. *Epilepsia*, 55(12):2017-27. doi: 10.1111/epi.12839.

Kan AA, van Erp S, Derijck AA, de Wit M, Hessel EV, O'Duibhir E, de Jager W, Van Rijen PC, Gosselaar PH, de Graan PN, Pasterkamp RJ (2012), Genome-wide microRNA profiling of human temporal lobe epilepsy identifies modulators of the immune response. *Cell Mol Life Sci*, 69(18):3127-45. doi: 10.1007/s00018-012-0992-7.

Kretschmann A, Danis B, Andonovic L, Abnaof K, van Rikxoort M, Siegel F, Mazzuferi M, Godard P, Hanon E, Fröhlich H, Kaminski RM, Foerch P, Pfeifer A (2015),

Different microRNA profiles in chronic epilepsy versus acute seizure mouse models. *J Mol Neurosci*, 55(2):466-79.

Krook-Magnuson E, Armstrong C, Bui A, Lew S, Oijala M, Soltesz I (2015), In vivo evaluation of the dentate gate theory in epilepsy. *J Physiol*, 593(10):2379-88.

McKiernan RC, Jimenez-Mateos EM, Sano T, Bray I, Stallings RL, Simon RP, Henshall DC (2012), Expression profiling the microRNA response to epileptic preconditioning identifies miR-184 as a modulator of seizure-induced neuronal death. *Exp Neurol*, 237(2):346-54.

Pitkänen A, Lukasiuk K (2009), Molecular and cellular basis of epileptogenesis in symptomatic epilepsy. *Epilepsy Behav*, 14(1 Suppl. 1):16-25.

Pitkänen A, Lukasiuk K (2011), Mechanisms of epileptogenesis and potential treatment targets. *Lancet Neurol*, 10:173-86.

Risbud RM, Porter BE (2013), Changes in microRNA expression in the whole hippocampus and hippocampal synaptoneurosome fraction following pilocarpine induced status epilepticus. *PLoS One*, 8(1):e53464. doi: 10.1371/journal.pone.0053464.

Song YJ, Tian XB, Zhang S, Zhang YX, Li X, Li D, Cheng Y, Zhang JN, Kang CS, Zhao W (2011), Temporal lobe epilepsy induces differential expression of hippocampal miRNAs including let-7e and miR-23a/b. *Brain Res*, 1387:134-40.

Zwart R, Sher E, Ping X, Jin X, Sims JR Jr, Chappell AS, Gleason SD, Hahn PJ, Gardinier K, Gernert DL, Hobbs J, Smith JL, Valli SN, Witkin JM (2014), Perampanel, an antagonist of α -amino-3-hydroxy-5-methyl-4-isoxazolepropionic acid receptors, for the treatment of epilepsy: studies in human epileptic brain and nonepileptic brain and in rodent models. *J Pharmacol Exp Ther*, 351(1):124-33.